VARIABILITY IN FORMS AND FLUXES OF CARBON DIOXIDE IN THE ARABIAN SEA

Thesis submitted for the degree of

DOCTOR OF PHILOSOPHY

in

MARINE SCIENCE

to the

GOA UNIVERSITY

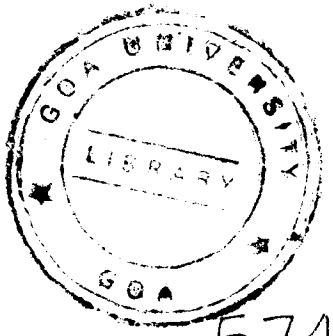

by

V.V.S.S. Sarma

National Institute of Oceanography
Dona Paula - 403 004, Goa, India

December 1998

CERTIFICATE

This is to certify that the thesis entitled **"VARIABILITY IN FORMS AND FLUXES OF CARBON DIOXIDE IN THE ARABIAN SEA"**, submitted by Mr. **V.V.S.S. Sarma** for the award of the degree of Doctor of Philosophy in Marine Science is based on his original studies carried out by him under my supervision. The thesis or any part thereof has not been previously submitted for any other degree or diploma in any universities or institutions.

Place: Dona Paula

Date:

Dr. M. DILEEP KUMAR

Research Guide,
Scientist E I
Chemical Oceanography Division
National Institute of Oceanography
Dona Paula - 403 004, Goa.

HEAD
DEPARTMENT OF MARINE SCIENCE
&
GOA UNIVERSITY.

STATEMENT

As required under the University ordinance 0.19.8 (vi), I state that the present thesis entitled "**VARIABILITY IN FORMS AND FLUXES OF CARBON DIOXIDE IN THE ARABIAN SEA**" is my original contribution and the same has not been submitted on any previous occasion. To the best of my knowledgem the present study is the first comprehensive work of its kind from the area mentioned.

The literature related to the problem investigated has been cited. Due acknowledgments have been made wherever facilities and suggestions have been availed of.

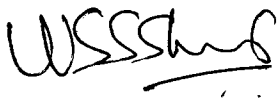

V.V.S.S. SARMA

To

My Parents

INDEX

7. Carbon Budgets

ACKNOWLEDGEMENTS

Ever since I started my research career, there are numerous people who are my friends and well wishers whose generous support helped me to reach my goal. I have a great pleasure to acknowledge the following colleagues and individuals involved with this work or otherwise helped in consolidating my research persuit.

I have no words to express my deep sense of gratitude to **Dr. M. Dileep Kumar**, my Research Guide. It is only his encouragement, inspiration and help that has made me carry out this work. Since beginning of my research career, he never failed to share his interests in new adventures in science. He provided a working environment in such a way, I felt free to work, think and grow. It is an ideal atmosphere for any researcher to brighten his research career. I take this opportunity to express indebtedness and respect to him. My interaction has not ended with him and has extended to his family members and their affection is highly appreciable.

Dr. S.W.A. Naqvi, Assistant Director, Chemical Oceanography Division, N.I.O. for his constant encouragement and valued guidance in my work. Thanks are also due to his valuable and critical assessment of the thesis in amazingly short time. This kind help qnd support that enabled me to get trained at CEREGE, France on Mass spectrophotometer and also all through my career so far, are highly acknowledged.

My gratitude to **Dr. E. Desa**, Director, National Institute of Oceanography, Goa for his kind encouragement, moral support and providing necessary infracture facilities and award of fellowship under Joint Global Ocean Flux Study programme (JGOFS - Arabian Sea. I also thank **Dr. S.Y.S. Singbal**, Head, Chemical Oceanography, for support and encouragement.

I am indebted to the Department of Ocean Development for supporting me with a Reseach Fellowship under the national programme, JGOFS. With this financial aid I could complete this task. I particularly take this opportunity to thank **Drs. B.N. Krishnamurthy** and **K. Somasundar** of DOD, New Delhi.

Thanks are also due to JGOFS namely **Drs. S.N. de Sousa, M.D. George, S. Sardessai, P.V. Narvekar, M.S. Shailaja, P.V. Shirodkar, Ch. Kesava Rao** and **Mr. D.A. Jayakumar,** Chemical Oceanography, **M. Madhupratap, P.M.A. Bhattathiri, N. Ramaiah, S. Raghu Kumar and Lata Raghu Kumar** from Biological Oceanography, **S. Prasanna Kumar, P.M. Muraleedharan, V.S.N. Murty, Y.V.B. Sarma** and **Mr. Almeida**, from Physical Oceanography and **V. Ramaswamy and Mr. Fernando**, from Geological Oceanography, for their help during cruises and allowing me to use their unpublished data. The discussions made with them, have been exciting and greatly helped me.

Prof. S. Krishnaswami is highly appreciated for his excellent leadership to JGOFS group. Just before SK121 cruise, our Coulometer developed a problem. **Dr. M. Sarin**, Physical Research Laboratory is highly appreciated for his great help by providing their Coulometer.

I am greateful to **Dr. Catherine Goyet**, Woods Hole Oceanographic Institution (WHOI), USA for providing underway pCO2 measurement system for continuous pCO_2 measurements in the Arabian Sea and Bay of Bengal and allowed to me utilize the data in my thesis. She offered several helpful discussions at different stages of this work and I acknowledge the same. **Mr. Greg Eischeid** of WHOI is highly appreciated for the training offered and technical support provided to utilize underway surface pCO_2 analyzer and in processing the raw data sets.

Thanks are due to **Dr. Ferial Louanchi** and **Dr. Nicolas Metzl**, Universite de Marie et Currie, Paris, France for helpful discussions especially when I used their model in chapter 6.

My thanks are also due to **Dr. Richard Sampere**, Universite de Luminy, **Dr. Gus Cauwet** of France and **Dr. Edward Peltzer**, MBARI, USA for their help in the discussions.

I learned the fundamentals and new frontiers in paleoceanography at CEREGE, France and my sincere thanks are to **Prof. Edouard Bard, Prof. Bruno Hamlein** and **Mrs. Frauke Rostek** whose expertise helped me to learn much about the subject.

My sincere thanks also goes to my best friend **Dr. Damien Cardinal**, France for his help and suggestions during his stay in India and as well as my stay in France.

I would like to thank **Profs. D. Satyanarayana, N.S. Sarma** and **Dr. I.M. Rao**, Andhra University, Visakhapatnam for their encouragement.

My thanks also goes to **Profs. U.M.X. Sangodkar, G.N. Naik, Drs. M. Vishnu Murty**, and **Upadyaya** Goa University, Goa for their encourage and help provided at several stages of my work.

I would like to acknowledge **Mr.Louis** and **Mr. V.N. Choadankar** from NIO workshop who helped me to prepare semi-automated coulometer sampling system. My thanks also goes to **Mr. Rajaram Patil, H.S. Dalvi, Fotu Gauns** and **M.J.M. Gilbert** for their secretarial and laboratory assistance.

I greatly acknowledge **Mr. E.P. Rama Rao and Vishwa Kiran** their help during my stay in hostel (especially good dinners!!) and at several stages of this work.

My special thanks also due to my friend Mr. **Mangesh Gauns** for his help during cruises and in laboratory.

I greatly appreciate the friendship, goodwill and support of my best friends **Ms. Chanda Nasnolkar, Vibha Salkar** and **Jyoti Borkar** and their help during cruises also highly appreciated.

I appreciate my friends and colleagues **Damodar Shenoy, Hema Naik, Patil, Bhaskar, Thamban, Balakrishna Nair, Mishra, Subodh** and many others at the National Institute of Oceanography, Goa.

Last but not least, I am indebted to my parents but for whom I would not have been existing. Their unending love and unrelented support and guidance only moulded me to what I am today. I find no appropriate words to express my feeling and gratitude to them. I am sure they do not expect this from me either. So affectiionate and dedicated they are. However, I am elated and proud to write these few words. My appreciation also goes to all my family members and friends back home in Andhra Pradesh.

V.V.S.S.SARMA

PREFACE

The northern Indian Ocean is different from other oceanic areas in terms of its geographical setting and circulation patterns. The Indian subcontinent splits the region into two contrasting hydrographical regimes. The Arabian Sea occupies the area bounded by the African and Asian landmasses in the west and north, the Indian subcontinent and the Maldives in the east and the main Indian Ocean in the south. The Arabian Sea is characterised by strong, seasonal oscillations in biological productivity forced by winds. The wind, which is the key to physical forcing in the basin, blows from the northeast during winter (December to February) also known as the NE (Northeast) monsoon. The wind, however, blows in the reverse direction during the SW (Southwest) monsoon (June-September). Inter-monsoon transitions occur during October-November and March-May. Monsoonal coupling between atmosphere and ocean is vigorous and the seasonal shift in wind pattern causes semi-annual reversal of surface currents in the Arabian Sea. This gives rise to the greatest seasonal variations in surface water characteristics seen in any ocean basin.

In addition to the temporal variations, considerable spatial variations also occur. Strong gradients in biogeochemical processes in the pelagic zone are created by the asymmetric effects of the monsoon within the basin. Upwelling occurs in a few coastal zones of the Arabian Sea, along the Somali and Omani coasts besides the Southwest coast of India. This is driven by offshore Ekman transport of surface water under the influence of winds parallel to the coast. Upwelling is most pronounced off the coasts of Oman and Somalia while comparatively weaker upwelling has been

off the Southwest coast of India. During the SW monsoon, a narrow, low-level, atmospheric Findlater Jet generates strong gradients in the wind stress over the Arabian Sea. To the northwest of the jet axis, a positive wind stress curl drives divergence (open-ocean upwelling) through Ekman pumping whereas to the southeast of the jet the curl is negative causing convergence (sinking) of surface waters. The nutrient-rich upwelled water promotes primary production during the SW monsoon. This makes this basin one of the most productive regions in the world's oceans. Higher rates of primary production results in very low levels of dissolved oxygen in intermediate waters of the Arabian Sea. This oxygen minimum zone (OMZ) occurs between ~100 and 1200 m of the water column and is the most pronounced in the central and northern Arabian Sea. The reducing environment in the OMZ has important biogeochemical consequences for nitrogen and carbon cycling, as it is conducive for microbial-mediated process such as denitrification. The only other open oceanic sites that experience mid-depth nitrate reduction are located in the eastern tropical Pacific Ocean off Mexico and Peru. Rate of water column denitrification in the Arabian Sea has been estimated to be 12-33 Tg N y^{-1}. These results indicate that the Arabian Sea is an area of global significance, accounting for ca. 10-30% of the total oceanic water-column denitrification.

Dissolved organic carbon (DOC) in sea water represents the largest pool of organic matter in aquatic environments. Diverse opinions exist on the behaviour of DOC in the deep sea. Initially, it was thought to be conservative, subsequent studies supported a non-conservative behaviour. DOC behaviour in the Arabian Sea shows lower concentrations in the water column in the northern Arabian Sea than in south. These

differences could be due to their chemical and biological systems, triggered mainly by variations in reducing nature, microbial biomass, primary productivity and consequent denitrification or nitrification processes.

The surface waters of the northern Indian Ocean are found to be supersaturated with respect to partial pressure of carbon dioxide in air and also to both calcite and aragonite. The change-over from supersaturation to undersaturation occurs at ~500m for aragonite. However, the deep water seems to be generally at near-equilibrium with calcite. Considerable regional variability in the degree of undersaturation of deep waters were observed.

In view of the complexity of the north Indian Ocean and its importance to biogeochemical cycling of carbon a detailed study has been undertaken, mostly as a part of the Indian JGOFS programme.

The results obtained during JGOFS and other cruises and inferrences drawn on the variability in inorganic forms of carbon and their fluxes at air-water interface forms the major theme of this Thesis and are addressed in nine chapters.

Chapter 1 discusses on the carbon in the earth system and their interchange among different reservoirs. It introduces study area which covering central and eastern parts of the Arabian Sea (i.e., 11° N to 21° N and 64° E to 78° E) with brief accounts of oceanographic aspects, with particular emphasis on the present understanding of

carbon cycling. The scientific rationale and major objectives of this study were highlighted.

Chapter 2 gives detailed account of sampling procedures, analytical instruments used and methods adopted in this study. In order to achieve the goals specified ten oceanographic cruises were undertaken on boards ORV Sagar Kanya and FORV Sagar Sampada. The best available techniques were used to obtain precise and accurate data sets. Details of computed parameters such as partial pressure of carbon dioxide, carbonates, apparent oxygen utilization and nitrate deficit etc. are described.

Chapter 3 deals with the hydrographical features of the Arabian Sea. Seasonal and spatial changes in physical parameters and circulation were discussed in detail. Influence of changes in circulation and physical forcing on biological productivity and the consequent reducing conditions in subsurface layers were highlighted.

Chapter 4 discusses the variability in forms of inorganic carbon components in time and space in the Arabian Sea. Physical and associated biological processes substantially effect dissolved inorganic carbon components. Winter convective mixing and SW-monsoonal upwelling bring nutrients and carbon rich subsurface waters into the surface as a result of which surface productivity increases. High productivity lowers total carbon dioxide (TCO_2), partial pressure of carbon dioxide (pCO_2) but increases carbonate ions concentrations and pH. Increased respiration rates in the suboxic waters, on the other hand, enhances TCO_2 and pCO_2 whereas pH, TA and carbonates reduce as proton is released during organic matter decomposition. The detailed

discussion on these topics, along with seasonal and temporal variations, was presented in this chapter that also include skeletal carbonates dissolution.

Chapter 5 focuses on organic carbon dynamics in the Arabian Sea. DOC mainly originates from metabolic processes including the breakdown of cells during grazing and also is an intermediate in the conversion of particulate organic matter into inorganic carbon dioxide. DOC is known to play a pivotal role in food chain processes as it serves as substrate for micro-organisms. The POC can occur in visible and invisible forms. Of these the invisible form is generally referred to as Transparent Exopolymer Particles (TEP) formed from dissolved carbohydrates. As TEP plays an important role in carbon cycle than the rest of particles we studied this class of particles in detail. In view of the intense water column denitrification in the Arabian Sea and higher rates of sinking particles in the Bay of Bengal data on TEP were collected from the North Indian Ocean during August 1996 to understand their role in the biogeochemical processes. This chapter presents the dynamics of Dissolved Organic Carbon and Transparent Exopolymer Particles, possible inter-conversions between them and their importance to biogeochemical processes.

Chapter 6 describes the air-sea fluxes of carbon dioxide in the Arabian Sea. Surface pCO_2 is generally higher in surface waters than atmospheric concentrations throughout the year suggesting that Arabian Sea is a pernnial source for atmospheric carbon dioxide. Due to the pumping of carbon rich subsurface waters into the surface by different physical process, emission of CO_2 into the atmosphere occurs except in a few coastal regions where fresh water dominance is more. Winds play major role

controlling these fluxes. The effect of physical and biological processes on surface pCO_2 concentrations are discussed using one dimentional model and through linear relationships.

Chapter 7 outlines the carbon budgets for the study regions. The study area has been taken as one box but with different layers and lateral and vertical fluxes in to the box were studied using velocities obtained from the run of MOM model. To these model results the presently observed biogeochemical data have been combined to arrive at carbon budgets of the study area.

Chapter 8 attempts to study the effect of soil-water interactions on pH of the estuarine waters. Biogeochemical processes occurring in estuaries may modify the concentrations of river or sea water borne substances. The pH of river waters may be governed by the nature of rocks in the catchment area. If the terrain rocks are acidic, the pH will be in the acidic range. If so, this will result in an increase in pCO_2 in water. Discharge of industrial and aquaculture effluents can also alter the carbonate equilibria based on the acidic/alkaline nature of the effluents. Thus, the changes in dissolved pCO_2 will lead to change in its gradient between air and water that determines the direction of the flux.

A summary of the present work with salient features was outlined in **Chapter 9**.

This chapter is followed by a complete list of references cited in the text in alphabetical order.

Chapter 1

INTRODUCTION

1.1 Carbon in the earth system

Carbon is one of the few essential elements for the existence of life on earth. It is the principal constituent of both the organic soft tissue and inorganic (skeletal) parts of living beings. The life on this planet largely depends on the atmospheric carbon dioxide (CO_2) fixed photosynthetically by plants, that will be carried over to higher trophic levels. Furthermore, the life has been sustained over the geological periods by the warmth generated because of the trapping of long wave length radiation (greenhouse effect) by CO_2 together with water vapour, methane and nitrous oxide in the atmosphere. However, in spite of the life saving and sustaining roles of CO_2, one of the most important problems its accumulation in the earth's atmosphere threatens the humanity today by raising the rise in atmospheric temperature. The increasing use of fossil fuels and deforestation results in the accumulation of CO_2 in the atmosphere. Carbon dioxide content of the atmosphere was around 280 ppmv in the pre-industrial era (Siegenthaler and Sarmiento, 1993) that increased to 360 ppmv at present. Since the beginning of the industrial era, about 200 x 10^3 Tg (1 Tg = 10^{12} g or Mega tonnes) of carbon has been released into the atmosphere as CO_2. The present annual increase is estimated to be ~1.5 ppmv amounting to a build up of $3.4x10^3$ Tg in the atmosphere (Fig. 1.1; Table 1.1). This rate far exceeds the natural variability. For example, an increase in atmospheric carbon dioxide over the last glacial - interglacial transition, by 80 - 90 ppmv, occurred over a few

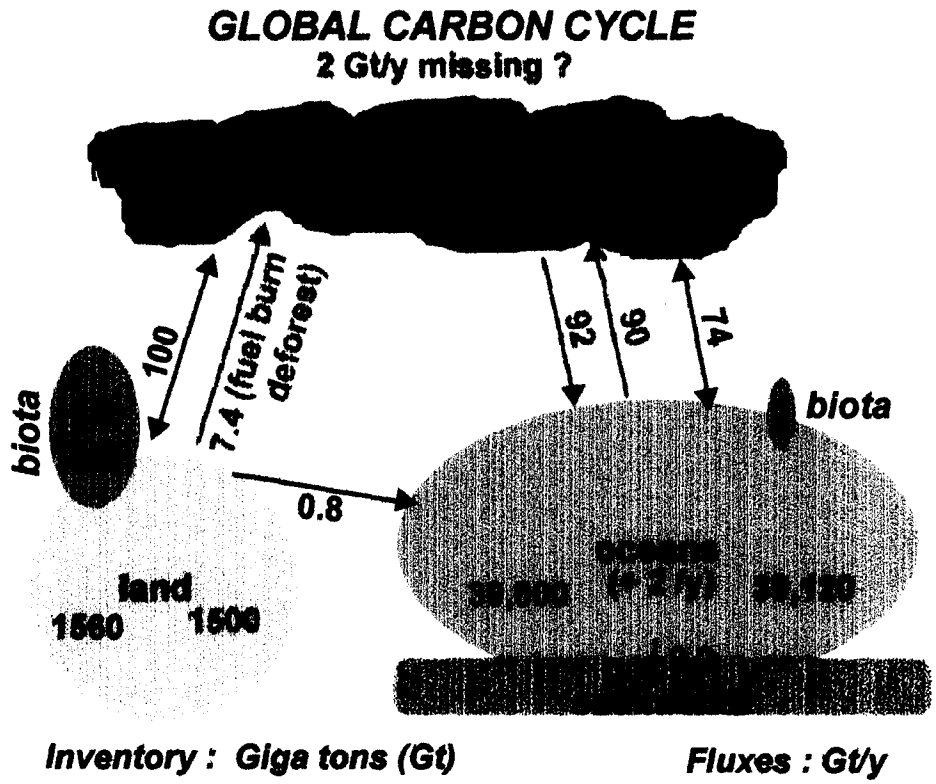

Fig. 1.1. Schematic diagram showing the global carbon cycle (after Siegethlar and Sarmiento, 1993)

thousand years whereas man has brought about an increase of almost the same magnitude in less than two centuries. Studies on ice cores of Antarctica have shown a convincing positive correlation between changes in temperature and in atmospheric CO_2 (UNESCO, 1979). Table 1.1 reveals that carbon dioxide is released by humans at rates exceeding that of its absorption by major carbon reservoirs on the earth surface thereby raising concerns about the 'missing carbon'. Whether the missing carbon dioxide is mainly absorbed by the land ecosystems or by the ocean is still being debated (Keeling and Heinemann, 1986; Keeling *et al.*, 1989; Sarmiento *et al.*, 1992; Tans *et al.*, 1990; Broecker and Peng, 1992; Kauppi *et al.*, 1992; Quay *et al.*, 1992; Siegenthaler and Sarmiento, 1993). The latest information, however, suggests that a large part of this missing carbon could go into enhanced primary production at high latitudes in the Northern Hemisphere (Tans, 1998). Such concerns emphasise the need for an improved understanding of carbon cycling through global efforts that eventually shaped into the Global Change Programme (International Geosphere-Biosphere Programme).

Among the earth's reservoirs, the largest amount of carbon is present as carbonate sediments while it is the least in air (Table 1.2). The largest aquatic body on this planet covering ~71% of its surface is ocean in which about 38,100 Tg C resides in inorganic forms, in addition to 700 Tg C present as dissolved organic substances. The oceans are estimated to absorb about 2 Tg

Table 1.1:The average anthropogenic carbon budget (in x 10^3 TgC y^{-1})

CO_2 sources	
(1) Emissions from fossil fuel combustion and cement production	5.5 ± 0.5
(2) Net emissions from changes in tropical land-use	1.6 ± 1.0
(3) Total anthropogenic emissions = (1) + (2)	7.1 ± 1.1
Partitioning amongst reservoirs	
(4) Storage in the atmosphere	3.2 ± 0.2
(5) Ocean uptake	2.0 ± 0.8
(6) Uptake by Northern Hemisphere forest regrowth	0.5 ± 0.5
(7) Additional terrestrial sinks (CO_2 fertilisation, nitrogen fertilisation, climatic effects)=[(1)+(2)]-[(4)+(5)+(6)]	1.4 ± 1.5

Table 1.2: Amount of carbon in various reservoirs (Tg CO_2 equivalent) (after Bolin et al., 1977)

Reservoir	Amount
Atmosphere	2
Biomass (living matter)	30
Soils (organic carbon)	25,000
Oceans and freshwater (in soln.)	140
Carbonate sediments	150,000
Fossil fuels (plus organic carbon disseminated in sediments)	27

C of anthropogenic carbon released to air annually. The amount of CO_2 penetrating the ocean has been found to increase by a factor of two during the last forty years (Pearman *et al.*, 1983). Although, the sizes of carbon in air and oceans are small compared to those in sediments and soils, the small quantity in air regulates the temperature of this reservoir. Atmospheric CO_2, however, a function of its exchange between the atmosphere and oceans (Fig. 1). Oceans control the atmospheric CO_2 concentration over a period of 1×10^5 years (UNESCO, 1979). Therefore, there is a need to study the variability of carbon in the ocean and to understand the changes in the extent of its transfer across the air-sea interface that have implications for regulating the atmospheric temperature.

1.2 Carbon cycle in oceans

While carbon dioxide is the major form of inorganic carbon in the atmosphere it comprises of four different species in sea water: gaseous carbon dioxide [CO_2], carbonic acid [H_2CO_3], and bicarbonate [HCO_3^-] and carbonate [CO_3^{2-}] ions. Transformations among these species can be shown by the following equilibria:

$$CO_2 + H_2O \text{ <==> } H_2CO_3 \text{ <==> } H^+ + HCO_3^- \text{<==> } 2\,H^+ + CO_3^{2-}$$

Total carbon dioxide (TCO_2) or dissolved inorganic carbon (DIC) refers to the sum of these four inorganic carbon species, i.e.,

$$TCO_2 = [CO_2] + [H_2CO_3] + [HCO_3^-] + [CO_3^{2-}]$$

Gaseous CO_2 is the only species that can be exchanged with air. However, $CO_{2\,(g)}$, $CO_{2(aq)}$ and H_2CO_3 are nearly indistinguishable in water since their interconversions are fast. Thus, partial pressure of carbon dioxide (pCO_2) is generally used to represent the sum of these three forms. At pH values <3 negligible ionization occurs and thus the dissolved inorganic carbon existing almost entirely as $CO_{2\,(aq)}$ + H_2CO_3. At a pH of 5.5 only ≈15% of the total inorganic carbon is in the form of HCO_3^-. The percentage of CO_3^{2-} is not significant at pH <7.5. However, above 7.5 CO_3^{2-} becomes significant and dominates at pH>9. At a normal sea water pH range (7.5 to 8.3) bicarbonate ion is the predominant form (Skirrow, 1975).

A large amount of atmospheric CO_2 is absorbed by the ocean especially in high latitude regions (Takahashi, 1961; Keeling, 1968; Takahashi *et al.*, 1980). The geographical variations in carbon dioxide absorption by the ocean is mainly due to the increased CO_2 solubility with decreasing temperature (Weiss, 1974). The equatorial regions of the world oceans and vast areas in the north-eastern

Pacific Ocean are noted to be sources of atmospheric CO_2 (Takahashi, 1989; Tans *et al.*, 1990).

Both Physical and biological pumps regulate the dissolved carbon in the ocean. Transport of waters from one region to an other and from one depth to an other results in the transfer of dissolved substances as well. The main means of transportation are advection and diffusion. Oceanic processes such as convection in winter and seasonal upwelling lead to supply of carbon from the subsurface to the surface layer. These physical processes ultimately drive the magnitude of biological processes by controlling the availability of nutrients. Therefore, the physical pump exerts a control over the biological production, with the eventual regulation of carbon dioxide at a given location in the sea by both the processes.

About 3×10^3 Tg of carbon is stored in the surface biota (Fig. 1.1). A part of the biogenic debris produced in the euphotic layer sinks into the deep ocean, which is subjected to microbial oxidation. The calcium carbonate in skeletal materials of some organisms is the primary source of mineral carbonate in marine sediments. These transport processes together are referred to as the **biological pump**. If this pump acts with high efficiency the level of atmospheric CO_2 could be reduced. However, the complex physical, chemical and biological factors determine the overall efficiency of the pump. The phytoplankton

biomass is recycled within a few weeks, and most (90%) of this recycling occurs in the mixed layer. Transport of particulate detritus from the euphotic zone to the deep ocean can be of the order of 3-10% of primary production (Broecker, 1974a). The oceanic organic carbon reservoirs are living matter, detrital particulate organic carbon and dissolved organic carbon. The Dissolved Organic Carbon (DOC) is the most abundant followed by detrital, planktonic and bacterial forms. The remaining organic forms are of insignificant sizes compared to planktonic forms.

The overall cycle of carbon among the atmosphere, biota, soils and ocean has a residence time of about 100,000 years; most of which is spent in the deep sea. The upward transport by physical processes and sinking through biological pumping greatly vary seasonally and geographically. These processes, coupled with a slow air-sea CO_2 transfer rate are responsible for the high degree of CO_2 disequilibrium between the oceanic surface layers and the atmosphere.

1.3 Significance of northern Indian Ocean

The northern Indian Ocean is different from other oceanic areas in terms of its geographical setting and circulation patterns. The Indian subcontinent splits the region into two contrasting hydrographical regimes. The Bay of Bengal

(north eastern Indian Ocean) is essentially tropical, lying to the south of 22° N and its maximum zonal extent is about 1200 km. Irrawady, Brahmaputra, Ganges and Godavari discharge annually ~1.5 x 10^{12} m^3 of fresh water into the bay (Martin *et al.*, 1981). In addition, annual rainfall over the bay varies between 1 m off the east coast of India to more than 3 m in the Andaman Sea and in the coastal region to the north of the latter (Baumgartner and Reichel, 1975). Large amounts of fresh water inputs in to the north-eastern Indian Ocean cause strong thermohaline stratification which greatly inhibits vertical mixing (Ku and Luo, 1994; Naqvi *et al.*, 1994; Rao *et al.*, 1994).

The Bay of Bengal is an area of positive water balance. A large excess of precipitation and river runoff over evaporation leads to very low surface salinities. In addition to supplying large amounts of dissolved and suspended materials, the runoff is also expected to influence the chemistry by controlling circulation and mixing. The rivers from this region are known to make disproportionately large contributions to the global suspended load to the ocean (Milliman and Meade, 1982). The lithogenic substances strongly influence the sedimentation of biogenic matter (Ittekkot *et al.*, 1992). This is expected to significantly alter the water column regeneration processes, the extent of which remains unknown. Unlike Arabian Sea, the Bay of Bengal does not appear to be an active denitrification site although this region also contains nearly sub-oxic intermediate waters (Rao *et al.*, 1994).

The north-western Indian Ocean (Arabian Sea), on the other hand, is a region of negative water balance; where the evaporation far exceeds precipitation and runoff; consequently, the upper layers in this region are much more saline and relatively weakly stratified as compared to those in the Bay of Bengal. The multi-layer watermass structure in the Arabian Sea is modified seasonally with variable extents of evaporation in the Arabian Sea and its neighbouring bodies, the Persian Gulf and the Red Sea. In the Arabian Sea, the Arabian Sea High Salinity (ASHSW) watermass forms at the surface whereas those in intermediate and deep waters, such as Persian Gulf Water (PGW), Red Sea Water (RSW), Antarctic Intermediate Water (AAIW), Circumpolar Water (CW) and Antarctic Bottom Water (AABW), originate elsewhere (Wyrtki, 1973).

The flux of terrigenous material, apart from inputs of high salinity waters through the Gulf of Oman and the Gulf of Aden, into the north-western Indian Ocean could significantly influence the carbon budget (Table 1.3).

Overall, carbon budget of the Arabian Sea appeared to be negatively balanced that could possibly be balanced by the carbon supply through Antarctic Bottom Water (AABW). Bethoux (1988) emphasized the importance of the transport of materials (carbon, nutrients and oxygen) through the Red Sea outflow on the geochemistry of intermediate waters of the adjacent Indian Ocean. The Arabian Sea is the most productive part of the Indian Ocean (Qasim, 1977).

Table 1.3. Carbon budget of the Arabian Sea (after Somasunder et al., 1990)

Reservoir	Carbon Flux (Tg y^{-1})
Inputs	
Rivers runoff	2.62
Persian Gulf	80.24
Red Sea	316.00
Surface Production	50.66
TOTAL	449.52
Outputs	
Persian Gulf	91.91
Red Sea	358.80
Sedimentation	1.74
Flux to atmosphere	75.73
TOTAL	528.18
Net	-78.66

The actual values of surface primary productivity (Babenerd and Krey, 1974) show a wide variation, ranging between 1 and 74 mg C m^{-2} d^{-1} in low-productive zones and between 2450 and 5790 mg C m^{-2} d^{-1} in high-productive zones. The Indian Ocean, in general, has a mean productivity higher than the other oceans. High surface productivity, especially in the northern region, leads to a large sinking carbon flux. As a result, near anoxic conditions occur in intermediate waters of the Arabian Sea (Sen Gupta *et al.*, 1976; Naqvi, 1987). Physical and biogeochemical processes in the northern Indian Ocean are strongly affected by seasonal changes associated with the monsoons.

1.4 Significance of Study Area - The Arabian Sea

The Arabian Sea occupies the area bounded by the African and Asian landmasses in the west and north, the Indian subcontinent and the Maldives in the east and equator in the south. The Arabian Sea is characterised by strong, seasonal oscillations in biological productivity (Yoder *et al.*, 1992) forced by winds. The wind, which is the key to physical forcing in the basin, blows from the northeast during winter (December to February), also known as the NE (Northeast) monsoon. The wind, however, blows in the reverse direction during the SW (Southwest) monsoon (June-September). Inter-monsoon transitions occur during October-November and March-May (Schott *et al.*, 1990). Monsoonal coupling between atmosphere and ocean is vigorous and the

seasonal shift in wind pattern causes semi-annual reversal of surface currents in the Arabian Sea. This gives rise to the greatest seasonal variations in surface water characteristics of the Arabian Sea than seen in any ocean basin.

In addition to the temporal variations, considerable spatial variations also occur. Strong gradients in biogeochemical processes in the pelagic zone are created by the asymmetric effects of the monsoon within the basin. Upwelling occurs in a few coastal zones of the Arabian Sea, along the Somali and Omani coasts besides the Southwest coast of India. This is driven by offshore Ekman offshore transport of surface water under the influence of winds parallel to the coast (Smith and Bottero, 1977). Upwelling is the most pronounced off the coasts of Oman and Somalia (Swallow, 1984) while comparatively weaker upwelling has been noticed off the Southwest coast of India (Wyrtki, 1973). During the SW monsoon, a narrow, low-level, atmospheric Findlater Jet (Findlater, 1969, 1974) generates strong gradients in the wind stress over the Arabian Sea. To the northwest of the jet axis, a positive wind stress curl drives divergence (open-ocean upwelling) through Ekman pumping whereas to the Southeast of the jet, the curl is negative causing convergence (sinking) of surface waters.

The nutrient-rich upwelled water promotes primary production during the SW monsoon. This makes this basin one of the most productive regions in the

world's oceans. The primary production ranges from <0.3 g Cm^{-2} d^{-1} in the oligotrophic gyre to >2.5 g C m^{-2} d^{-1} in the upwelling zone off the Oman coast (Owens *et al.*, 1993). The 'f-ratio' (new/total production) for phytoplankton varies between 0.1 in the oligotrophic waters to 0.9 in the upwelling region. The new production is defined as that equivalent to organic matter exported from the euphotic zone (Dugdale and Goering (1967). Higher rates of primary production results in very low levels of dissolved oxygen in intermediate waters of the Arabian Sea. This oxygen minimum zone (OMZ) occurs between ~100 and 1200 m of the water column and is the most pronounced in the central and northern Arabian Sea. Various hypotheses have been proposed for the maintenance of the OMZ, including slow advection of water allowing long periods for organic decomposition (Sverdrup *et al.*, 1942) and high local respiration rates due to enhanced production in surface waters (Ryther and Menzel, 1965). The dynamic processes required for the maintenance of the OMZ in the Arabian Sea have been studied recently by Olson *et al.* (1993); who estimated the residence time of water in the OMZ to be ~10 years. An oxygen budget constructed for the OMZ reveals that near-zero oxygen concentrations are maintained by moderate consumption in waters of initially low oxygen content which pass through the layer at a moderate speed (Olson *et al.*, 1993). Other recent estimates of the renewal time are lower down to 1 year (Naqvi, 1987; Somasundar and Naqvi, 1988; Naqvi and Shailaja, 1993; Howell *et al.*, 1997).

The reducing environment in the OMZ has important biogeochemical consequences for nitrogen and carbon cycling, as it is conducive for microbial-mediated process such as denitrification. The only other open oceanic sites that experience mid-depth nitrate reduction are located in the eastern tropical Pacific Ocean off Mexico and Peru (Codispoti *et al.*, 1992). Rate of water column denitrification in the Arabian Sea has been estimated to be 12-33 Tg N y^{-1} (Naqvi and Shailaja, 1993; Mantoura *et al.*, 1993). These results indicate that the Arabian Sea is an area of global significance, accounting for ca. 10-30% of the total oceanic water-column denitrification (Naqvi, 1987; Law and Owens, 1990; Naqvi and Shailaja, 1993).

Nair *et al.* (1989) found a strong seasonal variability in sedimentation using traps moored at 2000-3000 m in the Arabian Basin. The pattern of sedimentation was strongly correlated to the monsoon activity. The observation that biogeochemical processes such as sedimentation in the ocean interior can be related to atmospheric forcing, together with the decadal time-scale for the turn-over of the OMZ (Olson *et al.*, 1993), makes the Arabian Sea an important location to study ocean-climate interactions. Furthermore, the upwelling also facilitates the ventilation of greenhouse gases, generated in the OMZ, such as CO_2, CH_4, and N_2O to the atmosphere and provides a climatic feedback mechanism. The biogeochemical balance between such processes must be sensitive to the climatic changes. The Arabian Sea OMZ may therefore be a

sensitive 'marine barometer' for global climate change (Mantoura *et al.*, 1993). Thus, although the Arabian Sea is a small ocean basin, the diverse physical processes it experiences and biogeochemical regimes it houses has led to a spurt of in research activities in this region in recent years under numerous international programs, such as International Indian Ocean Expedition (IIOE), GEOSECS (Geochemical Ocean Sections, led by United States), World Ocean Circulation Experiment (WOCE) and Joint Global Ocean Flux Study (JGOFS).

1.5. Carbon dynamics in the Arabian Sea - State of the Art

The primary productivity in surface waters of the Arabian Sea is higher than in other open oceanic regions of the Indian Ocean (Qasim, 1977, 1982). Kabanova (1968) observed strong seasonal variations in surface productivity associated with changes in upper ocean circulation. During the Northeast monsoon, surface productivity in the Arabian Sea is less than 0.1 g C m^{-2} d^{-1}. The high surface primary productivity during the SW monsoon is due to upwelling. Brock *et al.* (1991) observed plankton blooms during the 1979 summer monsoon and attributed the same vertical nutrient fluxes caused by coastal upwelling but to local upward dynamics for a phytoplankton biomass in 1987. Time-series sediment trap experiments in the Arabian Sea revealed large temporal variability in particulate fluxes primarily controlled by seasonal changes in the upper ocean circulation driven by monsoon winds (Nair *et al.*,

1989). Similarly, using the remote sensing data on ocean colour Sathyendranath *et al.* (1991) showed that the SW monsoon promotes seasonal upwelling of deep water, which supplies nutrients to the surface layer and leads to a marked increase in phytoplankton growth. Strong seasonal variability in the distribution of phytoplankton may also influence the seasonal variation of sea surface temperature that has significant implications to ocean atmosphere interactions. Besides, surface sediments of the Arabian Sea are enriched with organic carbon and its distribution appears to be controlled by surface primary productivity, sedimentation rates and the oxygen concentration in the overlying waters (Slater and Kroopnick, 1984).

Dissolved organic carbon (DOC) in sea water represents the largest pool of organic matter in aquatic environments. Diverse opinions exist on the behaviour of DOC in the deep sea (Wangersky, 1978). Initially, it was thought to be conservative (Menzel, 1964; Menzel and Ryther, 1968), but subsequent studies supported a non-conservative behaviour (Craig, 1971). Sugimura and Suzuki (1988) demonstrated the presence of a large class of previously unknown organic compounds dissolved in sea water that could fuel deep-sea respiration. Kumar *et al.* (1990) studied DOC behaviour in the Arabian Sea while reporting lower concentrations throughout the water column in the northern Arabian Sea than in south. These differences could be due to their chemical and biological systems, triggered mainly by variations in extents of

oxygen-deficient environment, microbial biomass, primary productivity and consequent denitrification or nitrification processes.

The surface waters of the northern Indian Ocean are found to be supersaturated with respect to both calcite and aragonite (e.g., Kumar *et al.*, 1992; George *et al.*, 1994; and references therein). The change-over from supersaturation to undersaturation occurs at ~500m for aragonite (George *et al.*, 1994). However, the deep water seems to be generally at near-equilibrium with calcite. Considerable regional variability in the degree of undersaturation of deep waters were observed (George *et al.*, 1994). The northern Arabian Sea, where calcite saturation depth lies at ~1500 m, is the only region in the northern Indian Ocean that is undersaturated with respect to this mineral at these depths. Based on the observed changes in alkalinity, Anderson and Dyrssen (1994) found the dissolution of $CaCO_3$ to be significant below 600 m in the Arabian Sea.

Distribution of sediment organic carbon and calcium carbonate in the Arabian Sea has been studied by various workers (e.g., Paropkari *et al.*, 1992 and Calvert *et al.*, 1995). Paropkari *et al.* (1992) reported that the organic carbon content is generally high (4 to 12%) along the margins and exhibits a decreasing trend towards the centre of the basin. High organic enrichments (>4%) are observed along the mid-slope of the Arabian peninsula and western

India. The sediments of deep Arabian Sea are poor in organic carbon (<1%). It was also observed that the organic carbon distribution mirrors the surface productivity to some extent, being high in the peripheral portions and low in the open ocean. However, a critical examination of the data reveals that there is no direct correspondence between the intensity of primary productivity and the organic enrichment in the sediments beneath. This suggests that the primary productivity is not necessarily the fundamental control of the organic enrichment in the Arabian Sea. Calcium carbonate in the sediments was extremely high in shelf and upper parts of the slope, ranging up to 96% by weight, whereas at the deeper depths $CaCO_3$ ranged from 24 to 60% by weight (Calvert *et al.*, 1995). On the slope, the carbonate occurs as foraminiferal shells, which appear to show little evidence of dissolution (Von Stackelberg, 1972; Naidu, 1993), while on the shelf it occurred as reworked, relict macrofaunal shell debris, calcareous algae and oolites (Nair and Hashimi, 1980, 1981).

Somasundar *et al.* (1990) worked the carbon budget through inward and outward fluxes of carbon in the Arabian Sea (446 and 530 Tg y^{-1} respectively). Annually, ~74 Tg of carbon in the form of CO_2 escapes into the atmosphere from the Arabian Sea; this is higher than expected from the global average fluxes from the equatorial oceans. The occurrence of denitrification in the Arabian Sea appears to enhance the pCO_2 in the subsurface layers of the

Arabian Sea (George *et al.*, 1994). The Arabian Sea is found to serve as a significant source of carbon dioxide (74-79 Tg C y^{-1}) to the atmosphere (Somasundar *et al.*, 1990; Kumar *et al.*, 1992; George *et al.*, 1994). Using an average carbon concentration (including both particulate and dissolved forms) of 8.74 g m^{-3} in world rivers (Meybeck, 1982) the annual carbon flux into the Arabian Sea is calculated as ~2.32 Tg (Table. 1.3). Fluxes from rivers did not seem to be significant to the carbon balance. Burial of carbon through the sedimentation process is even less than input by rivers. The Arabian Sea has been found to be a carbon source for the Persian Gulf and the Red Sea. Based on the standing crop and net outfluxes, estimated residence time for carbon in the Arabian Sea is ~944 years (Somasundar *et al.*, 1990).

1.6 Importance and objectives of the present study

The Arabian Sea is a small ocean basin with a large number of unusual features. It is, for instance, the only ocean basin where a complete reversal of surface circulation occurs semi-annually basis. Although small on a global scale, the Arabian Sea also encompasses a wide range of oceanographic conditions. While some surface waters are almost devoid of nutrients, others are nutrient rich and extremely productive. On the otherhand, while the surface and deep waters are well oxygenated, waters between 100 and 1,200 m are sub-oxic. Based on these considerations it is obvious that the Northwest Indian

Unlike the Arabian Sea which seems to serve as a source of atmosphere CO_2 throughout the year, some parts of the north-eastern Indian Ocean act as sink for atmospheric carbon dioxide during NE and pre-SW monsoon seasons (Kumar *et al.*, 1996). However, not much is known about its behaviour during the SW monsoon. Also whether the estuarine regions, where high productivity and intense regenerative processes is expected, act as source or sink to atmospheric carbon dioxide is still not clear. Total Carbon dioxide (TCO_2) in global average river water is only about 750 μM (Meybeck, 1982) against its abundance in sea water of ≥1800 μM. Such low TCO_2 levels may result in lower pCO_2 in river and estuarine waters than in the atmosphere. Therefore, it is of extreme importance to understand the CO_2 exchange in estuarine regions, which might make a significant contribution to global air-water CO_2 flux.

Under this programme, a systematic study has been undertaken to understand the biogeochemical cycling of carbon in various regimes of the Arabian Sea with the following main objectives:

- to understand seasonal and spatial variability in carbon components,
- to understand the physical and biological controls on the partial pressure of carbon dioxide in surface layers,
- to quantify the air-sea CO_2 fluxes with respect to identifying its sink and source areas in the Arabian Sea and in the Bay of Bengal,

- to study the influence of dissolved organic carbon on the abundance of other carbon components and denitrification,
- to understand the role of transparent exopolymer particles in the biological pump,
- to quantifying the extent of regeneration of organic carbon,
- construction of carbon budgets in the Arabian Sea., and
- to understand the air-sea exchange of CO_2 in estuarine regions and its controlling mechanisms,

Chapter 2

MATERIAL AND METHODS

The Arabian Sea has been selected as one of four oceanic areas for detailed **process studies** as a part of the international JGOFS by the IGBP. A major portion of the present study was carried out under the multi-institutional and national project **JGOFS (India)** supported by the Department of Ocean Development, Government of India, New Delhi. Field observations for this study were made during a number of cruises in the Arabian Sea and the Bay of Bengal, in addition to local trips in the Mandovi-Zuari estuarine complex of Goa, west coast of India. Dissolved gas measurements in natural waters require extreme care from the time of sampling to the data generation. Even a slight contamination from atmospheric carbon dioxide during sampling would alter the pCO_2 value and the carbonate equilibria. Hence, utmost care has been taken in minimising the uncertainties and to generate quality data comparable with the international standards. The data generated under this programme will be accessible to the international community for global synthesis of data and for developing predictive models.

2.1 Sample collection

2.1.1. Oceanic expeditions

Nine cruises were undertaken in the Arabian Sea on boards ORV Sagar Kanya and FORV Sagar Sampada (Table. 2.1). Six (Fig. 2.1a) of these were under

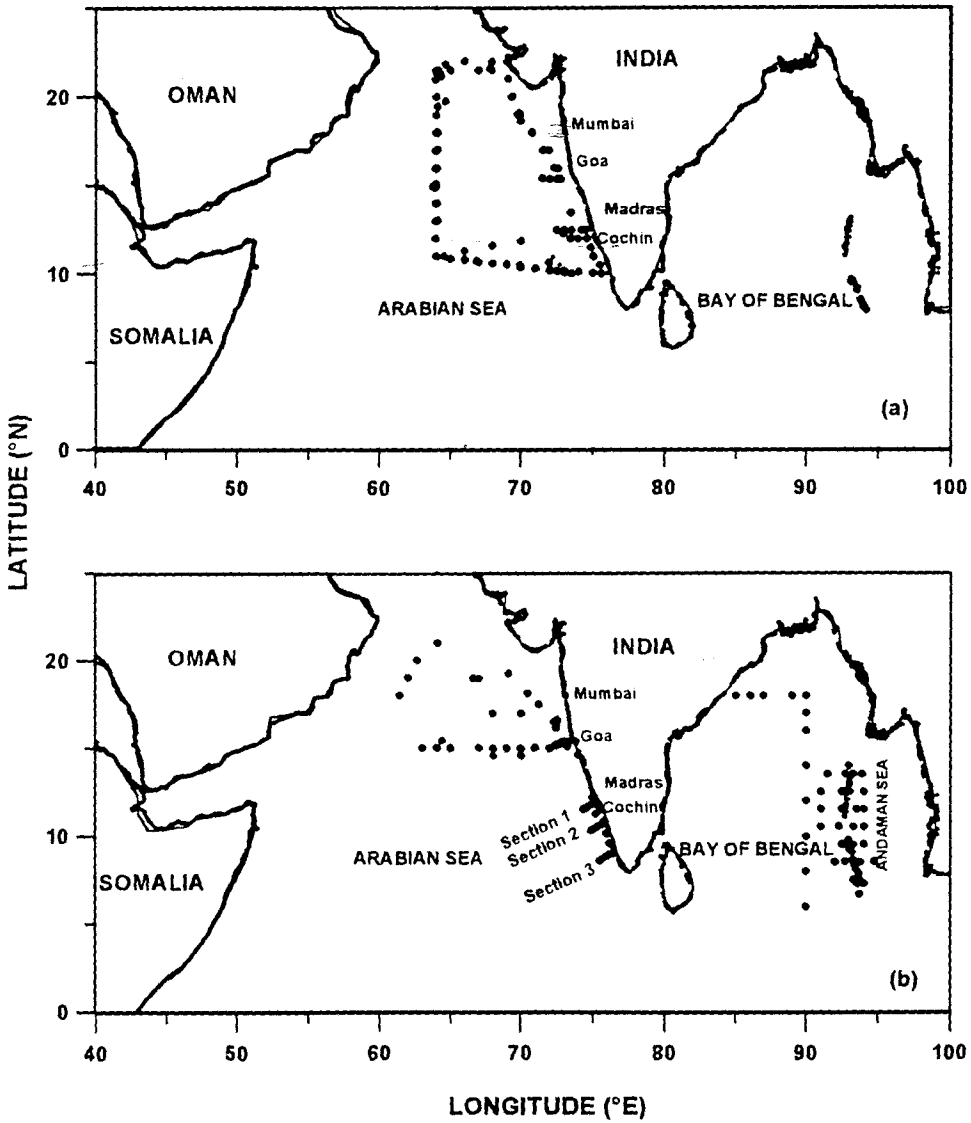

Fig. 2.1. Stations sampled (a) during five JGOFS cruises (SK91, SK99, SK104, SK115 and SK121). Reoccupation of the stations during different seasons overlap their positions and (b) during remaining cruises.

JGOFS (India) programme and were inter-disciplinary in nature. The tracks for the other cruises were shown in Fig. 2.1b including for expeditions in the Bay of Bengal.

The physical variables (temperature and salinity) and water samples were collected using a Sea Bird CTD (model SB9) having a rosette fitted with Niskin or Go-Flo bottles of 1.8/12/30 litre capacity. Water samples were sub-sampled in the order: dissolved oxygen, total carbon dioxide (TCO_2), pH, total alkalinity (TA), transparent exopolymer particles (TEP), dissolved organic carbon (DOC) and nutrients (nitrate, nitrite, phosphate and silicate). Care was taken to avoid trapping the bubbles during collection of water samples. All samples were measured on board within 24 hours of sampling, except for DOC the analysis for which was performed in the shore laboratory within two months.

2.1.2. Estuarine surveys

Sampling was carried out in the estuaries of Mandovi and Zuari, the two major rivers of Goa (Fig. 2.2). Southwest monsoon sampling was done on 22 August 1995 in the Zuari and on 25 August 1995 in the Mandovi and that of post-monsoon on the 2 November 1995 and on 5 December 1995 in the Mandovi and on 6 November 1995 and on 7 December 1995 in the Zuari. Since the Aguada Bay is closed for traffic during the monsoon, the work during this period was confirmed to the upstream position of the rivers. The monsoon

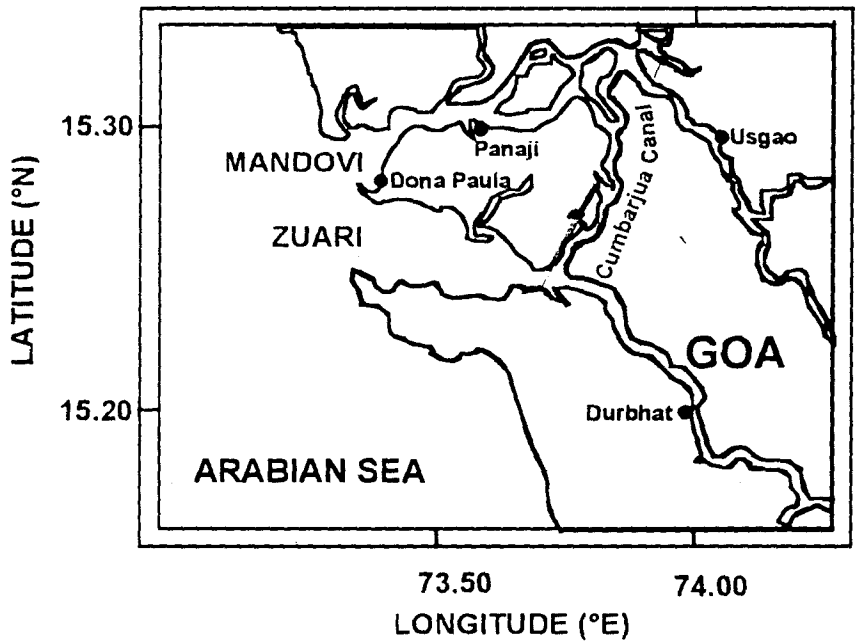

Fig. 2.2. Geological setting of the Mandovi and Zuari estuarine system in Goa.

Table: 2.1. Oceanographic expeditions undertaken for the present study.

No	Area	Period	Vessel	Cruise No.
1	Arabian Sea	April-May 1994	ORV Sagar Kanya	91
2	Arabian Sea	February-March 1995	ORV Sagar Kanya	99
3	Arabian Sea	June-July 1995	ORV Sagar Kanya	103
4	Arabian Sea	July-August 1995	ORV Sagar Kanya	104
5	Arabian Sea	September-October 1995	FORV Sagar Sampada	136
6	Arabian Sea	April-May 1996	FORV Sagar Sampada	141
7	Arabian Sea	June-July 1996	ORV Sagar Kanya	115
8	Bay of Bengal	July-August 1996	ORV Sagar Kanya	116
9	Andaman Sea Bay of Bengal	October-November 1996	ORV Sagar Kanya	118
10	Arabian Sea	February-March 1997	ORV Sagar Kanya	121

sampling in Zuari was performed in three sections half the way upstream. The post-monsoon sampling was done from Aguada bay to Usgao (~60 km upstream) in the Mandovi whereas it was from Dona Paula to Durbhat (~40 km upstream) in the Zuari. Since these rivers are freshwater dominated during monsoon, sampling strategy provided good coverage for studying the behaviour of CO_2 components at varying salinities.

The samples were collected using **Tarangini** a small research boat of 30 feet length. Surface samples were collected using a plastic bucket tied to a nylon rope. As the aim of this work is to understand the behaviours of TCO_2 and pH during the estuarine mixing, extensive collection of surface waters was made for covering the full salinity range. The water was subsampled in 125 ml stoppered glass bottles for salinity, pH and TCO_2. The bottles were rinsed well with the samples prior to collection. Samples for TCO_2 were preserved using 0.2 ml of saturated mercuric chloride. The preservative was added to inhibit the microbial activity in the sample which may change the original carbon dioxide concentration. The analyses of the samples were completed within 48 hours of the sampling. Salinity was analysed by argentimetric titration (Strickland and Parsons, 1972), pH by spectrophotometry and TCO_2 by coulometry. The latter two are detailed in the following sections. A brief account on methodologies used for various parameters studied along with the precisions obtained during the present study is given in Table 2.2. Ore samples for laboratory experiments

were collected from mine field whereas the soil samples were obtained from river banks beyond the head of the estuary.

2.2 Methodology - Experimental

2.2.1. Salinity and temperature

Measurements of temperature and conductivity were made using respective sensors fitted to a Sea-Bird CTD system (No. SB 9). Salinity values, calculated through conductivity, were calibrated against measurements made using an Autosal salinometer (model 8400). The salinity samples were filled, after three initial rinses, to bottle shoulder. The cap was then replaced and firmly tightened. These samples were stored in a temperature-controlled laboratory until analysis. Salinity values reported are in Practical Salinity Units (psu, Fofonoff, 1983). Temperatures sensed by CTD probes were also checked occasionally against those measured using reversing thermometers. Potential temperature and density were calculated based on the algorithms of Fofonoff (1983), the International Equation of State of sea water of Millero *et al.* (1980) and Bryden's (1973) formulation of adiabatic temperature gradients (Fofonoff, 1983).

Table: 2.2. Details of parameters studied, methods used along with the precisions.

S.No	Parameter	Method	Precision
1	Salinity	Conductivity probe	0.001 psu
2	Temperature	Temperature probe	0.01 °C
3	Dissolved Oxygen	Winkler method or Spectrophotometry	0.02 µM
4	Nitrite	Azo-dye method	0.02 µM
5	Nitrate	Reduction of NO_3 followed by Azo-Dye method	0.2 µM
6	pH	Multiwavelength spectrophotometric method involviing Cresol Red	0.002
7	Total Alkalinity	Multiwavelength spectrophotometric method involving Bromo Cresol Green	2 µM
8	Total Carbon dioxide	Coulometric analysis	2 µM
9	Dissolved Organic Carbon	High Temperature Catalytic Oxidation	5%
10	Underway partial pressure of carbon dioxide	Infra Red analyser	0.2 µM/M
11	TEP	Colorimetry	
12	pCO_2	computed from TCO_2 and pH	4 µatm
13	Carbonate	computed from TCO_2 and pH	1.7 µM

2.2.2. Dissolved Oxygen

Dissolved oxygen was measured by classical Winkler method during SK91, SK103, SK121, SS136 and SS141 and by colorimetric technique (Pai *et al.*, 1993) during other cruises.

The titrimetric determination of oxygen concentration in sea water is based on the method first proposed by winkler and modified subsequently by Carpenter (1965). The principle of the method is that oxygen in sea water sample reacts with Mn (II), in a strongly alkaline medium, and oxidises it to Mn (IV). In the presence of excess iodide Mn (IV) liberates iodine on acidification. The amount of oxygen was computed from the amount of thiosulphate used for neutralizing the I_2 liberated.

The colorimetric determination of dissolved oxygen in sea water is found to be more precise (Pai *et al.*, 1993) particularly at lower levels. The technique has been calibrated using potassium iodate as the standard (Fig. 2.3). After the fixed sample is acidified, the amount of iodine liberated is measured through the absorbance at 456 nm. While the liberated iodine was titrated with thiosulphate in Winkler method it is directly measured in colorimetry. The advantage of colorimetry, therefore, lies in eliminating the loss of molecular iodine by forcing the sample by applying nitrogen gas pressure into a flow cell

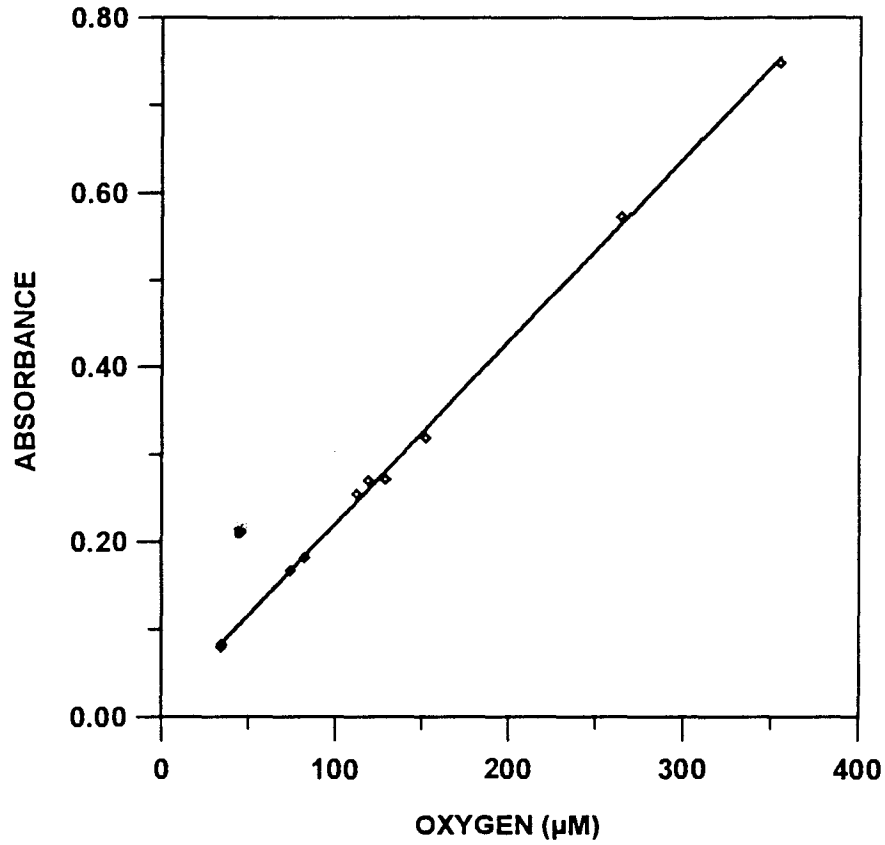

Fig. 2.3. Calibration of colorimetric technique of dissolved oxygen with potassium iodate. Oxygen is expressed in equivalents of iodate stardard.

(Fig. 2.4). Colorimetric method yielded a linear calibration curve for the oxygen range found in sea water. A comparison with the winkler titration showed that winkler method underestimates at high concentrations whereas the same overestimates under low oxygen conditions, due to loss of iodine during the transfer of solution and excess addition of thiosulphate at the endpoint, respectively (Figs. 2.5). Barring these minor differences the measured oxygen concentrations compared well between these two techniques.

2.2.3. Nutrients

2.2.3.1. *Nitrite, nitrate*

Nitrite, nitrate and silicate were measured using SKALAR (Model 5100-1) autoanalyser (Segmented Flow Analysis). Nitrite in the sample is allowed to react with an aromatic amine leading to the formation of a diazonium compound which on coupling with a secondary aromatic amine forms an azo-dye (Grasshoff *et al.*, 1983). The absorbance of the azodye is

measured. Nitrate in the sample was first reduced to nitrite in a reductor column filled with copper amalgamated cadmium granules. The conditions of the reduction column were adjusted such that the nitrate reduction was complete to nitrite and not reduced further. The principal reaction is

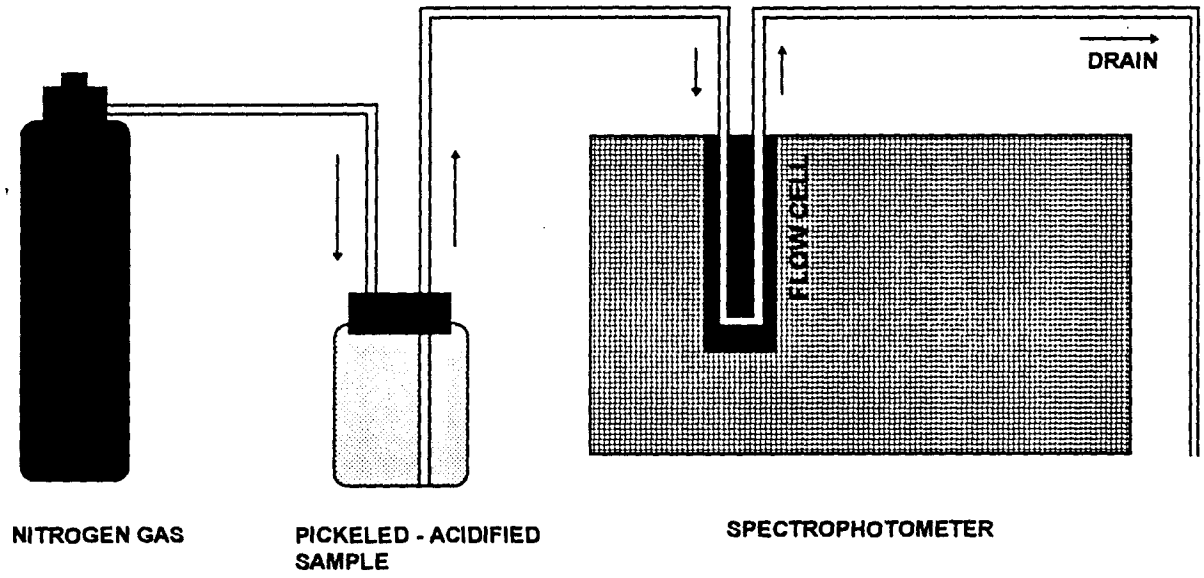

Fig. 2.4. Schematic diagram showing flow-injection system used in spectrophotometric dissolved oxygen measurements.

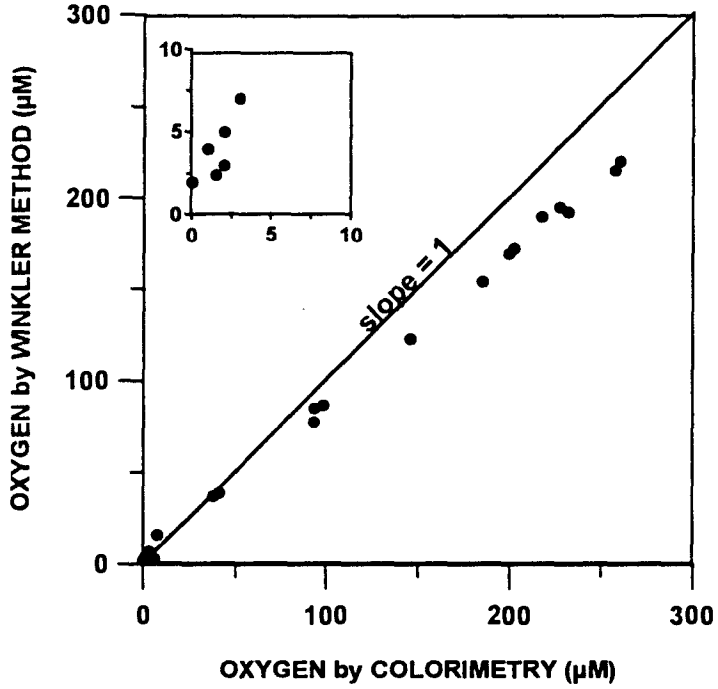

Fig. 2.5. Comparison of dissolved oxygen obtained using Winkler and spectrophotometric techniques. Inset shows comparison at low concentrations of oxygen.

$NO_3^- + Me_{(S)} + 2H^+ \Longrightarrow NO_2^- + Me^{++} + H_2O$

2.2.3.2. *Silicate*

The determination of dissolved silicon compounds in sea water is based on the formation of a yellow silicomolybdic acid when an acidified sample is treated with a molybdate solution. To this oxalic acid is added for two reasons: (1) to avoid reduction of the excess molybdate and (ii) to eliminate the interference of phosphate present in the sample. As the silicomolybdic acid has only a limited stability in the presence of oxalic acid, a reductant (ascorbic acid) is added immediately. The absorbance of the silicomolybdenum complex is measured using SKALAR autoanalyser.

2.2.3.3. *Phosphate*

Phosphate was measured following the method of Koroleff (1983). This method is based on the reaction of the phosphate ions with an acidified molybdate reagent to yield a phosphomolybdate complex, which is then reduced to a highly coloured blue compound by ascorbic acid. To suppress the interference from silicate, reaction pH is maintained to less than 1 and that the ratio of sulphuric acid to molybdate between 2 and 3. The absorbance of the blue complex was measured at 880 nm by JASCO spectrophotometer.

2.2.4. pH and Total Alkalinity

2.2.4.1. *pH*

The state of equilibria among different forms of inorganic carbon is dominantly controlled by the pH. Therefore, it is essential to measure the pH very precisely. The widely used potentiometric technique is prone for uncertainties such as liquid junction potential and stabilization of electrode. The multi-wavelength spectrophotometric techniques use acid-base indicators and are highly precise and sensitive (Byrne and Breland, 1989). Cresol red (a sulphonephthalein indicator) absorbance ratios provide the basis for spectrophotometric measurement of pH in sea water. The indicator occurs in protonated and unprotonated forms. The maximum absorption for these two forms occurs at 433 and 573 nm respectively.

The sea water sample, thermostated at 25±0.2°C in a water bath, was transferred to 10 cm long cylindrical quartz cuvette, with the least exposure to air and capped. Blank absorbances of this sample were measured at 730, 573 and 433 nm. Subsequently 50 μl of cresol red (2×10^{-3} M) was added to the sample in cuvette, dispersed well and measurements repeated. Absorbance measurements were made on a JASCO spectrophotometer (Model 7011). The absorbance at 730 nm wave length was to account for baseline drift, if any, between the

measurements. The ratio of cresol red indicator absorbances at 573 and 433 nm is used to calculate sea water pH using the following the equations:

$R = \lambda_{573} / \lambda_{433}$

$PH^{\circ}_{25} = 7.8164 + 0.004\ (35 - S) + \log\ ((R - 0.00286) / (2.7985 - 0.09025*R))$

where λ is the absorbance corrected for baseline drift and S is the salinity (Byrne and Breland, 1989). The pH thus obtained is on free ion scale.

2.2.4.2 *Total alkalinity*

Spectrophotometric procedure proposed by Breland and Bryne (1993) was used to determine total alkalinity of sea water. One-step volumetric acid addition followed by the spectrophotometric measurement of excess acid enabled precise estimation of total alkalinity. In the present case, excess acid was quantified using the sulphonephthalein indicator Bromocresolgreen (BCG). Measurement of bromocresolgreen absorbances at 444 and 616 nm at a temperature of t° C and a salinity of S yields molal scale total hydrogen ion concentrations ($[H^+]_T = [H^+] + [HSO_4^-] + [HF]$) according to

$pH_T = - \log [H^+]_T$

$$= \log_I B_{IT} + \log \{[R(25) - 0.00131] / [2.3148 - 0.1299\ R(25)]\}$$

where

$$R(25) = R_{(t)} [1 + 0.00907 (25 - t)$$

$$\log_I B_{IT} = 4.2699 + (2.578 \times 10^{-3}) (35\text{-}S) \text{ and}$$

$$R_{(t)} = (\lambda_{616} / \lambda_{444})$$

Using $[H^+]_T$ the TA of sea water is calculated from

$$(TA)_s V_s - M_a V_a = - [H^+]_T V_{sa}$$

where

$(TA)_s$ is total alkalinity of the sea water sample

M_a is the concentration of HCl added to the sample

V_a is volume of HCl added to sample

V_{sa} is total volume of sample and acid added

$[H^+]_T$ is the total excess hydrogen ion concentration in the sample after having been purged of CO_2 completely.

Required amounts of hydrochloric acid-BCG (0.1 N) mixture (ranging between 1.290 and 1.300 ml) measured using a high accuracy Radiometer Autoburette, were placed in dry 125 ml glass bottles. 50 ml of sea water sample was added to this mixture and purged with nitrogen gas for 10 minutes. Absorbances of original and treated samples were measured using a 10 cm long cylindrical quartz cell at 444, 616 and 750 nm on a JASCO spectrophotometer. Measurements at 750 nm were used to correct for the baseline drift, if any, between the measurements.

2.2.5. Total Carbon dioxide

We measured TCO_2 in sea water through coulometric titration. In coulometry the electrical current required to convert a particular chemical species to a different species is measured. The present coulometric titration involves electrolytic generation of a strong base to titrate the weak acid formed by the reaction between CO_2 and ethanolamine. Thus, CO_2 stripped from sea water is first quantitatively converted to hydroxyethylcarbamic acid which is then titrated by OH^- ions automatically generated through the reduction of H_2O at a platinum cathode. The equivalence point is detected photometrically with thymolphthalein as the acid-base indicator. The coulometric sequence includes neutralization, redox, and complexation reactions.

Neutralization:

$2CO_2 + 2NH_2(CH_2)_2OH \Longrightarrow 2HO(CH_2)_2NHCOOH$

ethanolamine hydroxyethylcarbamic acid

$2HO(CH_2)_2NHCOOH + 2OH^- \Longrightarrow 2HOH + 2HO(CH_2)_2NHCOO^-$

Oxidation - reduction:

$2Ag^\circ(s) \Longrightarrow 2Ag^+ + 2e^-$ Silver electrode (anode)

$2HOH + 2e^- \Longrightarrow H_2 + 2OH^-$ Platinum electrode (cathode)

Complexation:

$2Ag^+ + 4I^-$ (saturated KI) $\Longrightarrow 2AgI^{2-}$ (anode)

Net reaction:

$Ag^\circ(s) + 2I^- + CO_2 + NH_2(CH_2)_2OH \Longrightarrow AgI_2^- + 0.5H_2 + HO(CH_2)_2NHCOO^-$

To be quantitative, the reduction of H_2O must occur without the involvement of any other chemical species and each faraday of electrical current must bring about a chemical change corresponding to one equivalent of the analyte. If

true, 100% current efficiency is maintained even when the neutralization reaction is secondary to the electrode reaction, i.e., CO_2 is not required to directly participate in the electron transfer process at the electrode. The cell solution (supplied by the manufacturers, UIC Inc., U.S.A.) is originally blue since it contains thymolphthalein (blue at pH 10.5 and colourless at pH 9.3). The CO_2 stripped from sea water forms hydroxyethylcarbamic acid in the cell and reduces pH thereby increasing the transmittance (%T). This in turn triggers the redox reactions by generating current at a low (1-5mA) or high (50-100 mA) level depending on the magnitude of change in %T. The generated current is measured in coulombs that actually is displayed in µg C through a built-in conversion mechanism.

A semi-automated sampling system was developed to eliminate atmospheric carbon dioxide contamination during the sub-sampling and stripping for measurement. (Fig. 2.6). This involves drawing a specific aliquot of sub-sample followed by acidification with ortho-phosphoric acid and purging the sample by CO_2 free air. The titration of the liberated CO_2 was performed in coulometric cell. Air was used as a carrier gas that was passed through potassium hydroxide scrubber, followed by drierite and ascarite to remove CO_2 and moisture, respectively, from the carrier gas. A comparison made between CO_2 free air and nitrogen as carrier gases did not reveal any significant differences in the results and hence the former was preferred. However, extreme care was

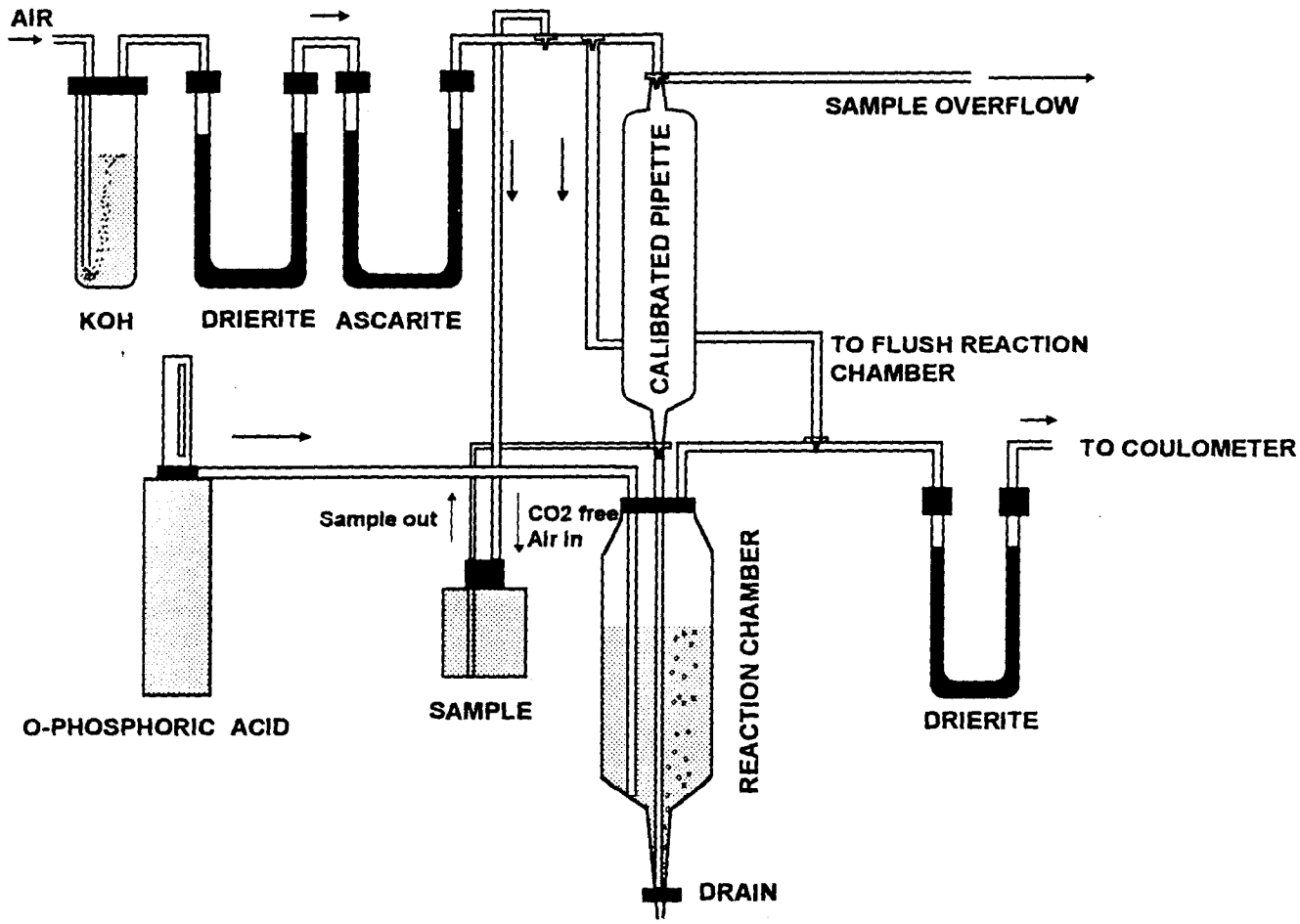

Fig. 2.6. Schematic diagram showing semi-automated system used in Coulometric total carbon dioxide analysis.

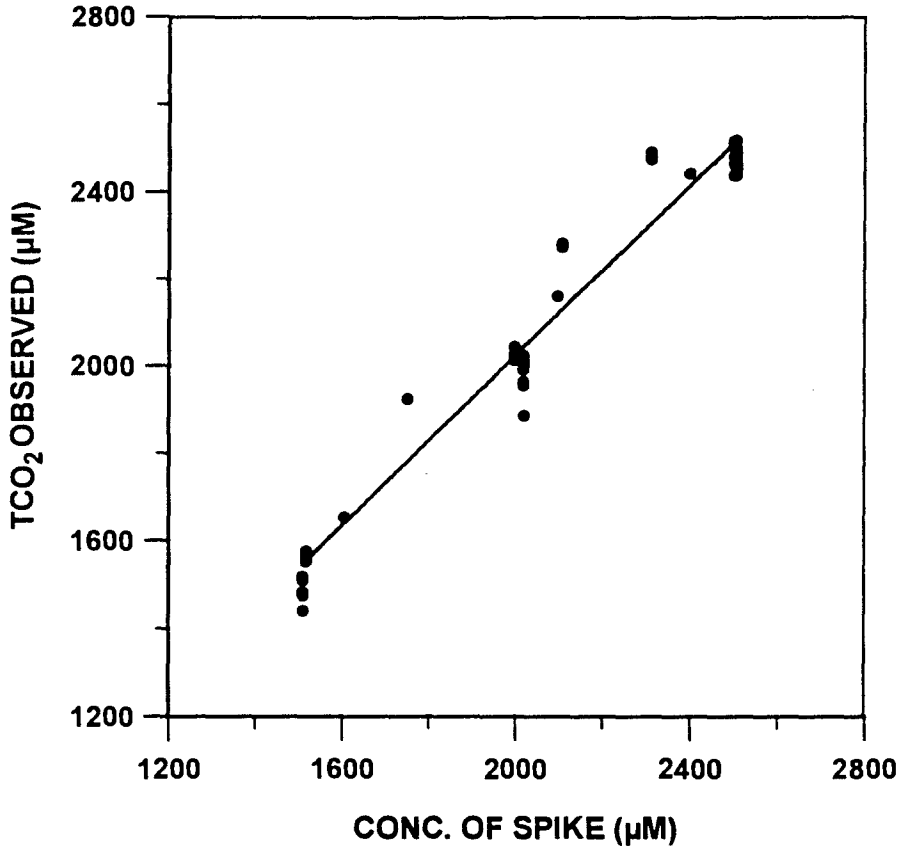

Fig. 2.7. Calibration curve using sodium carbonate standards for coulometric TCO_2.

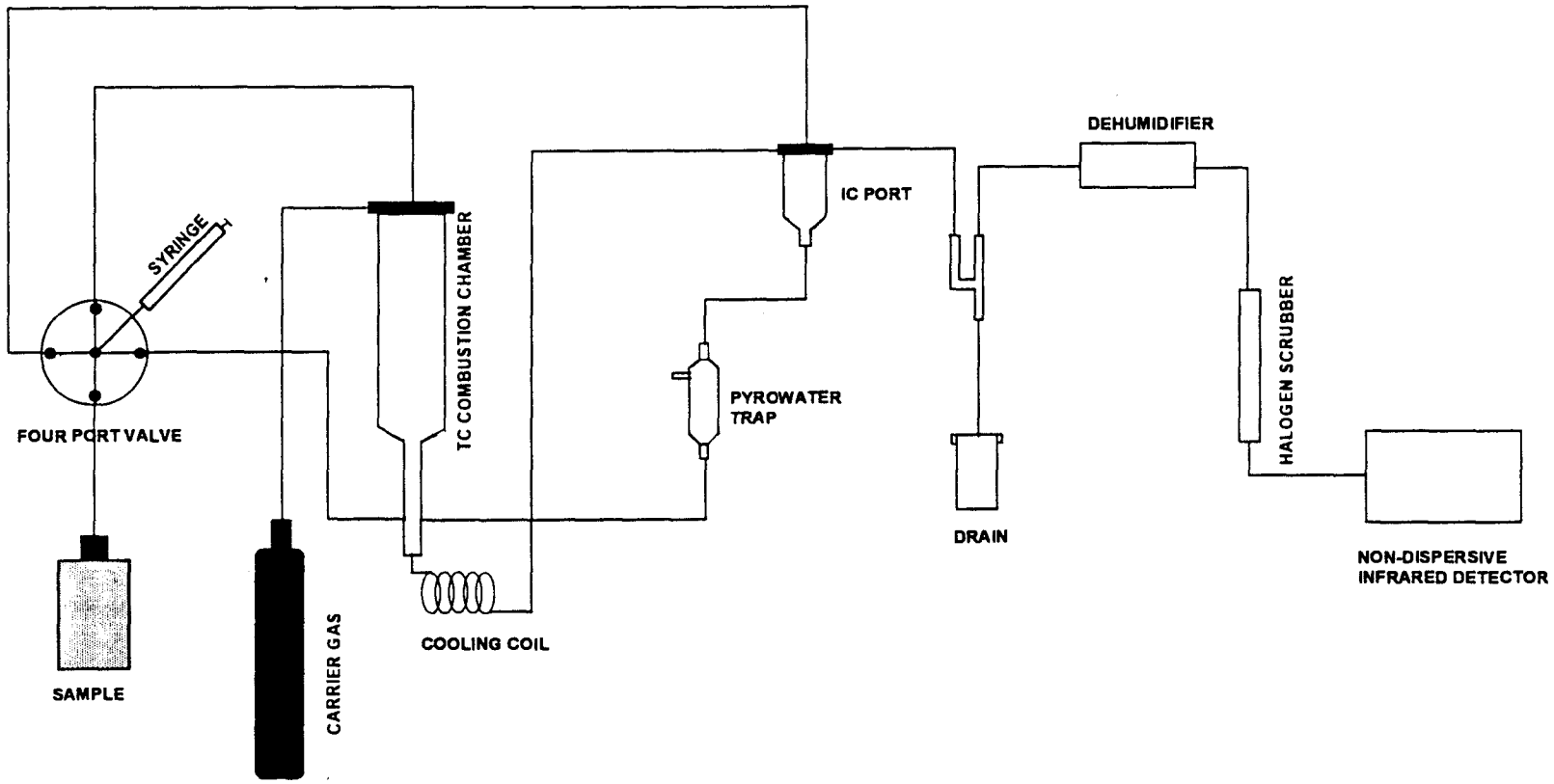

Fig. 2.8. Schematic diagram of Shimadzu TOC-5000 analyzer used in the determination of Dissolved Organic Carbon in seawater.

This zero water was used for the preparation of standards. Ultrapure blank check, a built-in programme, was run to find out the blank. This was carried out by injecting the ultrapure water a couple of times into the catalytic chamber and collecting the condensed water into a reservoir from where it was re-injected into the catalyst as a fresh sample. This cycle comprised 10 injections. The mean peak area of the last cycle was considered as the instrument blank which were 500-600 counts. This nearly equals 10-15 μM and was subtracted from samples. The instrument was calibrated against potassium hydrogen phthalate as the standard (Fig. 2.9).

Samples were collected in 30 ml polypropylene bottles. Before the cruise, these bottles were washed, soaked in 20% ortho-phosphoric acid for 24 hours and thoroughly rinsed with double distilled water. Samples were preserved with 1 ml of 85% o-phosphoric acid and stored in a refrigerator until analysis in the shore laboratory. Each sample was injected 4 to 6 times until the coefficient of variation obtained was less than 1%. The mean value of these injections was considered.

2.2.7. Transparent Exopolymer Particles

Water samples were collected in 125 ml glass bottles. Well shaken water samples were passed through polycarbonate (Nuclepore; 0.4 μm pore size) or

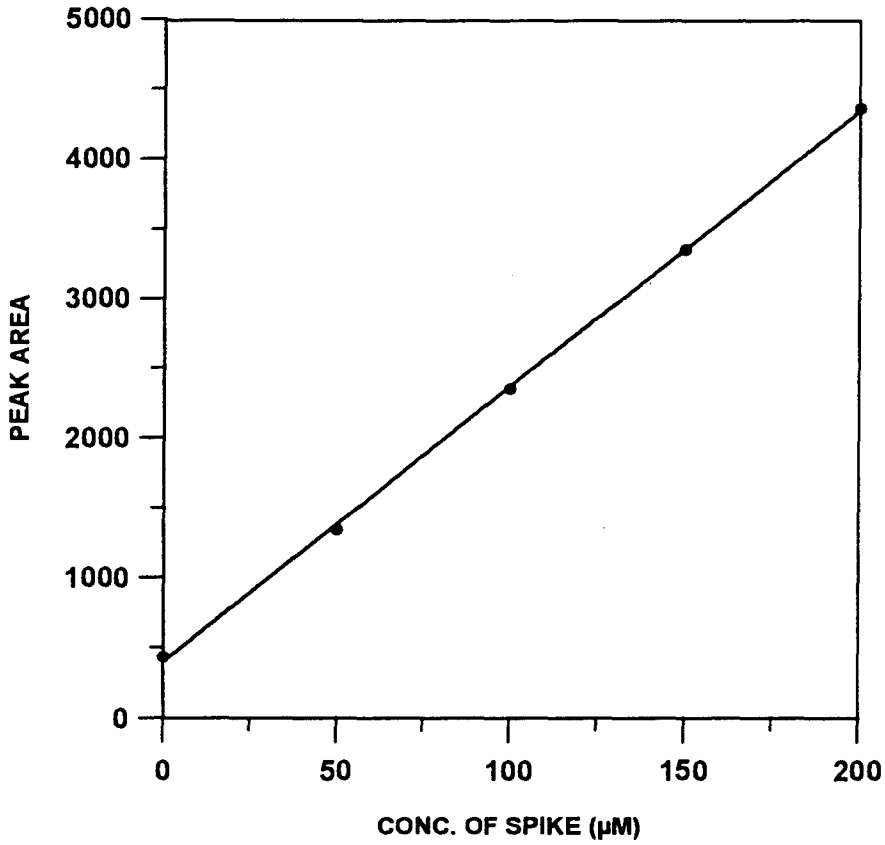

Fig. 2.9. Calibration of DOC made using potassium hydrogen pthalate as standard in ultrapure distilled water.

Durapore (0.45 μm) filters within a few hours of collection. Durapore filters have been found not to interfere with the colorimetric analysis, similar to Nuclepore filters. The concentration of TEP, expressed in terms of alginic acid (AA) was estimated using the alcian blue colorimetric method (Passow and Alldredge, 1995) with minor modifications. We found that although the TEP (in samples) dissolved in 80% sulphuric acid showed maximum absorbance at 787 nm, the alginic acid in the same acid medium exhibited inverse relation between its abundance and absorbance and that AA standard yielded a better (positive) linear relation at 745nm (Table 2.3). Nevertheless, TEP spectra revealed proportional changes in absorbencies at the wavelengths, 745 and 787 nm. Consequently, the TEP was measured at 745 nm since its abundance is represented in terms of AA. The Arabian Sea samples were analysed mostly in single, but in duplicates wherever possible, whereas the Bay of Bengal samples were done in quadruplicates.

Table 2.3: Absorbances of Alginic acid measured at wavelenghs 787 and 745nm.

Alginic Acid mg/l	Absorbance at 787 nm	Absorbance at 745 nm
0	1.261	1.104
10	1.227	1.131
20	1.178	1.142
30	1.140	1.162
40	1.106	1.185
50	1.046	1.198

2.2.8. pCO_2 underway measurements

Carbon dioxide partial pressures in air and water were determined using an underway pCO_2 measurement system during SK115. The mole fractions of CO_2 (xCO_2) in sea water equilibrated air and in atmosphere were continuously measured with an infrared detector. This automated underway CO_2 monitoring system consisted of a "shower-head" equilibrator and a non-dispersive infrared (NDIR) CO_2 and H_2O analyser (Li-COR 6262) with a solid state detector (Fig. 2.10). A system consisting of automated valves controls the frequent and regular switching of gas flows to the NDIR analyzer between sea water equilibrated air (SEA), marine air sampled from the bridge of the ship (AIR), and two gas standards (CO_2 concentrations of 412 and 325 μM/M, respectively).

The air intake system consisted of an inverted polyethylene funnel mounted at the top of the bridge of the ship using 3/8" inner diameter Dekoron line. Sea surface air was pumped by an Air Cadet pump at a rate of several litres per minute. After the pump line was split, part of the air supply went to the instrument. The remaining portion of the air (>500 ml/min) was used to flush a "ballast" chamber which was vented to ambient atmosphere. This ballast chamber was then used to maintain ambient pressure in the equilibrator headspace. When analysing marine air, a flowrate of 200 ml/min was

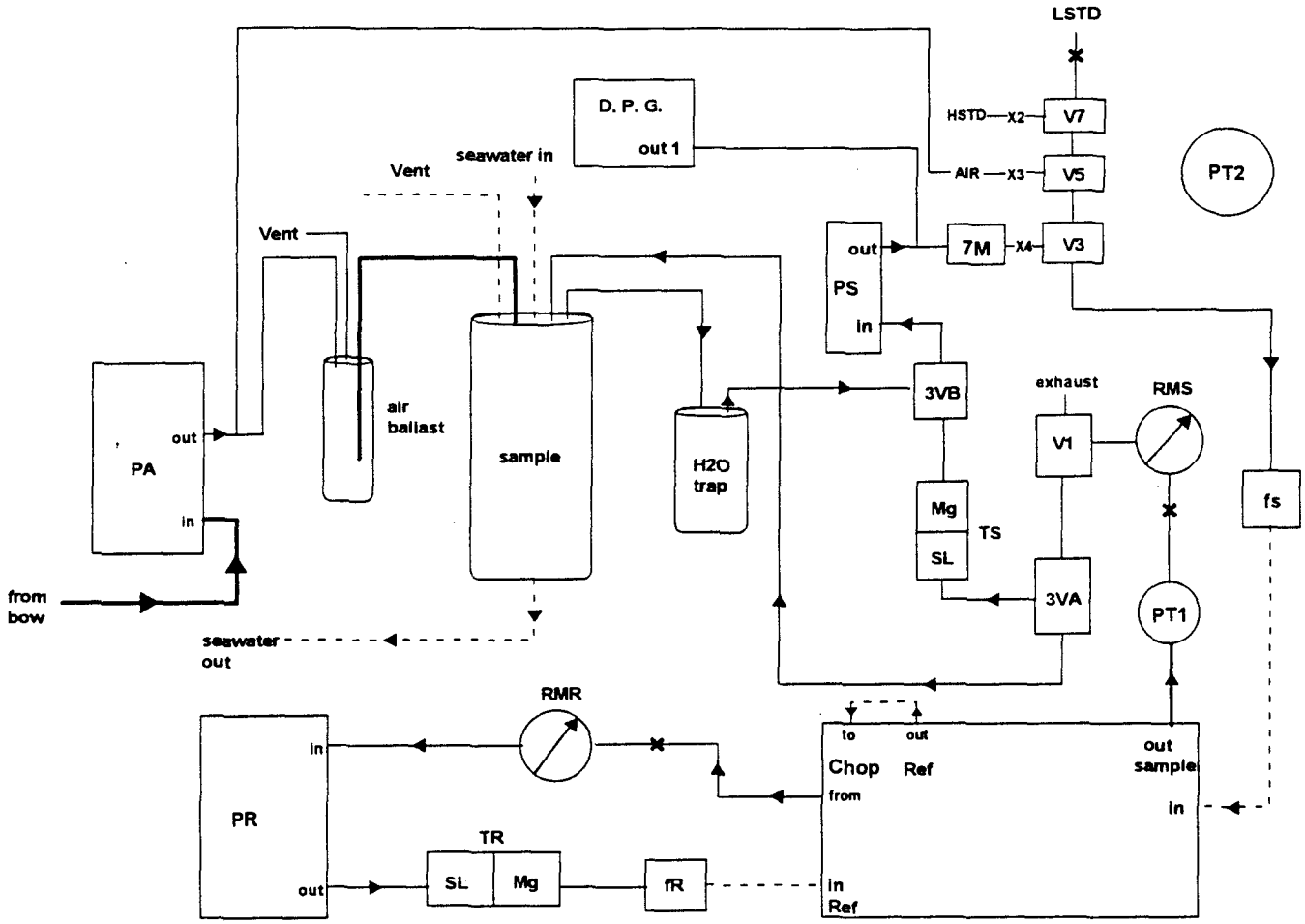

fR,fS=1.0μ filters; V1,V2,V3=3 way valves; PT1, PT2=Pressure Transducer; RMR, RMS= rotometer, TR, TS=sodalime and Mg perchlorite traps; PA= pump, air; PR=pump reference; PS=pump, sample; 3VA,3VB=3 way valves, X1-4=regulating valves; D.P.G.=Dew Point Generator, 7M=7μ filter

Fig. 2.10. Schematic diagram of infra-red analyzer based underway measurement system for the determination of pCO_2 in surface seawater.

maintained through the NDIR. Once in every 2 h the alternation of the two sample gases was interrupted for the measurement of the two reference gases according to 10 min cycle.

The small size (approximately 40 cm high) equilibrator consists of two concentric cylinders (stages) made of plexiglass, with a drain in the centre (Fig. 2.10). The sea water "showers" from the top of the equilibrator at a rate of 4 l/min, and the first stage of the equilibrator is vented to the clean marine air to maintain ambient atmospheric pressure. The gas phase is continuously re-circulated at a rate of 200 ml min^{-1} by an air pump, through a closed loop that passes through the infrared analyzer. The sea water temperature in the equilibrator together with both atmospheric pressure and the gas pressure in the closed loop is continuously monitored. The sea water temperature sensor in the equilibrator has been calibrated against a platinum resistance thermometer.

The CO_2/H_2O differential NDIR analyzer is of small size, precise and insensitive to vibrations and lateral accelerations. The Li-Cor CO_2/H_2O analyzer uses an internal algorithm to correct wet measurements to dry gas scale at one atmosphere pressure. Thus, this automated system allows direct monitoring of xCO_2 (mole fraction of CO_2 gas corrected to dry air at a pressure of 1 atm) in the gas phase without having to pretreat it (no drying nor gas

separation are required). This not only simplifies the analytical procedure, but also minimizes the potential errors in the measurements.

During SK 115 and SK 116 cruises the system was regularly calibrated once every 2 h, using the secondary CO_2 standard gases that were calibrated using primary standards. The 2 h calibration indicated that the infrared analyzer had been remarkably stable. The computer recorded one xCO_2 datum per minute which was an average of 10 readings taken every 6 s. A typical duty cycle consisted of a 5-min cell flush, followed by five 1-min averages. The same cycle was then repeated for the measurement of air.

The pCO_2 was computed from the measured xCO_2 using the relationship (UNESCO, 1987):

$$pCO_2 = xCO_2 \times \text{pressure} \times [1-(\text{vapour}/\text{pressure})]$$

where

$$\text{vapour} = 0.981 \times \exp(27.029 - 0.098T - 6163/T)$$

Here, "pressure" represents the ambient atmospheric pressure, "vapour" represents the saturation water vapour pressure at the air-sea interface, and T (°K) is the surface temperature in the equilibrator.

2.3. Methodology - Computations

2.3.1. Oxygen Utilization and Nitrate Deficits

2.3.1.1 *Apparent Oxygen utilization (AOU)*

Apparent Oxygen Utilization (AOU) is the amount of oxygen utilized during biological respiration. This is calculated by the difference between expected oxygen solubility (a function of temperature and salinity) and observed oxygen concentration, i.e.,

$$AOU = O_{2\,(exp)} - O_{2\,(obs)}$$

The oxygen solubility was evaluated according to Benson and Krause (1984):

$$O_{2\,(exp)} = e^{M}$$

where

$$M = -135.9025+1.575701\times10^{5}/T - 6.642308 \times 10^{7}/T^{2} + 1.243800 \times 10^{10} \times T^{3} - 8.621949 \times 10^{11} \times T^{4} - S\,(0.017674-10.754/T + 2140.7/T^{2})$$

2.3.1.2 *Nitrate deficit (δN)*

Nitrate deficit indicates the extent of nitrate lost as a result of denitrification occurring under suboxic conditions in water. It is obtained as the difference between the nitrate concentration expected in the absence of denitrification and the sum of observed nitrate and nitrite concentrations.

$$\delta N = NO^-_{3\,(exp)} - (NO^-_{3\,(obs)} + NO^-_{2\,(obs)})$$

Naqvi and Sen Gupta (1985) have proposed the use of NO, a derived semi-conservative property, to compute nitrate deficits. Broecker (1974b) originally proposed NO as the following

$$NO = 9.1\,(NO^-_3+NO^-_2)_{obs} + O_{2\,(obs)}$$

This approach is based on the assumption that NO behaves conservatively outside the denitrification zone and should therefore exhibit linear relationship with potential temperature, in accordance to the linear salinity-potential temperature relation. Naqvi *et al.* (1990) proposed the following set of revised equations to compute the nitrate deficit:

$$NO = 415.934 - 8.974\,\theta \qquad 10.39 \geq \theta \leq 27^\circ\,C$$

$NO = 490.254 - 16.126$ $\theta \leq 10.39°$ C

$\delta N = (NO - O_2)/9.1 - NO^-_3 - NO^-_2$

Here θ refers to potential temperature (°C) and 9.1 is derived from Redfield ratios of oxygen and nitrate.

2.3.2. Carbon components

Appropriate equilibrium constants are a prerequisite in the quantitative evaluation of the carbon dioxide components. Use of these constants along with any two of the measured variables among pH, alkalinity, pCO_2 and total carbon dioxide (TCO_2) enables the quantification of all the CO_2 species. The relevant procedures and equations used in the present study are summarized below.

2.3.2.1. *pH conversion from free ion scale to Total scale*

Spectrophotometric pH method yielded hydrogen ion concentration on the free ion scale at 25° C and atmospheric pressure ($pH°_{25}$). We first converted this $pH°_{25}$ to pH in $_{situ.}$, according to Millero (1979). pH as a function of temperature,

pressure and salinity was computed using the constants given by Hansson (1973) and Mehrbach *et al.* (1973).

$$pH^{\circ}_{t} = pH^{\circ}_{25} + A\,(t-25) + B\,(t-25)^{2}$$

Here t refers to the temperature of the sample, in situ, and

$$10^{3}\,A = -9.702 - 2.378\,(pH_{25} - 8) + 2.885\,(pH_{25} - 8)^{2}$$

$$10^{4}\,B = 1.123 - 0.003\,(pH_{25} - 8) + 0.933\,(pH_{25} - 8)^{2}$$

pH°_{25} was obtained from the spectrophotometric measurements at 25° C (please see section 2.2.4.1.). These equations are valid for ranges in t of 0 - 40° C, salinity of 30 - 40 psu and pH°_{25} of 7.6 - 8.2 (Millero, 1979).

The effect of pressure in the ocean on pH_{t}° was estimated using

$$pH^{p}_{\text{in situ}} = pH_{t}^{\circ} + AP$$

The slope A is a function of temperature and salinity

$$-10^{3}A = 0.424 - 0.0048\,(S-35) - 0.00282t - 0.0816\,(pH^{\circ}_{t} - 8)$$

and is valid for salinity range of 32 - 38 psu and t of 0 - 25° C. P is the pressure, in situ, in decibars.

Hydrogen ion concentration on total scale is ($[H]_f$ = free proton)

$$[H^+]_T = [H]_f + [HSO^-_4] + [HF]$$

Bisulphate ion effect was computed using the formulations given by Hansson (1973) for the conversion of $pH_{in\ situ}$ to pH_T since the effect of fluoride ion will be insignificant (Dickson, 1993).

The equilibrium constant for bisulphate/sulphate is

$$\text{Log } K_{HSO_4^-/SO_4} = 747.39/T - 7.1833 + 0.020234.T - 9.94466 \times 10^{-3}.S + 3.9813.10^{-5}\ S^2$$

this equation is valid for a salinity range of 20 - 45 psu (Hansson, 1973)

Total sulphate (SO_{4t}) was calculated from the salinity of the sample based on the 'constancy of ionic composition in sea water' principle.

$$SO_{4(t)} = 0.02823 \times S/35$$

$pH_T = pH_{in\ situ} - \ln (SO_{4(t)})$

$\ln (sulf) = \text{Log} (1+K_{HSO4^-/SO4} * SO_{4(t)})$

The effect of pressure on above equations were computed from

$\Delta 10^3 V = -18.03+0.0468*t+0.316/t^2$

$\Delta 10^3 K = -45.3+9 * 10^{-2} * t$

2.3.2.2. *Carbonic acid constants*:

The apparent dissociation constants of carbonic acid (K_1, K_2), determined by Goyet and Poisson (1989) at atmospheric pressure and on Total pH scale, were used in the present study. These are

$pK_1^* = 812.27/T + 3.356 - 0.00171 \times S \times \ln (T) + 0.000091 \times S^2$

$pK_2^* = 1450.87/T + 4.604-0.00385 \times S \times \ln (T) + 0.000182 \times S^2$

where the constants K_1^* and K_2^* are expressed in moles kg^{-1} of solution

The effect of pressure on the apparent ionization constants of acid in sea water were done according to Culberson and Pytkowicz (1968):

$$\ln (K_1^*{}_p/K_i^{*0}) = -(\Delta V_i/RT)\, P + (0.5\Delta K_i/RT)P^2$$

where ΔV_i and ΔK_i are the volume and compressibility change for the ionization.

The values of ΔV_i and ΔK_i have been fit to equation of the form

$$-\Delta V_i = a_o + a_1 (S - 34.8) + a_2 t$$

$$-10\, \Delta K_i = b_o + b_1 (S - 34.8) + b_2 t$$

Coefficients in these equations are

a_o=25.50: a_1=0.151; a_2=-0.1271;

b_o=3.08; b_1=0.578; b_2= -0.0877

Using the evaluated pH_T, acidity constants and TCO_2 (or TA in some cases) the CO_2 components, particularly pCO_2, HCO^-_3, and CO^{2-}_3 were computed.

2.3.3. Solubility of carbon dioxide

The equation given by Weiss (1970) is used for calculating the carbon dioxide

solubility in sea water.

$$\ln K^\circ = A_1 + A_2 (100/T) + A_3 \ln (T/100) + S [B_1 + B_2 (T/100) + B_3 (T/100)^2]$$

where

$A_1 = 60.2409$; $A_2 = 93.4517$; $A_3 = 23.3585$;

$B_1 = 0.023517$; $B_2 = 0.023656$ and $B_3 = 0.0047036$

where K° is expressed in moles dm^{-3} at T of °K.

2.3.4. Carbonate saturation

The thermodynamic solubility products of aragonite and calcite were found from the equations given by Mucci (1983):

$$\text{Log } (K^\circ_{sp} \text{ (arag)}/ K^\circ_{sp} \text{ (calc)}) = 0.0385 + 63.974/T$$

and

$$\text{Log } K^\circ_{sp}\text{(arag)} = -171.945 - 0.077993T + 2903.293/T + 71.595 \log T$$

T is in K.

The following equation was used to find the temperature and salinity dependence of stoichiometric solubility constants of calcite and aragonite in sea water.

$$\text{Log } K^{*}_{sp(i)} - \text{log } K^{\circ}_{sp\,(i)} = (b_o + b_1 T + b_2/T)S^{0.5} + C_o S + d_o S^{1.5}$$

along with the following constants:

solid	b_o	$b_1.10^3$	b_2	C_o	$d_o.10^3$	σ
calcite	-0.77712	2.8426	178.34	-0.07711	4.1249	0.010
aragonite	-0.068393	1.7276	88.135	-0.10018	5.9415	0.009

The pressure dependence of the solubility product was estimated by the following formula (Millero, 1979).

$$\ln (K^{*P}_{sp(i)} / K^{*\circ}_{sp(i)}) = -(\Delta V_i/RT)P + (0.5\Delta K_i/RT)P^2$$

2.3.5. Air-Sea fluxes

The net flux of CO_2 across the air-sea interface was calculated from:

$$Flux = K \alpha (P_{atm} - P_s)$$

where K is the transfer velocity (cm h^{-1}) α is the CO_2 solubility at the temperature and salinity at the surface, P_{atm} is the partial pressure of CO_2 in atmosphere (µatm) and P_s that in surface sea water (µatm).

The transfer velocity of a gas is a function of wind speed and temperature (Liss and Merlivat, 1986; Tans *et al.*, 1990; Wanninkhof, 1992). The formulations of Wanninkhof (1992) was used for transfer velocity computations. Wanninkhof (1992) derived a quadratic relation between wind speed and the transfer velocity, where a proportionality factor of 0.36 was found for discretely measured wind speeds (u)

$$K = 0.36 (u^2) (Sc/660)^{-0.5} \quad \text{(discrete winds)}$$

The Schmidt number (Sc) is defined as the kinematic viscosity of water divided by diffusion coefficient of the gas; it was computed using the following equation (Wanninkhof, 1992)

$$Sc = A - Bt + Ct^2 - Dt^3$$

Coefficients A to D are:

A=2073.1 B=125.62 C=3.6276 D=0.043219 t= temperature (°C)

2.3.6. Quantification of regenerated carbon

2.3.6.1. *Based on Redfield Ratio*

The regenerated carbon dioxide can be computed using the C/O_2 ratio. Based on these ratios regenerated carbon can be computed using the formulation

$Reg.CO_2$ = (AOU * C/O ratio)

These ratios for the study area were evaluated on a seasonal basis and were found to be:

NE monsoon	+1.025
Inter monsoon	+1.366
SW monsoon 95	+1.233
SW monsoon 96	+1.207

2.3.6.2. *Based on Kroopnick's formulations*

The carbon dioxide regenerated from the soft tissue and hard parts was

evaluated following the generalizations made for global oceans by Kroopnick (1985):

$TCO_{2\,(n)} = (TCO_2 * 35.000)/S$

$TCO_{2\,(pre)(n)} = 2233\text{-}10.36*\theta$

$TCO_{2\,(reg)} = TCO_{2\,(n)} - TCO_{2\,(pre)(n)}$

where suffixes 'n', 'pre' and 'reg' indicate normalized, predicted and regenerated carbon dioxide, respectively. θ is the potential temperature (°C) and S is salinity (psu).

Chapter 3

HYDROGRAPHIC FEATURES

3.1. Introduction

The Indian Ocean in the north comprises of the Arabian Sea, the Bay of Bengal, the Andaman Sea and the Laccadive Sea in addition to the adjoining Persian Gulf and Red Sea. Although, the geographical setting is somewhat similar the hydrographical and hydrochemical characteristics widely differ between the first two regions (see 1.3 and 1.4).

The Arabian Sea receives very little river runoff as most of the Indian rivers discharge into the Bay of Bengal (Subramanian, 1993). In the Arabian Sea evaporation far exceeds precipitation and runoff, except off the west coast of India where annual precipitation slightly in excess of evaporation (<20 cm) (Venkateswaran, 1956). The domination of evaporation over the precipitation is maximal (100-150 cm y^{-1}) off the Arabia coast that decreases steadily towards Southeast. The excessive evaporation results in high surface salinities in the Arabian Sea. The two marginal seas, viz. the Red Sea and the Persian Gulf, lying in arid zones experience still more intense evaporation. Surface salinities in these regions are among the highest in the oceans. This, together with winter cooling in the north, leads to the formation of high-density water masses which sink and renew deep-waters in the Red Sea and Persian Gulf (Dietrich, 1973). These deep high-salinity waters flow at subsurface levels into the Arabian Sea through the Gulfs of Oman and Aden. In order to balance the

outflow as well as the excess evaporation, there is an inflow of Arabian Sea surface waters into the Red Sea and the Persian Gulf (Grasshoff, 1969, 1975; Morcos, 1970; Hartmann *et al.*, 1971).

Wyrtki (1971) has extensively dealt with physico-chemical characteristics of the Arabian Sea and identified the major watermasses and their density (sigma theta (σ_θ)) surfaces. Table 3.1 summarises various water masses (Kumar and Li, 1996) in the Arabian Sea along with their physico-chemical characteristics and approximate depths of occurrence. Among these, the shallow salinity maximum water (SSMW, σ_θ=25.0) could be traced throughout the Arabian Sea but the Persian Gulf Water (PGW) flows mostly in the southeast direction east of 63° E (Ramesh Babu *et al.*, 1980). However, the PGW effect could be found even in the central Arabian Sea (Wyrtki, 1971). Wyrtki (1971) also noticed that spreading of Red Sea Water (RSW) is mostly southward while Ramesh Babu *et al.* (1980) could not find it north of 17° N. The SSMW is formed due to mixing between Southern Subtropical water and the Arabian Sea High Salinity Water (Wyrtki, 1971). Other important watermasses reported to occur in the Arabian Sea (Kumar and Li, 1996) are waters originating in the Central Indian Ocean and from the western Pacific Ocean (Indonesian Throughflow Water). The Bay of Bengal Low Salinity water (BBLS) flows, predominantly, along the southwest coast of India in winter (Shetye, 1993.). Kolla *et al.* (1976) and Warren (1978) found the entry of Antarctic Bottom Water (AABW), having a potential

Table 2.4. Watermasses in the Arabian Sea and their physico chemical properties.

Water mass	Depth (m)	Potential temp. (°C)	Salinity (psu)	Density (°θ)	Dissolved Oxygen (μM)	TCO_2 (μM)	Total Alkalinity (μM)
AABW	4709	-0.615	34.659	27.888	246	2245	2354
MNADW	2055	1.769	34.77	27.838	206	2237	2348
CIWW	1383	3.811	34.743	27.638	124	2296	2374
ITWW	723	7.415	34.763	27.215	124	2238	2333
PGW	233	22	36.5	26.880	200	2150	2400
AAIWW	4	6.492	33.726	26.525	305	2093	2269
IW	17	29.13	34.188	21.423	212	1889	2247
BBLS	9	28.107	33.25	21.097	209	1872	2217
RSW	759	11.06	35.699	27.309	15	2281	2360
ASHSW	5	28.897	36.754	24.082	195	2034	2386

temperature (θ) of 1.2° C near 10° N, into the Arabian Basin through the Somali Basin Besides the presence of the above water masses, Somasundar *et al.* (1987) observed the occurrence of 22° and 9° discontinuities in the Arabian Sea. These two discontinuities have been proposed to originate from mixing between SSMW and PGW, and RSW and North Indian Bottom Water, respectively.

In addition to several watermasses present in the Arabian Sea at different depth horizons the mechanisms of mixing vary with seasonal changes in wind regimes. The dominants of these are upwelling (Shetye *et al.*, 1990) and divergence (Muraleedharan and Prasanna Kumar, 1996) the Southwest monsoon and convective mixing during winter monsoon (Banse, 1984). As these processes influence the productivity pattern and hence have a control over the carbon cycle it is necessary/important to understand the detailed hydrography of the study area. This CHAPTER presents the detailed distributions of physical (temperature, salinity and wind speed) and chemical (oxygen and nitrate) properties in order to find the prevalent mixing processes in different seasons and their influence on biological productivity in order to understand carbon exchanges in the Arabian Sea.

3.2. Northeast monsoon

During the northeast (NE) monsoon period, the circulation in the Arabian Sea is

not very different from that in the northern Pacific and Atlantic Oceans. North of the equator, the flow is from east to west in the form of the NE monsoon current. Beginning in November this flow becomes the most intense in February and subsides by April (Wyrtki, 1973). A branch of the NE monsoon current turns north and flows along the west coast of India during November to January, bringing low salinity surface waters from the Bay of Bengal. The other branch turns south off Somalia, crosses the equator and merges with the South Equatorial Current. An equatorial counter current and an undercurrent are also found (Wyrtki, 1973). Surface circulation in the Arabian Sea is generally anticlockwise during this period.

The observed winds were predominantly north/north-easterlies during this season. Along the shelf, the observed wind speed varies between 4 and 10 m s^{-1}, except at 18° N where it is about 12 m s^{-1}. Along the northern shelf, the wind speeds are between 8 and 10 m s^{-1} decreasing to 4 to 6 m s^{-1} towards south. In the open ocean, along 64° E, the wind speed shows a gradual increase from about 2 m s^{-1} to 5 m s^{-1} towards the south and comparatively high wind speeds are observed north of 18° N reaching upto 8 m s^{-1}.

Latitudinal variations in wind speed, air temperature, sea surface temperature (SST) and mixed layer depth (MLD) shown in Fig. 3.1 to highlight the conditions in the top layer of the central Arabian Sea during winter, inter-

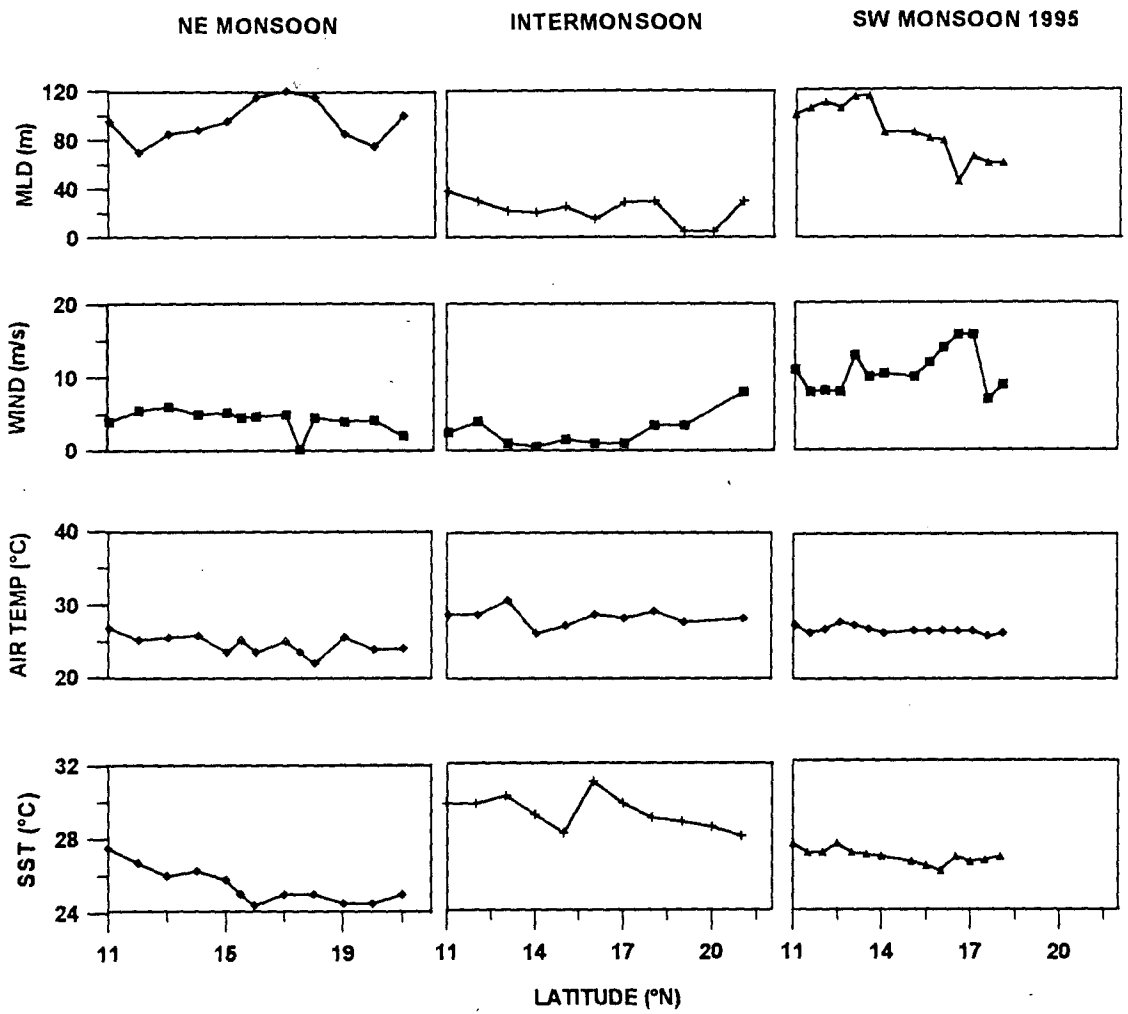

Fig. 3.1. Distribution of sea surface temperature (SST), air temperature, wind speed, mixed layer depth (MLD) during different seasons along 64° E.

monsoon and SW monsoon seasons. The air temperature increased from 22° C in the north to more than 26° C in the south. The SST rose about 3° C from north (25° C) to south (28° C). The MLD was generally deep (80 m) in the north with the deepest value of 120 m at 17° N. South of this latitude the MLD shoaled steadily to 65 m. Low air temperatures facilitated increased evaporation in the northern Arabian Sea wherein the latter results in convective mixing (Prasanna Kumar and Prasad, 1996; Madhupratap *et al.*, 1996). Below 500 m, there found to be no appreciable north-south gradients in temperature and salinity. Salinity structure showed the presence of ASHSW with >36.4 psu in the northern region, the core of which deepened towards south (Prasanna Kumar and Prasad, 1996). The surface salinity decreased from 36.4 psu in the north to less than 35.7 psu at 11° N. This low salinity water is representative of the North Equatorial Current (NEC) that carries waters from the Bay of Bengal as well as the eastern Indian Ocean into the western Arabian Sea.

Under the influence of north/north-easterly winds the possibility of upwelling along the eastern Arabian Sea in winter can be expected. However, the winds are too weak to induce any appreciable offshore Ekman transport (Madhupratap *et al.*, 1996). The specific humidity during this season was lower by 9 g kg^{-1} than in other seasons pointing to the prevailing dry air. The cool dry continental air over the northern Arabian Sea enhances evaporation leading to surface cooling. It is computed that the surface waters were cooled by 3° C

during this season (Prasanna Kumar and Prasad, 1996). Apart from the cooling due to evaporation, the decrease in solar insolation by 60 $W.m^{-2}$ results in a further cooling of surface waters. Thus, the reduced SST and deepened MLD in the northern Arabian Sea during winter result from a combination of enhanced evaporation and reduced solar insolation. Consequently, the Arabian Sea surface waters, north of 15° N, experience cooling and densification. This leads to sinking of surface water that sets in convective mixing which brings about injection of nutrients into the surface layers from the upper thermocline region.

The oxygen distribution in the subsurface waters showed lowest oxygen concentrations (below detection limits) in the northern parts. It actually reached near-zero levels during this season (Fig. 3.2). This could be due to enhanced productivity driven by winter convection. Nitrate was about 2 µM in surface waters of the northern latitudes in NE monsoon (Fig. 3.3). However, it was less than 1 µM in the south. This clearly suggests the influence of convection in making nutrients available to plankton in surface layers in the North. These data are consistent with the concurrent primary productivity measurements (Madhupratap *et al.*, 1996; Bhattathiri *et al.*, 1996). They observed a productivity of 643 mgC m^{-2} d^{-1} in the northern Arabian Sea during NE monsoon whereas it was 1097 mgC m^{-2} d^{-1} in SW monsoon 1996. Surprisingly, though the mixed layer is enriched with nutrients the winter productivity remained less

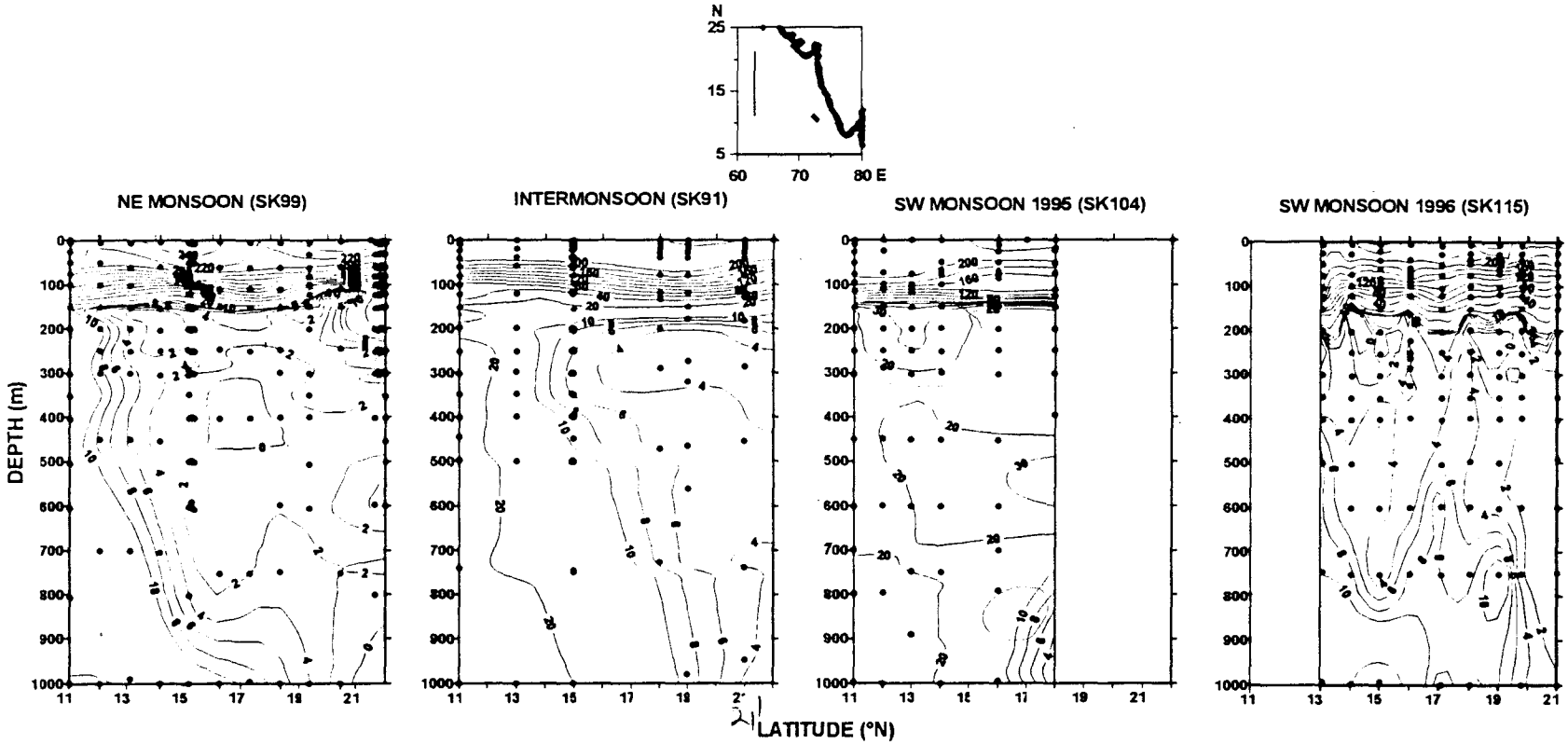

Fig. 3.2. Vertical distribution of dissolved oxygen (μM) along 64° E during three different seasons in the Arabian Sea.

than that in SW monsoon (Madhupratap *et al.*, 1996). Higher productivity at the surface results in the sinking of large amounts of organic matter that should be getting oxidized in intermediate layers, thus leading to more intense oxygen-deficient conditions (Fig. 3.2). For instance, at 15° N the measured sinking rates of particles using ^{234}Th export fluxes during NE- and intermonsoon are 371 and 848 mgC m^{-2} d^{-1} (Sarin *et al.*, 1996). Comparatively higher oxygen concentrations (>10 µM) were observed in the southern Arabian Sea because of the inflow of southern subtropical and polar waters in intermediate and deep layers.

The depth profiles of nitrate at any given depth show that its concentrations were lower in the north (Fig. 3.3). This results from nitrate consumption during the oxidation of organic matter. When oxygen is present at trace levels, the bacteria utilize nitrate as substitute oxidant in the decomposition of organic material. During this process nitrate gets reduced to molecular nitrogen as the end product with nitrite as an important intermediate. Thus the presence of secondary nitrite below the thermocline indicates the occurrence and intensity of denitrification process. Figure 3.4 depicts the relationships between nitrite and oxygen for the upper 1000 m water column. There are two distinct ranges of oxygen levels where nitrite was present. One is in the upper thermocline with oxygen concentrations of 175-275 µM and the other in intermediate depths with oxygen largely <10 µM While nitrite present in sub - oxic waters indicates the

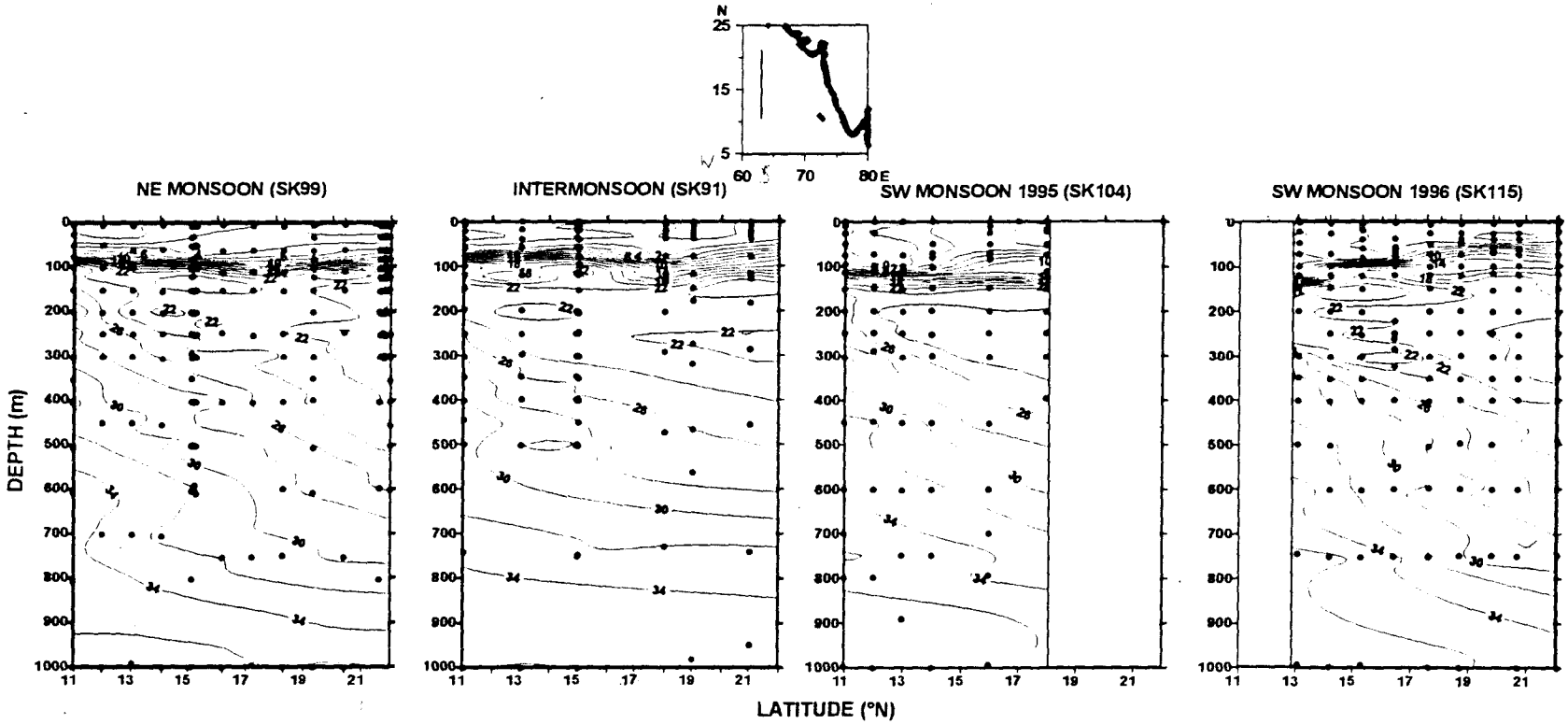

Fig. 3.3. Vertical distribution of nitrate (μM) along 64° E during three different seasons in the Arabian Sea.

occurrence of denitrification, that in the thermocline region originates from nitrification process and/or from assimilatory reduction (Sen Gupta *et al.*, 1976). Data in insets of Fig. 3.4 suggest that secondary nitrite predominantly occurs at trace levels of oxygen. Oxygen was the lowest in winter perhaps because of its enhanced consumption cumulatively triggered by the rain of organic matter from surface layers produced in winter and Southwest monsoon seasons.

The estimated nitrate deficit (Naqvi *et al.*, 1990), a measure of nitrate consumed during bacterial reduction and also an indicator of the extent of reducing conditions, ranged from 0 to ~10 µM in intermediate and deep waters. Figure 3.5 shows the relationships between dissolved oxygen and deficit in nitrate, at oxygen concentrations ≤60 µM. A large number of points have positive nitrate deficit values in winter particularly below 10 µM of oxygen. This is in good agreement with the nitrite data (Fig. 3.4).

Weakly stratified surface layer extended upto 100 m depth along the shelf. SST rose from about 24.2° C in the north (21.5° N) to about 29° C at 10° N, with an approximately 0.5° C increase per degree latitude (Prasanna Kumar and Prasad, 1996). The MLD was deep and varied between 120 m at 21° N and about 80 m at 10° N. The packed isotherms below 100 m, along the southern shelf indicate the occurrence of a strong thermocline. Salinity

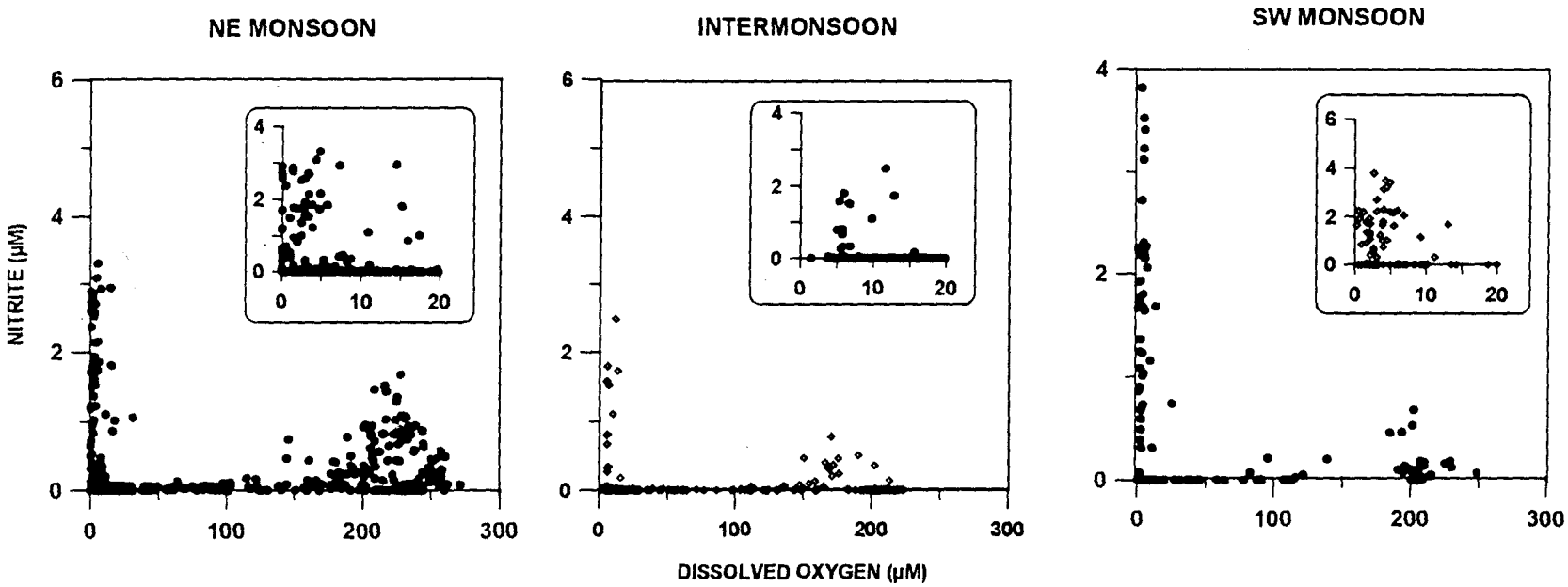

Fig. 3.4. Relation between dissolved oxygen (µM) and nitrite (µM) during three different seasons. Insets show relations of oxygen levels <20 µM.

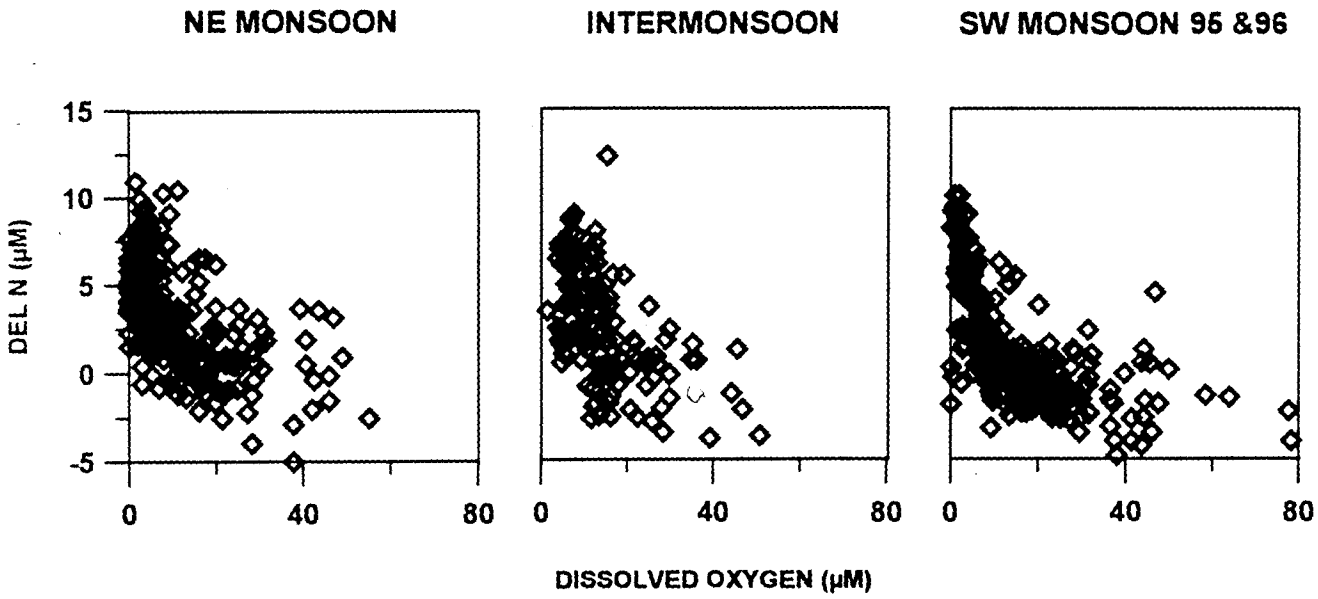

Fig. 3.5. Dissolved oxygen (µM) versus nitrate deficit (DELN, µM) during different seasons.

structure also showed a weakly stratified layer of high salinity (36.4 psu) in the north that thinned towards south. The high salinity surface waters (36.4 psu) in the north lead to the formation of the Arabian Sea High Salinity Watermass (ASHSW), the core of which deepens towards south (about 100 m depth) having a salinity of 36.0 psu (Prasanna Kumar and Prasad, 1996).

Fig. 3.6 depicts oxygen and nitrate distributions in waters along the west coast of India. Many contours of nitrate as well as oxygen rose from a depth of 180 m between 16 and 19° N whereas the same are deepened between 19° and 21° N in response to winter convection that must have triggered higher productivity. Along 21° N, dissolved oxygen concentrations were higher towards the coast due to enhanced productivity triggered by winter cooling. The oxygen concentrations were higher by 20-30 μM in the east where high productivity (860 mgC m^{-2} d^{-1}) was observed whereas it was 640 mgC m^{-2} d^{-1} in the west (Bhattathiri *et al.*, 1996). High nitrate concentrations (2 μM) were observed towards the coast.

The MLD along the 11° N zonal section increased gradually from about 50 m in the west to almost 100 m towards the east with SST, in general, greater than 28° C (Fig. 3.7). The presence of NEC brings about drastic changes in the surface salinity along this section (Fig.3.7) with very low salinity waters (34.6 psu) of Bay of Bengal over-riding the ASHSW. The core of the ASHSW (36.0

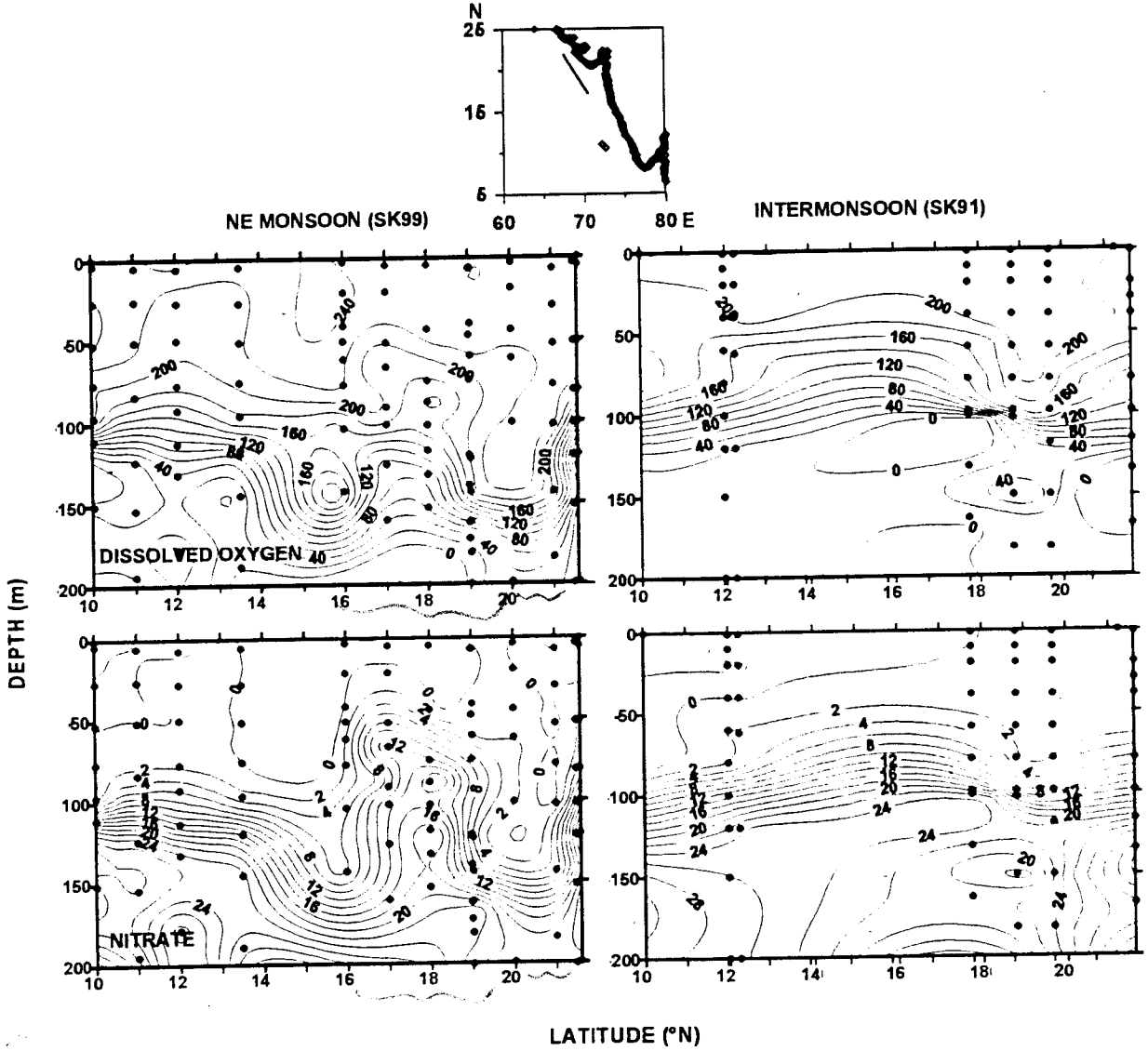

Fig. 3.6. Vertical distribution of dissolved oxygen (μM) and nitrate (μM) along 21 N the Arabian Sea during NE- and Intermonsoon seasons.

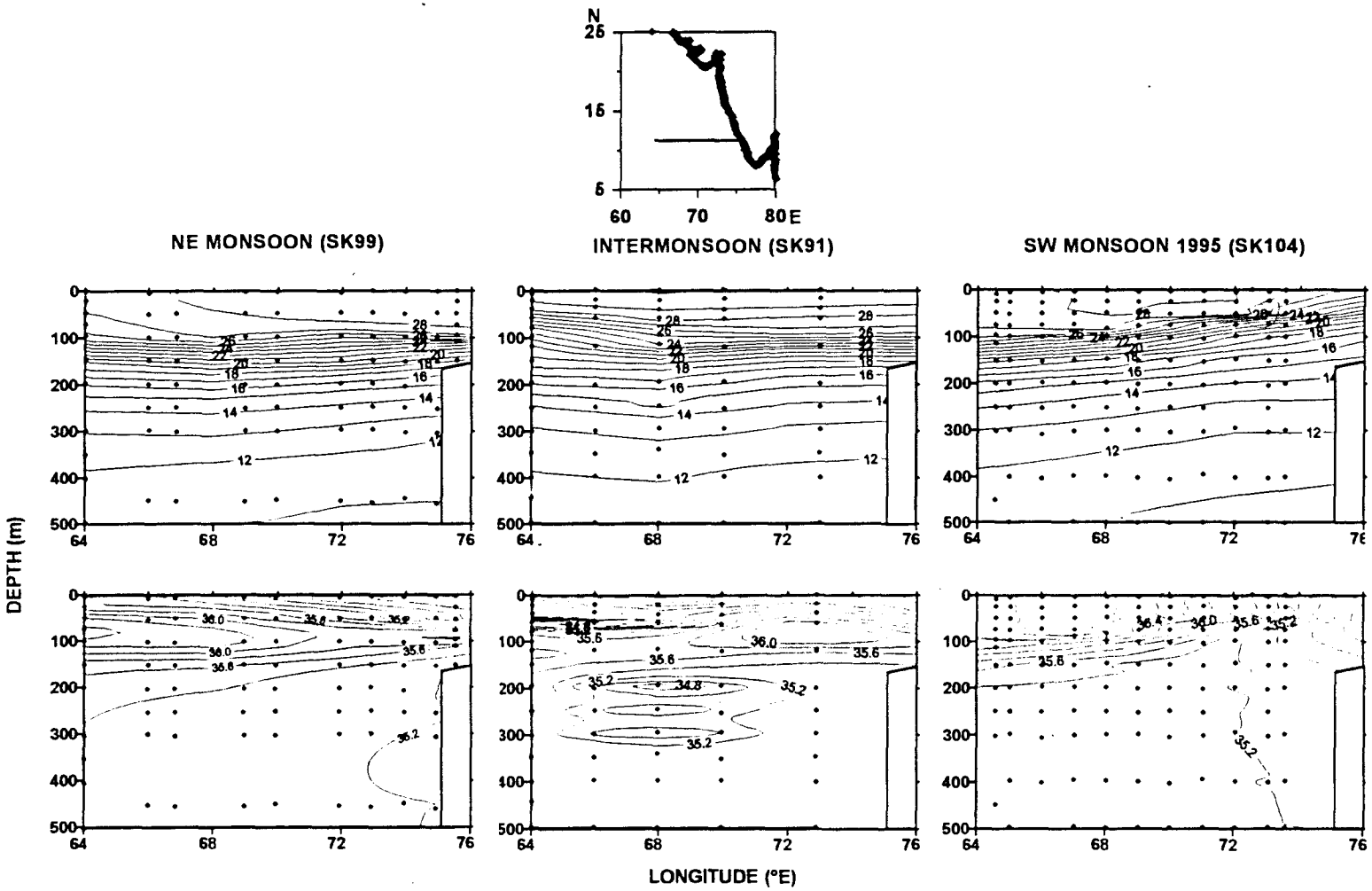

Fig. 3.7. Vertical distribution of temperature (upper panels, C) and salinity (lower panels, psu) along 11°N in the Arabian Sea in different seasons.

psu) consequently showed an eastward tapering and deepening. Dissolved oxygen concentrations in surface waters showed no significant east-west variations (~220 μM) and the water column was well stratified (Fig. 3.8). Nitrate distribution shows that the upper 50 m had undetectable nitrate with no meridional gradient. In the sub-surface layers low nitrate occurred closer to the western margins of India which could be due to consumption of nitrate from water immediately above the sediments or to upward diffusion of nitrate deficient pore waters.

The salient features in NE monsoon are:

- **Weak winds generally prevailed**
- **Winter convection occurred in the north**
- **Mixed layer deepened in the north**
- **Primary production enhanced in the north driven by convection**
- **Clear north-south subsurface gradients occurred in oxygen and nitrate**
- **Large nitrate deficits were associated with higher production/ sinking of organic matter**

3.3. Inter-monsoon (Pre-SW monsoon)

The inter-monsoon represent transition periods between NE and SW monsoons when the winds reverse direction during March to May (pre-

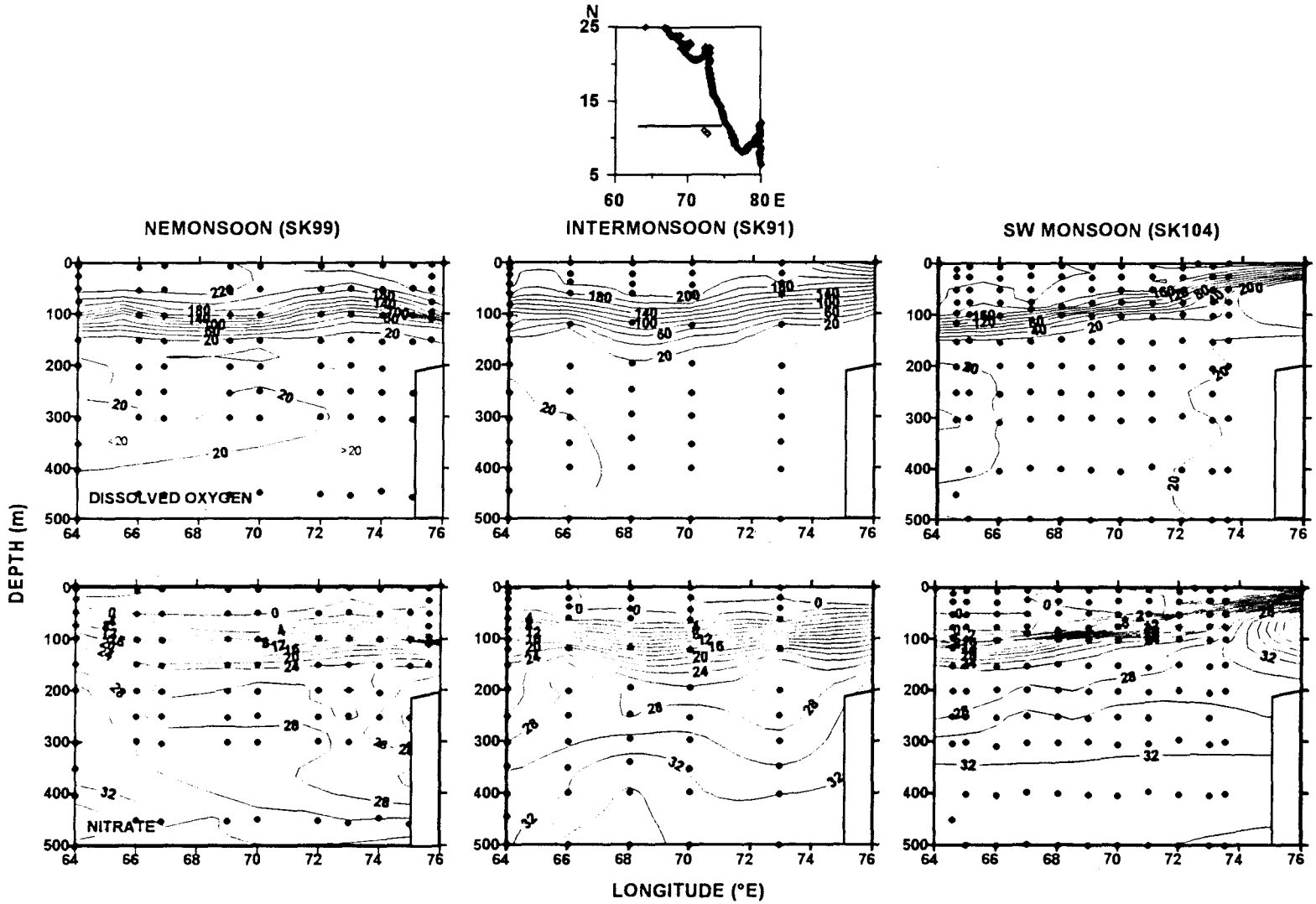

Fig. 3.8. Vertical distribution of oxygen (uM) and nitrate (uM) along 11 N in the Arabian Sea in different seasons.

monsoon) and October to November (post-monsoon). The surface winds south of 17° N during April-May were predominantly northerly and weak (<4 m s^{-1}) in the south but became westerlies and progressively stronger towards the north west. Along the north Indian shelf, wind speeds were between 8 and 10 m s^{-1}. Wind speeds were high north of 18° N reaching upto 8 m s^{-1} in the open ocean The air temperature along 64° E was, in general, around 28° C but reached up to 30° C at 13° N (Fig. 3.1). SST decreased from 30° C in the south to 29° C in the north with large variations (between 13° and 17° N). MLD was shallow and varied between 30 and 35 m except at 19-20° N where it further shallowed to 10 m. Along the western shelf, thermal structure revealed thin mixed layer that varied from 10 m to 25 m with SSTs more than 30° C (Fig. 3.1). More or less uniformly high salinity waters (36.4 psu) were encountered along the northern shelf (north of 16° N). However, along the southern shelf, relatively low salinity waters were seen in the upper 20 m. The core of ASHSW was closer to the surface in the north but deepened to about 80 m in the south (Prasanna Kumar and Prasad, 1996).

The oxygen isopleuths were well stratified up to a depth of 150 m with no significant gradient between northern and southern Arabian Sea. Comparatively low surface oxygen (200 µM) concentrations were observed than in the NE monsoon (240 µM) which could be due to high production in the latter season (Fig. 3.2). Surface waters are nearly devoid of nitrate during the

inter-monsoon period (Fig. 3.3). The 2 µM nitrate isoline was found at ~75 m whereas the same had surfaced in the north during NE monsoon. Although surface waters are depleted in nutrients, high nutrient concentrations were found at the base of the euphotic zone leading to subsurface chlorophyll maximum (SCM) (Bhattathiri *et al.*, 1996). The SCM was found to be prevalent at ~40 to 60 m during the inter-monsoon period. In this season surface primary production varied from 0.7 to 11.9 mgC m^{-2} d^{-1}. The surface production was comparatively higher in the north than in the south.

The oxygen concentrations at intermediate depths (4-20 µM) were higher than in the winter (0-10 µM). Although surface productivity was low, bacterial population has been found to be higher by several folds during inter-monsoon unlike July/August (Ramaiah *et al.*, 1996). Bacteria showed an increase from the northern to the southern Arabian Sea. Patches of *Trichodesmium* blooms were found in some areas of the southern Arabian Sea. Rapid turnover of bacteria during the inter-monsoon period of April/May suggests the predominance of a 'microbial loop' in the foodweb. The depth profile of nitrate (Fig. 3.3) shows that at any given depth the concentrations were lower at the northern latitudes. Nitrate deficits were low in this season than in winter as a consequence of which a large number of data points have moved to the right in Fig. 3.5.

The MLD remained thin showing a general deepening, though small, toward south, as also is the case along the western shelf. Salinity structure resembled that in February-March, except for the reduced spatial extent of the low salinity water in the southern region. The thick isohaline layer seen in the north, during winter, was no longer present. Instead, high salinity water (36.6 psu) intruded into the column, indicating the spreading and deepening of the ASHSW towards south. Unlike in winter, the sigma-t structure showed the presence of low-density waters uniformly from 21° N to 11° N with strong stratification. The upper thermocline showed a overall trend of deepening from 21° N to 11° N, except between 13.5° N and 15.5° N where isotherms greater than 20° C shoaled, that appeared to be a signature of a meso-scale (cold core) eddy (Prasanna Kumar and Prasad, 1996).

Along the Indian western margin, oxygen was lower than in NE monsoon by 20 µM (Fig. 3.6) with increasing concentrations towards the north. Nitrate concentrations were also comparatively higher in the north during inter-monsoon (Fig. 3.6). This could be attributed to a remnant of injected nitrate concentrations by winter convective mixing that might not have been used completely. Primary productivity was 310 mgC m^{-2} d^{-1} during this season perhaps because of the availability of nitrate in surface waters.

Thermal structure along 11° N revealed extremely shallow MLD that was at least 2° C warmer than in winter (Fig. 3.7). Oxygen contours in the upper 150 m were well stratified and showed no east-west gradient. But high surface oxygen concentrations were observed close to the coast because of high productivity. Surface nitrate was undetectable but appeared (Fig. 3.8) at the base of the euphotic zone (60-70 m) leading to the formation of SCM. Subsurface oxygen concentrations showed large east-west gradient having higher concentrations in the west (Fig.3.8). Low concentrations of oxygen in the east coincides with high concentrations of nitrate suggesting intense remineralisation of organic matter closer to the coast.

The salient features in inter-monsoon are:

- **Wind speeds increased in the north**
- **Water column well stratified, in general**
- **Mixed layer was shallow**
- **Subsurface chlorophyll maximum occurred**
- **North-south gradients in oxygen and nitrate were evident**
- **Bacteria were more abundant than in other seasons**
- **Northern coastal waters experience conditions similar to those in winter, i.e. higher oxygen and nitrate, and relatively deep mixed layer than in south**

3.4. Southwest monsoon

The flow pattern seen in winter changes completely with the onset of the SW monsoon.. The reversal actually starts in February and is completed by May. The westbound NE monsoon current is replaced by an eastbound monsoon current. During SW monsoon the overall direction of winds over the north Indian Ocean is from the southwest and surface currents flow towards the equator (Muraleedharan and Prasanna Kumar, 1996). A prominent feature of the large-scale surface circulation in the Arabian Sea during the SW monsoon is the Somali Current System. The northward flowing Somali Current reaches its greatest strength in July (Schott, 1983). Düing (1970) has studied the dynamic topographies of sea surface during this season, which are dominated by a complex pattern of cyclonic and anticyclonic vortices. The eastward drift observed by Düing (1970) is also seen in the ship-drift charts of Cutler and Swallow (1984). The same charts indicate that in the coastal region of India a southward flow occurs. Nevertheless, the occurrence of upwelling is, by far, the best characteristic of Southwest monsoon season in the Arabian Sea. Open ocean regions and continental margins of India have been covered in the present study (please see Fig. 2.1).

3.4.1. Central Arabian Sea

A prominent signature of the onset of the SW monsoon is the cross equatorial

wind component in the northern hemisphere. During May this low-level flow progressively moves northward along the East African coast where it accelerates and produces the Somali Jet --the strongest persistent low-level wind system in the world. During June and July the jet splits over the Arabian Sea when its northern branch progresses across the Indian subcontinent and the southern branch moves eastward to the south of India.

The observed wind speeds ranged between 1.6 and 16.7 m s^{-1}. Winds along 64 ° E were stronger, ranging from 8.6 to 16.7 m s^{-1} with the highest values occurring near the Jet axis (16-17° N). The winds were highly variable along the coast with speeds of 1.6-10.2 m s^{-1}. To the Northwest of the jet axis extreme values of positive (cyclonic) wind stress curl occur which induce a divergent Ekman transport in the upper ocean with vertical velocities of the order of 1-2 m d^{-1} (Yoshida and Mao, 1957; Smith and Bottero, 1977). This divergence stimulates an intense biological bloom over ~40% of the surface area of the basin during the SW monsoon (Smith and Bottero, 1977; Brock *et al.*, 1991). To the southeast of the jet axis, the curl is negative (anti-cyclonic) and drives downward Ekman pumping. This results in a warm and deep mixed layer (Bauer *et al.*, 1991).

Considerable inter-annual variability in the strength and position of the Findlater Jet leads to variability in divergence. A weaker or broader jet induces

weaker cyclonic curl, leading to weak divergence. Whenever the jet is stronger, winds largely have southerly component, while at other times they have westerly component, although the axis of the jet remains nearly stationary. The paleoceanographic records provide evidences of extreme variability in the strength of the Findlater Jet and the associated divergence over glacial/interglacial cycles (Luther *et al.*, 1990; Prell *et al.*, 1990). During glacial times (i.e., ~18 ^{14}C kyr before present), the difference in surface heating between the Indian Ocean and the Asian continent was less, due to variations in the Earth's orbital parameters, that drove a weaker jet with weak divergence. About 9 kyr B.P., when the northern hemisphere summer insolation was its maximum, the differential heating increased relative to the present day conditions that resulted in a stronger jet and enhanced intensity in divergence (Luther *et al.*, 1990).

The mixed layer was found to be deep in the south and shallow in the north in consistence with the processes expected to the south and north of the Jet axis, respectively. Dissolved oxygen in surface layers did not show much variation between seasons (Fig. 3.2). Nevertheless, the notable features were: (a) comparatively higher concentrations in subsurface layers during the SW monsoon of 1995, probably due to increased inflow or oscillations of PGW, and (b) values higher by ~10 μM at the surface at 18-19° N in 1996. The former is supported by the fact that relatively high concentrations in oxygen nearly

coincided with higher salinity representative of PGW. The latter may be due to enhanced biological production at these latitudes triggered by higer availability of nutrients. Nitrate was at undetectable or very low levels in the upper 50 m (Fig. 3.3), except that a lens of high nitrate was found at 17° N during SW monsoon of 1995 and at 19° N in 1996. Nitrate abundance at these locations was about 4.5 μM in 1995 but was low (< 2 μM) in 1996. The nutrients apparently are supplied by upwelling/divergent. Oxygen levels in the subsurface layers of the Arabian Sea during 1996 Southwest monsoon were nearly the same as those in winter but were lower than those found during 1995 Southwest monsoon. This probably indicates annual variability in water mass composition and the consequent changes in water column chemistry.

During the summer of 1995, vertical thermal structure showed surfacing of 27° C isotherm north of 14° N (Muraleedharan and Prasanna Kumar, 1996). The isotherms in the upper thermocline (above 200 m), in general, showed a northward shoaling (upward Ekman pumping). A reverse trend was observed in the lower thermocline. Earlier similar observations have been reported from this region (Bauer *et al.* 1991). However, during 1996 SW monsoon, though there was no outcropping of isotherms but cold SSTs (<27°C) prevailed all along 64° E and shoaling of the upper and deepening of the lower thermocline waters, respectively, were consistent with those in the previous summer. Prasanna Kumar *et al.* (submitted) hypothesised that lateral advection from the western

Arabian Sea upwelling regions could be the major factor in maintaining the high nutrient concentrations in open ocean waters in this season. These processes obviously led to the enrichment of nutrients in surface layers. Thus, a pronounced subsurface chlorophyll maximum associated with nitracline (at about 50-60 m), that is usually found in the oceans, was not discernible in summer; instead higher pigment concentrations were observed throughout the mixed layer.

Satellite images show higher surface pigment concentrations over large areas in the Arabian Sea (Yentsch and Phinney, 1992). The contemporary observations showed that high production indeed occurred also in the interior Arabian Sea during summer, which is not confined to just northern regions despite varying physical regimes between north and south. In SW monsoon 1996, higher surface pigment concentrations (up to 0.54 mg m^{-3}) and primary production (22 mgC m^{-3} d^{-1}) occurred in the north (19° N, 64° E) compared to those of 0.32 mg m^{-3} and 8.3 mgC m^{-3} d^{-1}, respectively, in the south (13° N, 64° E). The observations along 64° E revealed highest productivity of 1782 and 1760 mgC m^{-2} d^{-1} at 15° N in 1996 and at 12° N in 1995, respectively. High production in southern latitudes during summer was also found during the US - JGOFS observations (Barber *et al.*, 1998) in 1995 at 10° and 14° 30'N along 65° E (1600 mg C m^{-2} d^{-1} at both stations In July, 600

and 1600 mgC m^{-2} d^{-1}, respectively in August). Interestingly, the chlorophyll *a* concentrations and production rates in the open central waters are comparable to those from the active upwelling fields off the Somalia coast in July-August 1992 (Veldhuis, 1997). The NE monsoon values observed during the present study were much lower when surface chlorophyll *a* varied from 0.064 to 0.27 mg m^{-3} and primary production ranged between 3.80 and 6.7 mgC m^{-2} d^{-1} in south (11° N, 64° E) and north (19° N, 64° E), respectively. Maximal biological production in surface layers probably leads the subsurface layers with large quantities of organic matter. As the intermediate waters in the Arabian Sea are suboxic, nitrate is used as oxidant that can be seen from the presence of secondary nitrite (Fig. 3.4).

3.4.2. Coastal waters of western India

A comprehensive study made by Banse (1968) established the occurrence of cold upwelled water along the west coast of India. However, its extension to the north of 15° N is unknown. Shetye *et al.* (1990) found intense upwelling along the Southwest coast of India which weakened towards the north. Although, the overall direction of winds over the northern Indian Ocean is from the southwest, departures from this can be noticed from the distribution of climatic monthly mean winds in July (Hastenrath and Lamb, 1979). Off the west coast of India the direction of winds varies from roughly west-southwest in the north to

approximately west-northwest in the south. Shetye *et al.* (1984) computed the climatic annual cycle of the along-shore component of the wind stress off the southwest coast of India, and compared it with the annual cycle of the mean thermal structure on the shelf given by Sharma (1968). This comparison revealed that winds control the upwelling along the coast. Shetye and Shenoi (1988) studied the annual cycles of wind stress and ship-drift along the coast and could that local winds could drive the surface circulation.

It has been noted that upwelling along SW coast of India begins sometime in February (Longhurst and Wooster, 1995), well before the onset of upwelling-favourable southwest monsoon winds. Longhurst and Wooster (1995) suggested that the most important element of this process is the Rossby wave radiation from the Kelvin waves propagating poleward along the western margin of the Indian subcontinent. Shankar and Shetye (1997) studied the dynamics of lakshadweep high and low in the Arabian Sea and suggested that a consequence of the remotely forced Kelvin wave is the formation of a weak, but nonetheless upwelling-favourable coastal current off Southwest India. The coastal Kelvin waves may be generated locally by along-shore winds or forced remotely by along-shore winds in the Bay of Bengal or winds in the equatorial Indian Ocean.

During the present study period the local winds were generally from west-northwest. High eastward wind component (10 m s^{-1}) has been observed to be associated with moderately strong southward component (6 m s^{-1}) (Muraleedharan and Prasanna Kumar, 1996). Along 10° N, the observed wind showed a steep rise in both cross-shore (positive towards east) and along-shore (positive towards north) components. Along this transect, the negative along-shore component (northerly wind) dominates over the positive cross-shore component (westerly wind), with their magnitudes exceeding 6 and 4 m s^{-1}, respectively. The shoaling of the isotherm with low SST indicated strong upwelling and is well correlated to the prevailing winds. Shetye *et al.* (1990) observed along-shore component of winds towards equator and showed a decrease from south to north. The cross-shore wind component is generally larger than the long-shore by a factor of 10 (Shetye *et al.*, 1990).

The shoaling of isotherms with decreased SST towards coast in a section off-Goa studied during SK104 indicate the continuance of upwelling to the north. Muraleedharan and Prasanna Kumar, (1996) attributed this to the strong cross-shore wind present at this latitude, bringing the low saline surface water, diluted by fresh water influx from land, thereby supressing the upwelling. Thus along-shore as well as cross-shore components play significant role in determining the magnitude of the upwelling The thermal structure off Goa exhibits gentle upsloping towards the coast. However, this trend is reversed in

the sub-thermocline region. Surface salinities near the coast were almost 0.8 psu lower than in the offshore.

Figures 3.7 and 3.8 depict the signatures of upwelling in the eastern side of the east-west section along 11° N during SW monsoon (SK104). This occurred to the east of 72° E where the surface temperatures were less than 28° C. Increase in nutrients in surface layers due to upwelling results in higher productivity. For example, the primary productivity was 1760 mgC m^{-2} d^{-1} off Mangalore (12° 30'N, 73° 30'E), 660 mgC m^{-2} d^{-1} off Cochin (10° N, 75° 35'E) and 440 mgC m^{-2} d^{-1} off Bombay (Bhattathiri *et al.*, 1996). This shows patchiness of surface production. The intensity of upwelling along the Southwest coast of India can be suppressed by land run-off. Consequently, variable run-off may have caused the observed patches in productivity (de Sousa *et al.*, 1996). However, during inter-monsoon it was 199 mgC m^{-2} d^{-1} near Cochin (Bhattathiri *et al.*, 1996) which is considerably less than that in SW monsoon.

Fig. 3.9 depicts the signatures of upwelling observed during SW monsoon (SK103) along the 9 °N, 10° N and 11° N (hereafter referred to as transects 1, 2 and 3, respectively). Strong upwelling has occurred along 10° N although its signatures can be seen at 9°N also. Thermal structure showed surfacing of 24 ° C isotherm in coastal waters. Salinity distribution showed that surface waters in

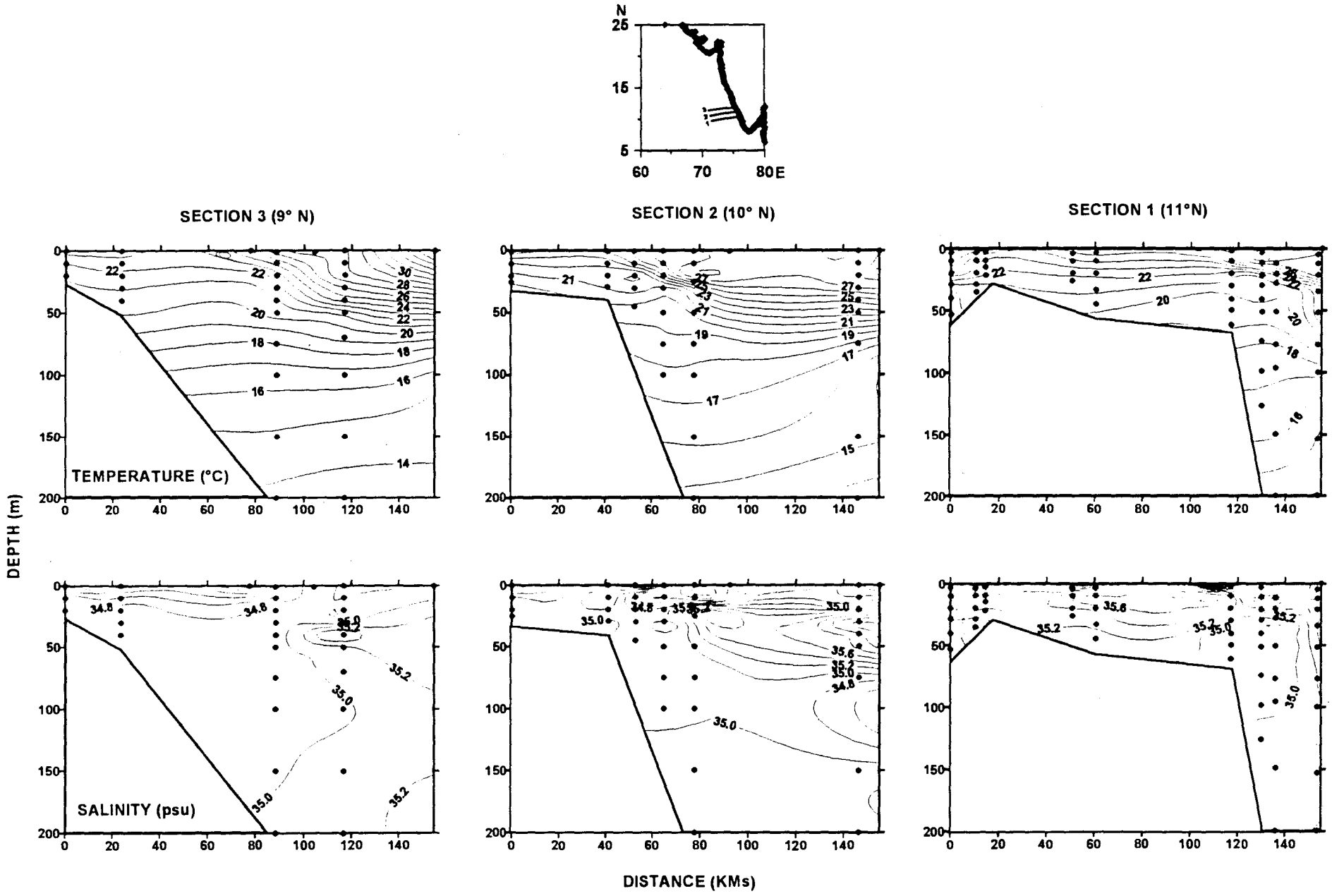

Fig. 3.9. Distribution of temperature and salinity along the three sections in the Arabian Sea during SW monsoon.

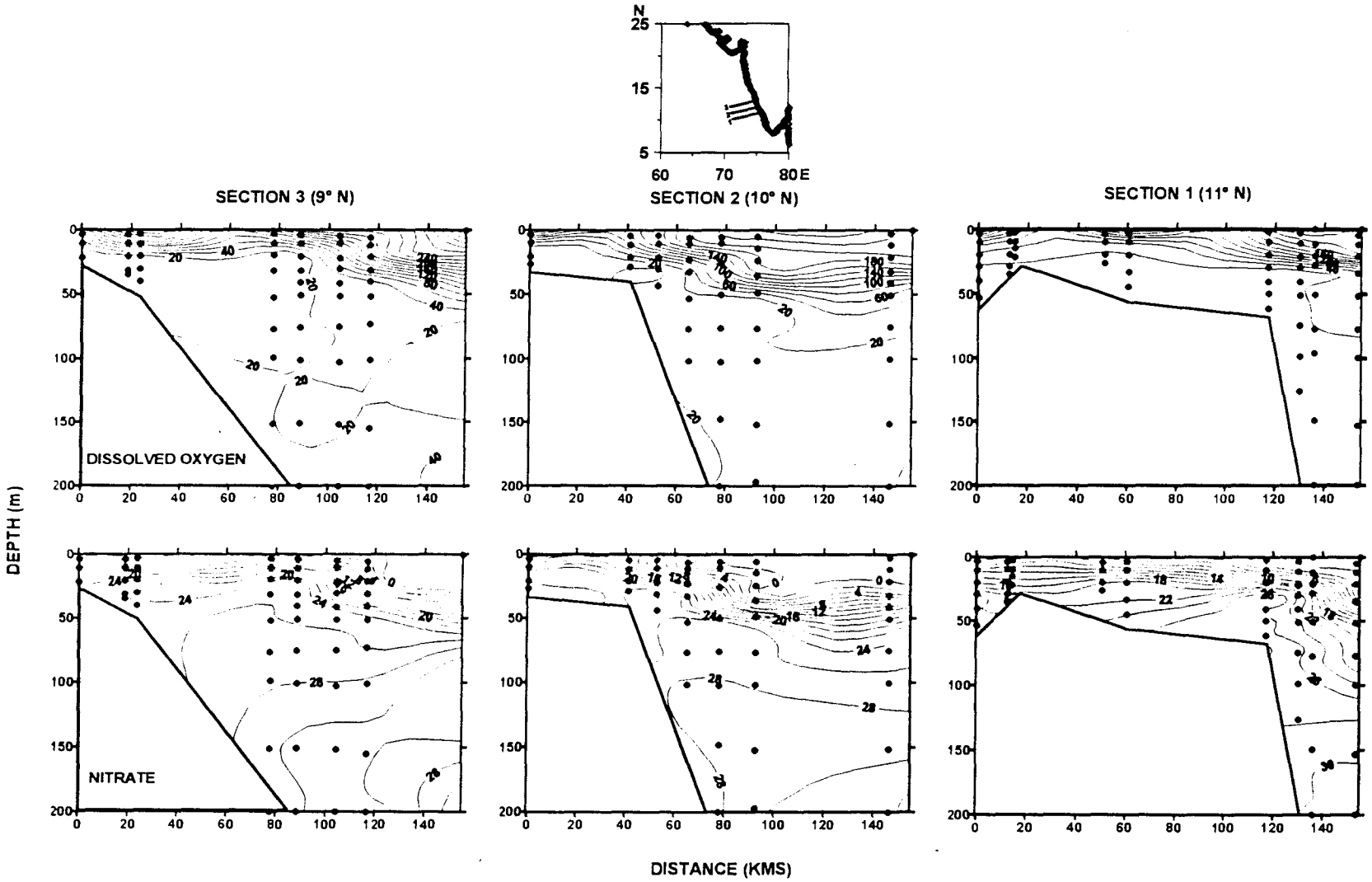

Fig. 3.10. Vertical distribution of dissolved oxygen (μM) and nitrate (μM) along the three sections in the Arabian Sea during SW monsoon.

the coastal regions were occupied by the low salinity waters whereas high salinity upwelled waters remained below (transect 2 in particular) suggesting that run-off from land supresses the upwelling intensity (Fig. 3.9). Oxygen and nitrate distributions revealed that nutrient depleted fresh waters were capping the nutrient enriched upwelled waters. The surface oxygen concentrations fall to values as low as 90 µM (section 2) occurred (Fig. 3.10). In concurrence, surface nitrate concentrations were as high as 16 µM (Fig. 3.10). But for upwelling these values would be found only at a depth of 100 m in the Sea.

The vertical thermal structure off Goa (along 15° N) exhibited upsloping of isotherms towards the coast (Fig. 3.11). This occurred to the east of 72° E where the surface temperature was low during post SW monsoon (28° C) than in other seasons (29° C). The 20° C isotherm, which generally lies in the middle of the upper thermocline in the north Indian Ocean (Wyrtki, 1971), rose from a depth of more than 150 m to a depth of less than 50 m across the length of the transect. The salinity distribution (Fig. 3.11) exhibits that fresh water inflow inhibits upwelling at this place as well.

Dissolved oxygen contour surfaced from deep layers near the coast (Fig. 3.12). Surface concentrations were ≥180 µM. In general, this concentration occurs in the middle of the thermocline. Nitrate contours upslopped from a depth of 80-150 m. Surface nitrate concentration near the coast was 2 µM (Fig. 3.12) which

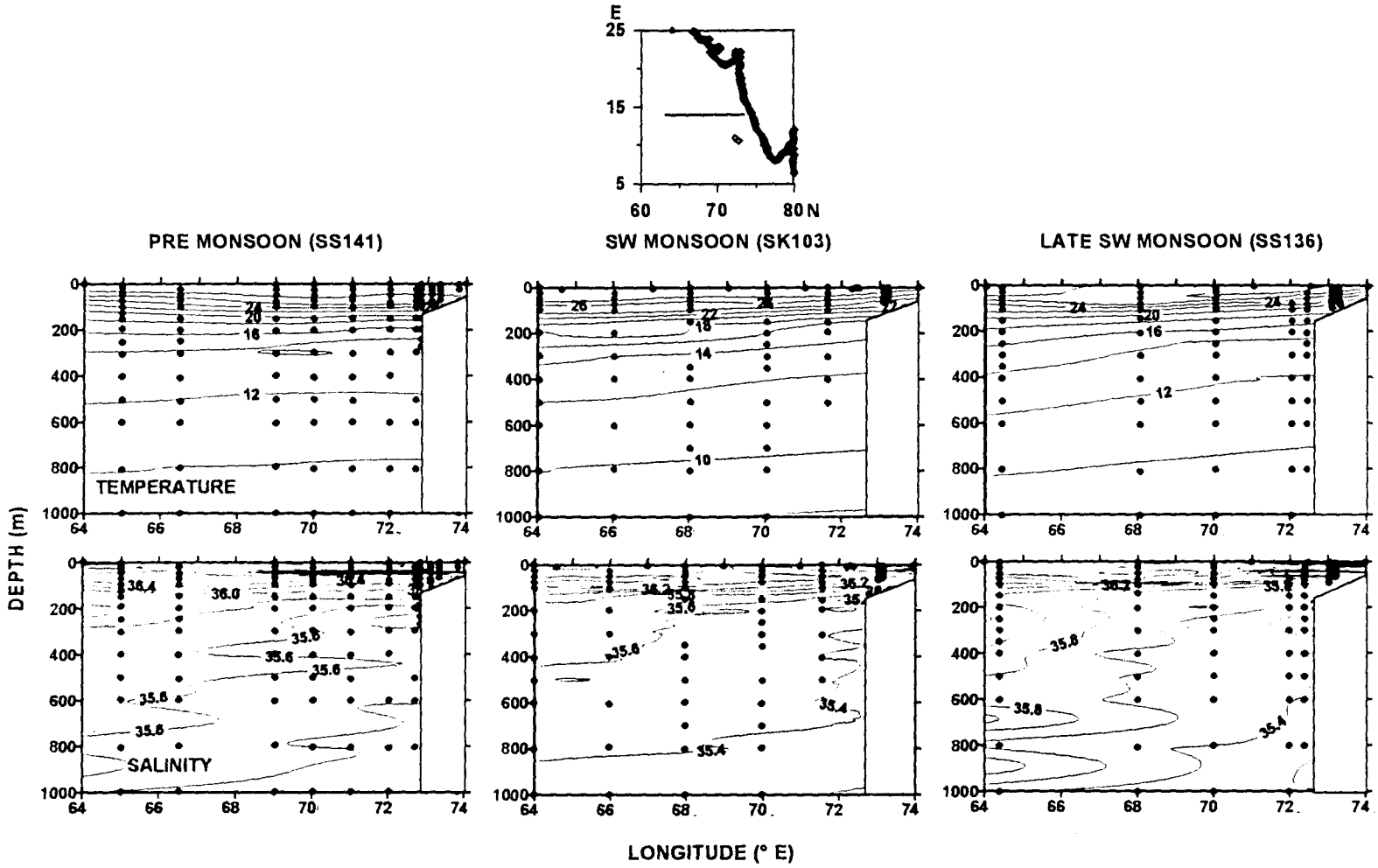

Fig. 3.11. Distribution of temperature (°C) and salinity (psu) along 15° N during three different seasons in the Arabian Sea.

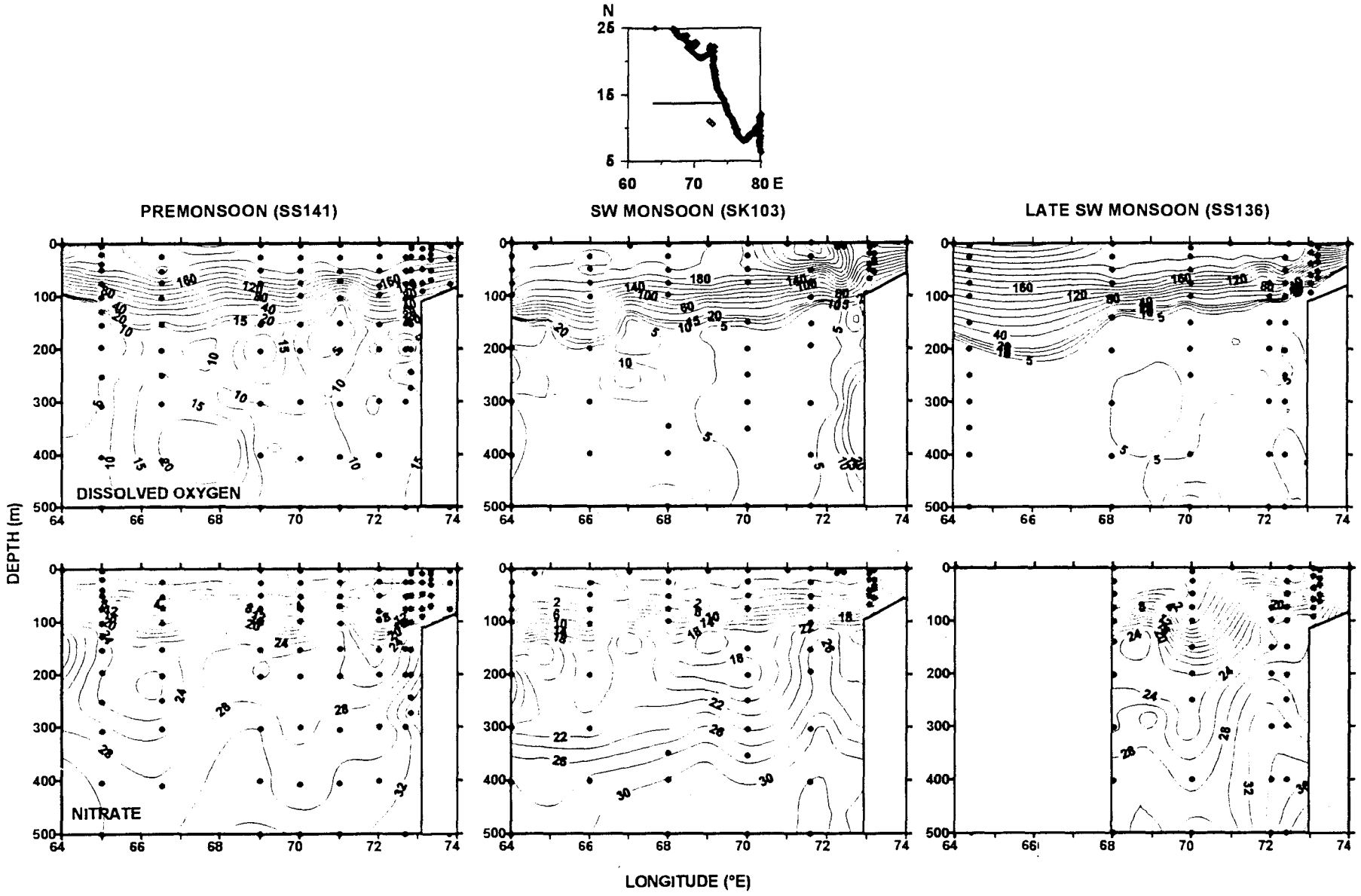

Fig. 3.12. Vertical distribution of oxygen (uM) and nitrate (uM) along 15 N in the Arabian Sea in different seasons.

might enhance primary productivity. Oxygen distribution in the suboxic waters showed that lower oxygen concentrations were observed in the east (<5 μM) compared to those in the west due to higher rates of decomposition in proportion to the organic matter supply. Westward increase in oxygen in intermediate waters is in agreement with comparatively high oxygen concentrations observed along 64° E during the same season of 1995 (Fig. 3.2). Nitrate concentrations lower by 2 μM, compared to those in off-shore regions, were found near the coast indicating that this decrease might have been due to bacterial respiration near sediment-water interface.

3.5. Late SW-Monsoon (Sept. - Oct. 1996)

Observations along 15° N during September-October, 1996 depicted features mostly of SW monsoon. Surface temperature ranged between 28 and 28.5° C where lower values were found closer to the coast. The 28° C isotherm rose from a depth of 50 m to the surface suggesting the occurrence of upwelled waters near the coast (Fig. 3.11). Salinity shows the low salinity cap near the coast (Fig. 3.12). The occurrence of a subsurface current was noted by the presence of low salinity water at a depth of about 50-60 m (Fig. 3.11). Dissolved oxygen upslopped from depths of 80-150 m. Low oxygen and nitrate of 2 μM concentration were observed closer to the coast driven by upwelling.

Low oxygen concentrations (<5 μM) were found in the sub-surface waters leading to denitrification.

The salient features of the present observations during Southwest monsoon are:

- **Strong winds prevailed over most of the study area**
- **Inter-annual variability in water column conditions were evident**
- **Nutrients in the surface layers enriched due to upwelling/divergence/lateral advection**
- **Biological production in the offshore regions also was high**
- **River influx reduced upwelling intensity in coastal regions**
- **Monsoonal conditions off Goa continued to occur even in the late-monsoon period**

Chapter 4

VARIABILITY IN INORGANIC FORMS OF CARBON

Carbon dioxide exists in different forms (see 1.2) in sea water whose distribution patterns needs to be clearly understood for the assessment of CO_2 fluxes across the Arabian Sea air-sea interface and their dynamics in the water column. Thus, to evaluate the variations in different species of dissolved inorganic carbon a systematic study was carried out on total carbon dioxide, partial pressure of carbon dioxide, regenerated carbon dioxide, carbonate and bicarbonates distribution in association with total alkalinity and pH. Different physical and biological processes play important roles on the inorganic carbon system. For instance, physical processes bring nutrient rich subsurface waters into the surface leading to an increase in productivity. These relatively cold waters influence the solubility of carbon dioxide to some extent. Increased surface productivity would influence water column carbon chemistry since phytoplankton fixation of carbon dioxide increases pH marginally. The opposite occurs in subsurface layers. The variability in carbon dioxide chemistry in the Arabian Sea is not much known Therefore, this chapter examines the spatial, seasonal and inter-annual changes in the dissolved inorganic carbon species in the Arabian Sea.

4.1. Variability in pH_T

As stated earlier, pH is a key variable controlling the inorganic carbon system. A chemical change in carbonate equilibrium brings corresponding shift in pH.

pH in oceanic surface layers generally ranges from 7.8 to 8.2. It decreases to about 7.5 in the oxygen minimum/sub-oxic zone. In sea water pH is represented in pH on free (pH_F), National Bureau of Standards (pH_{NBS}) and total (pH_T) scales. In this work data are presented on pH_T (see 2.3.2) since this scale is more appropriate here in view of the proton complexation with the dominant sulphate ion in sea water. Precision of our measurements are comparable to measurements made by experts in carbon dioxide methodologies else where (Table 4.1).

Figure 4.1 exemplifies the vertical distribution of pH_T in the Arabian Sea. It shows low values in intermediate waters with a sharp fall in thermocline layers. Protons are used during primary production leading to an increase in pH in surface waters (Anderson and Dyrssen, 1994) whereas it decreases in sub-oxic zone due to release of protons during organic matter decomposition (Redfield *et al.*, 1963):

$$(CH_2O)_{106}\,(NH_3)_{16}H_3\,PO_4 + 138\,O_2 \Longrightarrow 106\,CO_2 + 16\,NO_3^- + HPO_4^{-2} + 18\,H^+ + 122H_2O \qquad (4.1)$$

The northward decrease in pH_T in sub-surface waters during all the seasons (Fig. 4.2) is in agreement with dissolved oxygen (Fig. 3.2) and it is caused by proton release during the decomposition of organic matter, in response to high

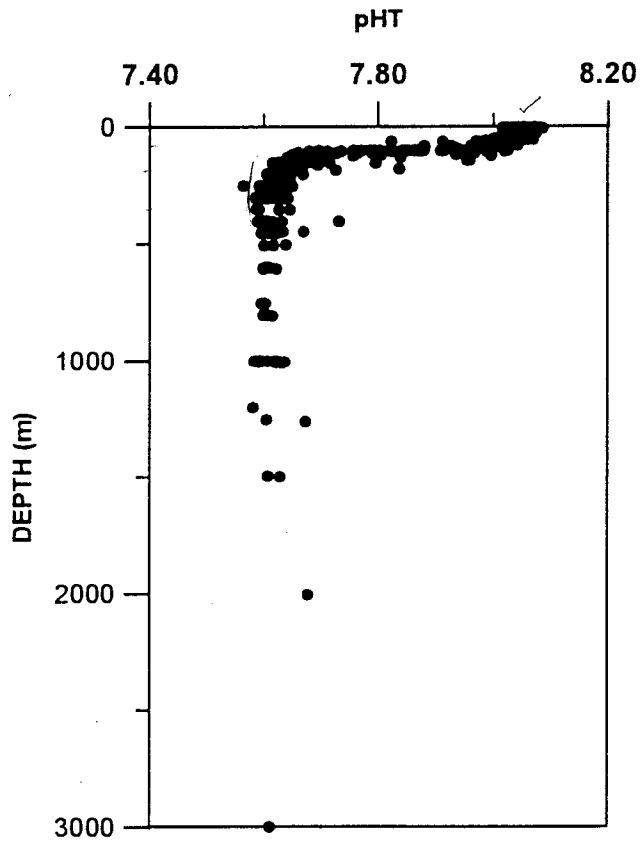

Fig. 4.1. Vertical profile of pH_T (total scale) in the Arabian Sea during NE monsoon.

Table 4.1. Precision of our measurements are compared with measurements made by experts in carbon dioxide methodologies else where.

Parameter	Precision of our study	Method used	Precision of other workers	Method they followed	Reference
pH	0.002	Colorimetry with Cresol Red	0.0005	Colorimetry with Cresol Red	Byrne and Breland, 1989
			0.0004	Colorimetry with m-purple	Clayton and Byrne, 1993
			0.002	Potentiometry	Millero et al., 1993
Total alkalinity	2 µM	Colorimetry with BCG	2 µM	Colorimetry with BCG	Breland and Byrne, 1993
			4 µM	Potentiometry	Millero et al., 1993
			2 µM	Potentiometry	Millero et al., 1993
Total carbon dioxide	2 µM	Coulometry	2 µM	Coulometry	Millero et al., 1993
			1 µM	Coulometry	Johnson et al., 1993
			0.3-1.3 µM	Coulometry	Goyet and Hacker, 1992
Partial pressure of carbon dioxide	4 µatm	Computed using TC & pH	2 µatm	Computed from TC & pH	Millero et al., 1993
	0.2 µatm	Infra Red	0.5 µatm	Infra Red	Wanninkhof and Thoning, 1993

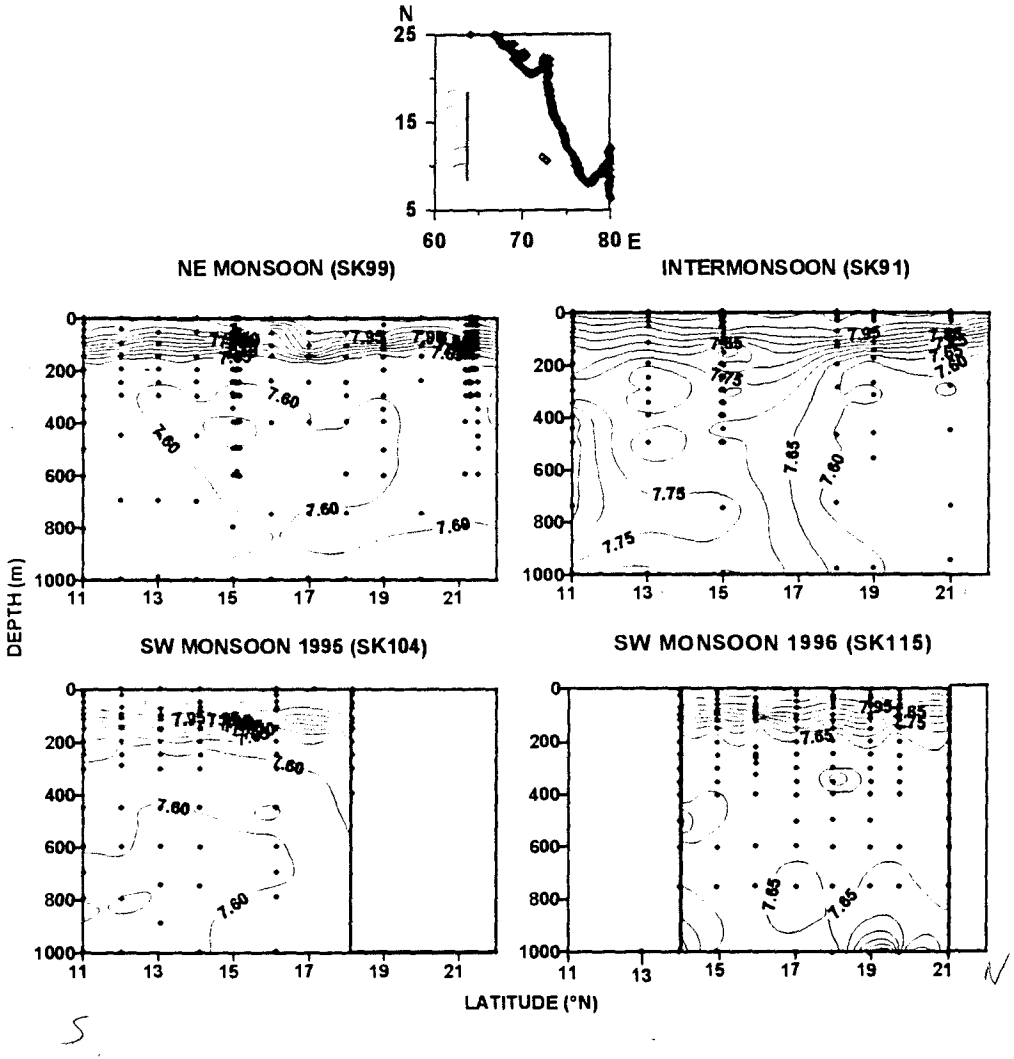

Fig. 4.2. Distribution of pH_T along 64° E during different seasons in the Arabian Sea.

productivity in the north. A large extent of regeneration of soft tissue and the prevalence of reducing conditions result in a decrease in pH_T in the subsurface waters of the Arabian Sea (George *et al.*, 1994).

4.1.1. Meridional variability in pH_T

Along 64°E, pH_T in surface waters varied from 8.0 to 8.10 during NE monsoon and Southwest monsoon 96 (Fig. 4.2) with no significant north-south gradients. This is not as expected because the values should have been higher in the north because of higher production. However, the productivity was triggered by convected or upwelled/diverged waters having their origin in thermocline region that have relatively low pH_T. Therefore, mixing between thermocline waters and high productive surface waters in the north resulted in no pH_T gradient meridionally. This distribution pattern is in agreement with dissolved oxygen (Fig. 3.2). Winter convection was evidenced by the shoaling of 2 µM nitrate isoline (Fig. 3.3) from a depth of 100 m to the surface (de Sousa *et al.*, 1996). Column productivity varied from 643 mgC m^{-2} d^{-1} in the north to 335 mgC m^{-2} d^{-1} in the south. On the other hand, pH_T is comparatively lower (~8.00) during inter-monsoon. Low pH_T values in this season could arise both from low primary productivity (Bhattathiri *et al.*, 1996) and higher bacterial activities (Ramaiah *et al.*, 1996). Mostly, the primary productivity was $\leq$ 310 mgC m^{-2} d^{-1} except at 21° N where it was 1097 mgC m^{-2} d^{-1}.

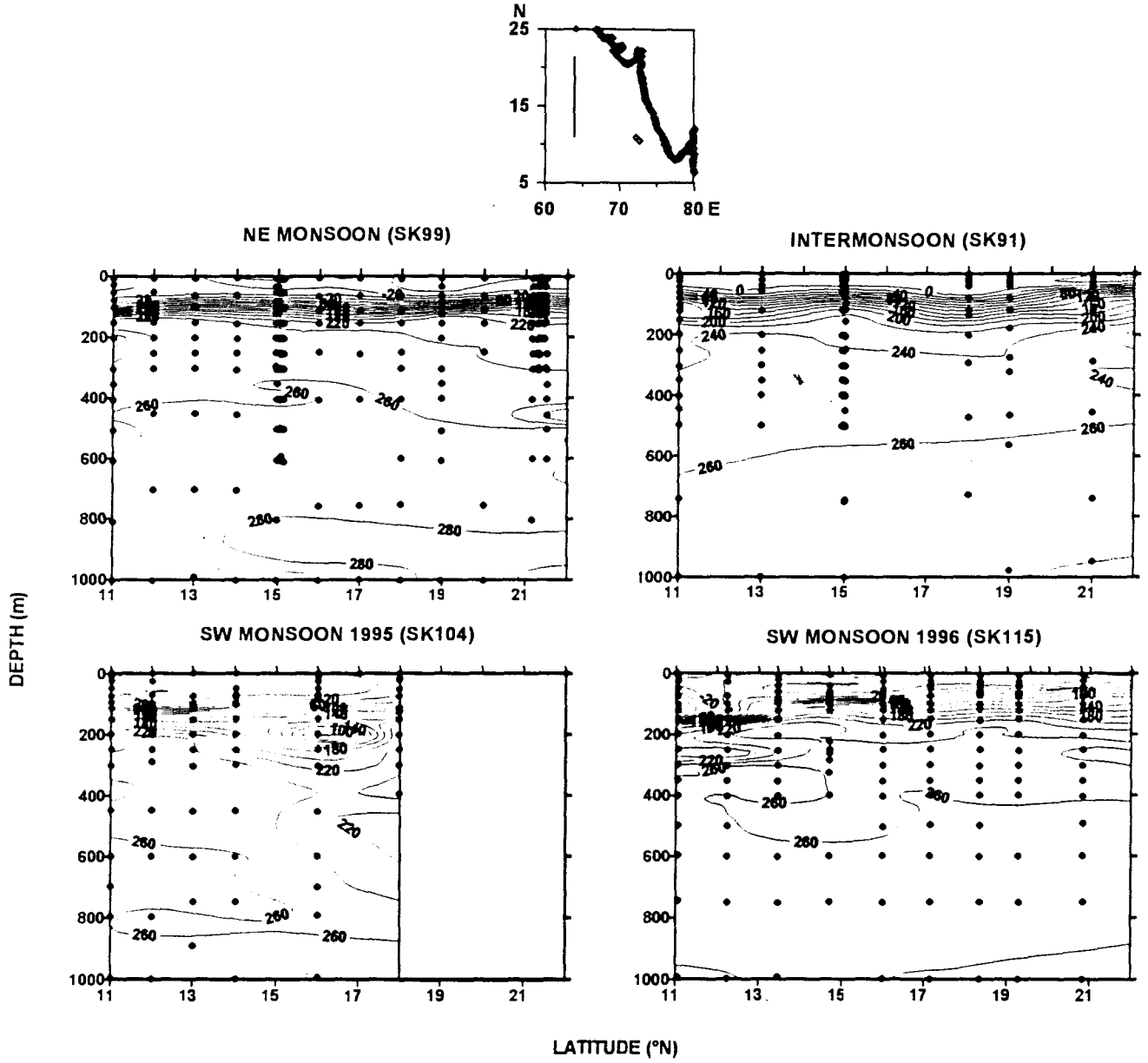

Fig. 4.3. Distribution of AOU (μM) along 64° E during different seasons in the Arabian Sea.

In suboxic waters, low pH_T waters of ~7.60 were observed in the study region during NE monsoon and SW monsoon (Fig. 4.2). Infact, values <7.60 were common during NE monsoon and SW monsoon whereas they varied between 7.60 to 7.85 in intermonsoon. pH_T in suboxic waters is mainly controlled by decomposition of soft tissue (eq. 4.1). Dissolution of Calcium carbonate increases pH. During the decomposition of organic matter oxygen is utilized. The oxygen utilized in this process can be evaluated (see 2.3.1.1) as Apparent Oxygen Utilization (AOU). The AOU higher during NE monsoon and 1996 SW monsoon than during intermonsoon and 1995 SW monsoon (Fig. 4.3). The seasonal variations in AOU agreed well with productivity patterns. AOU generally showed north-south variations. Denitrification is a bacterial process in which nitrate is reduced to molecular nitrogen under low oxygen conditions. There is a good correspondence in spatial and seasonal distributions of nitrate deficits (Fig. 4.4), pH_T and AOU. The negatve relation between AOU and pH_T (Fig. 4.5) is caused by alterations in organic matter synthesis/decomposition. Relationship between nitrate deficit (see 2.3.1.2), a measure of the extent of denitrification, and pH_T (Fig. 4.5) does show explicit negative relation as observed between the latter and AOU, mainly because the pH_T has already reached near minimum when the deficit turned positive. On the other hand, Fig. 2 does not suggest any significant differences in sub-surface pH_T values between 1995 and 1996 SW monsoon seasons.

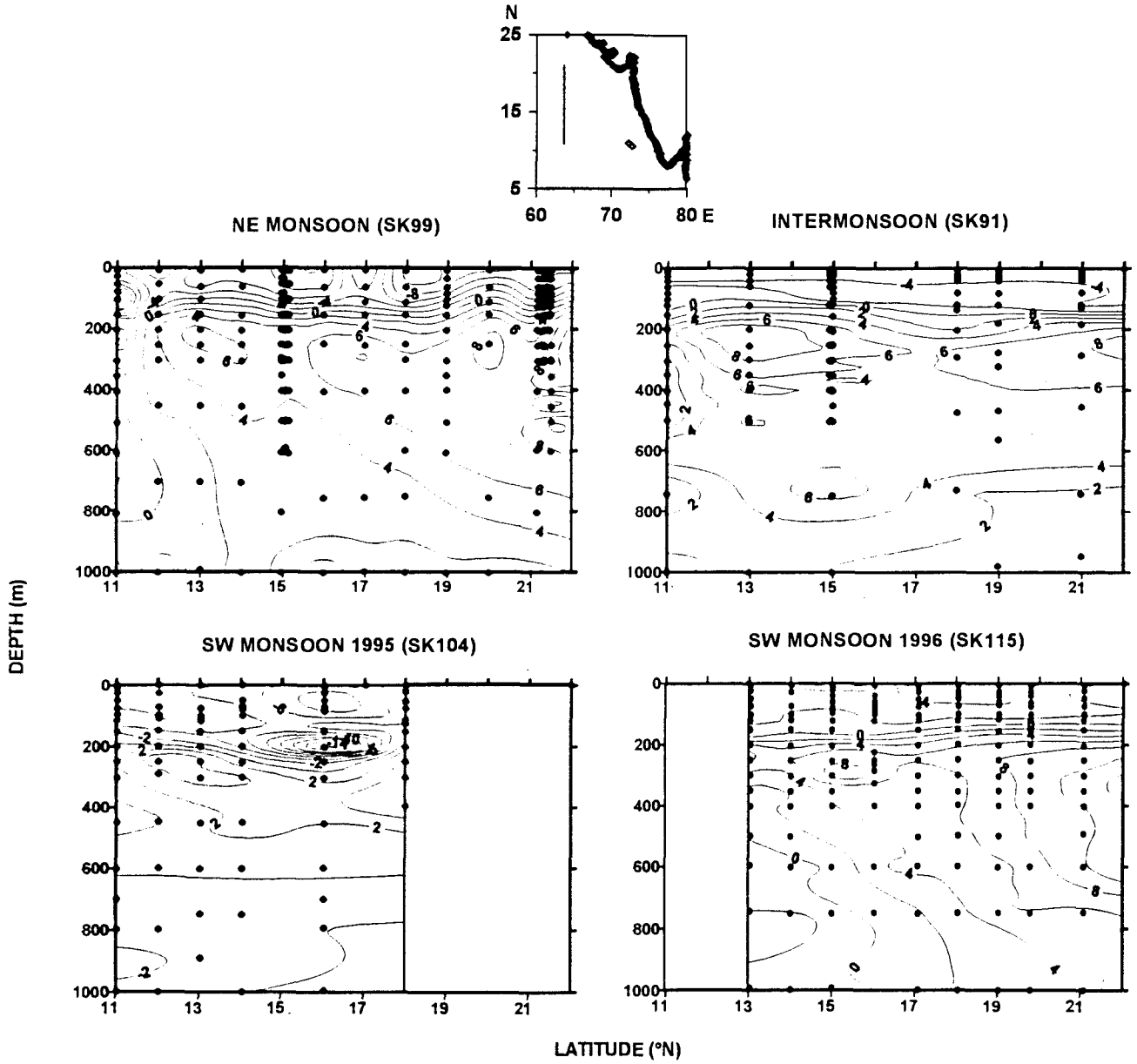

Fig. 4.4. Vertical distribution of nitrate deficit (μM) along 64°E during different seasons in the Arabian Sea.

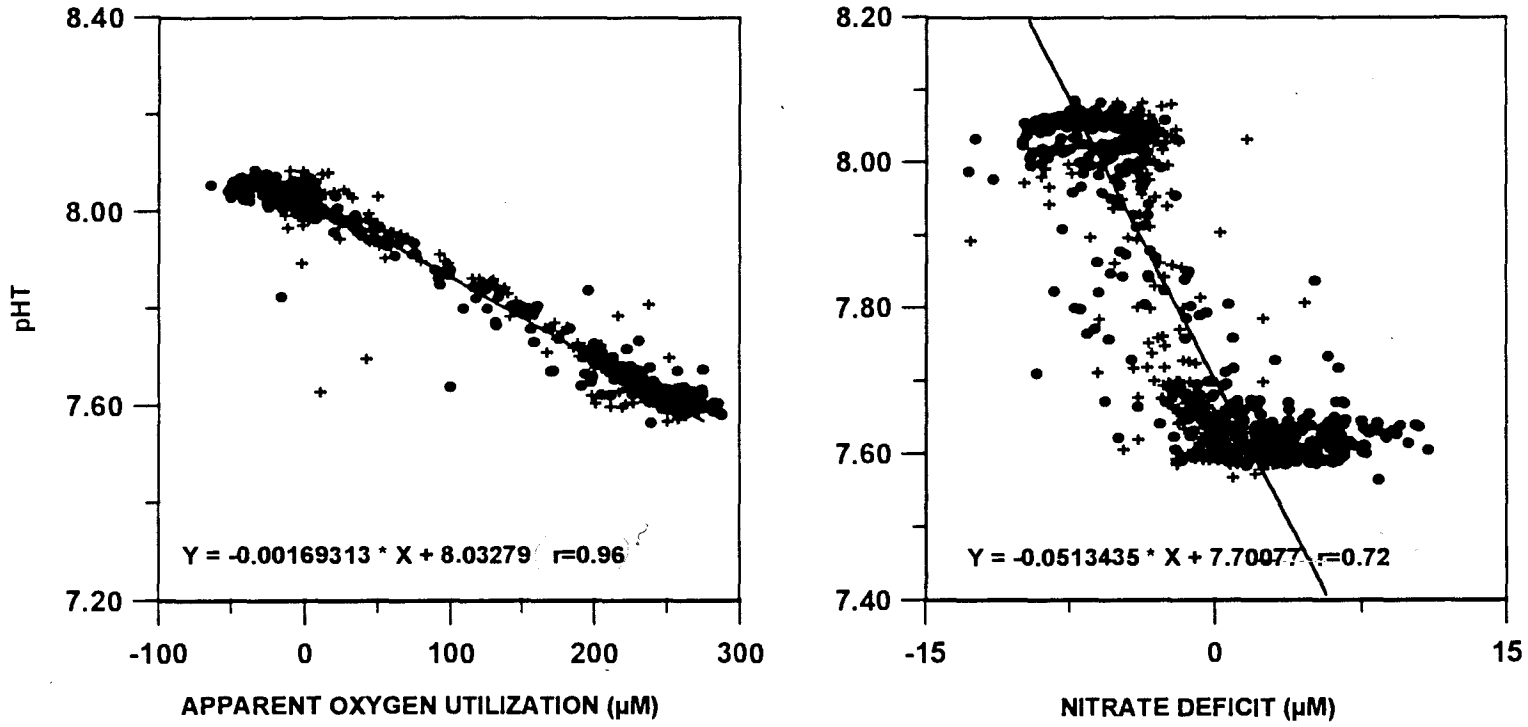

Fig. 4.5. Relations between pH_T and AOU and the former and nitrate deficit in all seasons.

4.1.2. Zonal variability in pH_T

Zonal variability in pH_T was studied along three sections, along 21° N, 15° N and 11° N. Along 21° N, the observations could be made only during NE monsoon and inter-monsoon seasons. Inclement weather conditions in 1995 and time constraints in 1996 prevented us from covering this section during SW monsoon. The pH_T values in surface waters were mostly ~8.00 when the 7.99 isoline has deepened towards coast in winter (Fig. 4.6) due to intense convective mixing off-Gujarat coast as evidenced by nitrate distribution where 2 µM isoline surfaced (Fig. 3.6). Column productivity was also high in the east (860 mgC m^{-2} d^{-1}) than in the west (643 mgC m^{-2} d^{-1}). Surface pH_T was >7.98 but < 8.00 during inter-monsoon. The sub-surface pH_T in near-shore waters is marginally higher in the west (Fig. 4.6). AOU showed strong variability between these two seasons with variations between 100 and 220 µM, and 100 and 140 µM during NE monsoon and inter-monsoon, respectively (Fig. 4.7). Nitrate deficit was found to be correspondingly intense (≥ 4 µM at 200 m) during NE monsoon which does not seem to be significant during inter-monsoon (Fig. 4.8). pH_T distribution in sub-surface layers is in accordance with those of oxygen and nitrate deficits.

Along 15°N, observations were made during pre-monsoon, (SS141), SW monsoon (SK103) and late-SW monsoon (SS136). The surface pH_T varied from

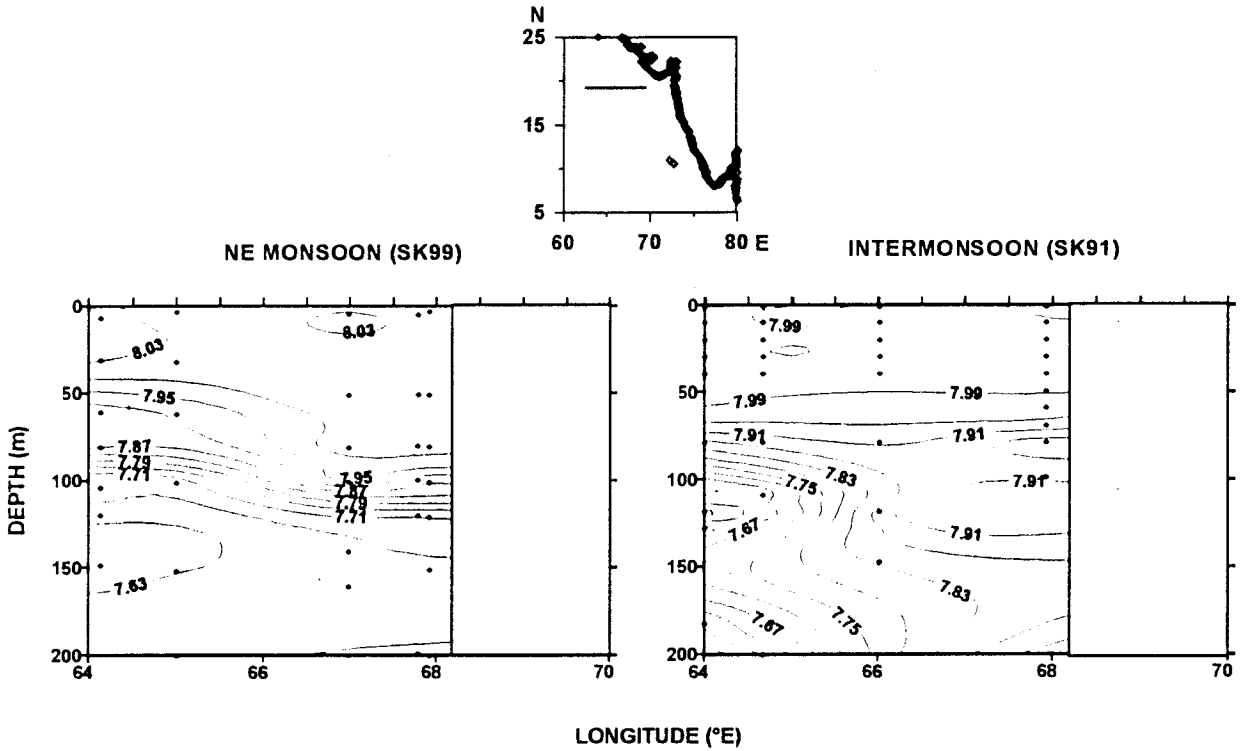

Fig. 4.6. East-west vertical variations in pH along 21° N in the Arabian Sea.

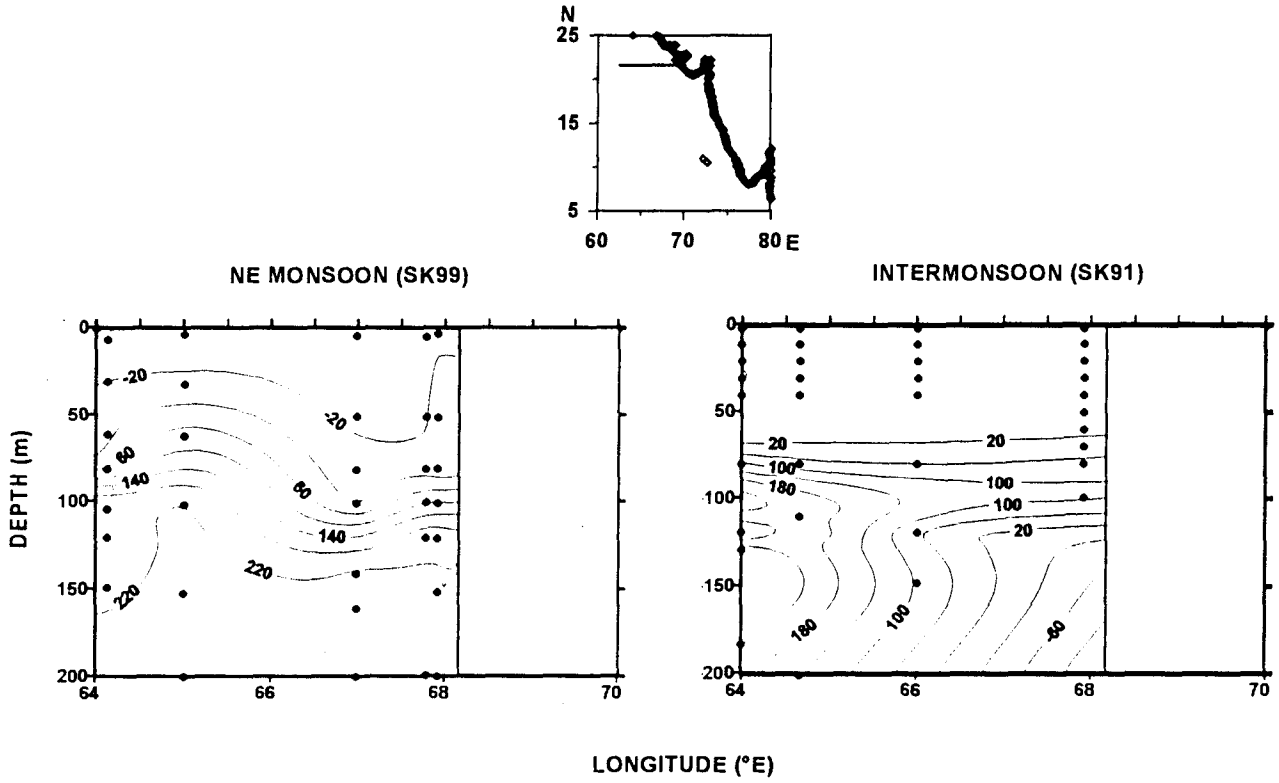

4.7. Vertical distribution of AOU (μM) along 21° N in the Arabian Sea.

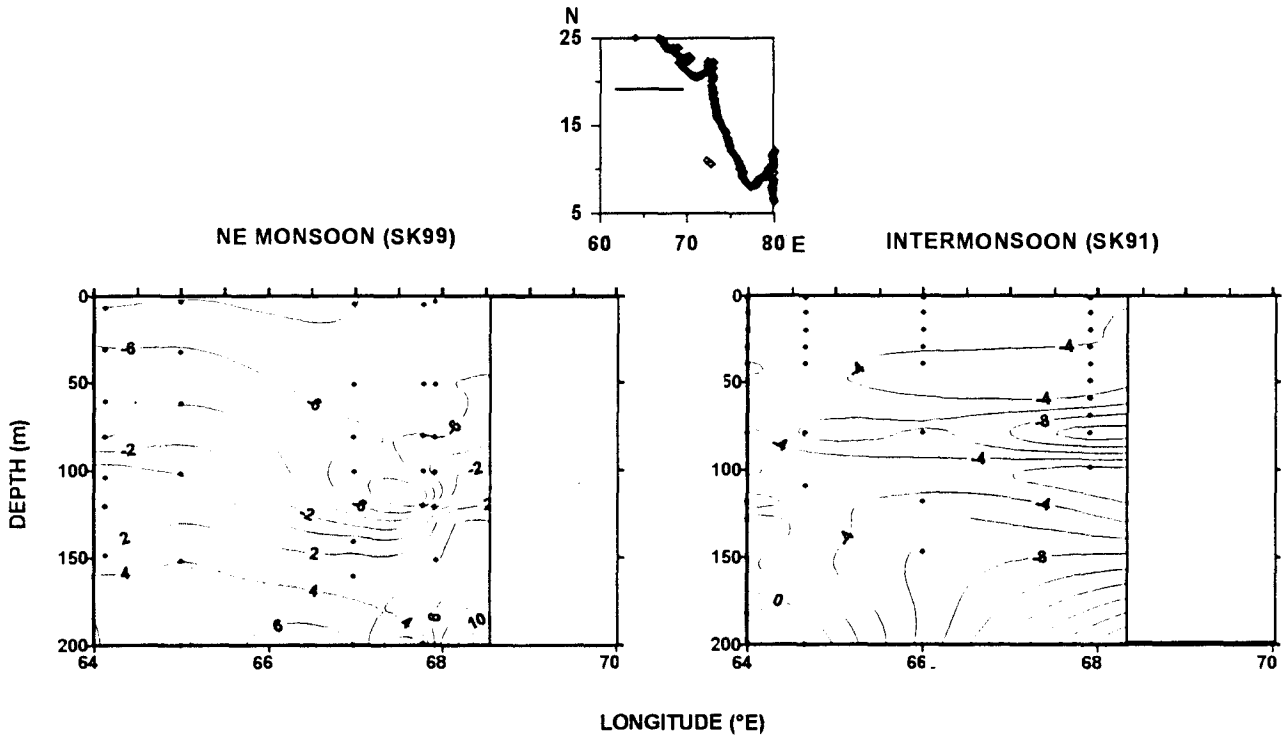

Fig. 4.8. Variations in nitrate deficit (μM) along 21° N in the Arabian Sea.

8.00 to 8.05 during SS141 and SS136 monsoon whereas it was >8.10 during SK103 (Fig. 4.9) due to higher rates of primary production driven by coastal upwelling. The upwelling resulted in enrichment of nutrients in surface layers along the coast (Fig. 3.12). The 2 μM nitrate contour has risen to surface from a depth of 150 m. During all periods of observations comparatively higher pH_T was observed in coastal regions than in open sea regions.

In sub-oxic waters, pH_T was low and centred around 7.65 which is due to decomposition of higher loads of organic matter in response to NE monsoon overturning and upwelling driven primary production. Intensity of decomposition depends also on the time lag between production and bacterial response (Ducklow, 1993), rates of sinking flux and availability of dissolved oxygen. Low pH (<7.60) in shallow coastal waters could again be due to higher rates of remineralization. Higher amounts of oxygen utilization (>250 μM; Fig. 4.10) and high nitrate deficits (2-6 μM; Fig. 4.11) observed during the SW monsoon suggest prevalence of reducing conditions which trigger denitrification.

Along 11° N, surface pH_T was mostly around 8.03 during all seasons (Fig. 12), except for high pH values in the coastal region (~8.10) during SW monsoon as a consequence of upwelling driven productivity. The isolines become shallower towards coast during SW monsoon due to wind induced upwelling. Lower pH_T values prevailed in the sub-oxic waters during SW monsoon than in inter-

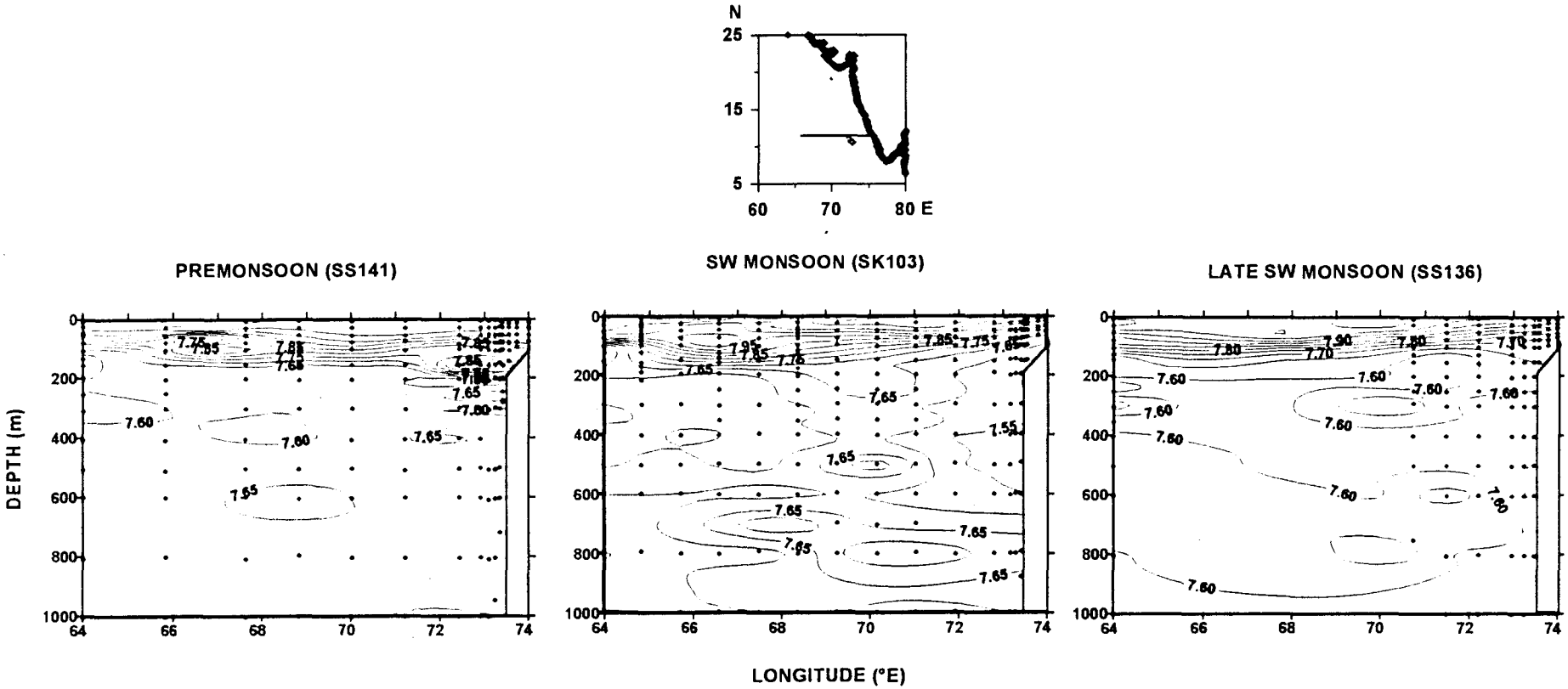

Fig. 4.9. Distribution of pH_T along 15° N during different seasons in the Arabian Sea.

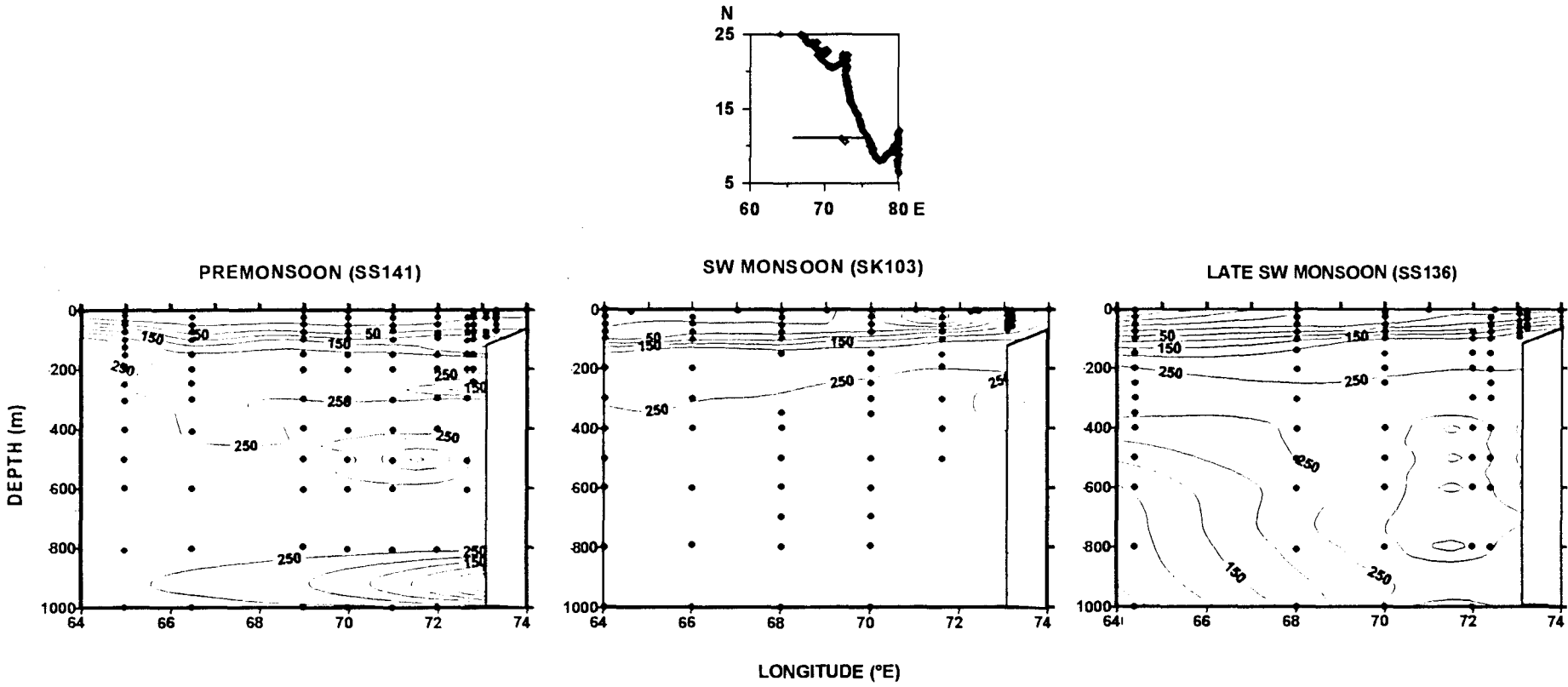

Fig. 4.10. Variations in AOU (μM) along 15° N in different seasons in the Arabian Sea.

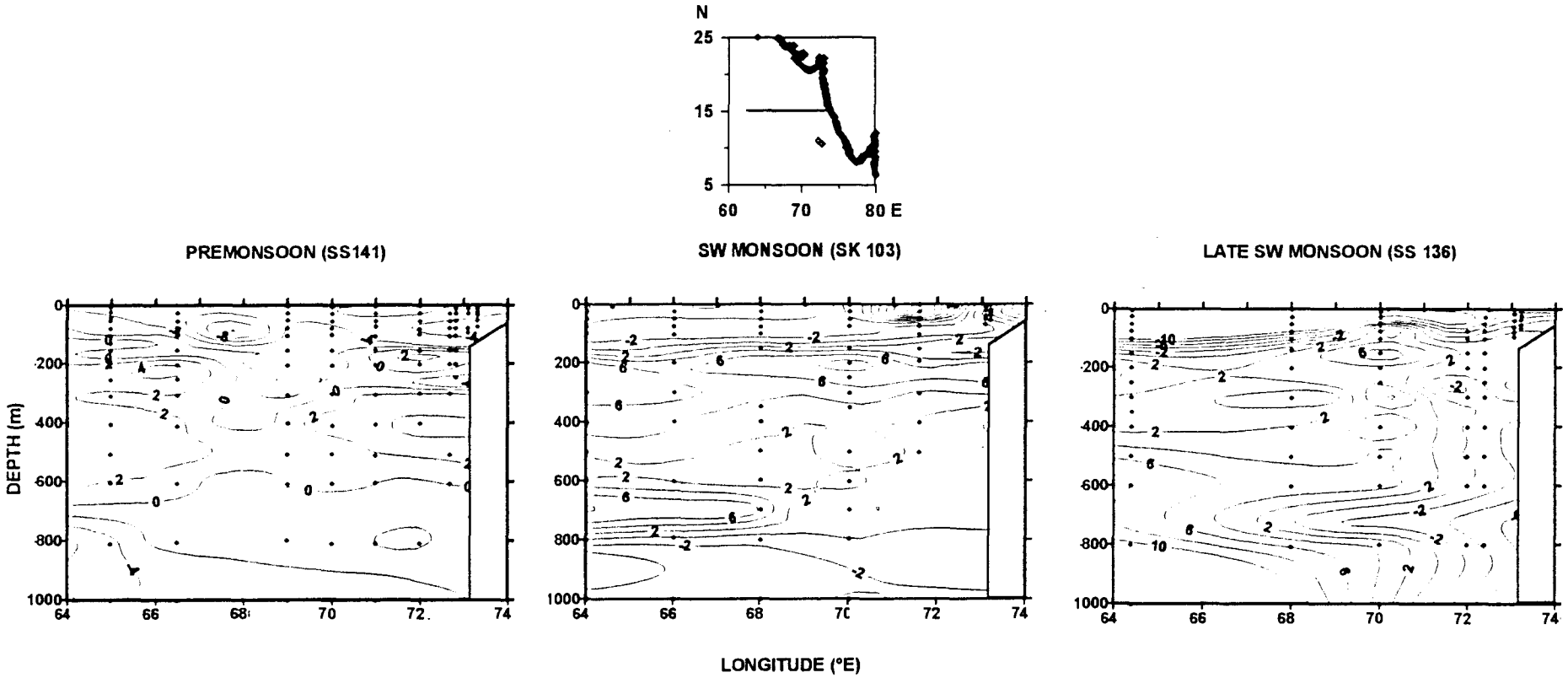

Fig. 4.11. East-west variations in nitrate deficit (μM) along 15° N in different seasons in the Arabian Sea.

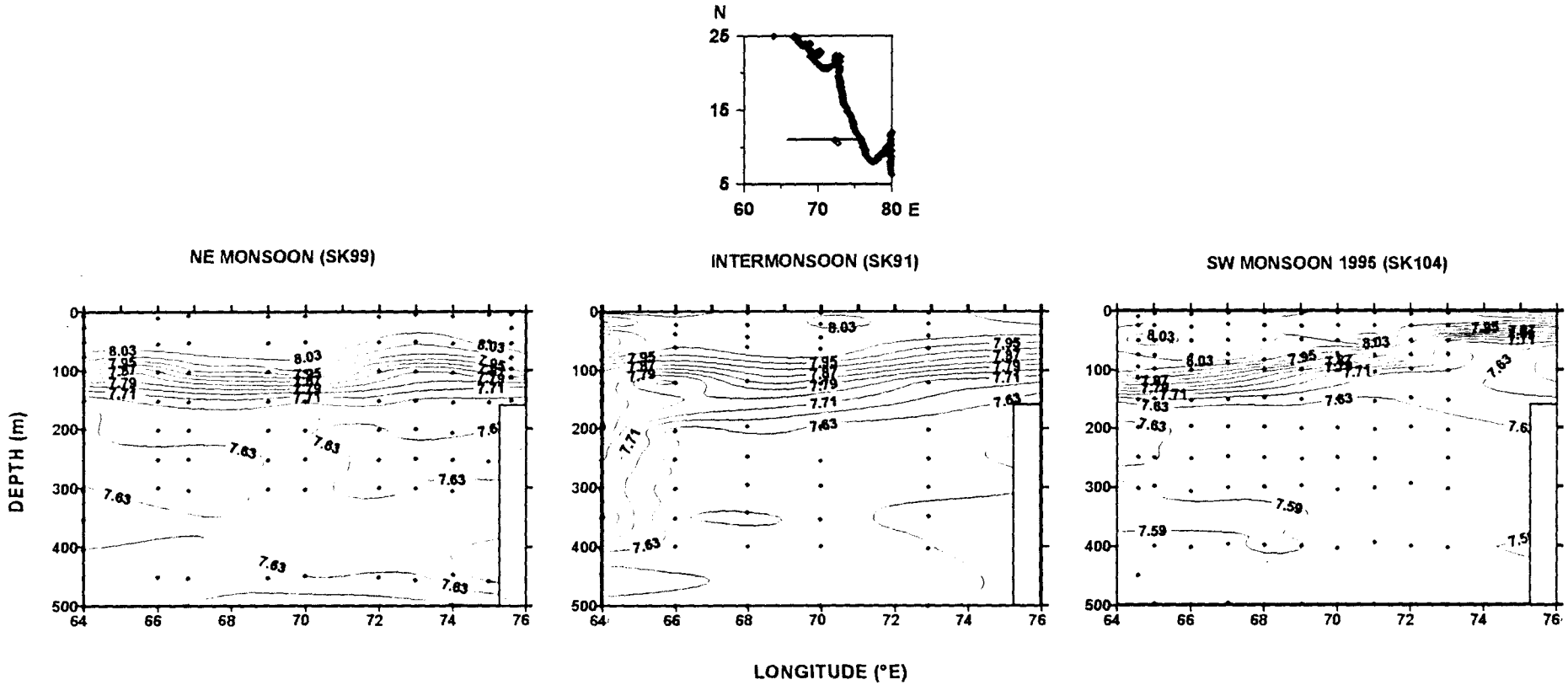

Fig. 4.12. Distribution of pH_T along 11° N during different seasons in the Arabian Sea.

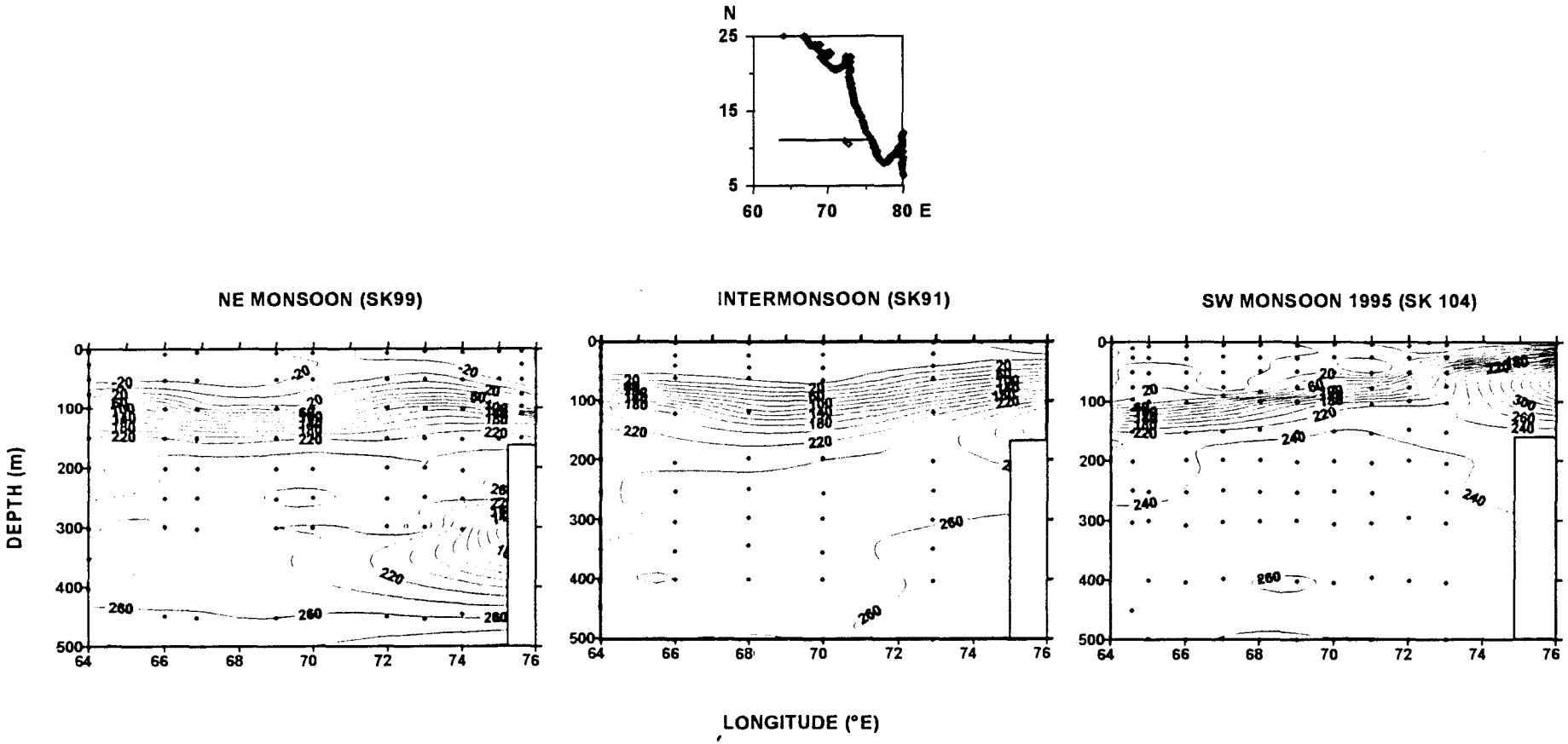

Fig. 4.13. Variations in AOU (μM) along 11° N in the Arabian Sea during different seasons.

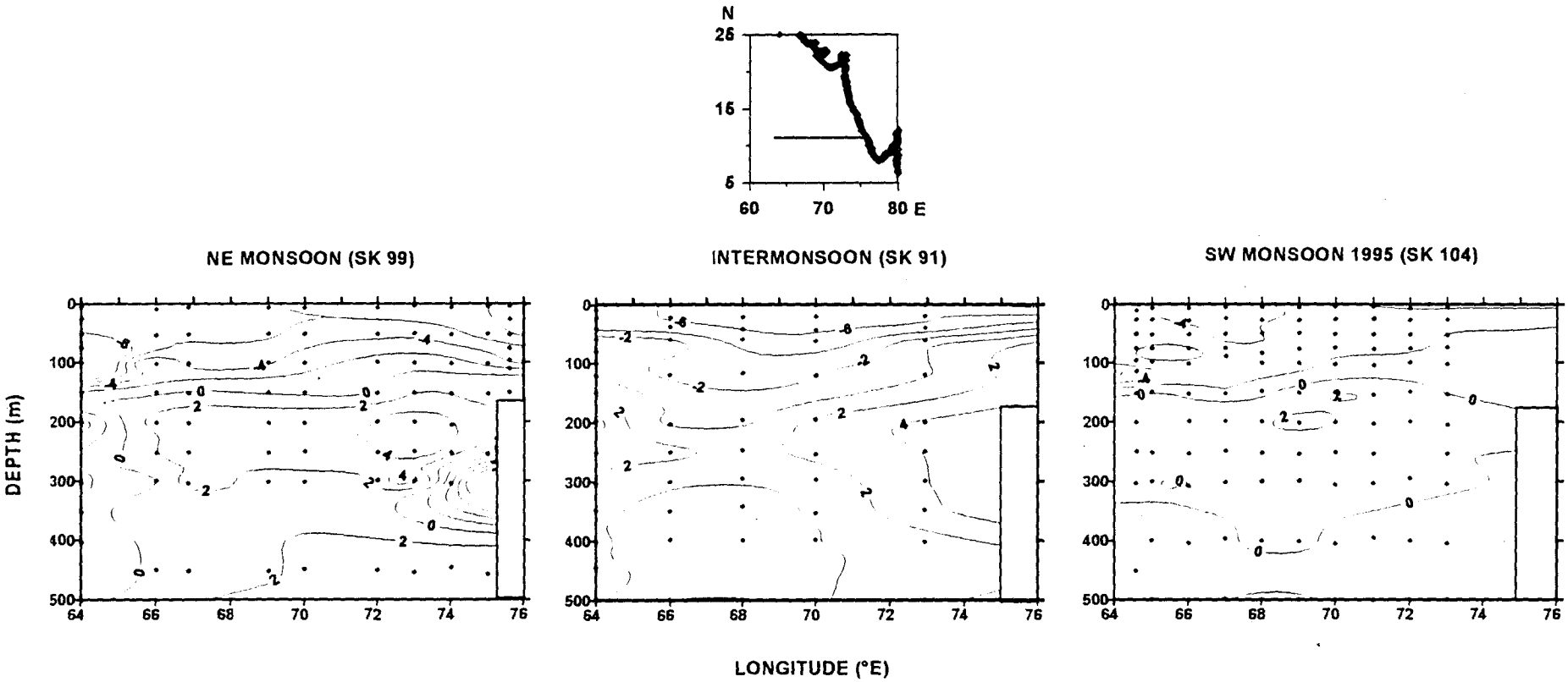

Fig. 4.14. Distribution of nitrate deficit (μM) along 11° N in the Arabian Sea during different seasons.

monsoon and in NE monsoon due to higher rates of regeneration. The AOU distribution appears to be nearly the same in all seasons (Fig. 4.13) while the nitrate deficit seems to be high during the NE monsoon (2-4 μM; Fig. 4.14).

pH_T along 90° E, in the Bay of Bengal, showed significant north-south variability (Fig. 4.15). pH_T in surface waters varied from >8.03 to <7.99 from north to south. High pH_T in the north can be attributed to high productivity and to influx of fresh waters where 32.200 psu salinity was observed. In sub-oxic waters pH_T was lower in the north due to intense remineralization. AOU was > 240 μM (Fig. 4.16) in subsurface layers that increased northward due to high rates of remineralization in the north whereas no deficit in nitrate seemed to occur (Fig. 4.16) in concurrence with the results of George *et al.* (1994). The measured pH_T in the Andaman Sea (SK 118) agree with the vertical trends shown in Fig. 4. 15. While the values in surface ranged between 8.00 and 8.10, at 1000 m they were ~7.65. The former (surface) were higher whereas the latter were lower when compared to those to the west of the Andaman Sea (see Fig. 4.15). This might have been due to higher productivity in the Andaman Sea than in open Bay of Bengal.

Meridional and zonal variabilities suggest that pH_T reflects a net effect of biological and physical forcings in the surface waters. Winter cooling and SW monsoonal upwelling inject nutrients into surface leading to enhancement in

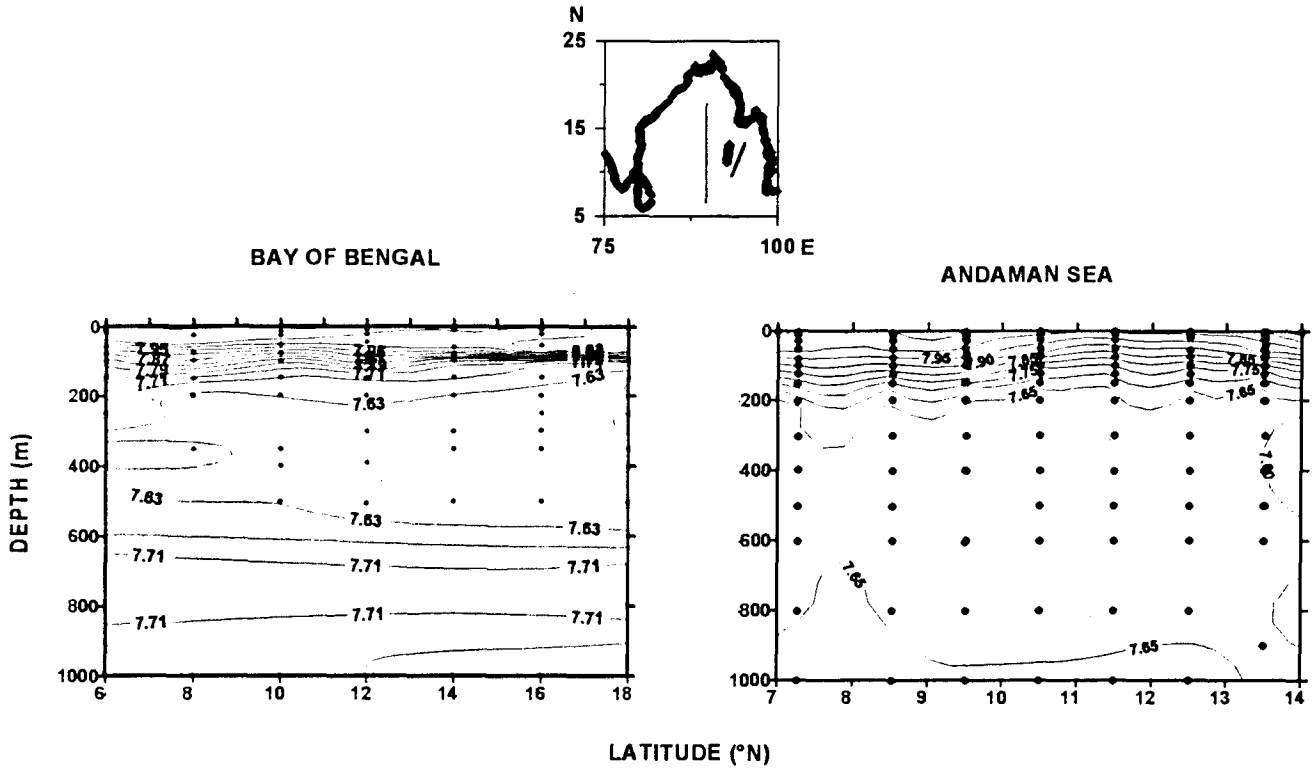

Fig. 4.15. Distribution of pH_T in the Bay of Bengal and Andaman Sea.

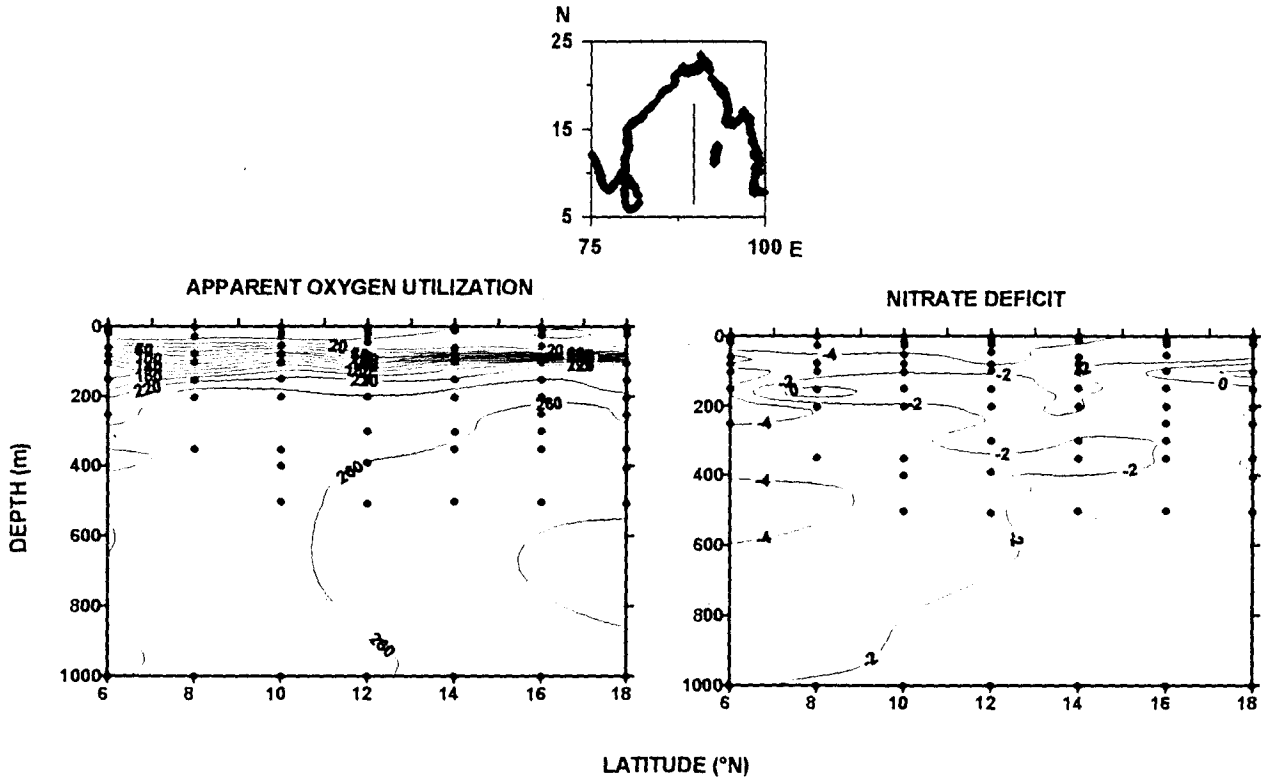

Fig. 4.16. Distribution of AOU (μM) and nitrate deficit (μM) along 90° E in the Bay of Bengal.

surface productivity. Such injected waters are of low pH_T. Consequently, pH_T does not exhibit a definite northward increase since the observed one is net from both these forcings. Bacterial decomposition and/or denitrification processes play major roles in regulating the pH_T in sub-surface layers. High organic matter input from surface layers during monsoons leads to intense reducing conditions in subsurface waters. As proton is released during decomposition processes (eq.1) it leads to lowered pH_T values in sub-oxic waters. During inter-monsoon seasons, however, the conditions appear to be different. Surface waters are depleted in nutrients and oligotrophic. Although, organic matter synthesis is less the regeneration of organic matter produced in the earlier seasons continues in inter-monsoon. Furthermore, Ramaiah *et al.* (1996) have observed a several fold increase in bacterial population during inter-monsoon compared to monsoons. This accounts for the northward decrease in pH_T, particularly in intermediate waters.

From the foregoing the highlights in pH_T variability are:

- **Neither seasonal nor north-south gradients in pH_T in surface waters in Arabian Sea could be discerned but northward increase in Bay of Bengal was evident in surface layers.**
- **Coastal surface waters have relatively high values**

- **Surface values reflect net pH_T resulting from physical and biological forcings**
- **Sub-surface values are low in the north in all seasons in Arabian Sea and Bay of Bengal**
- **No great seasonal variability occurred in intermediate layers**
- **pH distribution was consistent with trends in AOU and nitrate deficits**

4.2. Variability in Total Alkalinity

Total Alkalinity (TA) is defined as the amount of hydrogen ions required to neutralize all the carbonate, bicarbonate and borates in 1 kg of sea water

$$TA = 2\,CO_3^{2-} + HCO_3^{-} + B(OH)_4^{-} + OH^{-} - H^{+} \qquad (4.2)$$

A shift in inorganic carbon system occurs as a result of primary production/ decomposition processes

$$106\,CO_2 + 16\,NO^{-}_3 + MgHPO_4 + 16\,H^{+} + 122H_2O \Longrightarrow$$
$$(CH_2O)_{106}(NH_3)_{16}(MgHPO_4)_{(org)} + 138\,O_2 \qquad (4.3)$$

that can alter alkalinity levels. According to the above reaction, the shift in alkalinity will be +15 units since 16 H^+ and one base are removed. During

decomposition this reaction will be reversed and consequently the hydrogen ion increases with corresponding decrease in alkalinity. In case of denitrification

$$2\ NH_{3\,(org)} + 1.5\ O_2 \text{ ===> } N_2 + 3\ H_2O \qquad (4.4)$$

15 units organic nitrogen consumes 11.25 units of oxygen instead of 30 units required for the formation of nitrate

$$NH_{3\,(org)} + 2\ O_2 \text{ ===> } H^+ + NO_3^- + H_2O \qquad (4.5)$$

In calcium carbonate formation 2 moles of bicarbonate ions are consumed for each mole of calcium ion (eq. 4.6) and one mole each of calcium and CO_2 lead to shifts by 2 and 1 units, respectively, in alkalinity and total carbon dioxide. The released CO_2 goes either to atmosphere or consumed by plankton.

$$Ca^{2+} + 2\ HCO_3^- \text{ ==> } CaCO_{3(s)} + CO_2 + H_2O \qquad (4.6)$$

$$CO_2 + H_2O \text{ ===> } CH_2O_{(org)} + O_2 \qquad (4.7)$$

In general, carbohydrate production is about five times larger than the carbonate production in open ocean. Thus, this will facilitate increase in pH

(Dyrssen, 1992) due to autoprotolysis (eqs. 4.8 or 4.9)

$$2\,HCO_3^- \text{===>} CO_2 + H_2O + CO_3^{2-} \qquad (4.8)$$

or

$$H^+ + HCO_3^- \text{===>} CO_2 + H_2O \qquad (4.9)$$

Decomposition of organic matter facilitates simultaneous calcium carbonate dissolution (eq. 4.10)

$$CaCO_{3\,(s)} + CH_2O_{\,(org)} + O_2 \text{ ===> } Ca^{+2} + 2\,HCO_3^- \qquad (4.10)$$

Precision of our TA measurements was shown in Table 4.1. A typical total alkalinity profile in winter (Fig. 4.17) in the Arabian Sea depicts a general low (at ~200 m) compared to that in surface and deep layers. In relation to deep waters surface waters have low alkalinity because of the removal of carbonate ion through precipitation of calcium carbonate by organisms belonging to foraminifera, pteropoda and cocolithophoridae in the euphotic zone. Such precipitation triggers the **carbonate pump** (Sabine *et al*, 1995), which is a part of the **biological pump**. After the death of organisms these skeletal tests sink into deep waters that are under-saturated with respect to the carbonate mineral

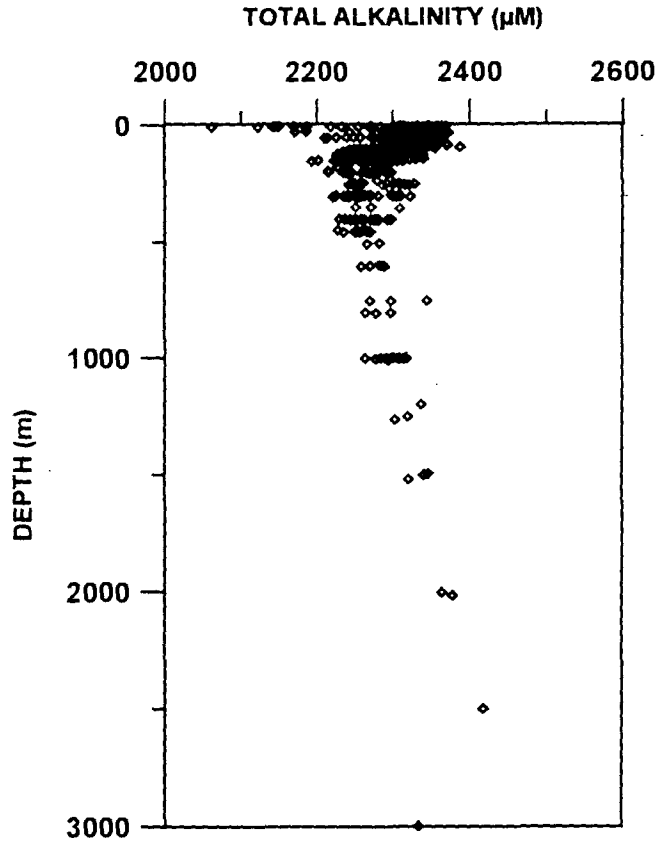

Fig. 4.17. Vertical profile of total alkalinity during NE monsoon in the Arabian Sea.

phase. The consequent dissolution of these tests in deep ocean releases carbonate ions thereby increasing the alkalinity of the deep waters. The rapid decrease in TA with depth in the upper 200 m water column is because of the effect of oxidation of organic matter (eq. 4.3) on alkalinity. In these layers the magnitude of organic matter decomposition dominates over that of carbonate minerals and hence a net decrease in TA. Below 500 m, TA begins to increase since dissolution of carbonate minerals become more important than soft tissue regeneration.

4.2.1. Meridional variability in Total Alkalinity

Total alkalinity exhibited significant variability along 64° E in the Arabian Sea (Fig. 4.18). Surface TA varied from 2200 to 2350 µM during NE monsoon whereas it varied between 2400 and 2420 and from 2320 to 2360 µM during SW monsoon and inter-monsoon, respectively. TA values in SW monsoon 1996 seem to be slightly higher than in other periods shown in Fig. 4.18. Comparatively higher values of TA were observed in the north, by about 40-60 µM than in southern Arabian Sea, due to higher productivity. The productivity was much higher along this meridional section ranging between 347 and 1782 mgC m^{-2} d^{-1} compared to that in other seasons. In both the SW monsoon seasons of 1995 and 1996 TA increased around 17° N, as shown by surfaced relatively higher TA contours, because of sub-surface/lateral inputs driven by

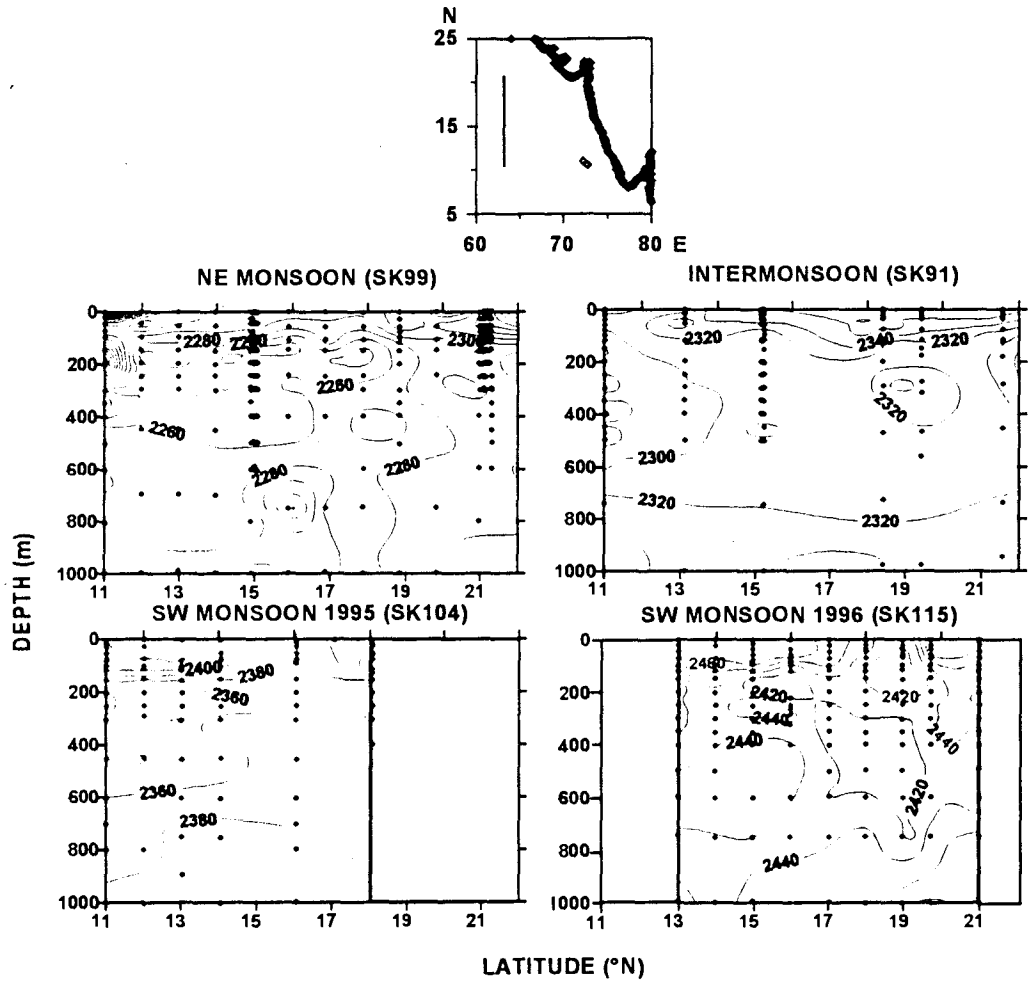

Fig. 4.18. Distribution of total alkalinity (μM) along 64° E in the Arabian Sea during different seasons.

divergence or coastal upwelling processes. These higher surfaced TA signatures (Fig. 4.18) are in corroboration with those of oxygen (Fig. 3.2), nitrate (Fig. 3.3) and pH_T (Fig. 4.2) in SW monsoon.

TA in the sub-surface waters showed large variations during all three seasons. Low alkalinity waters (of 2260-2280 µM) observed during NE monsoon are due to a decrease in pH triggered by intense organic matter decomposition. Higher AOU (Fig. 4.3) and lower pH (Fig. 4.2) values provide evidence for this, particularly in the north. Relatively low TA in NE monsoon is also in association with the largest extent of denitrification (Fig. 4.2). During inter-monsoon, TA varied from 2280 to 2320 µM in intermediate waters. Although, oligotrophic conditions prevail during this season, bacterial activity was observed to be several folds higher than in other seasons which was in response to increased organic matter supply promoted by NE monsoon convective mixing (Ramaiah *et al.*, 1996). Higher oxygen utilization (Fig. 4.3) and deficit in nitrate (Fig. 4.5) suggest the prevalence of reducing conditions that lead to a decrease in pH. Although low pH waters are corrosive to skeletal bodies the decrease in alkalinity in these waters is due to complexation of released carbonate ion by proton. Below the oxygen minimum zone, TA increased with depth due to increase in dissolved carbonate ions, through enhanced dissolution of calcium carbonates, at high pressures. Sediment trap experiments along 15° N (Nair *et al.*, 1989) revealed invariable carbonate fluxes from east to west, although, the

productivity is higher in the coastal upwelling regions of eastern and western Arabian Sea (Qasim, 1977). Therefore, the high TA values can be accounted for excess dissolution under reducing conditions (George *et al.*, 1994). The denitrification processes obviously plays a major role on the dissolution of carbonate minerals in the Arabian Sea, in particular.

4.2.2. Zonal variability in Total alkalinity

Along 21° N, TA varied from 2280 to 2340 µM with low values towards the coast during NE monsoon whereas it centred around 2360 µM during inter-monsoon (Fig. 4.19). Low alkalinity isolines reaching the surface near the coast are driven by NE monsoon cooling. The convective mixing brings relatively low alkalinity waters, from the upper thermocline region (Fig. 4.17), upward. As this mixing triggers higher productivity (860 mgC m^{-2} d^{-1}) large amounts of skeletal carbonates might have been produced. Sub-surface TA concentrations were low (2280 to 2300 µM) during NE monsoon whereas they were from 2300 to 2380 µM during inter-monsoon due to intense remineralization following increased productivity in the NE monsoon. AOU distribution (Fig. 4.7) supports this since it is higher by ~100 µM during NE monsoon than in inter-monsoon. Nitrate deficit was 2-6 µM during NE monsoon while no deficit occurred in inter-monsoon (Fig. 4.8) suggesting that regeneration processes largely control alkalinity in the sub-oxic waters. Low pH (Fig. 4.6) values were also observed

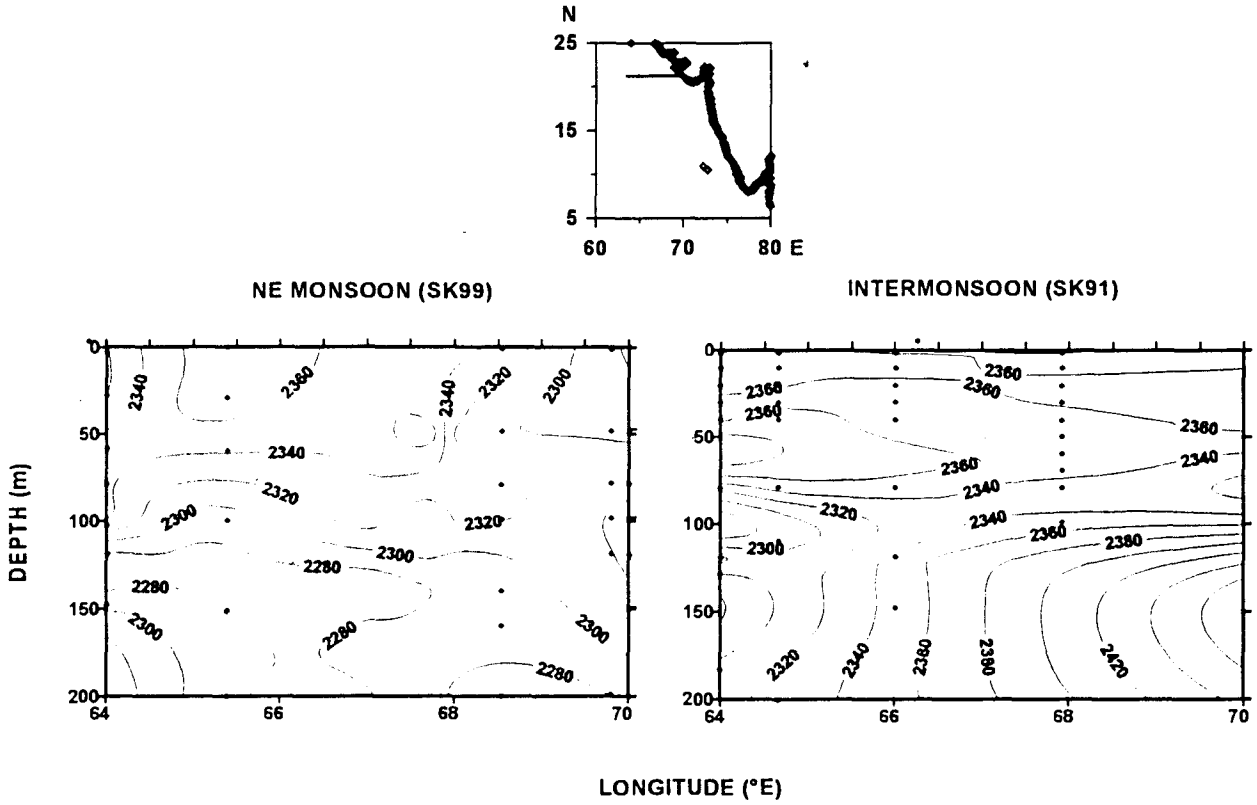

Fig. 4.19. Seasonal variations in total alkalinity (μM) along 21° N in the Arabian Sea during different seasons.

during NE monsoon compared to those in inter-monsoon. These observations support intense remineralization as the mechanism for the observed low alkalinity values in the oxygen minimum zone.

While there was no significant east-west gradient in TA in surface layers along 11° N in inter-monsoon season the differences were greater in winter and SW monsoon (Fig. 4.20). For instance, between 71 and 74° E at 20 m the TA changes by nearly 200 μM in SW monsoon. TA was also higher during SW monsoon than in other two seasons (Fig. 4.20). Coastal waters contained very low TA (<1900 μM) than in the offshore waters in SW monsoon due to high river discharge. Widespread low alkalinity waters in the sub-surface layers were in agreement with high AOU (Fig. 4.13) and nitrate deficits (Fig. 4.14) which is a reflection of extent of organic matter decomposition. Low pH values were also in accordance with this (Fig. 4.12).

TA was generally lower in the Bay of Bengal than in the Arabian Sea (Fig. 4.21). The GEOSECS data (Weiss *et al.*, 1983) showed slightly lower values in the upper 500 m of the water column in the Bay. There was no significant difference in waters deeper than 500 m. In the surface layers, TA decreased northward in accordance with the salinity distribution (Fig. 4.21) while there were no significant north-south gradients in subsurface layers of the Bay of Bengal. The measured TA in the Andaman Sea (SK 118) agrees with the

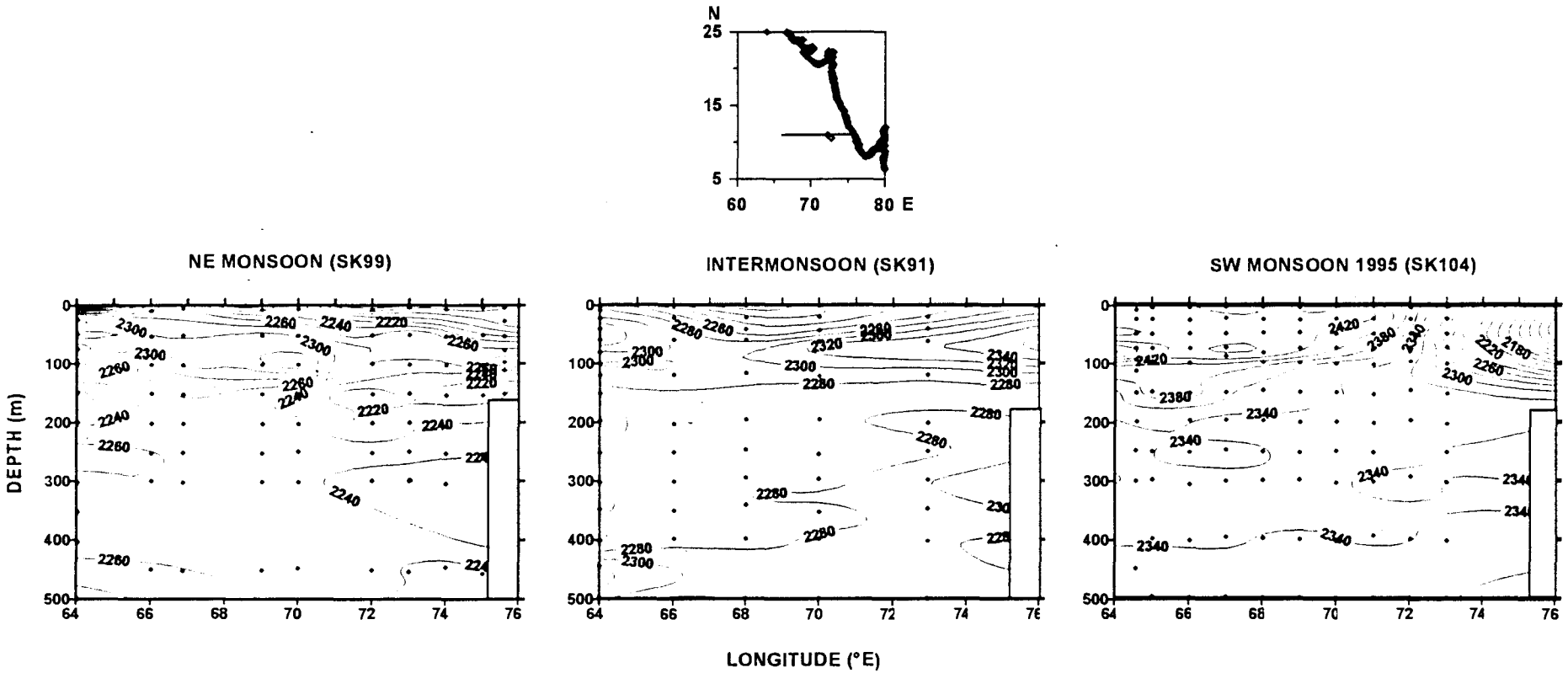

Fig. 4.20. Distribution of total alkalinity (μM) along 11° N during three seasons in the Arabian Sea.

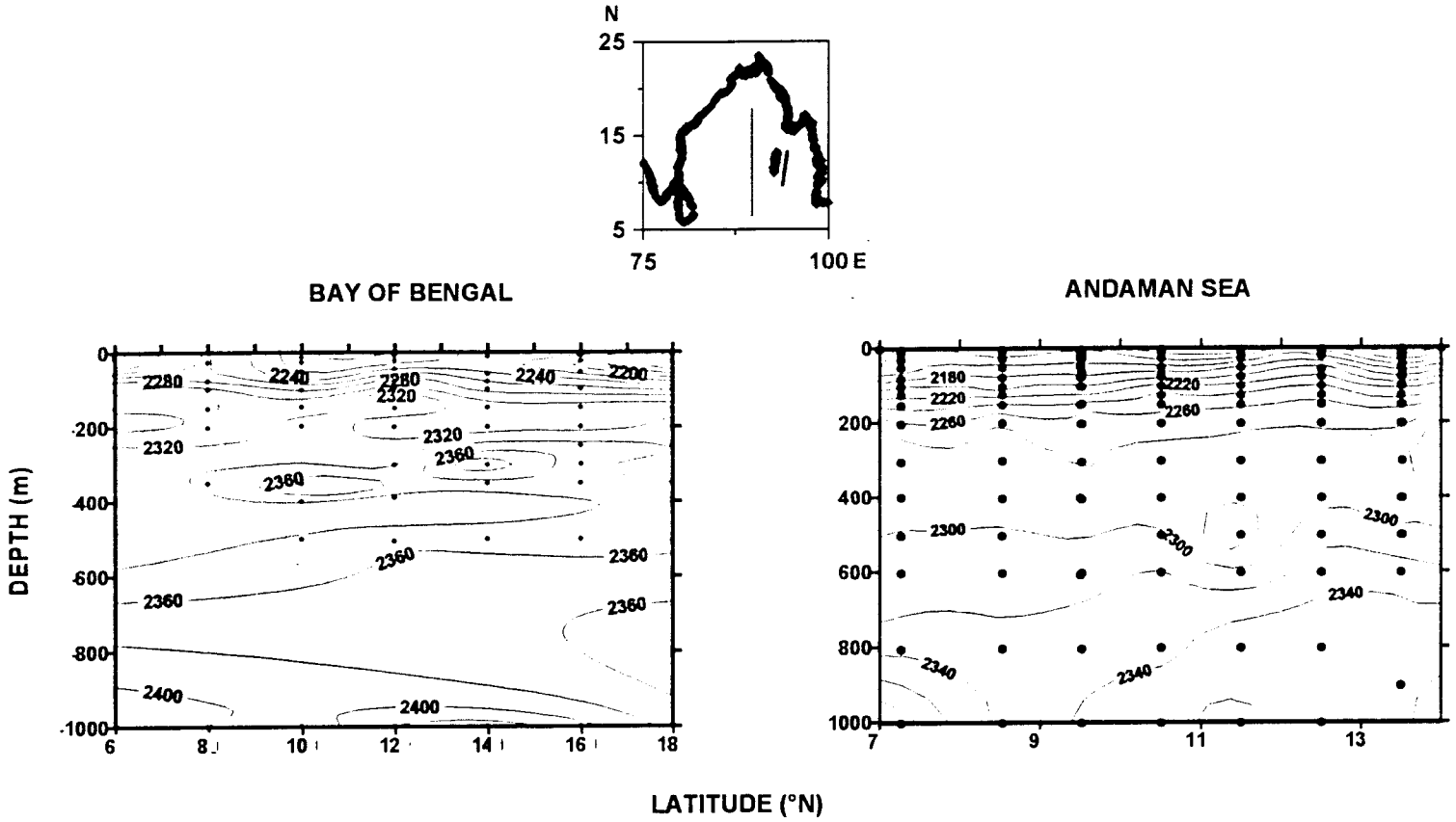

Fig. 4.21. Distribution of total alkalinity (μM) in the Bay of Bengal and Andaman Sea.

vertical trends shown in Fig. 4. 21. While the values in surface ranged between 2100 and 2160 μM, at 1000 m they were between 2320 and 2340 μM and lower values in the surface waters of northern Andaman Sea could be due to influx of river waters from Irrawady-Salween system. Surface salinities are lower (32.2-32.8 psu) in the north and increased towards the south (32.3-33.4 psu). Comparatively, lower values were observed in the northern Andaman Sea than in the eastern Bay of Bengal could be due to influence of water discharge from Irrawady-Salween system (Varkey *et al* 1996) and also due to high rates of precipitation which exceeds evoporation by atleast 0.80 m y^{-1} (Ramanathan and Pisharoty, 1972). Surface waters alkalinity were lower throught the water column when compared to those to the west of the Andaman Sea (see Fig. 4.21). This might have been due to higher productivity in the Andaman Sea than in open Bay of Bengal.

A plot of salinity versus alkalinity in the Arabian Sea (Fig. 4.22) shows that TA behaves nearly conservatively in surface waters despite the precipitation of calcium carbonate. Subsequent dissolution of these skeletal tests and the consequent alkalinity enrichment in deep waters can be clearly be seen in Fig. 4.22 when low salinity waters (<35.500 psu) deviated from the main positive relationship. On the other hand, lower TA in surface low salinity waters together with higher temperatures suggest that these low salinity warm water have their origin in the Bay of Bengal (Fig. 4.22). The Total Alkalinity decrease at 10-20^{o} C

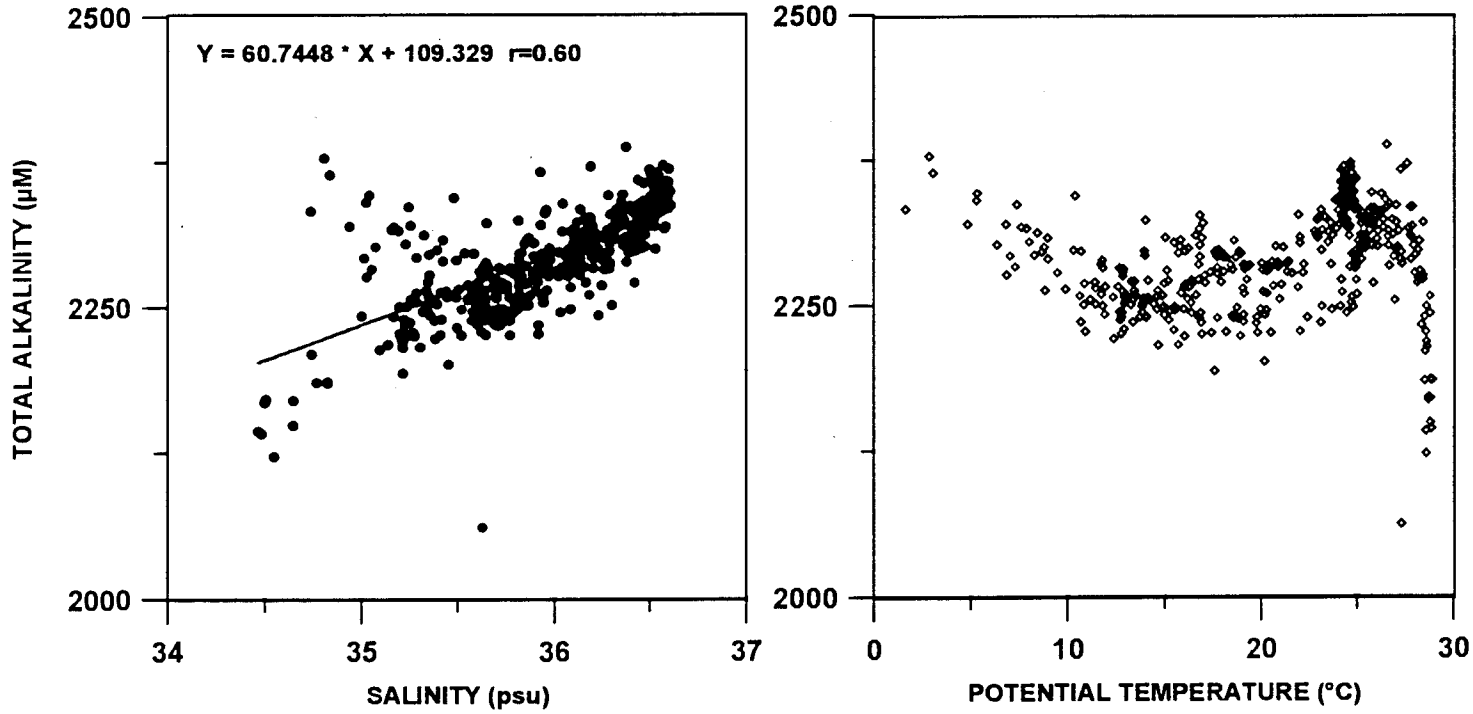

Fig. 4.22. Relation of total alkalinity with salinity and potential temperature in the Arabian Sea.

corresponds to its low in the sub-oxic zone (Fig. 4.17). The increase at $\theta \leq 10°$ C is due to increased dissolution of skeletal matter in deep waters under pressure. The relation between pH_T and alkalinity (Fig. 4.23) is positive, in general, but with two clusters of points with somewhat negative relations at both ends of the positive curve. The cluster with high pH belongs to surface waters since biological production ideally leads to higher pH_T and lower TA. The other at lower pH_T represents deep waters where pH_T variation is not so great but TA increases due to pressure effect. In spite of the expected aragonite dissolution TA decreases in sub-oxic waters due to the dominant release of proton during organic matter regeneration. This is well supported by the observed TA relation with AOU, which is exactly the opposite of trend with pH_T (Fig. 4.23). These relations suggest three segments in TA relations with pH_T and AOU; one each for surface and deep waters while the other for thermocline and sub-oxic waters. The relations for alkalinity with salinity and potential temperature in the Bay of Bengal are shown in Fig. 4.24. Alkalinity is strongly correlated to salinity and temperature exhibiting its conservative behaviour although a break in each relation is obvious separating surface and intermediate waters. The relation with salinity is in excellent agreement with the Bay of Bengal trend noted by Takahashi *et al.* (1982) based on limited data obtained in GEOSECS expedition. Its relations with pH_T and AOU (4.25) however exhibit opposite relationships compared to those observed for the Arabian Sea (Fig. 4.23). These relations are also a result of low salinity and

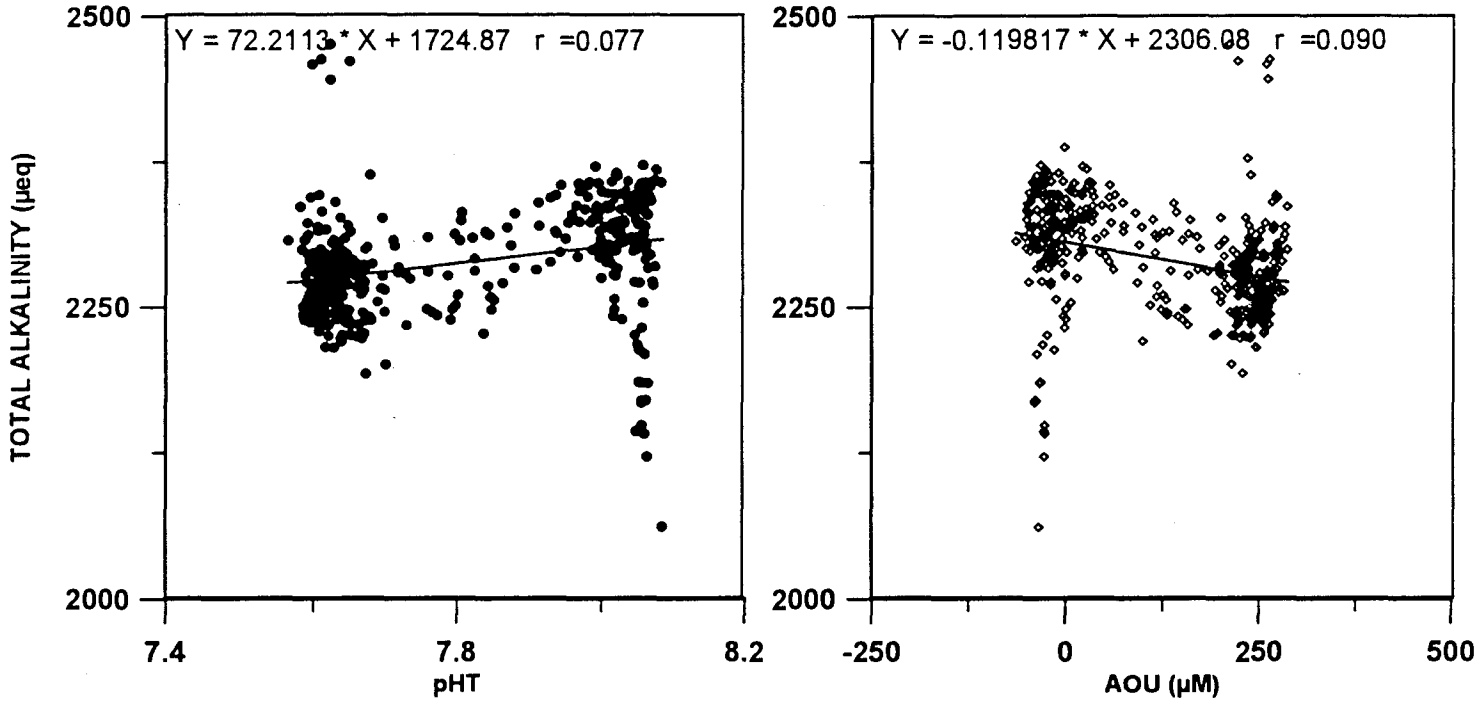

Fig. 4.23. Relation of total alkalinity (µM) with pH_T and AOU (µM) in the Arabian Sea.

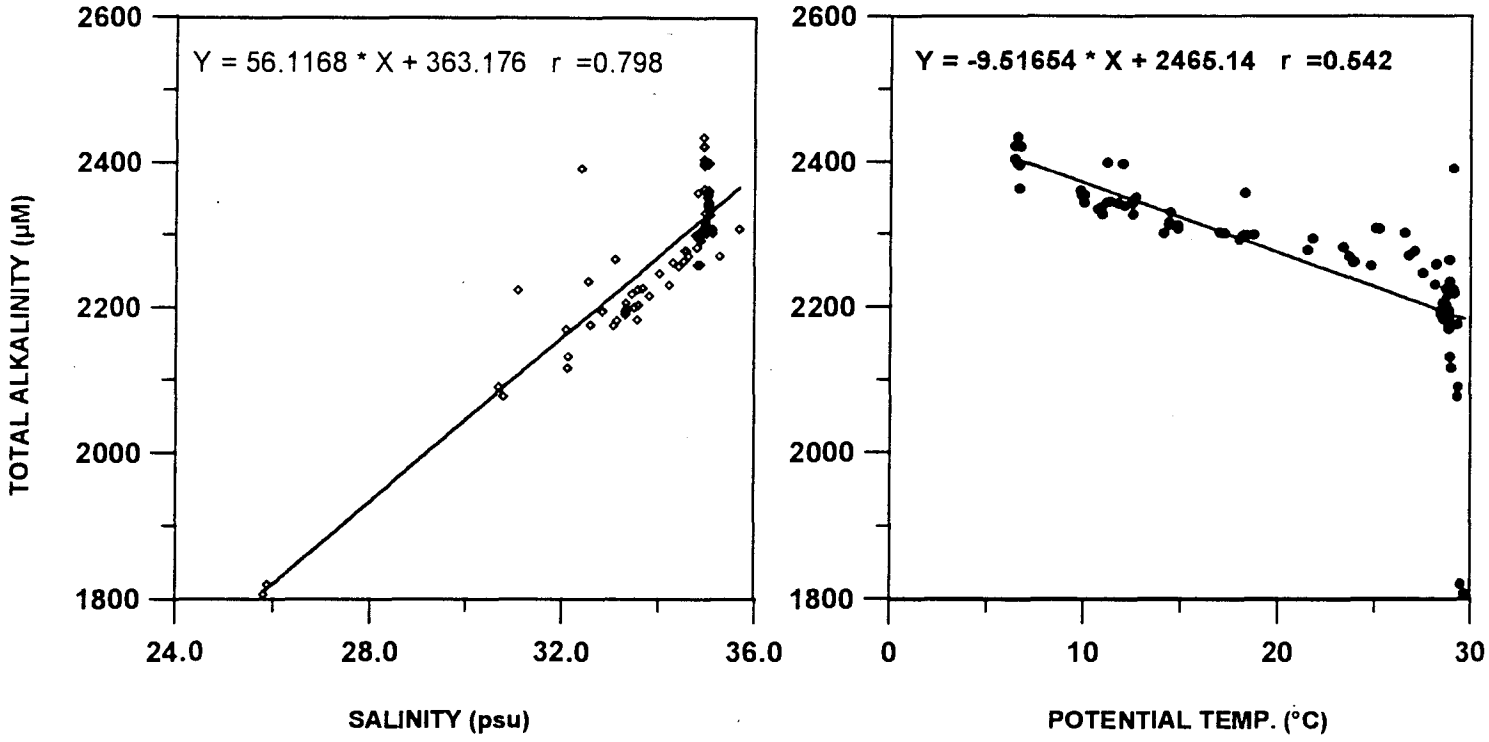

Fig. 4.24. Total alkalinity relations with salinity and potential temperature in the Bay of Bengal.

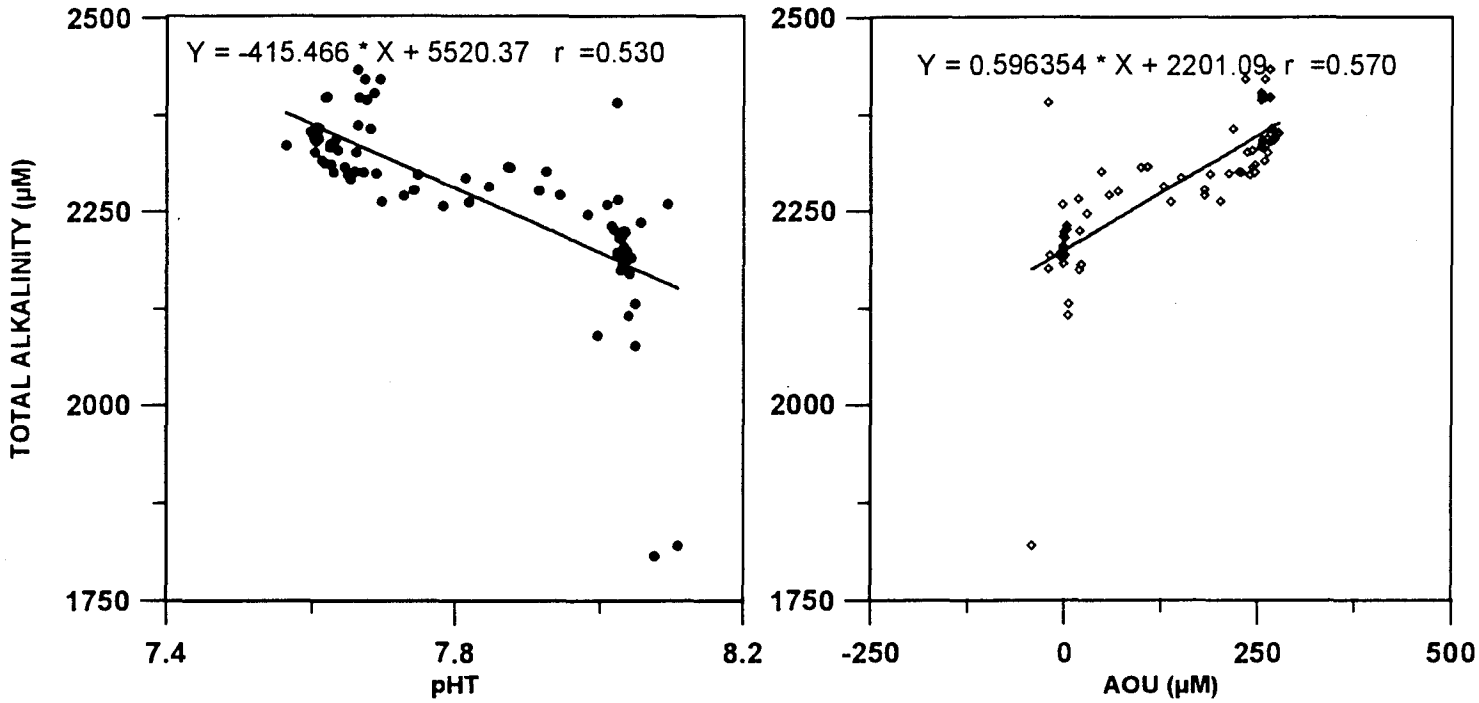

Fig. 4.25. Total alkalinity relations with pH_T and AOU in the Bay of Bengal.

low alkalinity in Bay of Bengal surface waters that have higher pH_T and lower AOU values.

The specific alkalinity, i.e., alkalinity normalised to salinity, distribution should indicate the changes in alkalinity due to the calcium carbonate precipitation or dissolution, since this derived property is a corrected one for mixing of watermasses. Wattenberg (1933) used the term 'specific alkalinity' in the Atlantic waters and found a constant value of 0.123. Koczy (1956) found this to range varies between 0.119 and 0.130 in all the oceans. Sen Gupta and Pylee (1968) observed specific alkalinity to vary between 0.120 to 0.126 in the Arabian Sea along 68° E. Figure 4.26 compares the vertical variations in specific alkalinity in the Arabian Sea. Large difference at the surface is due to variations in the extent of productivity between north and south. High productivity leads to higher TA. As the reducing nature in intermediate waters increases northward the specific alkalinity is lowered in the upper intermediate waters at 21° N compared to that in south. As per eqs. 4.1 and 4.3 the decomposition of organic matter would reduce pH_T that enhances the dissolution of calcium carbonate. On the other hand, proton release from organic matter oxidation would enable the formation of bicarbonates by complexing the carbonates dissolved from skeletal materials. Nevertheless, the concave nature of profiles in Fig. 4.26 suggests the dominance of organic matter regeneration over skeletal dissolution in the oxygen minimum zone.

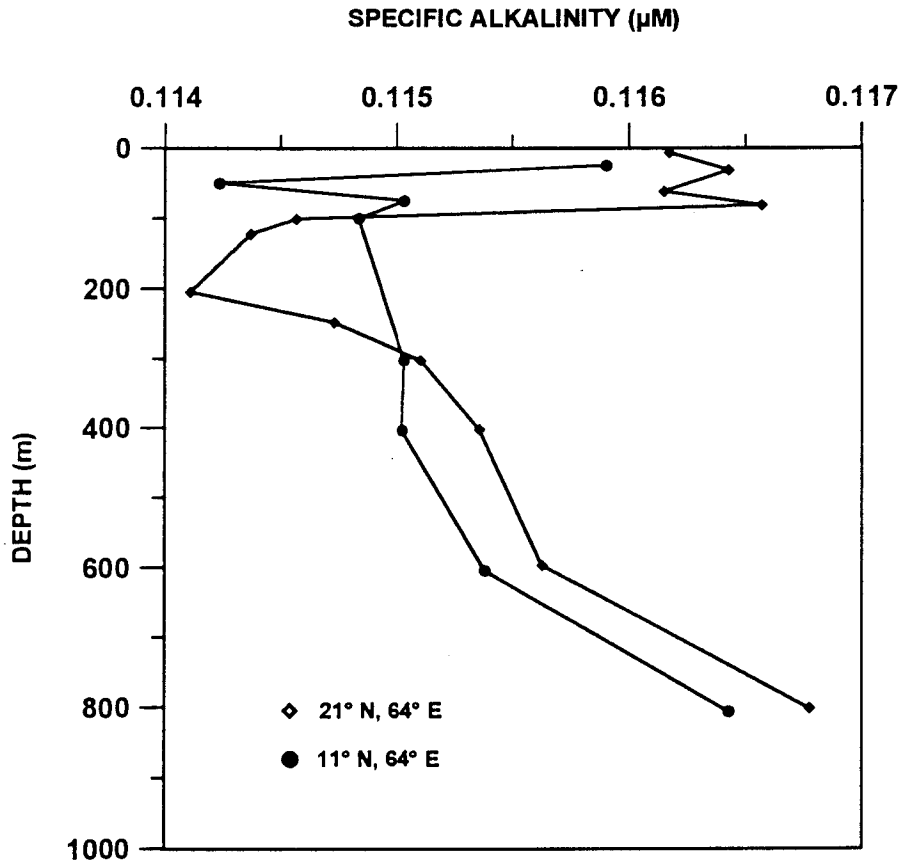

Fig. 4.26. Vertical distribution of specific alkalinity in the Arabian Sea.

Increase in specific alkalinity in deep layers is a result of dominance of dissolution of carbonates which again appears to be more in the north. In the Bay of Bengal the specific alkalinity values between 0.119 to 0.122 while in the Andaman Sea the range was 0.115 - 0.120. These two latter regions have relatively higher pH and also the waters are not reducing unlike the Arabian Sea.

The salient features related to TA in the study area are:

- **Clear seasonal variability observed in surface TA**
- **Surface TA is higher in SW monsoon driven by divergence/upwelling than in other seasons**
- **Coastal-offshore gradients are obviously the most significant in SW monsoon**
- **Surface TA are largely controlled by circulation, including in the Bay**
- **Low TA and low salinity surface waters in the Arabian Sea actually originate in the Bay**
- **Well defined TA minimum occurred at ~200 m because of intense remineralisation of organic matter**
- **TA exhibits linear relations with pH_T and AOU stemmed by two clusters belonging to thermocline and sub-oxic waters in the Arabian Sea but opposite in the Bay of Bengal**
- **Specific alkalinity reflected the productivity trends**

4.3. Variability in total carbon dioxide

The total dissolved inorganic carbon content of sea water may be defined for convenience as:

$$TCO_2 = [CO_2] + [HCO_3^-] + [CO_3^{2-}] \quad (4.11)$$

where brackets denote the total concentrations of respective components in solution (μM) and $[CO_2]$ represents the concentration of all the unionised carbon dioxide species present (as H_2CO_3, hydrolysed CO_2 and $CO_{2\,(aq)}$). The precisions obtained in this study is comparable to the best found elsewhere (Table 4.1), in spite of the fact that we used semi-automated sampling system.

Total carbon dioxide gradually increases from surface to bottom with a sharp increase across the thermocline (Fig. 4.27). Unlike TA (Fig. 4.17), TCO_2 does not decrease with depth in the upper 500 m of the water column (Fig. 4.27) since CO_2 is released both by the oxidation of organic matter and skeletal dissolution. While the former is dominant in the upper few hundred meters the latter becomes significant in deeper layers.

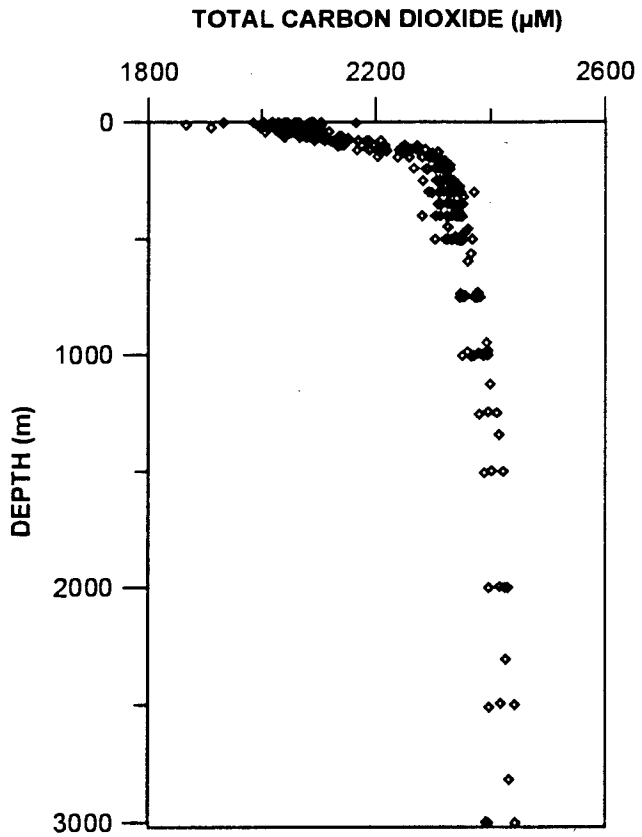

Fig. 4.27. Vertical profile of total carbon dioxide in the Arabian Sea.

4.3.1. Meridional variability in Total Carbon dioxide

Mixing and biological processes largely control the concentrations of dissolved substances in surface waters of the oceans. The TCO_2 distribution in upper layers of the Arabian Sea exhibited lowest values during the 1995 SW-monsoon and highest during the NE monsoon seasons in the central Arabian Sea (Fig. 4.28). Nitrate was found to be relatively higher around 16° N during the 1995 SW-monsoon (~4 µM; de Sousa *et al.*, 1996), whereas it was ~1 µM in the same season in 1996 (Fig. 3.3). Availability of high nitrate might have resulted in lower TCO_2 in 1995 through biological fixation. Primary production is found to be the highest in the SW monsoon (347-1782 $mgC.m^{-2}.d^{-1}$) followed by that in NE monsoon (337-643 $mgC.m^{-2}.d^{-1}$) and inter-monsoon (119-1097 $mgC.m^{-2}.d^{-1}$, the highest at 21° N) seasons (Dr. M. Madhupratap, personal communication 1996). The surface TCO_2 decrease in the north during the 1995 SW monsoon is accompained by a concomitant decrease in alkalinity only by ~15 µeq. This small decrease is perhaps due to minority carbonaceous groups where the diatoms dominated the phytoplankton populations (Sawant and Madhupratap, 1996). Presence of high nitrate with TCO_2 decrease in 1995 indicates that the CO_2 fixation could have been largely due to siliceous organisms. Senescent phytoplankton blooms, together with thick mucus that clogged the zooplankton nets, were noticed during 1996. Hence the elevated TCO_2 levels, than those in 1995 might have been due to rapid regeneration of

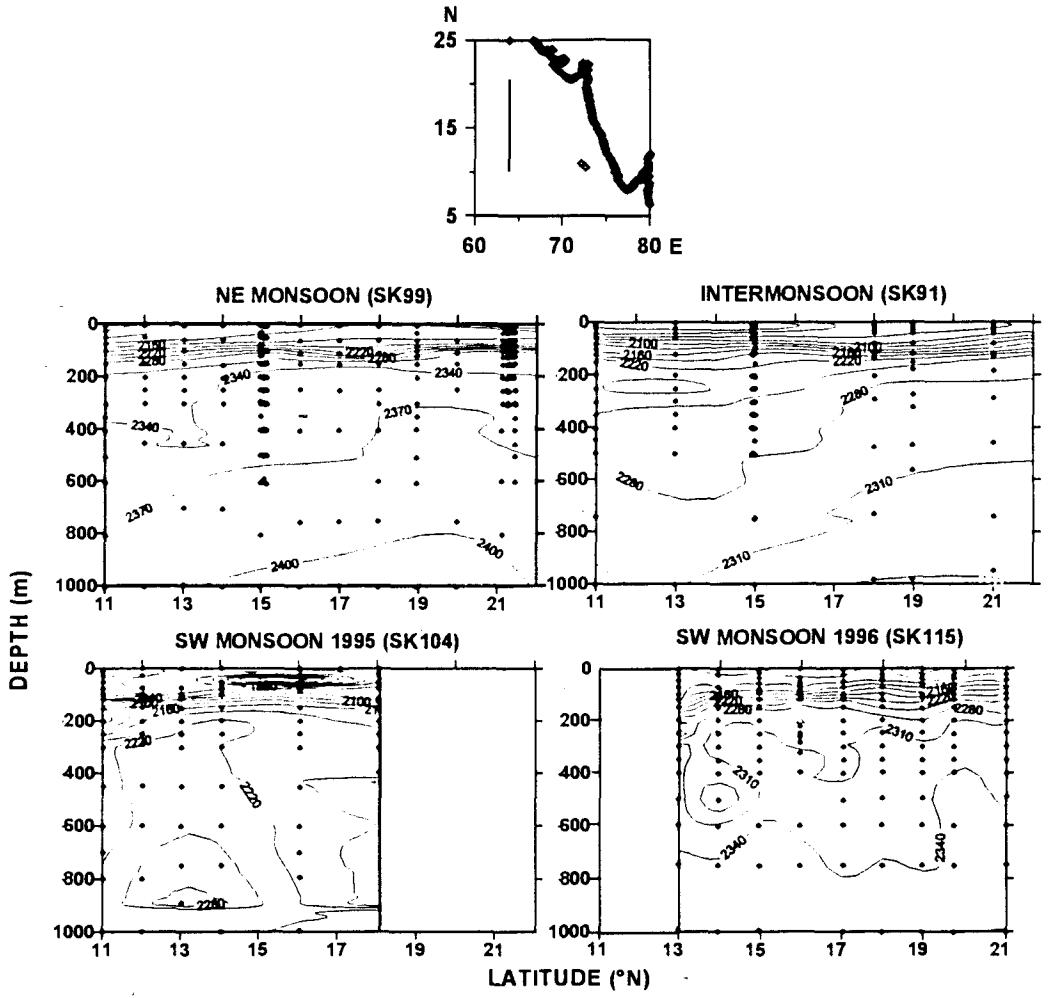

Fig. 4.28. Distribution of Total carbon dioxide (μM) along 64° E in the Arabian Sea during different seasons.

organic material in the upper layers in 1996, in addition to that laterally advected (Waniek *et al.*, 1996) and regenerated, in situ. The Findlater Jet (Findlater, 1969) is expected to drive divergence to the north of its axis in the Arabian Sea (Muraleedharan and Prasanna Kumar, 1996). This may have led to the observed patterns in nitrate during the 1995 SW monsoon (de Sousa *et al.*, 1996) and TCO_2 (Sarma *et al.*, 1996, 1998), particularly to the north of 15° N. The highest TCO_2 during the NE monsoon (Fig. 4.28), particularly in the north, is due to convection. However, in spite of relatively high surface nitrate in the north (~2 μM) (Fig. 3.3) the primary production surprisingly has remained lower than in the SW-monsoon (Madhupratap *et al.*, 1996).

The high rate of biological production at the surface results in higher respiration rates in sub-surface layers. Intense regeneration of organic matter leads to the development of sub-oxic conditions (Figs. 3.2 and 4.4) and to relatively lower pH values (Fig. 4.2). North-south gradient, in the suboxic zone, generally shows 80-100 μM more TCO_2 in the north due to the export of large quantities of particulate organic carbon from the euphotic zone and its subsequent decomposition. Application of Suess (1980) model, by which sinking fluxes can be expected from the surface production, revealed that POC fluxes were ten times higher at a depth of 3000m in the north (1.6 Tg 3months^{-1}) than in the southen Arabian Sea (0.16 Tg 3 months^{-1}). Hence, higher TCO_2 concentrations in the north can be attributed to a combination of higher

biological production and the consequent regeneration processes, in addition to the ageing of subsurface waters. The northward increase in TCO_2 in sub-surface waters of the Arabian Sea is in agreement with previous results (Kumar *et al.*, 1990,1992; George *et al.*, 1994). The seasonal trends in deep TCO_2 concentrations are consistent with those observed in surface layers. The differences in TCO_2 have, however, decreased from ~100 μM in the upper layers to ~80 μM around 1000 m between NE monsoon and inter-monsoon. The seasonal gradients in TCO_2 agree well with the nitrate distribution (Fig. 3.3). The nitrate concentrations were less than expected from the general trends and consequently nitrate deficit was significant during the NE monsoon and 1996 SW monsoon (~10 μM) than that in inter-monsoon of 6 μM (Fig. 4.4). This larger nitrate deficit is caused by enhanced oxidant demand by sinking organic material because of very low concentrations of oxygen (<5 μM) during NE monsoon and 1996 SW monsoon. Relatively high concentrations of oxygen during 1995 SW monsoon can be attributed to the increased influence of Persian Gulf Water (Sarma *et al.*, 1996) that might have annual variations/oscillations. The salinity distribution in intermediate layers (Fig. 4.29) clearly indicated the increased influence of Persian Gulf Watermass (PGW), farther south, during 1995 SW monsoon compared to that in other seasons. This could be due to seasonal variations in the distribution of PGW outflow in the Arabian Sea. For instance, the wind fields suggest that the PGW outflow might be carried along the western Arabian Sea during the NE monsoon but

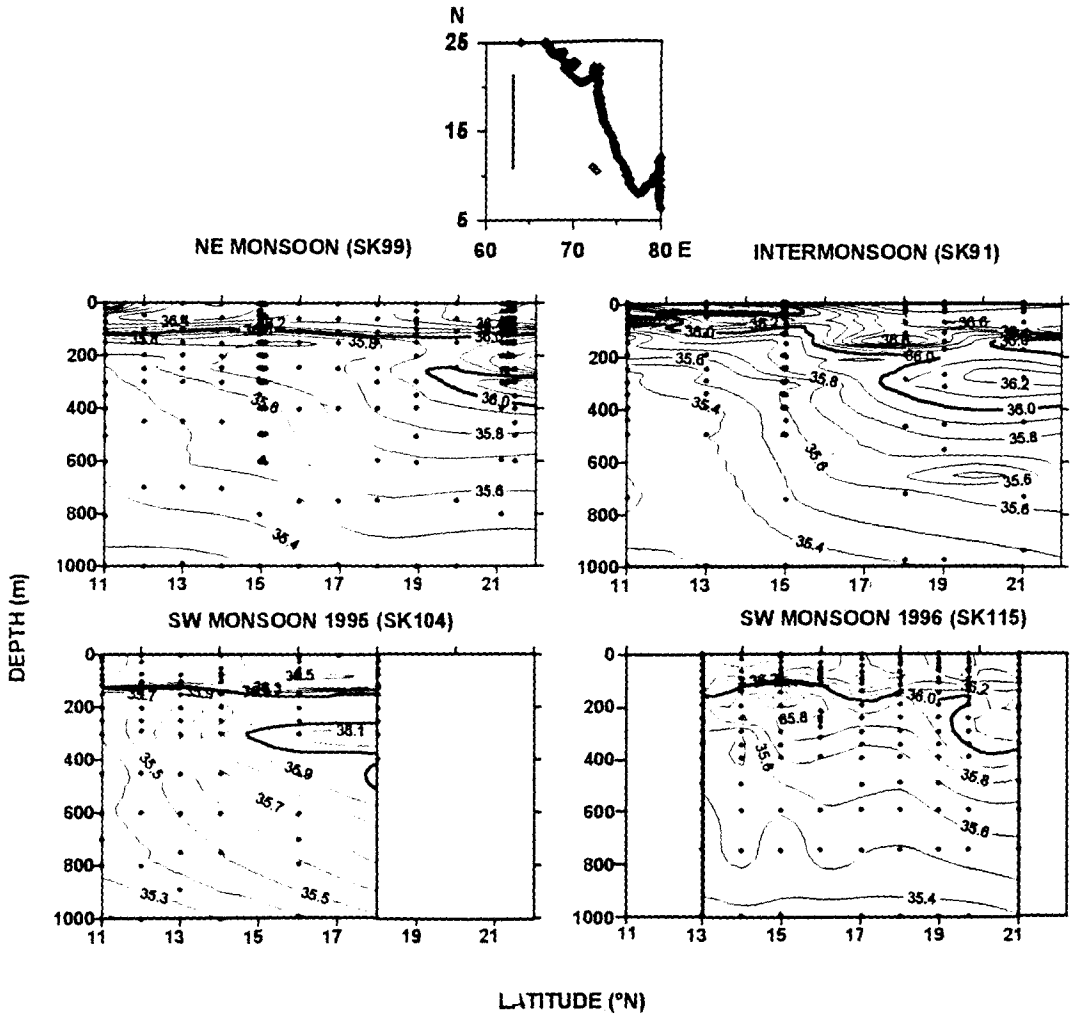

Fig. 4.29. Distribution of salinity (psu) along 64° E in the Arabian Sea during different seasons.

along the eastern part in monsoon (Dr. S. Prasanna Kumar, personal communication 1996). The PGW is relatively depleted in TCO_2 having ~2150 μM (Brewer and Dyrssen, 1985) in relation to that in intermediate waters of even the southern Arabian Sea. Hence, lower TCO_2 observed in 1995 SW monsoon in intermediate layers of the Arabian Sea is due to dilution by PGW. This is augmented by Fig. 3.2 where PGW (rich in oxygen with ~190 μM) leads to relatively higher oxygen concentrations (~50 μM) in 1995 SW monsoon compared to those in other seasons in subsurface waters of the Arabian Sea.

4.3.2. Zonal variations in total carbon dioxide

To examine the longitudinal variations in TCO_2, data have been collected along 11° N and 21° N during NE monsoon (February), pre-monsoon (April-May) and 1995 SW monsoon (July-August) but along 21° N data could not be collected during SW monsoon due to technical problems. Besides JGOFS cruises, data were also collected along 15° N during pre-monsoon (April-May; SS141), SW monsoon (June-July; SK103) and towards the end of SW monsoon (September-October; SS136). Extensive sampling was also done close to the coast along 9° N, 10° N and 11° N (hereafter called as transect 1,2 and 3 respectively) during SW monsoon to examine the upwelling intensity and relative effects on inorganic carbon distribution.

Along 21° N, higher TCO_2 concentrations were observed (Fig. 4.30) during NE monsoon as a result of convective mixing which brings CO_2 rich sub-surface waters into surface layers. Nitrate was higher during NE monsoon (~2μM; Fig. 3.6) whereas oligotrophic conditions prevailed in inter-monsoon. Surface TCO_2 values ranged between 2145 and 2160 μM during NE monsoon while these were comparatively lower by 80 μM (2060-2080 μM) during inter-monsoon. Availability of high nitrate might have triggered high primary production since column productivity was 860 $mgC.m^{-2}.d^{-1}$ in winter as compared to 310 $mgC.m^{-2}.d^{-1}$ in inter-monsoon. Sub-surface TCO_2 concentrations were higher by 40 μM during NE monsoon than in intermonsoon because of higher respiration rates. AOU was higher by ~80-100 μM during NE monsoon than in inter-monsoon (Fig. 4.7). As a result reducing conditions developed during NE monsoon leading to denitrification (Fig. 4.8) as also revealed by lower pH_T (Fig. 4.6).

During the pre-monsoon season surface TCO_2 concentrations ranged from 1960 to 2040 μM in the west and east, respectively along 15° N (Fig. 4.31). Lower concentrations in the east can be attributed to the influence of fresh waters. Low surface TCO_2 (1840-1940 μM) concentrations were encountered during 1995 SW monsoon compared to those in other two seasons (Fig. 4.31). TCO_2 contours of 2000 μM was found at a depth of 15-20m in the east. Fresh water from the river appears to play a major role in the biogeochemical cycling of carbon. Similar to that in the Bay of Bengal, the present fresh water lens

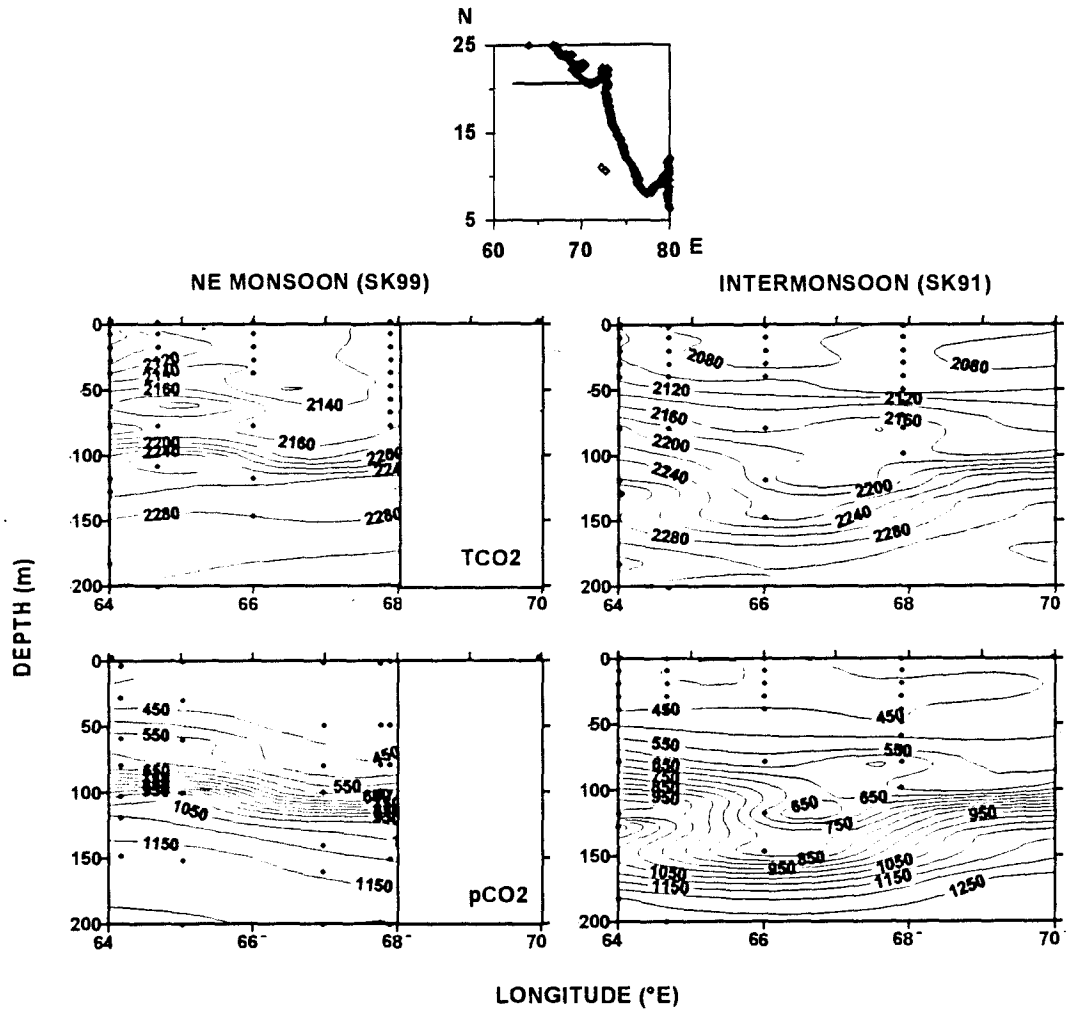

Fig. 4.30. Distribution of total carbon dioxide (μM) and partial pressure of carbon dioxide (μatm) along 21° N in the Arabian Sea.

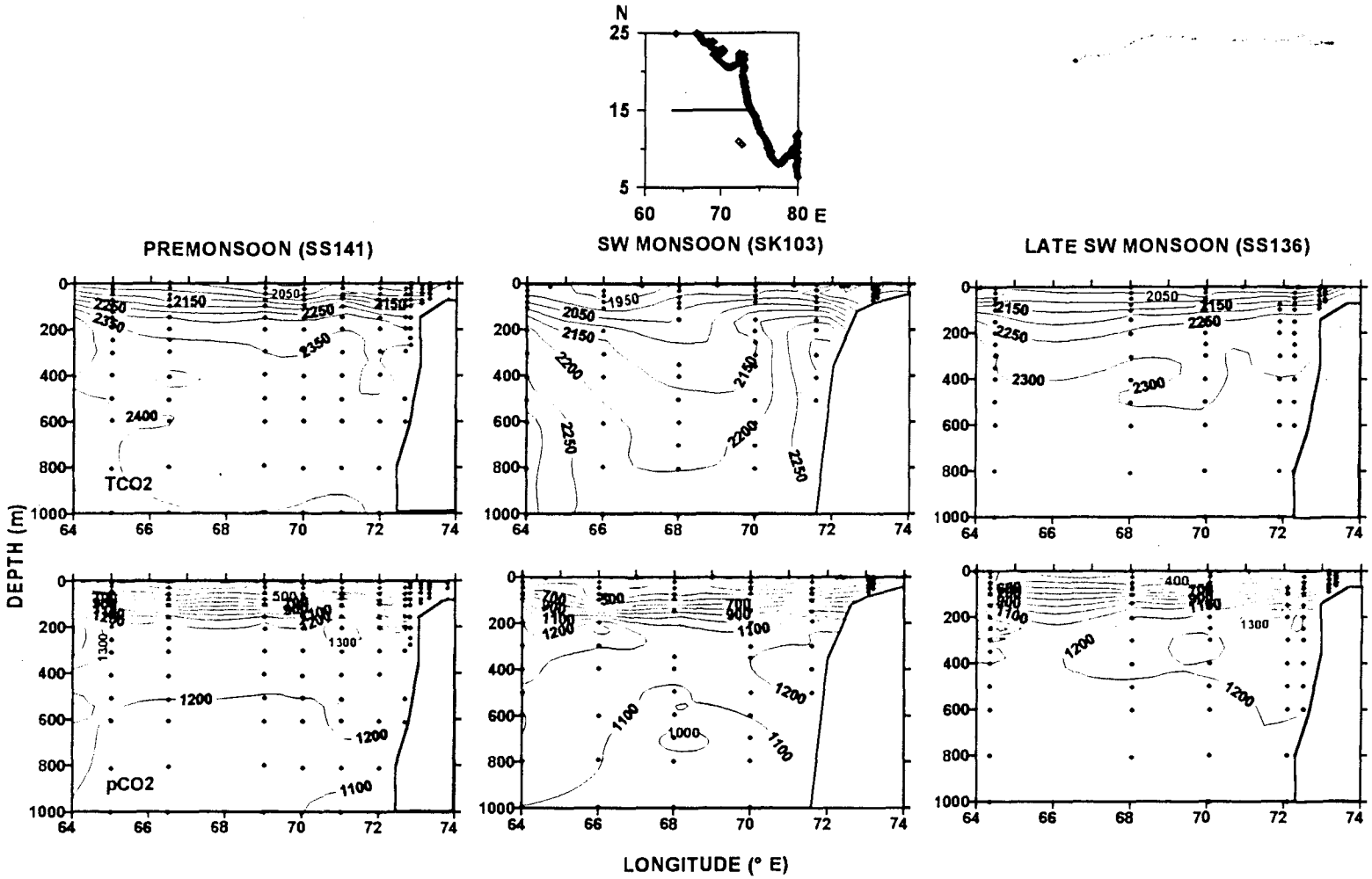

Fig. 4.31. Distribution of total carbon dioxide (μM) and partial pressure of carbon dioxide (μatm) along 15° N in the Arabian Sea.

does not allow upwelled subsurface waters to reach surface. With the receding discharge in the late SW monsoon the upwelled water reaches the surface (Fig. 4.31, top third panel). Salinity increased from 35.3 to 36.8 from peak SW monsoon to end of the season (Fig. 3.11). The seasonal trends in deep TCO_2 concentrations are consistent with those observed in surface layers. This is because of the fact that the increased surface TCO_2 will be associated with the supply of nutrients from the base of thermocline that could enhance biological production in the upper layer. Subsequent sinking and regeneration of this material in the sub-surface layers would lead to proportional increase in TCO_2. Concentrations were higher throughout the water column during pre and late SW monsoon seasons compared to those in peak monsoon season. These could be due to higher respiration rates in response to increased organic matter inputs driven by upwelling where a certain time lag is imminent for bacteria to respond (Ducklow, 1993; Azam *et al.*, 1994). Nitrate deficit was higher in the west, in general (Fig. 4.11) and comparatively higher values were found in the water column during SW monsoon probably due to drawing of upwelled waters at sub-surface from the west.

Along 11° N, relatively higher TCO_2 occurred at shallower depths towards the coast during SW monsoon due to upwelling (Fig. 4.32); this can also be seen in the shoaling of 27° C isotherm to 10 m from 100 m (Fig. 3.7). Surface TCO_2 was 1800 μM and contours appear to be upsloped from a depth of 100 m (Fig.

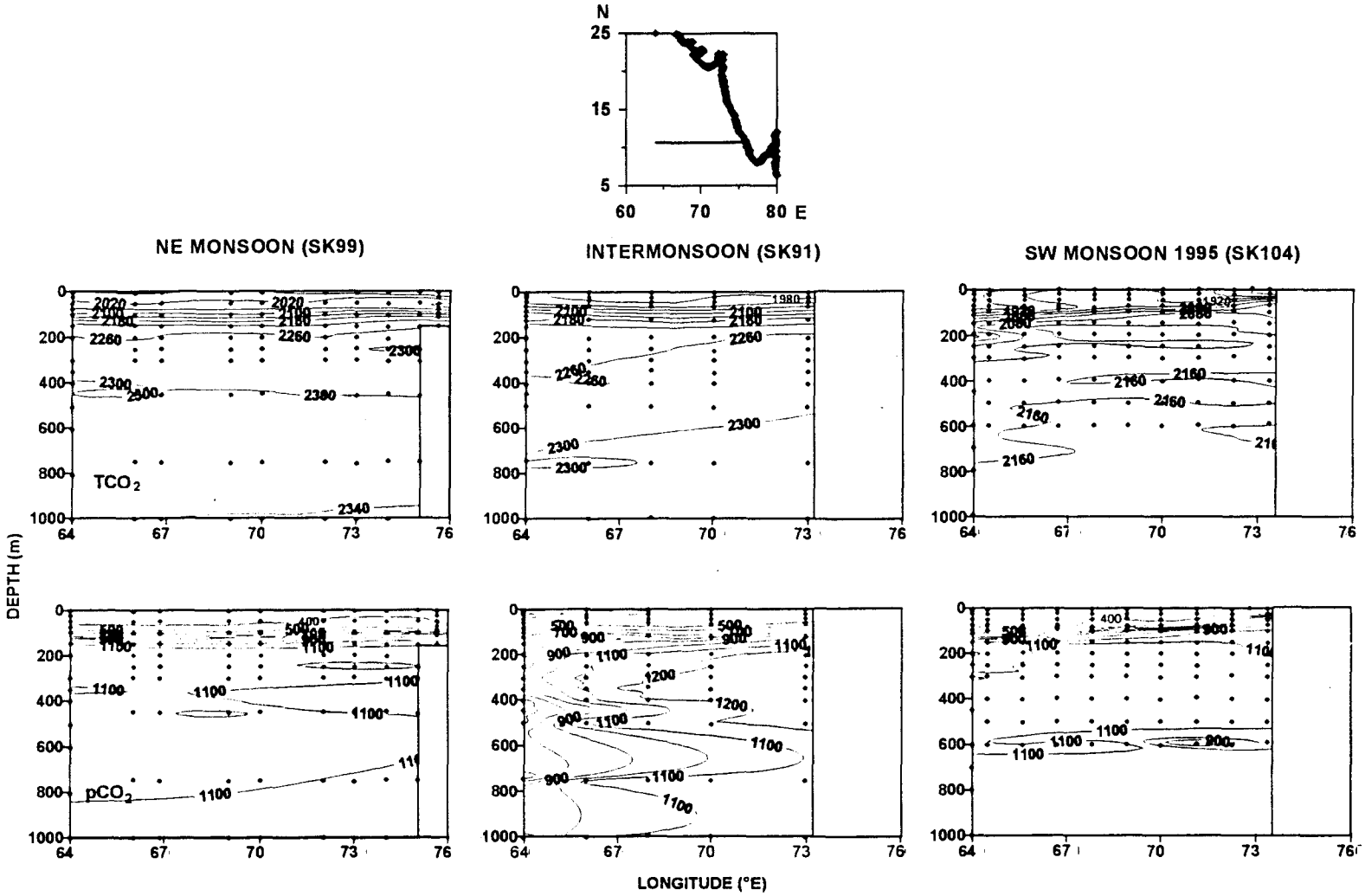

Fig. 4.32. Distribution of total carbon dioxide (μM) and partial pressure of carbon dioxide (μatm) along 11° N in the Arabian Sea.

4.32). A patch of low TCO_2 waters near the coast is an effect of river discharge. In agreement with this a large variation in surface TCO_2 parallels with the eastward decrease in salinity, due to the influx of fresh water with lower TCO_2 from land. Consequently, the TCO_2 gradient between surface and 20 m was about 180 µM in the east that decreased to 20 µM in the west. On the other hand, surface TCO_2 concentrations were high 2002 and 2018 µM during inter-monsoon and NE monsoon seasons, respectively. TCO_2 in sub-surface waters exhibited a clear eastward increase. Comparatively lower concentrations during the SW monsoon might be due to faster removal of organic matter from the water column, along with river discharged particles.

As a result of upwelling, surface nitrate was as high as 16 µM with very low oxygen levels (90 µM; Fig. 3.10) near the coast (along transect 2; Fig. 4.33). Very high TCO_2 of 2047 µM was found because of the intense upwelling. Maxima in surface TCO_2 concentrations were 1944 and 1874 µM, respectively, along transects 1 and 3 (Fig.4.33). All contours were upsloped from a depth of 75m. The salinity distribution (Fig. 3.9) shows the influence of fresh water in inhibiting the upwelled waters reaching the surface. Occurrence of high TCO_2 waters below the low saline waters leads to a large gradient (>150 µM) between surface and waters at 10 m.

Horizontal gradients in TCO_2 in surface waters of the Bay of Bengal were

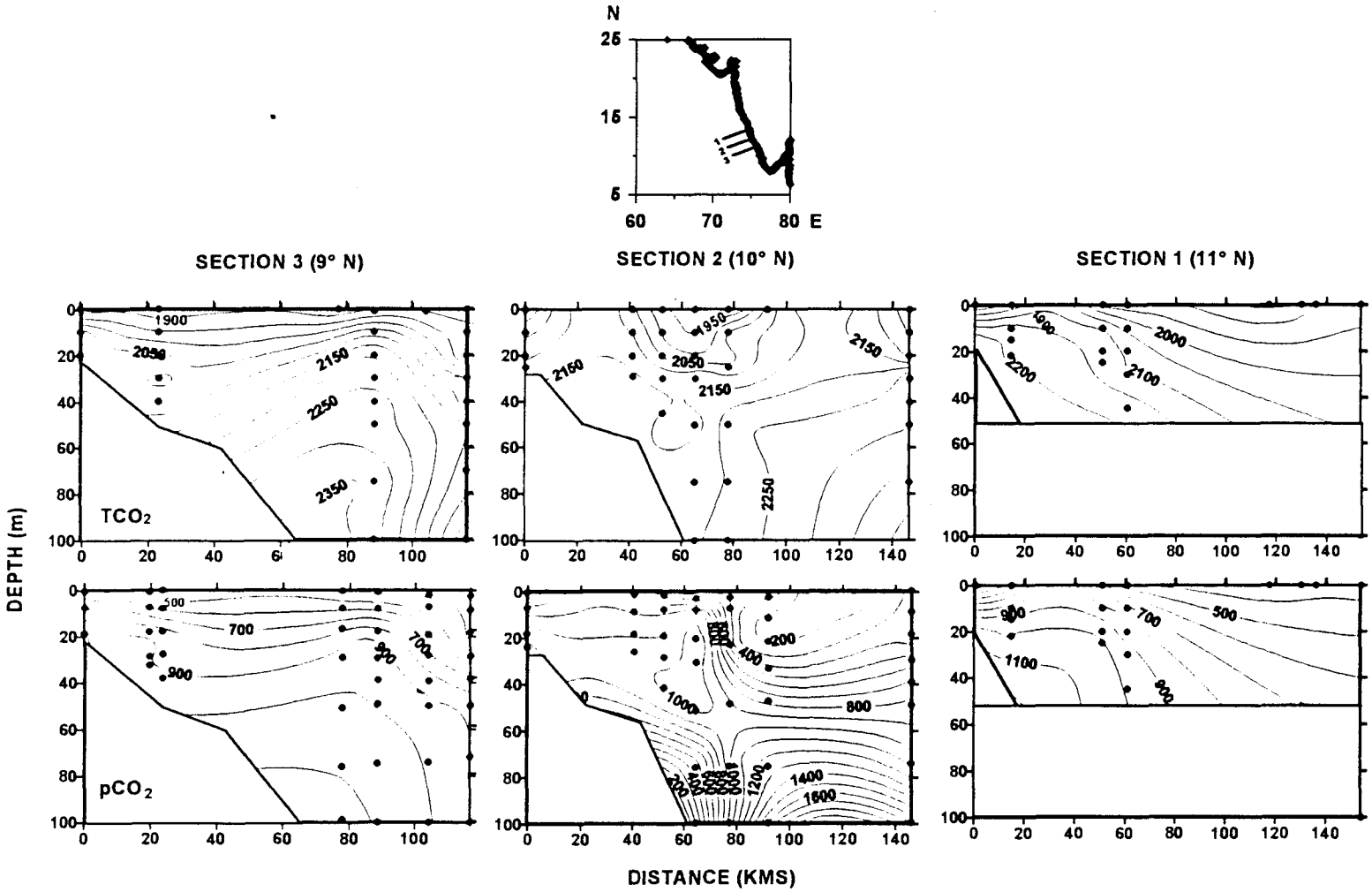

Fig. 4.33. Distribution of total carbon dioxide (μM) and partial pressure of carbon dioxide (μatm) along sections 1, 2 and 3.

evident (Fig. 3. 34). Concentrations were lower in the north mainly because of dilution by river waters. In the deep, however, there were no apparent north-south gradients with the values centring about 2300 µM. Concentrations in the Bay are relatively lower than those in the Arabian Sea, in the same 1996 SW monsoon season. These observations are in accordance with the earlier observations (George *et al.*, 1994; Kumar *et al.*, 1996) despite the fact that the seasons covered between these studies were different. George *et al.* (1994) studied CO_2 system during pre-SW monsoon while Kumar *et al.* (1996) during pre- and post- SW monsoon seasons. These comparisons reveal that the differences in CO_2 contents between the Arabian Sea and Bay Bengal and between northern and southern parts of the Bay exist in all seasons. The computed TCO_2 in the Andaman Sea (SK 118) agrees with the vertical trends shown in Fig. 4. 34. While the values at the surface ranged between 1800 and 1850 µM at 1000 m they were between 2250 and 2300 µM. Lower values in the surface waters of the northern Andaman Sea could be due to influx of river waters from Irrawady-Salween system. Surface waters alkalinity were lower throughout the water column when compared to those to the west of the Andaman Sea (see Fig. 4.34). This might have been due to higher productivity in the Andaman Sea than in the open Bay of Bengal and the consequent less intense regeneration in the subsurface waters of the Bay.

4.3.3. Variations in total carbon dioxide along the coast

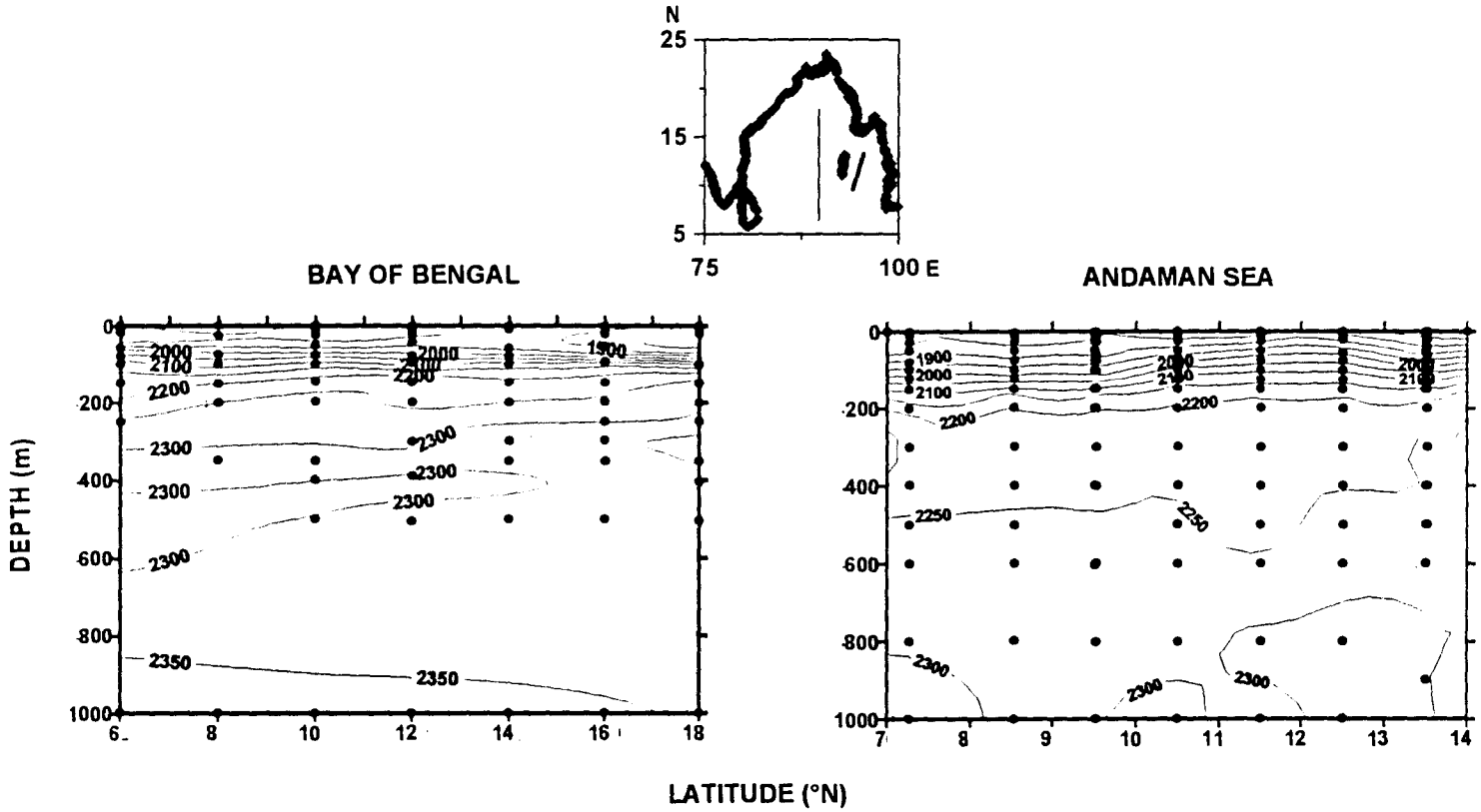

Fig. 4.34. Distribution of total carbon dioxide (μM) in the Bay of Bengal and Andaman Sea.

Fig. 4.35 depicts variations in TCO_2 during three seasons along the Indian coast of the Arabian Sea. Surface TCO_2 concentrations ranged between ~2020 and 2160 µM with an increase of 140 µM from south to north during NE monsoon. The NE monsoon convective mixing (Fig. 3.6) drives this increase in the north. The range and gradients are less (2010-2060 µM) in inter-monsoon. Surface nitrate concentration was >1 µM during NE monsoon but below detection limits during inter-monsoon. Column productivity is higher in winter (860 $mgCm^{-2}d^{-1}$) than in inter-monsoon season (310 $mgCm^{-2}d^{-1}$). During SW monsoon, low concentrations (1800 µM) in the south are due to fresh water drainage from the land and comparatively higher productivity (50 $mgCm^{-3}d^{-1}$ at 10° N 75° E whereas in the north it was 12 $mgCm^{-3}d^{-1}$ at 18° N 70°E with higher surface TCO_2 of 1970 µM). The influence of fresh water leads to stratification because of which high plankton production occurs below the surface but within the euphotic zone. Around 20 m at 12°N, 74° E a primary production of 71 $mgCm^{-3}d^{-1}$ was observed. TCO_2 concentrations were lower up to 100m during SW monsoon compared to inter-monsoon. North-south gradients in TCO_2 were not significant in winter and inter-monsoon but were barely significant in SW monsoon.

In order to examine controlling factors of TCO_2, the same has been correlated to salinity and potential temperature (Fig. 4.36). TCO_2-salinity plot shows that

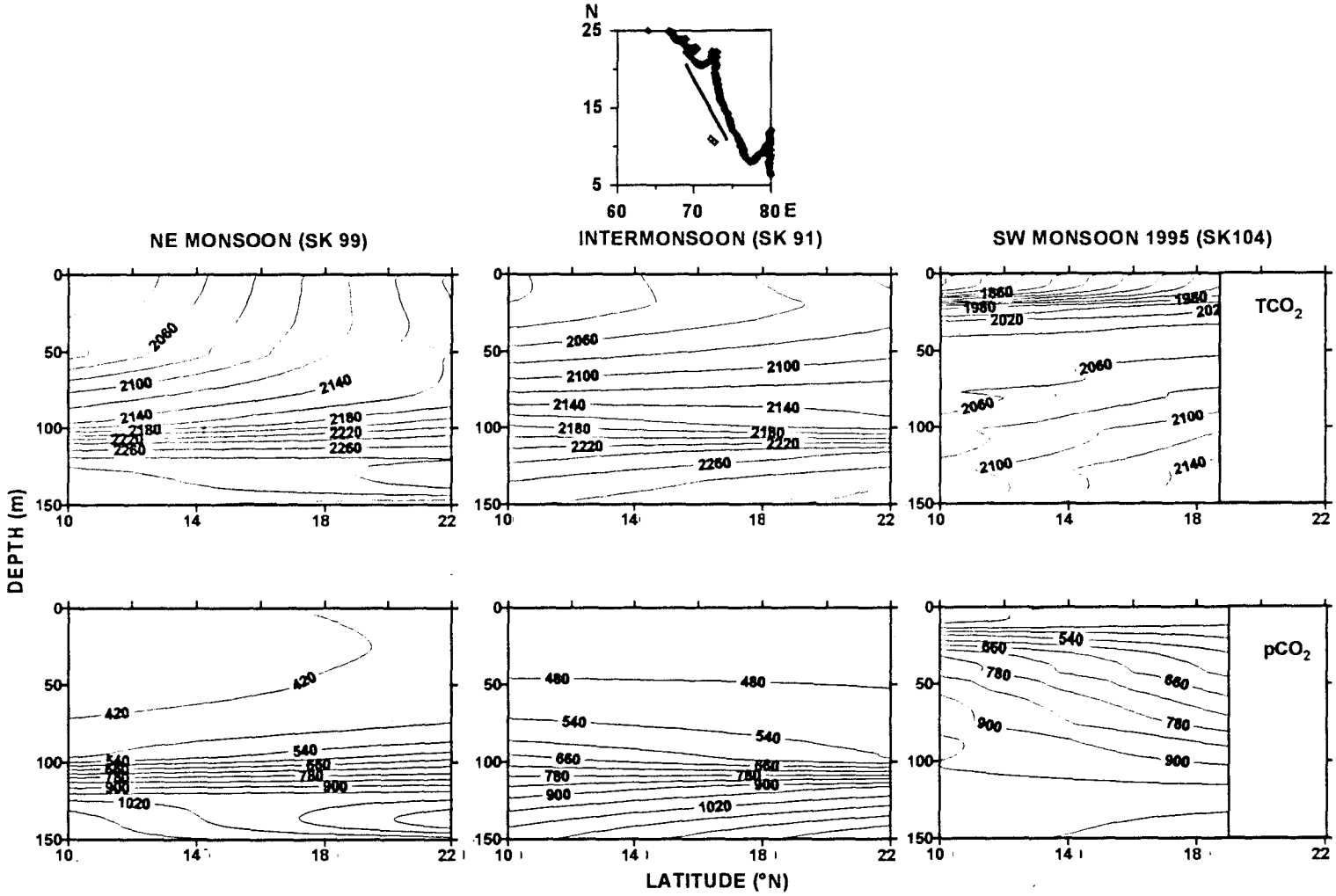

Fig. 4.35. Total carbon dioxide (µM) and partial pressure of carbon dioxide (µatm) distribution along the west coast of India.

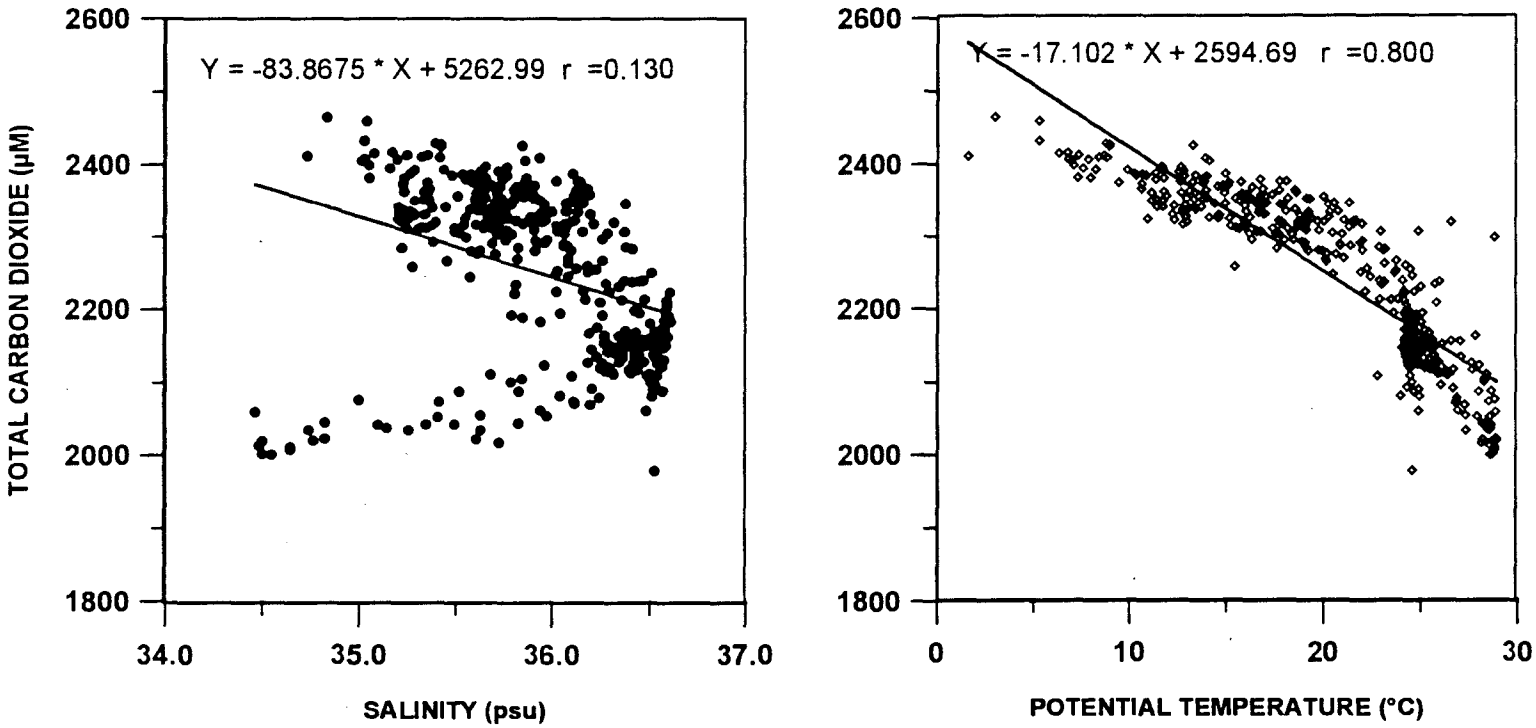

Fig. 4.36. Relations of total carbon dioxide with salinity and potential temperature in the Arabian Sea

these are linearly correlated in surface and deep regimes where they exhibited positive and negative trends, respectively. On the contrary, the clear negative correlation between TCO_2 and potential temperature (Fig. 4.36) suggests a near conservative behaviour. Nevertheless, linearity with respect to potential temperature stems from two pools of data points representing depths shallower than 100-150 m and deeper than oxygen minimum zone. The regeneration processes in the oxygen minimum zone actually cause the hump. These relations (Fig. 4.36) clearly reveal that TCO_2 in the Arabian Sea is largely controlled by physical processes although the large scatter, in each segment of the relationship, is because of biological processes. Better linear relations (Fig. 4.37) for TCO_2 with pH_T and AOU support the role of biological processes in regulating the TCO_2 in intermediate waters (OMZ). Apparently, mixing processes seem to chiefly influence TCO_2 distribution both in surface and deep layers.

The main highlights from the results and discussion on TCO_2 are:

- **Large seasonal and spatial variability in TCO_2 was found**
- **The variability was driven by physical and biological pumps**
- **Very high TCO_2 levels surfaced in upwelling regions**
- **River discharge prevented ventilation of TCO_2 rich upwelled sub-surface waters**
- **Winter convection also enhanced TCO_2 in surface layers**

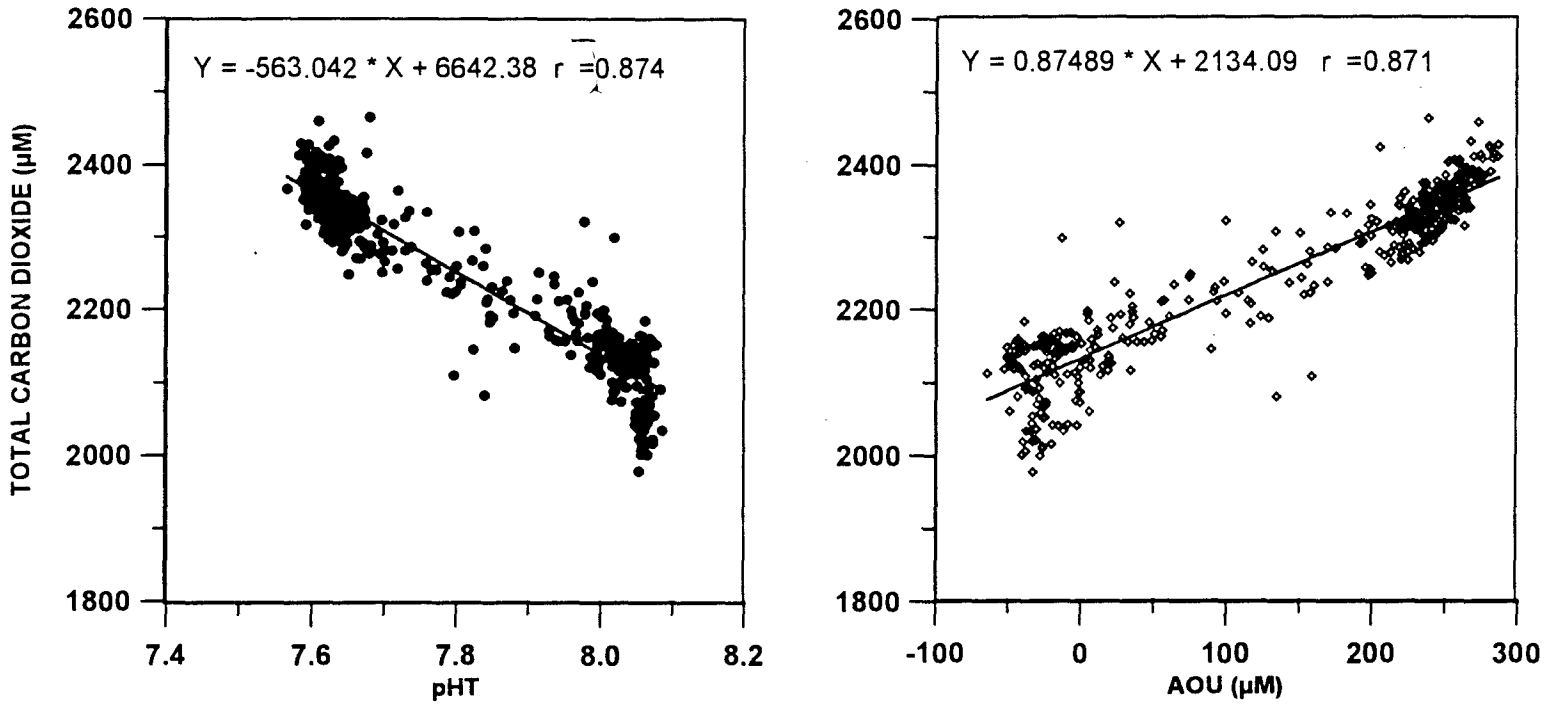

Fig. 4.37. Relation of total carbon dioxide with pH_T and AOU in the Arabian Sea.

- **Seasonal variability in TCO_2 complimented nitrate, in particular**
- **TCO_2 in coastal waters is seasonally and spatially (at surface) variable**
- **Gradients in TCO_2 between Arabian Sea and Bay Bengal exist in all seasons**
- **Mixing processes appear to be dominant in regulating TCO_2 over biological ones**

4.4. Variability in partial pressure of carbon dioxide

Among all the inorganic carbon species, pCO_2 is the most representative of inorganic carbon available to phytoplankton during photosynthesis. Transfer across air-water interface can occur only in this form. The typical vertical distribution of pCO_2 in the Arabian Sea (Fig. 4.38) shows that pCO_2 increased from surface to a depth of about 300-400 m and gradually decreased thereafter. Lower values in the surface layers are due to consumption by phytoplankton and continuous exchange with atmosphere. In addition to this, surface pCO_2 depends on temperature, salinity and on regeneration. Higher concentrations in intermediate layers are due to its release during decomposition of organic matter. Increase in TCO_2 (Fig. 4.27) and decreases in TA (Fig. 4.7) and pH_T (Fig. 4.1) are in good agreement with the higher pCO_2 values in intermediate layers. Therefore, OMZ is an important zone for production CO_2 that can influence pCO_2 levels in surface layers and thereby

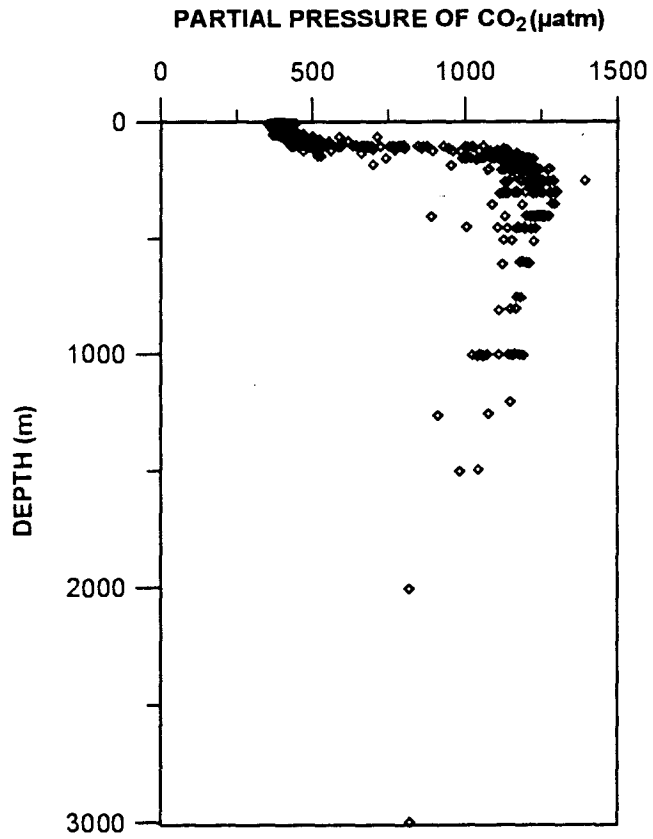

Fig. 4.38. Vertical profile of partial pressure of carbon dioxide in the Arabian Sea during NE monsoon.

the magnitude of air-sea exchanges. Gas exchange across the thermocline would depend on diffusion coefficients and on its concentration gradient in surface and intermediate layers. Decrease in pCO_2 in deep waters is because of decreased organic matter oxidation in addition to pH increase since these waters originate at surface in polar regions. Enhanced dissolution of skeletal carbonates at high pressures could also result in increased pH_T (Fig. 4.1).

4.4.1. Meridional variability in partial pressure of carbon dioxide

pCO_2 values in surface waters were higher than in atmosphere (355 µatm) during all the seasons. It mostly centred around ~420 µatm during NE monsoon but ranged from 360 to 420 µatm during the other periods (Fig. 4.39). Higher concentrations during NE monsoon and 1996 SW monsoon seasons seems to be driven by physical mixing and by bacterial activity during inter-monsoon. A patch of high pCO_2 waters at surface were observed during 1995 SW monsoon at 16°N (Fig. 4.39) which could be the result of divergence caused by Findlater jet or lateral advection of upwelled Oman waters (Waniek *et al.*, 1996).

Regeneration of CO_2 from soft tissue and the prevalence of reducing conditions result in a build up of pCO_2 that lowers the pH_T in sub-surface waters of the Arabian Sea. AOU (Fig. 4.3) and nitrate deficits (Fig. 4.4) distributions show intense reducing conditions during the NE monsoon and 1996 SW monsoon

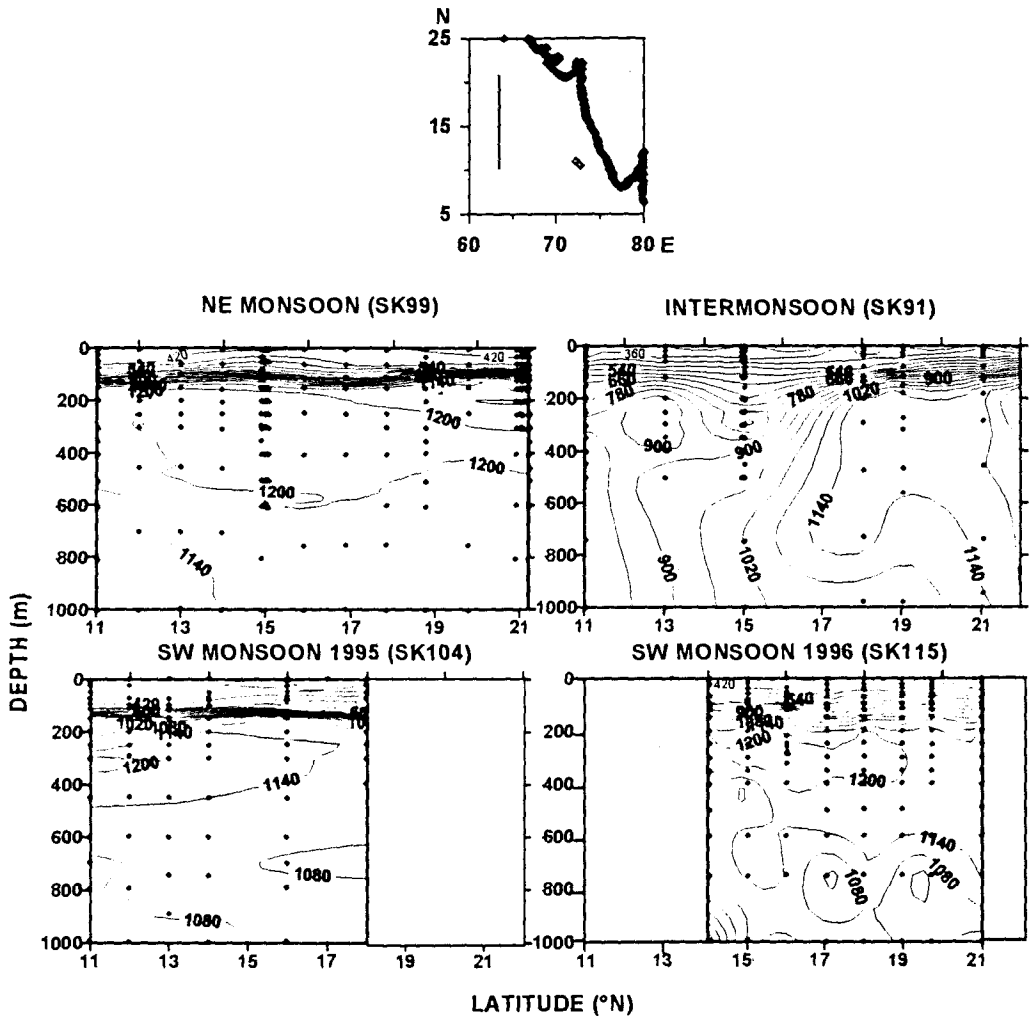

Fig. 4.39. Distribution of partial pressure of carbon dioxide (µatm) along 64° E in the Arabian Sea in different seasons.

seasons as a consequence of higher sinking fluxes of organic matter from the base of euphotic zone. The reducing conditions intensified northward. Consequently, pCO_2 increased to 1100±100 µatm in intermediate waters (200-1000 m) with clearly discernible seasonal variations (Fig. 4.39). In general, pCO_2 in intermediate waters were higher during NE monsoon compared to other seasons. The pCO_2 peak generally occurred in denitrifying zone and did not coincide with AOU maximum (1000-1200m) due to intense remineralization in this zone (George *et al.*, 1994). Even though sub-surface pCO_2 concentrations were 1100-1200 µatm in other seasons also, the depth range covered by 1200 µatm contour was larger during the NE monsoon season.

4.4.2. Zonal variability in partial pressure of carbon dioxide

Along 21° N, pCO_2 was studied during NE monsoon and inter-monsoon seasons (Fig.4.30). Higher pCO_2 concentrations were observed in NE monsoon as a result of convective mixing, that brings CO_2 rich upper thermocline waters to the surface. Surface pCO_2 ranged between 470 and 480 µatm whereas during inter-monsoon these were comparatively lower (by 20 µatm). High surface pCO_2 values were associated with high nitrate. This is in agreement with the trends in column productivity. It was 860 $mgC.m^{-2}.d^{-1}$ during NE monsoon whereas it was 310 $mgC.m^{-2}.d^{-1}$ in the inter-monsoon at 21°N and 67°E.

Along 15° N, high surface pCO_2 of ≥400 µtam occurred at 15-20 m during SW monsoon that seem to have surfaced in the late season (Fig. 4.31). It was prevented from reaching the surface at the peak of SW monsoon by the low salinity cap (Fig.3.11). Surface salinity increased from ~35.300 to ~36.800 psu from peak to late SW monsoon indicating the decreasing of river influx. During pre-SW monsoon season also surface pCO_2 of >420 µatm occurred. The pCO_2 concentrations were higher in surface as well as in intermediate waters in pre-monsoon and late SW monsoon seasons compared to those seen during the peak SW monsoon season due to higher respiration rates (see 4.1.1 and 4.1.2). Comparatively higher pCO_2 near the coast in the late SW monsoon might have been due to regeneration of sinking organic material produced during peak monsoon season along the margins. It can be seen from Fig. 4.31 that higher pCO_2 (by ~100 µatm) was found near the coast than in the west during September-October period whereas this difference was ~60 µatm during peak SW monsoon. This strongly indicates the influence of sinking organic matter produced during SW monsoon on the CO_2 regeneration particularly along the slope regions of western India.

Along 11° N, low surface pCO_2 concentrations of 345 µatm were found during NE monsoon (Fig. 4.32) which could be due to influence of fresh water from the land, where surface salinities ranged between 33.54 and 33.60 (Fig. 3.7). Below these layers high pCO_2 of 600 µatm occurred at 100 m (Fig. 4.32). There

was a large gradient in pCO_2 between surface and 10 m of 250-350 µatm, near the coast due to stratification in SW monsoon. Upwelling during SW monsoon led to high concentrations of pCO_2. Sub-surface waters showed similar trends as was shown by TCO_2. Moreover, pCO_2 increased towards the east during all the seasons. In fact, the gradient was more during inter-monsoon and NE monsoon (>60 µatm) whereas it was low during SW monsoon (Fig. 4. 32).

Very high surface pCO_2 of 682 µatm was recorded near the coast along transect 2 (Fig. 4.33) which has never been reported so far from this region. However, pCO_2 along the coast of Oman in July has been reported to be around 660 µatm by Goyet *et al.* (1998) and around 750 µatm by Kortzinger and Duinker (1997). The presently observed value is nearly twice that in atmosphere; therefore these regions can act like a chimney of CO_2 emission to the atmosphere during SW monsoon season as the winds are also usually strong. All contours upsloped from a depth of 75m (Fig. 4.33). It is clear from Fig. 3.9 that the influence of fresh water suppresses the intensity of coastal upwelling. The down slopping of high pCO_2 contours closer to the coast were due to prevalence of low density fresh waters that would not allow upwelled sub-surface waters to reach the surface. It is clear from Fig. 4.33 that high pCO_2 waters occurred immediately below the low saline waters. Surface pCO_2 concentrations were 550 and 600 µatm, respectively, at the shallow ends of transects 1 and 3. Effect of river water discharge could be seen here as well.

Vertical profiles in the Bay of Bengal (Fig. 4.34) are in concurrence with those of George *et al.* (1994). Higher levels of ~1200 µatm occurred in intermediate waters. Further, the depth range covering this concentration increased northward in accordance with the expected productivity patterns and the resultant decreasing AOU (Fig. 4. 16). The computed TCO_2 in the Andaman Sea (SK 118) agrees with the vertical trends shown in Fig. 4. 40. While the values at the surface ranged between 350 and 490 µatm, at 1000 m they were ~1000 µatm. Lower values in the surface waters of the northern Andaman Sea could be due to influx of river waters from Irrawady-Salween system. pCO_2 levels were lower by 100 µatm in the suboxic waters and this could be due to a less intense decomposition of organic matter.

4.4.3. Variations in partial pressure of carbon dioxide along the coast

Fig. 4.35 depicts the variations in pCO_2 during three seasons along the coast of India. The pCO_2 levels increased with a gradient of ~ 25-30 µatm from the south to north during NE monsoon. This increase to the north is obviously (Fig. 3.6) driven by convective mixing. Surface productivity was higher (21.4 mgC m^{-2} d^{-1}) during this season relative to inter-monsoon (8.76 mgC m^{-2} d^{-1}). During SW monsoon, all deeper contours shoaled up towards the south because of the wind-induced upwelling. The 600 µatm contour occurred at 25 m in the south during SW monsoon season and below 100 m in other seasons. But the

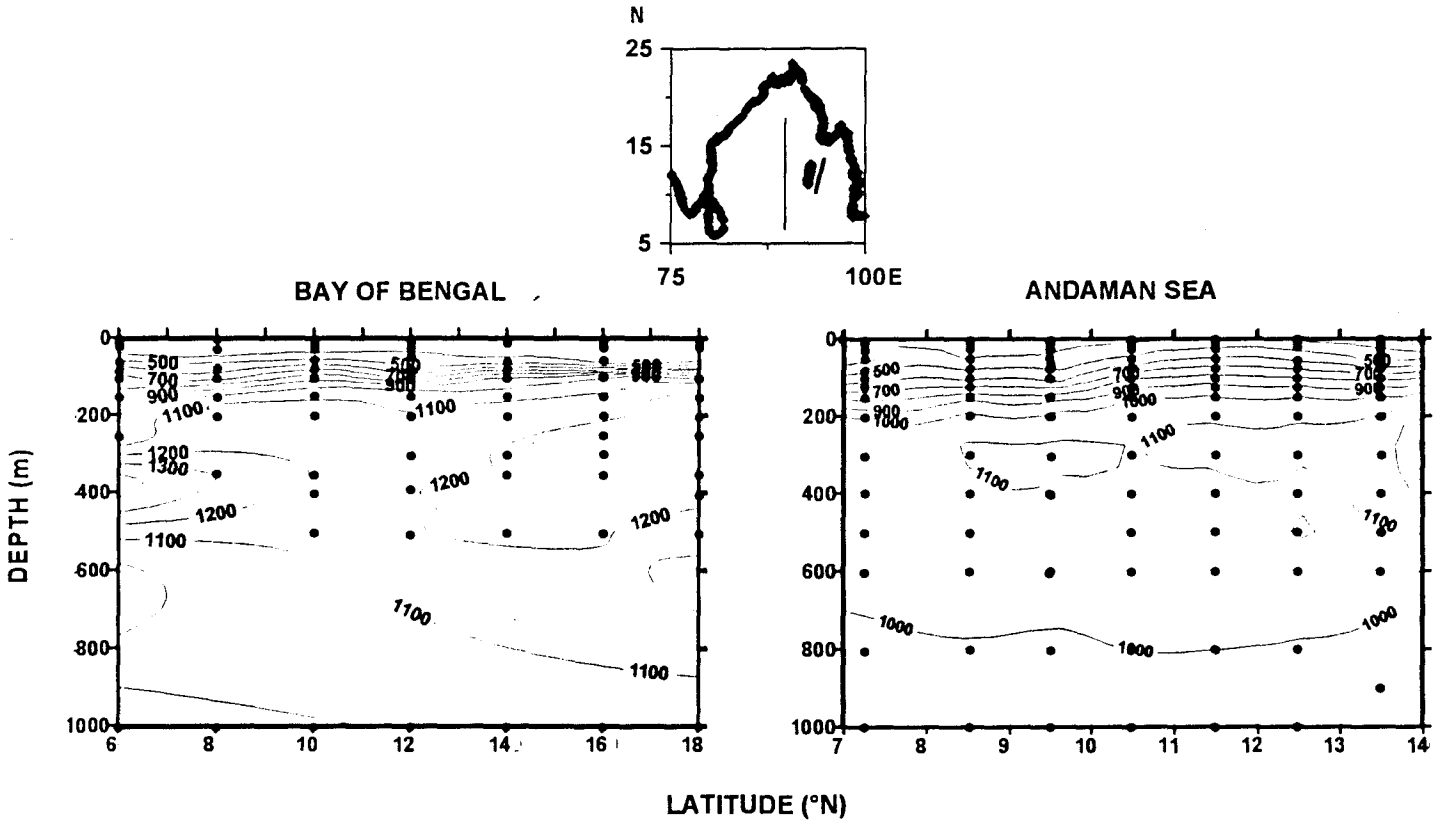

Fig. 4.40. Vertical distribution of partial pressure of carbon dioxide (µatm) in the Bay of Bengal and Andaman Sea.

surface pCO_2 was lowered by the influx of fresh water. Highly stratified pCO_2 contours during inter-monsoon and higher levels could be attributed to the influence of bacterial regeneration in response to increased inputs of organic matter, resulting from the high NE monsoon productivity.

Important points on pCO_2 are:

- **High seasonal and temporal variability occurred in surface pCO_2**
- **Very high pCO_2 values were associated with upwelling/divergence**
- **Coastal upwelling brings pCO_2 double to that in air in to top 20 m water column**
- **Increased in pCO_2 in sub-surface layers throughout the northern Indian Ocean**
- **Higher pCO_2 associated with nitrate rich upwelled waters and also with nitrate depleted sub-surface waters**

4.5. Carbonate solubility

Marine organisms secrete mainly two types of carbonate skeletal minerals. These are aragonite and calcite with same chemical composition ($CaCO_3$) but with slightly different crystal structures. In this section, regional and seasonal variability and biological influence on carbonate ion distribution with respect to

these polymorphs were studied. The surface ocean is generally supersaturated with respect to calcite by a factor of 5.5 in warm equatorial oceans and of 2.5 in the cold polar oceans (Takahashi, 1975). For aragonite, the saturation factor ranges from 3.7 to 1.7. This supersaturation persists up to considerable depths (Broecker and Takahashi, 1978). The tropical surface ocean will not become under-saturated with respect to aragonite and calcite until the partial pressure of carbon dioxide increases by 5.3 and 8.5 times, respectively, to the present atmospheric value (Broecker *et al.*, 1979). Surface water of the northern Indian Ocean have been found to be super-saturated with respect to both calcite and aragonite (Naqvi and Reddy, 1975; Naqvi and Naik, 1983; Kumar *et al.*, 1992; George *et al.*, 1994). Carbonate concentrations decrease from surface to deep sea due to organic matter synthesis in the former layer and decomposition in the latter.

Vertical distribution of carbonate ion (Fig. 4.41) is similar to that of pH (Fig. 4.1). Considerable variations occurred in carbonate ion distribution from south to north in coastal as well as in open seas that reflected productivity pattern (Fig. 4.41). During the SW monsoon carbonate concentrations in the southern surface waters were lower by 50 µM than in the north (Fig. 4.41) and this decrease might have been due to upwelling in the south. The difference was less (25 µM) during NE monsoon but no significant difference occured during inter-monsoon between the northern and southern Arabian Sea. Figure 4.41

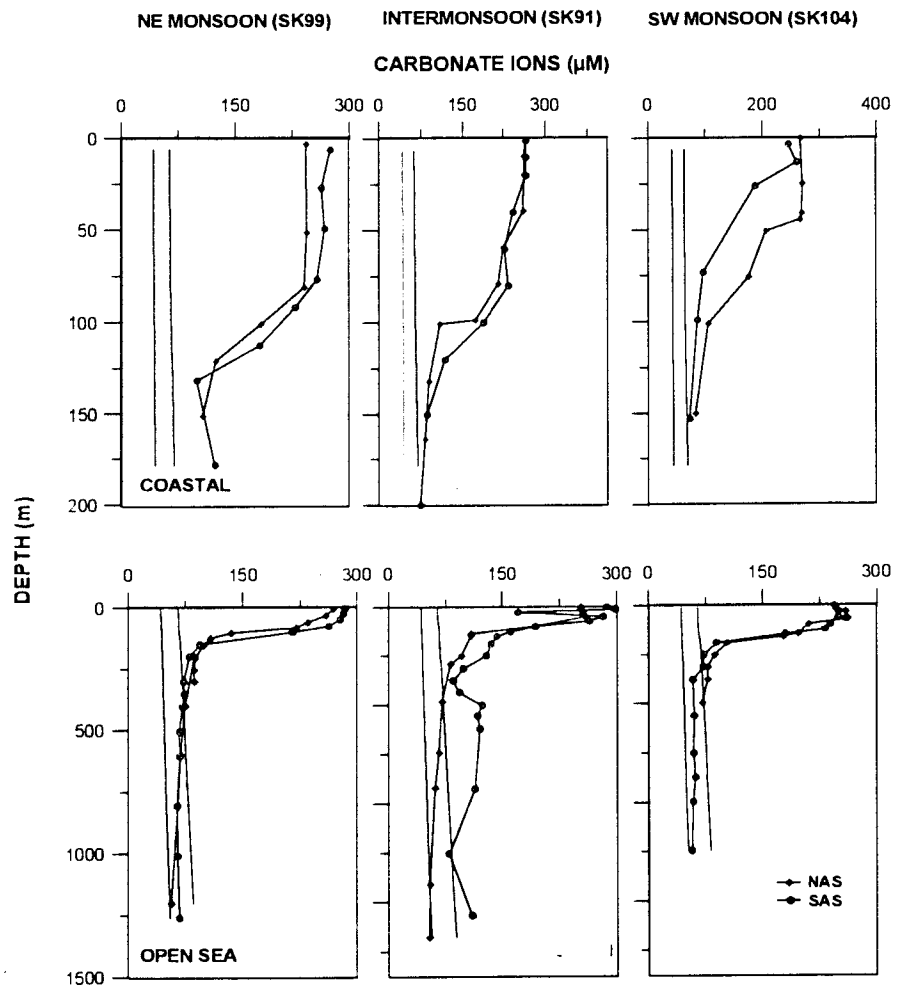

Fig. 4.41. Vertial distribution of carbonate ion (μM) during different seasons in coastal and open sea regions in the Arabian Sea.

shows that this difference is significant only up to a depth of 150 m. The general low carbonate content in the south is a consequence of lower production and lower salinities than in the north. The open sea results (Fig. 4.41) exhibit similar seasonal variations. Low carbonates (by 25-50 μM) were found during SW monsoon in the southern Arabian Sea in 1995 and 1996 compared to those in other seasons. It could be due to the higher productivity in the south (column productivity 119, 335 and 770 $mgC.m^{-2}.d^{-1}$, respectively, during intermonsoon, NE monsoon and SW monsoon at 11° N, 64° E) in this season. Figure 4.41 reveals that while carbonate ion is under-saturated with respect to aragonite at depths even shallower than 500m it is super-saturated with reference to calcite at all depths sampled.

Sub-surface carbonate distribution depends strongly on the extent of release of CO_2 from organic matter decomposition by bacteria. During this process the increase in CO_2 will lead to increased acidity of water thereby enhancing the corrosivness to carbonate skeletal matter

$$CaCO_3 + CO_2 + H_2O \rightarrow Ca^{2+} + 2\,HCO^-_3 \qquad \text{or}$$

$$CaCO_3 + H^+ \rightarrow Ca^{2+} + HCO^-_3$$

Aragonite appears to be more susceptible to these reactions since its saturation curve occurs within the oxygen minimum zone. Figure 4.42 depicts the variability in aragonite saturation depth (ASD) in the central Arabian Sea. During NE monsoon, saturation depth occurred at 400m in south and north but shallowed to 200 m at 17° N coinciding with the deep mixed layer at these latitudes (Fig. 3.1). Increased productivity in surface layers and consequent enhanced decomposition rates in subsurface layers lead to higher pCO_2 and lower in pH_T. Comparatively low pH_T was observed during NE monsoon (Fig. 4.2). At low pH_T waters are corrosive to skeletal carbonates and this leads to shallowing of ASD. Aragonite saturation depth occurred around 400-450 m in inter-monsoon with no significant north-south variations. During the SW, it varied from 200-400m. Seasonal change in productivity seems to be responsible for oscillations in ASD. The saturation horizons observed in the present study are in agreement with those reported in the literature. For instance, George *et al.* (1994) calculated the saturation horizon for aragonite to be at 500 m during pre-monsoon whereas Kumar *et al.* (1992) found it to be 200 m for aragonite just before the SW monsoon. However, these are shallower than that reported (500 m) by Mintrop *et al.* (1998)

Along 15° N, ASD showed large east-west variations (Fig.4.43). During all the seasons ASD shoaled up towards the coast which is in agreement with dissolved oxygen and nitrate. ASD was at 300m in the west but shallowed to

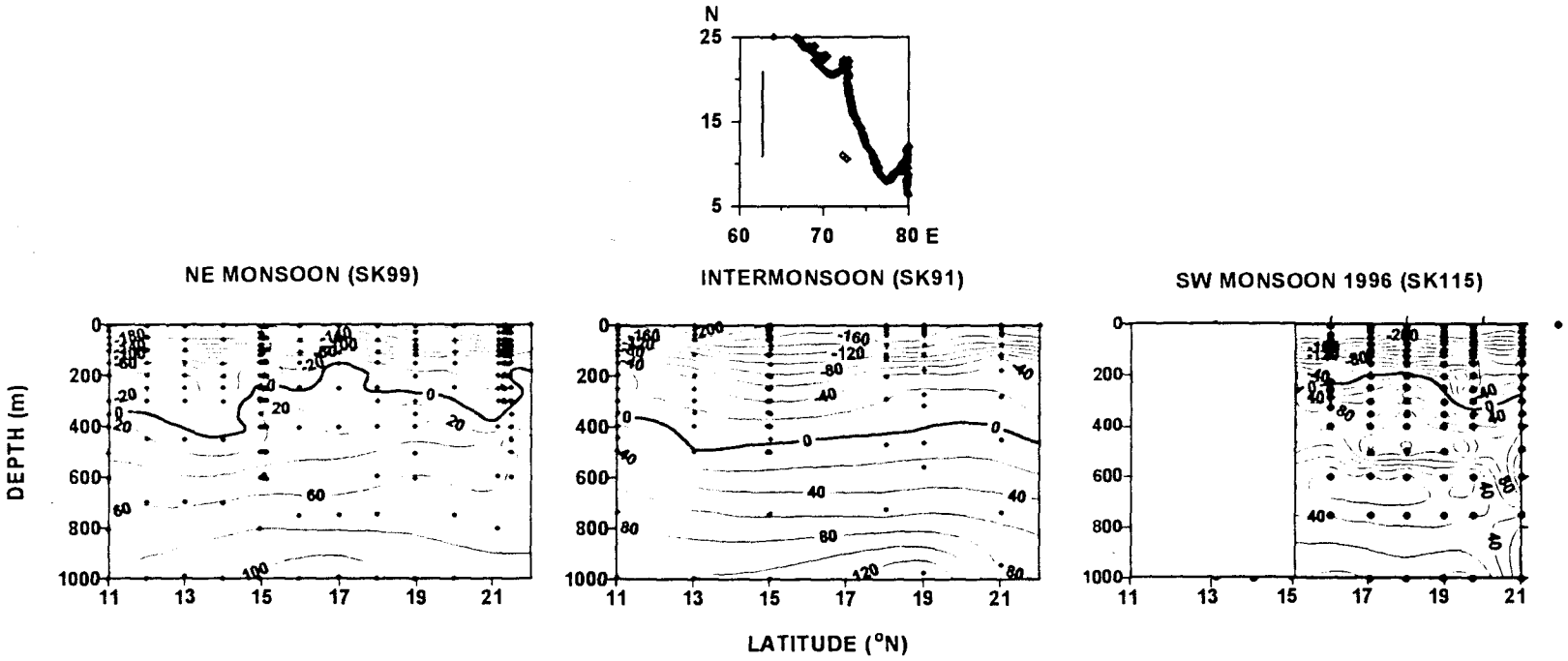

Fig. 4.42. Variations in Aragonite saturation depth (ASD, thick zero contour) during different seasons along 64° E in the Arabian Sea.

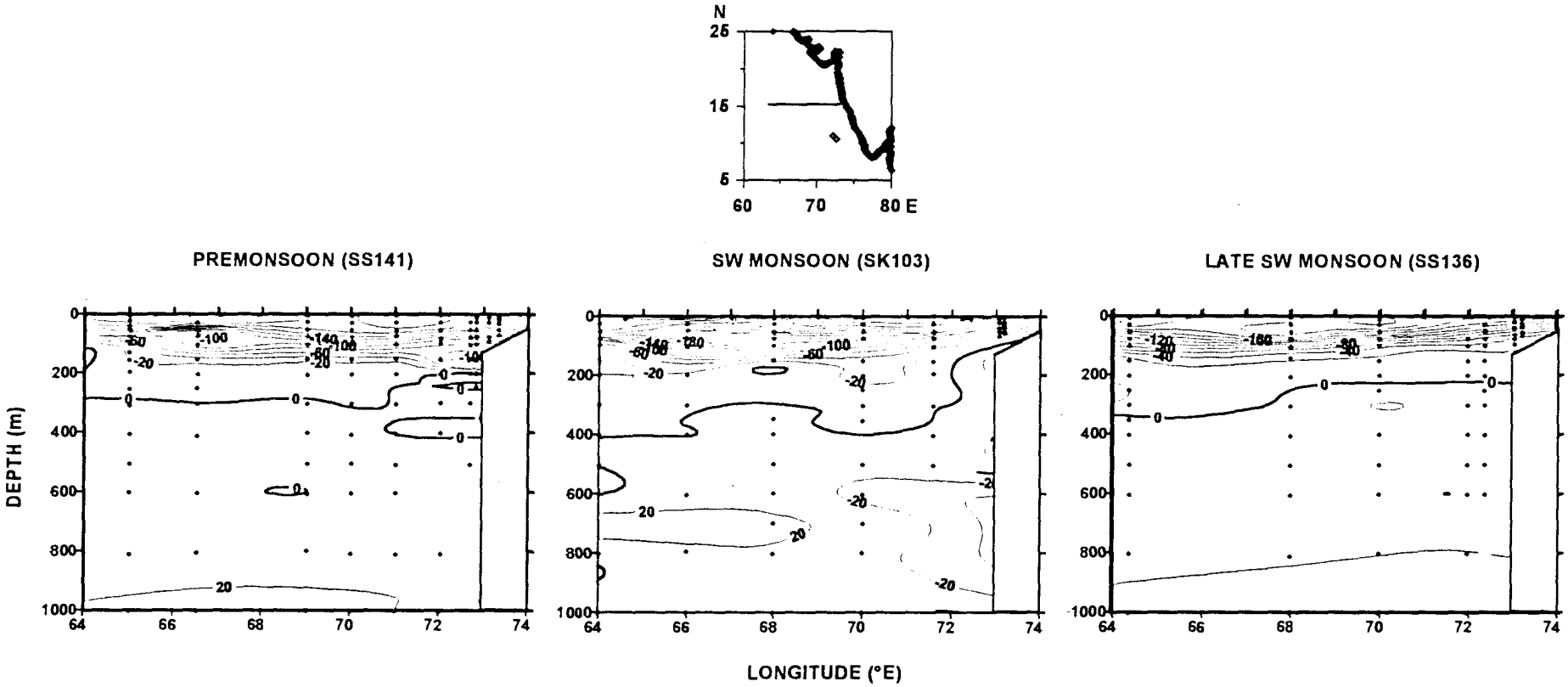

Fig. 4.43. Variations in Aragonite saturation depth (ASD, thick zero contour) during different seasons in the Arabian Sea along 15° N.

200m in the east during pre-monsoon whereas it varied from 400 m to 100 m during the SW monsoon. In the late SW monsoon, however, it did not show large great variation. Upwelling seems to account for the observed regional oscillations seen in Fig. 4.45.

Highlights of the skeletal carbonate dissolution are:

- **Mixing processes influenced carbonate ion abundance in surface waters**
- **Organic regeneration predominantly controls carbonate ion with in OMZ**
- **Seasonal variations in ASD seem to be brought in by changes in productivity**
- **Carbonate ion is super-saturated against calcite in the depth range studied**
- **Coastal upwelling lowers ASD near the coast.**

4.7. Variability in regenerated carbon dioxide

During photosynthesis CO_2 is absorbed from water thus lowering TCO_2. The fixed carbon sinks from surface to sub-surface waters as detritus. Most of the

organic detritus decompose according to equation 4.1 in the top 1000 m (Suess, 1980) thus returning the carbon back to dissolved form. The released carbon is generally referred to as regenerated CO_2. In general, the regeneration is expected to be more in the northern Arabian Sea where denitrification is dominant. Low oxygen concentrations (Fig. 3.2) in intermediate layers of the northern Arabian Sea in all seasons (de Souza *et al.*, 1996) is a result of higher inputs of organic matter from the surface layers. To assess the contribution of the biologically cycled carbon to that of TCO_2 observed the regenerated carbon dioxide was computed using (a) Redfield ratios, (b) Kroopnick's formulations and (c) mixing methods.

4.6.1. Redfield ratio method

According to eq. 4.1, for each mole of oxygen consumed, 0.76 moles of CO2 are liberated from organic matter. Hence, C/O should be 0.76 (Redfield *et al.*, 1963). The presently observed ratio varied considerably with significant seasonal and temporal changes. The C/O ratio was +1.025 during NE monsoon whereas it was +1.366, +1.233 and +1.207 during intermonsoon and during 1995 and 1996 SW monsoons, respectively. Using these ratios, regenerated carbon from the soft tissue was computed. The most intense regeneration (>340 μM) occurred during inter-monsoon season (Fig. 4.44) as bacterial population was very high in response to higher organic matter inputs from winter productivity and the inherent time lag. Bacterial population in inter - monsoon is higher by several

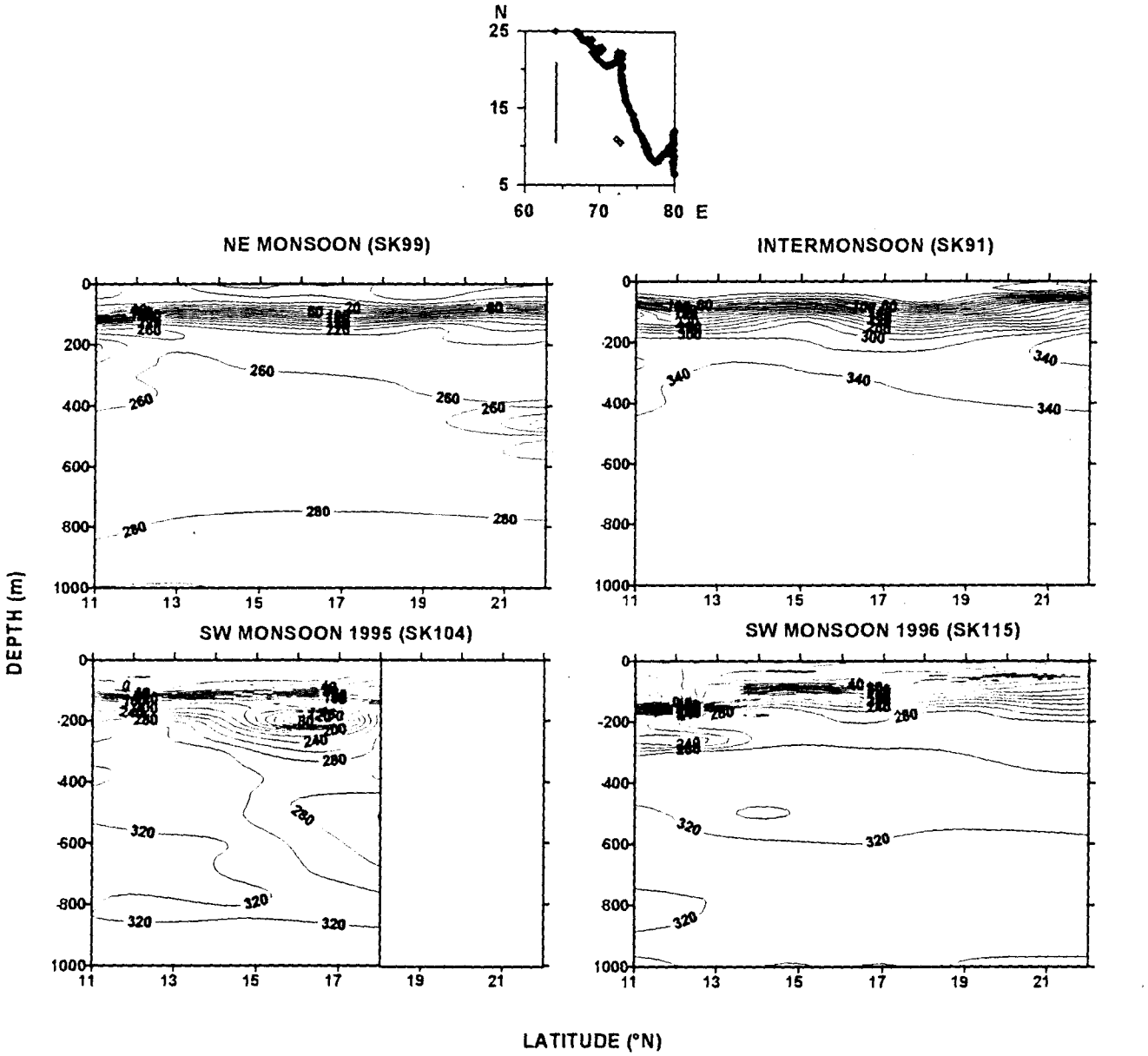

Fig. 4.44. Distribution of regenerated carbon dioxide (uM), which is computed using Redfield method, along 64° E in the Arabian Sea.

folds than in other seasons (Ramaiah *et al* 1996). During the SW monsoon season regenerated carbon amounted to >320 μM whereas it was about 280 μM during NE monsoon. Along 15° N, higher amounts of regenerated carbon (Fig. 4.45) were observed during pre- and late- SW monsoon with comparatively higher values towards the coast due to high productivity in the overlying waters. Regenerated carbon amounted to more than 360, 320 and 360 μM, respectively, during pre-, peak and late- SW monsoon seasons.

4.6.2. Kroopnick's method

Using the formulae given in section 2.3.6.2, the regenerated carbon dioxide (Fig. 4.46) was found to behave almost similarly to TCO_2 (Fig. 4.28). During the NE monsoon it is higher by 70-80 μM than in inter-monsoon and by more than 100 μM compared to that in 1995 SW monsoon. The regeneration amounted to a CO_2 release of 140 μM at 200-300m in inter-monsoon whereas it was about 230 μM, 80 μM and 180 μM, respectively, during NE monsoon, and SW monsoon of 1995 and 1996. During all the seasons there was a clear north-south gradient, i.e., increasing trend towards northern Arabian Sea at any depth level. Along 15° N, higher regeneration was observed in the west, except near the coast during the SW monsoon (Fig. 4.47). This is due to fixation of higher amounts of organic matter driven by upwelling. It amounted to ~240 and 160 μM during the peak and late SW monsoon, respectively.

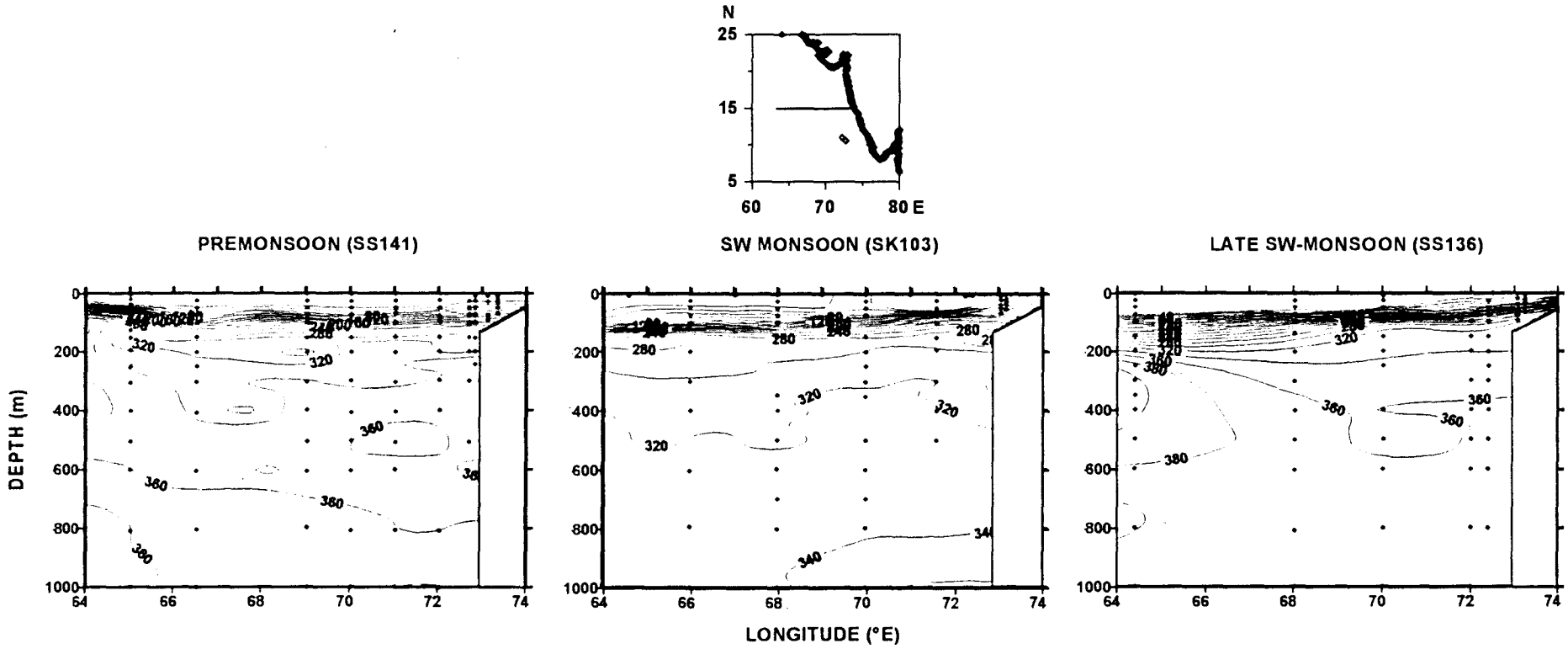

Fig. 4.45. Distribution of regenerated carbon dioxide (uM), which is computed using Redfield method, along 15° N in the Arabian Sea.

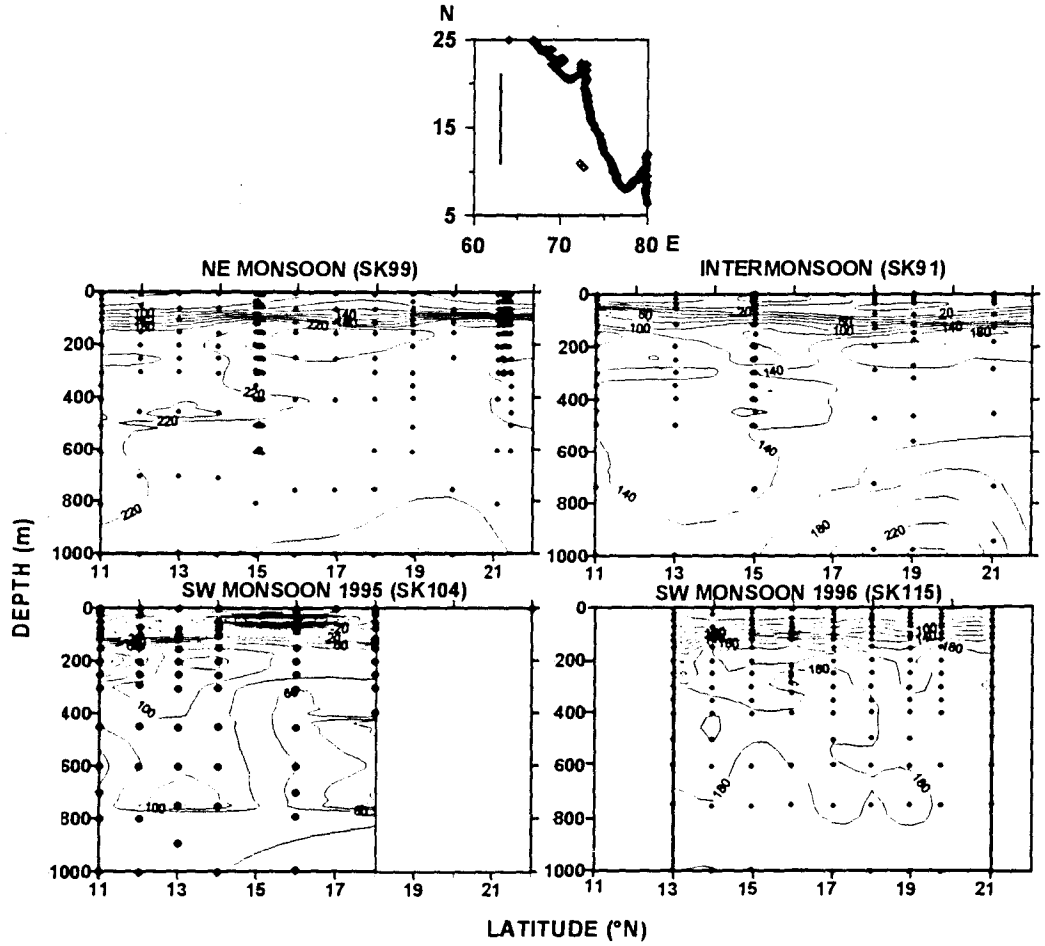

Fig. 4.46. Distribution of regenerated carbon dioxide (μM), which is computed using Kroopnick's method, along 64° E in the Arabian Sea.

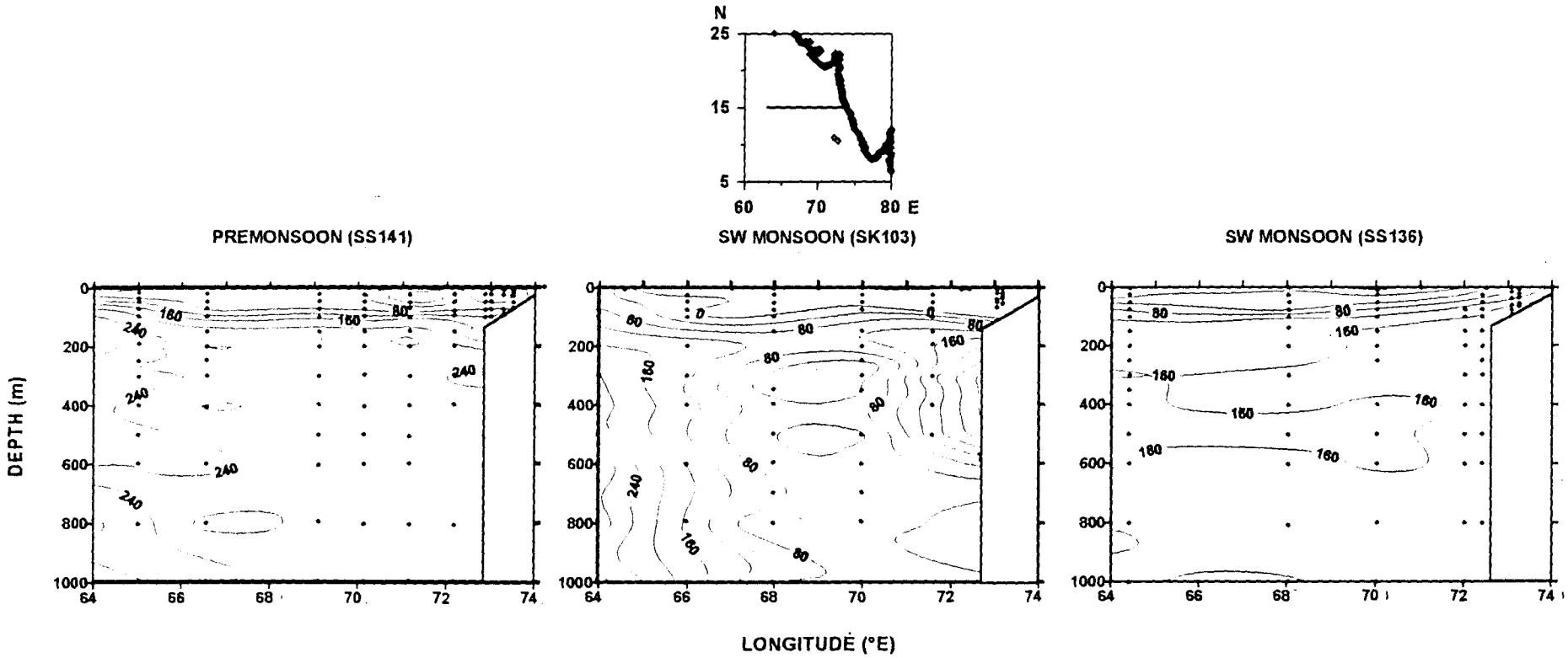

Fig. 4.47. Distribution of regenerated carbon dioxide (μM), which is computed using Kroopnick's method, along 15° N in the Arabian Sea.

Highlights on regenerated carbon are:

- Redfield regeneration decreased in the order inter-, SW and winter monsoons
- Kroopnick's generalizations yielded opposited to that of Redfield's, i.e., Winter, SW and inter- monsoons
- Considerable variability in regeneration between 1995 and 1996 SW monsoons occurred
- Regenerated carbon evaluation is highly subject to the method used

Chapter 5

DYNAMICS OF ORGANIC CARBON

Organic carbon occurs in dissolved and particulate forms in sea water. Dissolved Organic Carbon (DOC) represents the biggest pool of organic carbon in sea water. DOC mainly originates from metabolic processes including the breakdown of cells during grazing and also is an intermediate in the conversion of particulate organic matter into inorganic carbon dioxide. It is known to play a pivotal role in food chain as it serves as a substrate for micro-organisms. The nature and importance of various processes regulating the DOC pool, particularly in the Arabian Sea, are not well understood. Although DOC is largely produced at the surface by phytoplankton, bacteria play a major role in regulating its concentration through the processes of decomposition/ regeneration. Ducklow (1993) found mesopelagic bacterial carbon demand to be an order-of-magnitude greater than the sinking flux, in the Arabian Sea, suggesting a large scale DOC import into the mesopelagic zone from other sources such as lateral advection and vertical transport. Similarly Naqvi and Shailaja, (1993) found an imbalance between surface primary productivity and bacterial carbon demand in the denitrifying oxygen minimum zone. Measurements of electron transport system activity indicated that bacterial carbon demand was the highest beneath the offshore oligotrophic waters. Kumar *et al.* (1990) proposed that microbial population plays a major role in regulating the DOC contents in waters of this region. Their studies further suggested that denitrifying bacteria and other micro-organisms involved in nitrogen cycling in the Arabian Sea are related to DOC dynamics; their

increased abundance is responsible for decreased DOC concentrations in the north. Since the oceanic DOC pool is large and recycles faster than thought earlier (Toggweiler, 1988) it is important to study the dynamics of DOC which has implications to carbon cycling in sea water and in future to long term changes in atmospheric CO_2 concentration.

Tiny organisms such as plankton, bacteria etc. together with dead/detrital organic matter form particulate material. The POC can occur in visible and invisible forms. Of these, the invisible form is generally referred to as Transparent Exopolymer Particles (TEP) formed from dissolved carbohydrates. Dissolved carbohydrates constitute the major fraction of dissolved organic compounds in sea water. In view of the fact that TEP plays an important role in carbon cycle (Alldredge *et al.*, 1993) than the rest of particles, this class was studied in detail. TEP exists as discrete particles rather than as cell surface coatings (Alldredge *et al.*, 1993) that are probably formed abiotically from dissolved extracellular polysaccharides (Passow and Alldredge, 1994) which diatoms excrete copiously (Hama and Handa, 1983, 1987; Williams, 1990). During diatom blooms TEP occurs in abundance and sizes comparable to phytoplankton (Passow and Alldredge, 1994). Degradation of organic matter can be accelerated in the presence of TEP as these large particles appear to be more hospitable to bacteria than their source colloids (Kepkay, 1994). These particles are expected to have far reaching implications to aggregation

processes. Particle aggregation rates can be higher in the presence of TEP because surfaces of these are sticky and their size variation is quite large. Aggregation rates depend on concentrations and sizes of all particles present (Jackson, 1990). TEP are polysaccharides and so are easily consumed/decomposed by bacteria while playing a vital role in particle dynamics in aquatic systems (Fig. 5.1). In view of the intense water column denitrification in the Arabian Sea and higher rates of sinking particles in the Bay of Bengal data on TEP were collected from the North Indian Ocean during August 1996 to understand their role in the biogeochemical processes. DOC data were collected in the same season (SK 115) in the Arabian Sea. Due to unforeseen technical problems seasonal studies could not be performed in this study. Nevertheless, this is the first such effort to understand the processes involving organic carbon with respect to total carbon cycling. This chapter presents the dynamics of Dissolved Organic Carbon and Transparent Exopolymer Particles, possible inter-conversions between them and their importance to biogeochemical processes.

5.1. Variability in organic carbon

Vertical distribution of DOC (Fig. 5.2) suggests highly variable trend between north and south. Surface DOC concentrations varied from 90 to 120 μM. The patchy surface distribution seems to reflect variations in primary productivity.

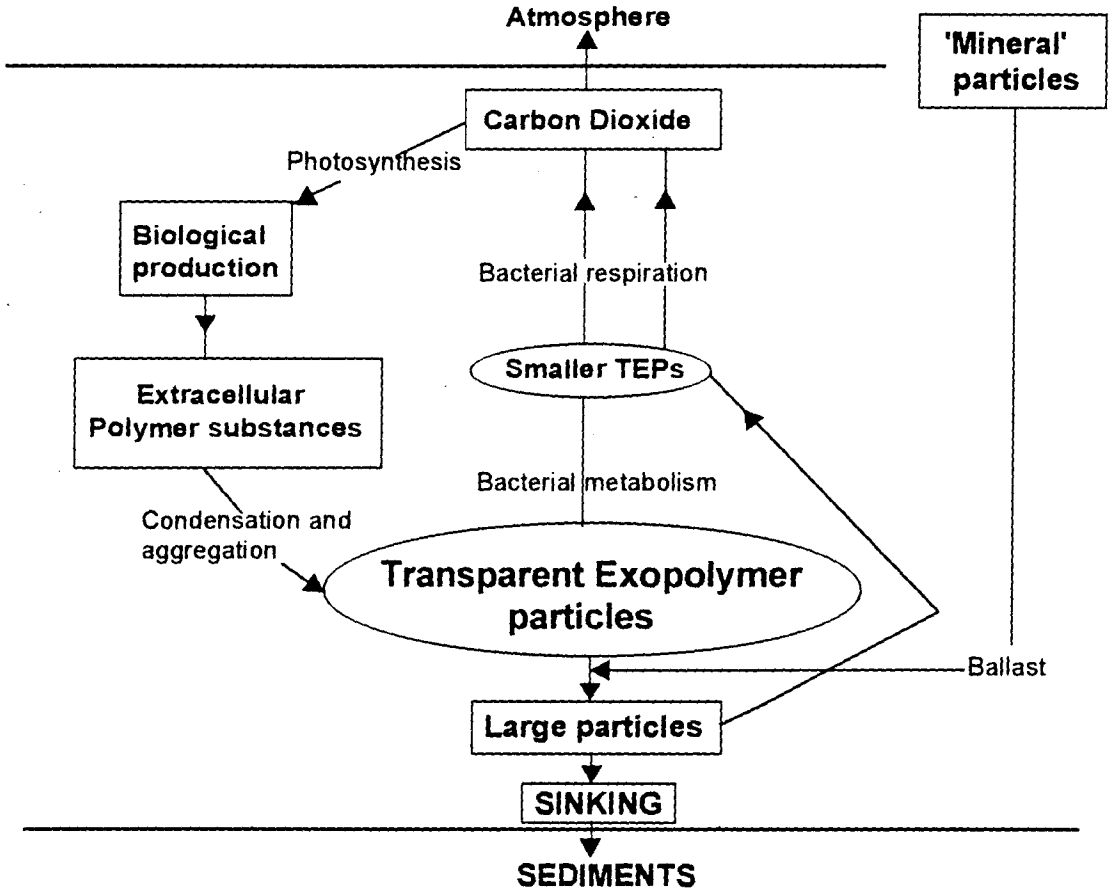

Fig. 5.1. Transparent Exopolymer Particles formation and implications to biogeochemical cycling of carbon in the oceans.

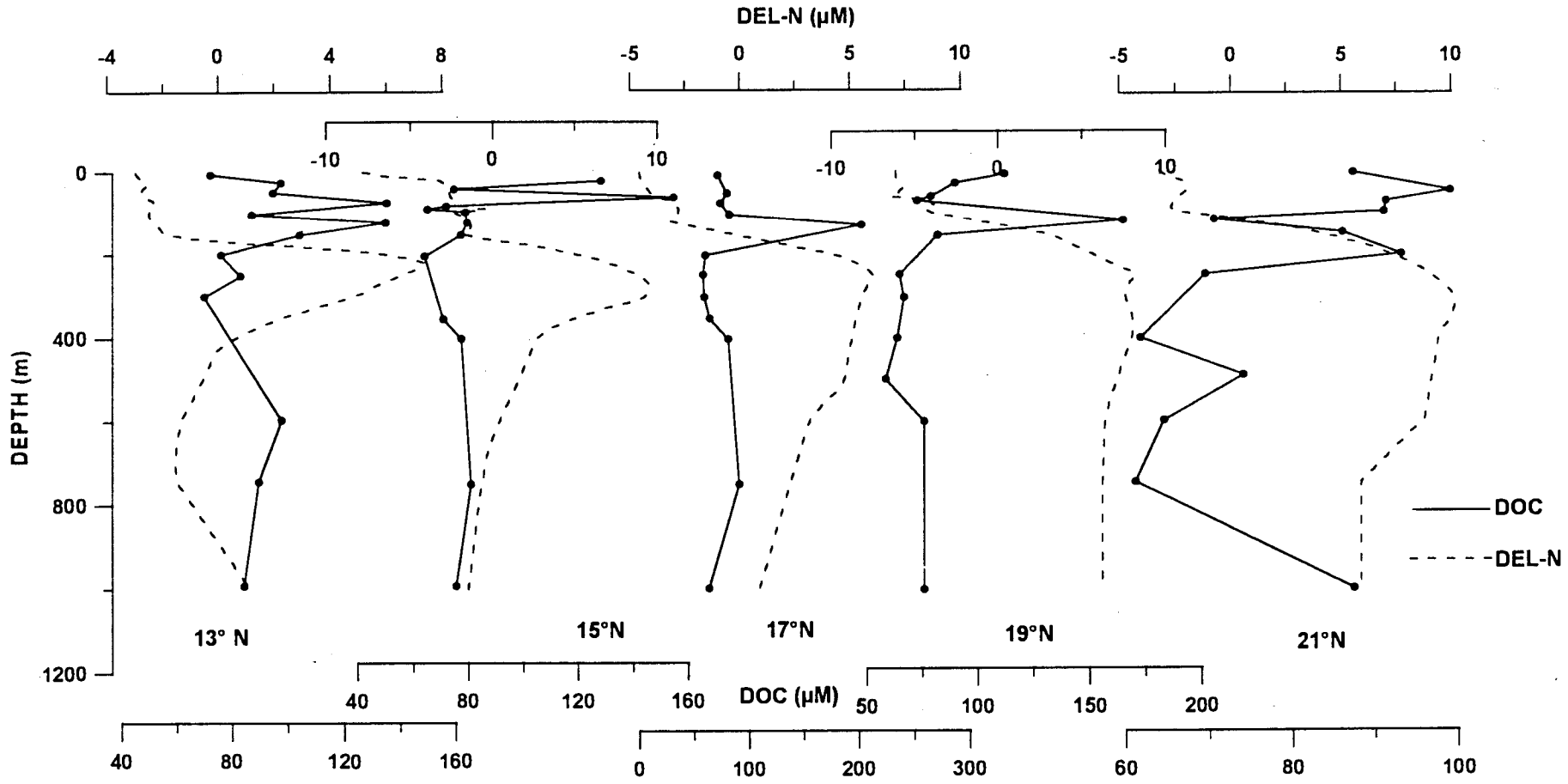

Fig. 5.2. Vertical distribution of Dissolved Organic Carbon in the Arabian Sea and its relation with nitrate deficit (DEL-N).

Relatively higher DOC in surface waters at 15° N is perhaps due to the dominance of production over its consumption which increases towards south as observed by Kumar *et al.* (1990). The primary production in August 1996 was the highest at 15° N. The production was found to be 792, 1782, 1030, 830 and 349 mgC m^{-2} d^{-1} at 13°, 15°, 17°, 19° and 21° N, respectively. Interestingly, at 17° and 19° N higher concentrations of DOC were observed at or below the thermocline (100-200 m). Figure 5.2 suggests DOC accumulation in thermocline waters with an increasing trend towards north. DOC concentrations varied from 60 to 100 µM in the sub-oxic waters when lower concentrations were observed in the northern parts. Decrease in DOC concentrations towards north could be attributed to high rates of respiration (Kumar *et al.*, 1990). Minima in DOC coincide with maxima in nitrate deficit suggesting its utilization in denitrification (Fig. 5.2). These profiles, in general, clearly suggest a negative relationship between DOC and nitrate deficits in the depth range 200 - 600 m.

Here, TEP are expressed as mg equivalents of alginic acid per litre. Concentrations of TEP were higher in the Arabian Sea than in the Bay of Bengal (Fig. 5.3). Higher TEP in Arabian Sea could have been a direct consequence of *Phaeocystis* blooms with diatoms in significant numbers during the study period (M. Madhupratap, Personal Communication, 1997). *Phaeocystis* blooms generally follow diatom blooms (Gieskes and Kraay,

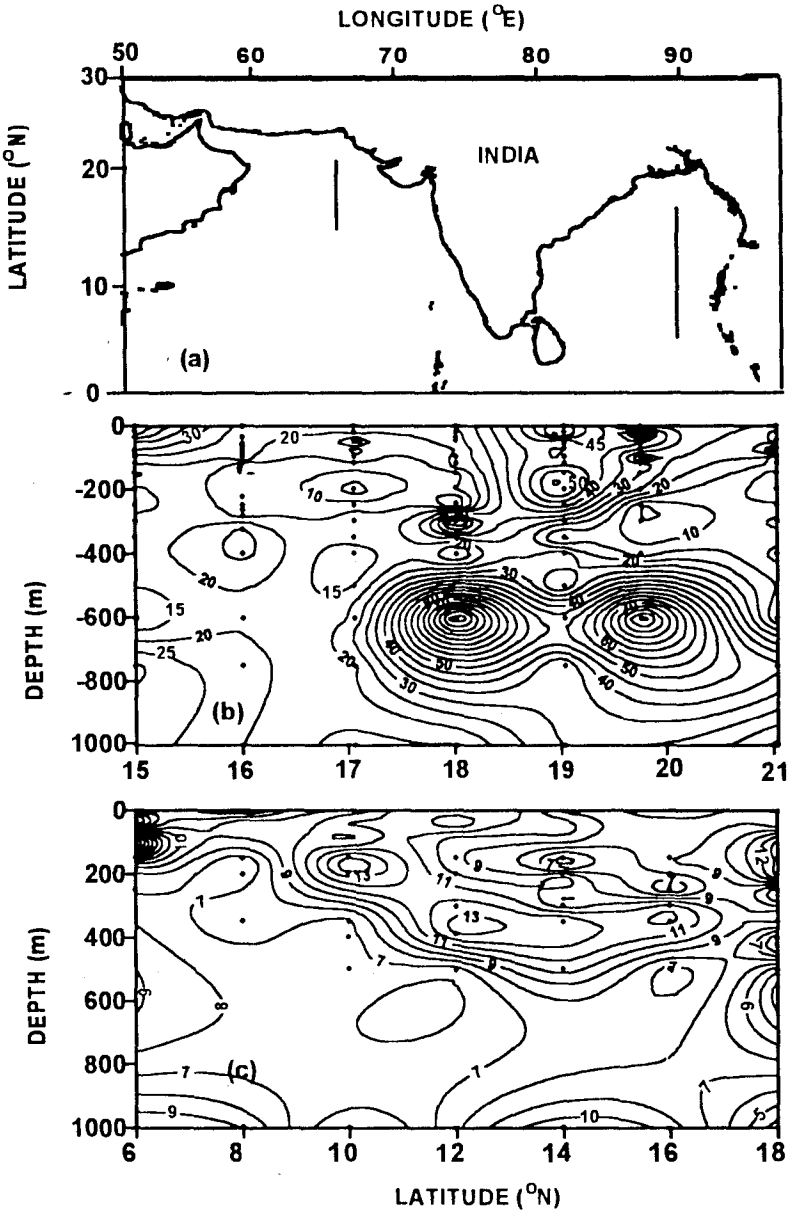

Fig. 5.3. (a) sections occupied during 1996 southwest monsoon in the Arabian Sea and the Bay of Bengal. TEP (mg equivalents of AA l^{-1}) distribution (b) in Arabian Sea and (c) in the Bay of Bengal.

1975). Polysaccharide exudates from *Phaeocystis* (Lancelot and Methot, 1985) and diatoms (Passow *et al.*, 1994) might have led to the observed higher TEP levels in Arabian Sea (Fig. 5.3). Lancelot (1984) observed that about 50% of the carbon fixed by photosynthesis is secreted as mucus by *Phaeocystis.* Surface TEP was higher (≥25 mg equivalents of AA l^{-1}) at 18-20° N in the Arabian Sea (Fig. 5.3) where upwelling signatures (a temperature of 26.3° C and nitrate >1 µM; Figs. 3.2 and 3.3) were evident. Availability of nutrients in these waters might have triggered intense biological production leading to a higher release of extracellular materials. Productivity was very high around these latitudes (1030 and 830 mgC m^{-2} d^{-1} at 17° and 19° N) that also corresponds well with the highest DOC values observed in the thermocline region (Fig. 5.2). Thick mucus materials in this region clogged the zooplankton net above the thermocline. The higher surface signatures of TEP, between 18° and 20° N, were conspicuous down to 300 m (Fig. 5.3). Very high concentrations of TEP (~102 and 94 mg equivalents of AA.l^{-1}, respectively) were, however, found at ~600 m at 18° and ~20° N, where upwelling occurred. These anomalous high concentrations might have been generated through bacterial activities, in situ (Passow and Alldredge, 1994) and/or due to sinking of aggregates from highly productive surface waters. Such concentration gradients were not seen in the Bay of Bengal where TEP varied within a narrow range (7-13 mg equivalents of AA.l^{-1}). Although the TEP concentrations were higher in Arabian Sea their numbers (Table 5.1) were low (130-350 ml^{-1}) in

contrast to those in Bay of Bengal (4400 to 7790 ml^{-1}) since the TEP sizes were relatively large in the former region than in the latter. In Table 5.1 the data from ~500 m are presented to understand the role of mineral-organic matter interactions in particle sinking mechanism. Higher productivity in Arabian Sea might have resulted in enhanced stickiness and hence in large TEP sizes. Bacterial numbers were higher in the bay thus aiding reduction in stickiness (Passow and Alldredge, 1995) and particle breakdown thereby increasing the TEP numbers. While these are the first measurements of bacteria from the central bay; the bacterial population in Arabian Sea seasonally vary by a factor of ~1000 (Madhupratap *et al.*, 1996; Ramaiah *et al.*, 1996).

The high concentrations of DOC below the mixed layer (~120 m) could be attributed to the release of DOC from TEP as somewhat negative trends observed between TEP and DOC at these depths (Fig.5.4). High bacterial carbon was also observed at this depth suggesting that TEP hydrolysis significantly contributes to the release of DOC. Since TEP is mainly comprised of polysaccharides, it is easily degradable/decomposible into small compounds. This view is supported by the observed association of the DOC maxima with a steep increase in nitrate deficit, (Fig. 5.2) particularly at 17° and 19° N. Cho and Azam (1988) hypothesized that bacteria attached to particle aggregates solublize these by hydrolytic enzymes. If DOC is produced much faster than its uptake by attached bacteria then most DOC tends to remain in

TABLE 5.1: Transparent Exopolymer Particle characteristics and bacterial counts in the North Indian Ocean

Lat. (°N)	Long. (°E)	Depth (m)	Bacterial Counts[a] (per ml)	TEP mean length[b] (μm)	TEP Total counts[a] (per ml)	TEP with mineral particles[c]	TEP without mineral particles[c]
				Arabian Sea			
15	64	600	2.94	37±42	0.026	3	5
17	64	500	1.64	92±97	0.013	1	5
19	64	500	1.29	21±23	0.033	1	6
21	64	500	3.40	42±67	0.035	4	3
				Bay of Bengal			
8	90	500	10.45	9±10	0.440	21	4
10	90	500	7.41	16±18	0.669	7	4
16	90	500	4.28	11±18	0.779	15	6
18	90	500	0.94	7±12	0.480	10	2

[a]Bacteria ($x10^4$) and TEP counts were total numbers in seawater.
[b]The mean lengths of TEP were determined from a minimum of 30 particles.
[c]TEPs associated with and without mineral particles were based on those counted in randomly selected 10 fields on each filter.

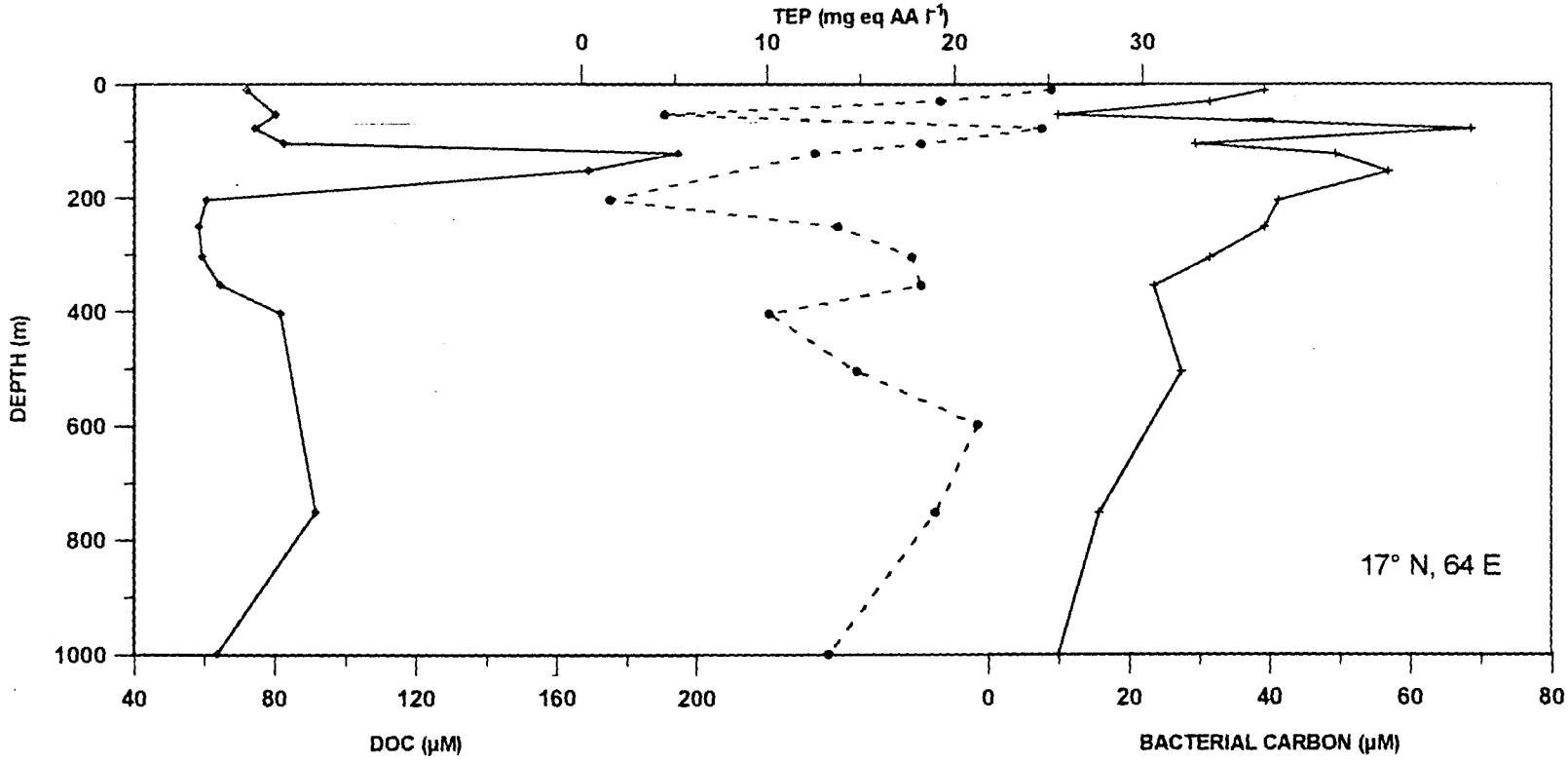

Fig. 5.4. Vertical profiles of DOC, TEP and bacterial carbon at 17° N, 64° E in the Arabian Sea.

sea water ('uncoupled solubilization'). The enzyme activity of bacteria on aggregates could generate slow-to-degrade DOC (Smith *et al.*, 1992) by creating high concentrations of hydrolytic products within the aggregate matrix. For instance, peptides and sugars produced by protease and glucosidase activities, respectively, can condense (Maillard, 1913) to form substances similar to humics which pelagic bacteria can not utilize rapidly (Keil and Kirchman, 1993). Azam *et al.* (1994) suggested that simultaneous and intense enzymatic activities on the structurally diverse and complex particulate aggregates produce a great variety of molecular species, some of which are not readily utilized. Mass aggregations during a bloom will thus result in a large-scale production of slow-to-degrade DOC. This may be particularly so around 19° N where mucus materials were found following the intense blooms triggered by upwelling.

The DOC depletion in sub-surface waters of northern Arabian Sea appears to be due to consumption by bacteria. Figure 5.2 clearly suggests that the depletion of DOC in the north is associated with higher oxidant utilization by bacteria. Naqvi (1994) argued that the carbon demand for denitrification in the sub-oxic zone can not be supported by the vertical particle flux alone and hypothesized it to be DOC lateral transport. Significantly, TEP levels were lower in 200-500 m range than those in layers above and below in Arabian Sea, particularly to the north of 18° N (Fig. 5.3). In contrast, there was no such

decrease in TEP levels in Bay of Bengal. Interestingly, decreased levels of TEP coincide with higher secondary nitrite and nitrate deficits (Fig. 5.5) suggesting the utilization of TEP in bacterial respiration/production in denitrifying layers. A few higher values, inside the dashed circles in Fig. 5.5 might have been due to sinking or in situ specific bacterial/coagulation processes (Kumar *et al.*, 1998).

5.2. Organic carbon relations

Negative relationships for AOU with DOC and TEP were found (Fig. 5.6). The observed higher values of AOU and lower values of DOC occurred in the oxygen minimum zone due to their consumption during bacterial metabolism (Kumar *et al.*, 1990). Depending upon whether the oxidation of POC to DOC or of DOC to CO_2 is dominant, the expected relations between oxidation and DOC would be negative or positive, respectively (Kumar *et al.*, 1990). Hence, the relation between oxygen/AOU and DOC/TEP should represent which process is dominant. In other words, if the rates of DOC production from POC/TEP and its subsequent oxidation to CO_2 are equal, and so the amounts of oxygen consumed are equal, no specific trend should be discernible. Alternatively, if POC oxidation directly proceeds to CO_2, as can occur at particle surfaces, the relationship of an oxidant with DOC should be random. The weak negative relationships between DOC/TEP and AOU (Fig. 5.6) illustrate the dominance of

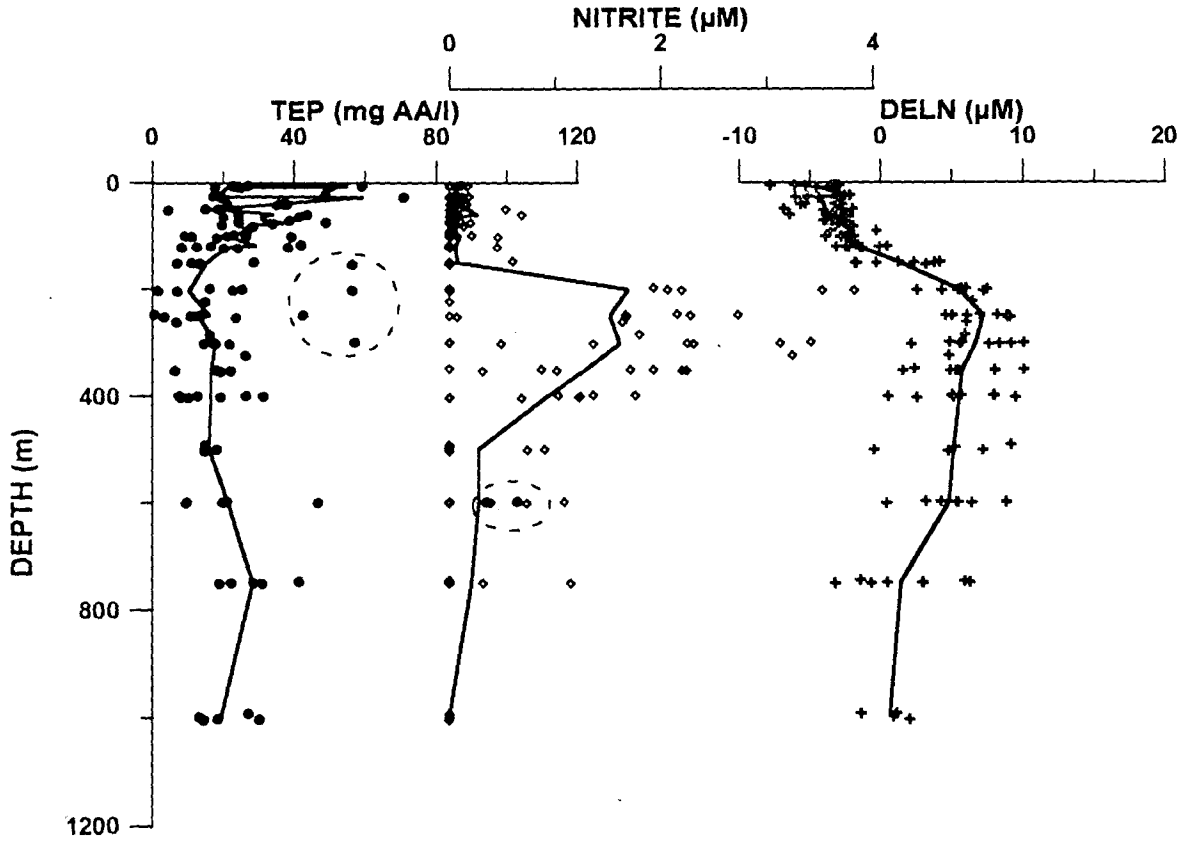

Fig. 5.5. Vertical profiles of (a) TEP (mg equivalents of AA l^{-1}), (b) nitrite (µM) and (c) nitrate deficit (µM) in the Arabian Sea. Solid lines are average curves. Points in dashed circles were not considered while averaging TEP.

DOC/TEP oxidation to CO_2. However, the scatter could be due to variations in organic matter flux, oxygen availability and bacterial activity. This scatter could have been also the result of POC oxidation to CO_2. Kumar *et al.* (1990) observed the weak negative correlation between AOU and DOC in the Arabian Sea and high scatter of points were attributed to the degradation of POC (detritus and other sinking biogenic particles), which might precede the in situ decomposition of DOC, should have consumed at least a part of subsurface oxygen. Menzel and Ryther (1968) opined that the in situ decomposition of organic matter does not necessarily account for the observed oxygen distribution. Our results show that not all of the sub-surface oxygen is used for the in situ decomposition of DOC alone, but that some could have been used for particle degradation, for example, TEP. This could also explain the DOC observations of Craig (1971) and of Ogura (1970), which accounted for about only one-third of the AOU. Results of Druffel *et al.* (1989) for a station in the central North Pacific Ocean revealed that oxygen was used not only for DOC but also for POC decomposition. The Arabian Sea intermediate layers experience widely variable reducing conditions where nitrate also acts as an electron donor (Fig. 4.4). Therefore, oxygen consumption may not solely represent the total oxidant used during the organic matter oxidation in sea water (Jackson and williams, 1988). Denitrification in subsurface layers of the Arabian Sea has been shown to be related to the occurrence of intermediate

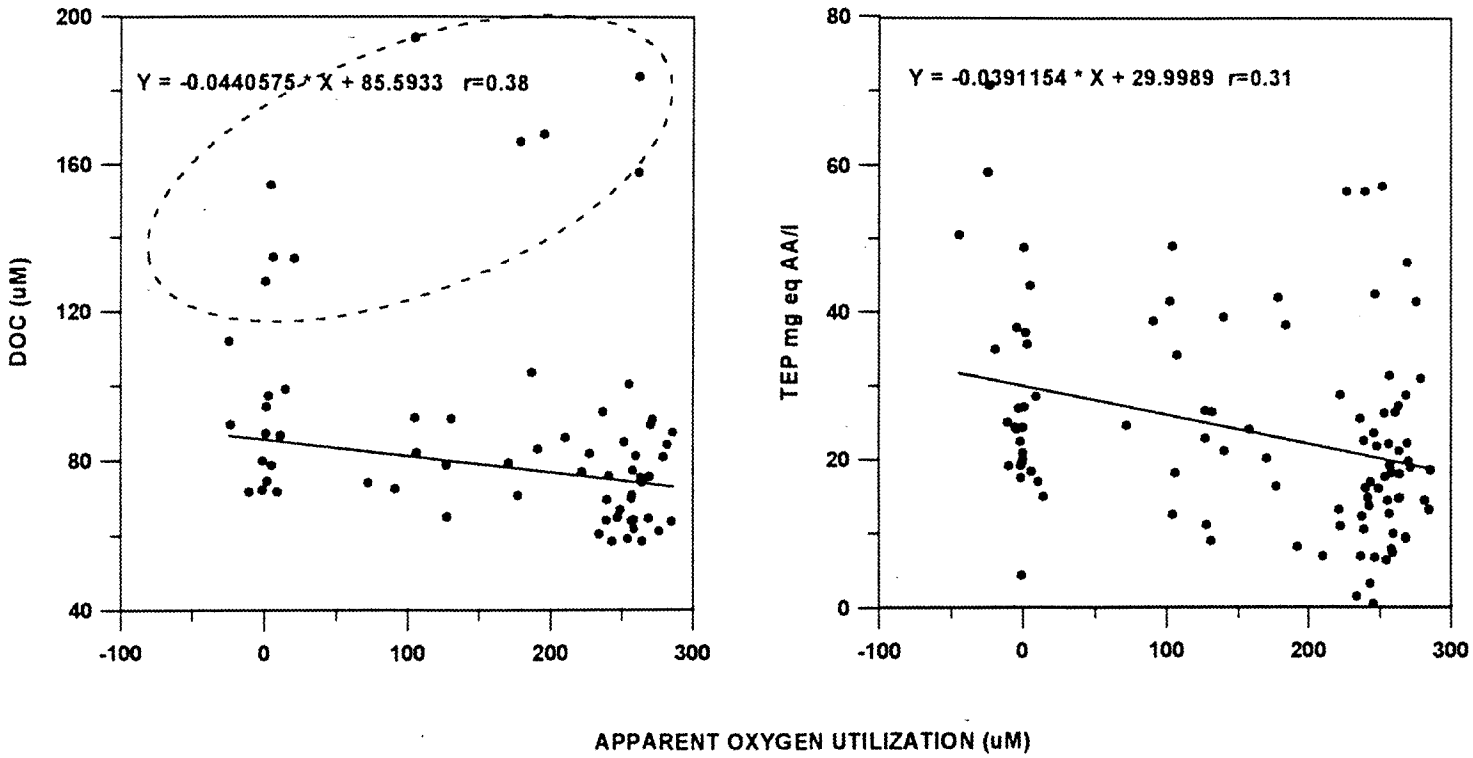

Fig. 5.6. Relations of AOU with DOC and TEP (mg equivalents of AA l^{-1}) in the Arabian Sea. Points in dashed circle were not taken into account in regression.

nepheloid layers (detectable by a transmissometer) and enhanced electron transport activity (Naqvi and Shailaja, 1993).

Dissolved organic carbon consumption occurs in denitrification (Kumar *et al.*, 1990) which is augmented by the negative relationship in Fig. 5.7 between DOC and nitrate deficit. North of 15° N particulate carbohydrates are found to be lower in intermediate waters in the Arabian Sea (Bhosle and Wagh, 1989). In agreement, respiration rates are comparatively higher in the upper 1 km of the Arabian Sea than in the Bay of Bengal (Naqvi *et al.*, 1996). Sinking fluxes of carbon (11.8 to 29.1 mg C m^{-2} d^{-1} at 100m; based on Ducklow, (1993) and Banse (1994)) have been found to be insufficient to meet the respiratory carbon demands of denitrifiers of 155 mg C m^{-2} d^{-1} (Naqvi *et al.*, 1993) and bacterial production of 173 to 758 mg C m^{-2} d^{-1} (Ducklow, 1993) in the sub-oxic layers of the Arabian Sea. Hence, the presently observed negative relation between TEP and nitrate deficits in the oxygen minimum zone (Fig. 5.7) is significant since some of these TEP may not sink rapidly but can remain in suspension, depending on the density structure of the surrounding medium and concentrations of extraneous/mineral particles, and in the meanwhile, can serve as substrate for respiratory activity. Alldredge (1998) estimated that the carbon content in marine snow could ranges from 17 to 39%. Consequently, this hitherto unknown carbon pool of TEP may account for a substantial part of the 'insufficient carbon substrate' required to satisfy the bacterial respiration

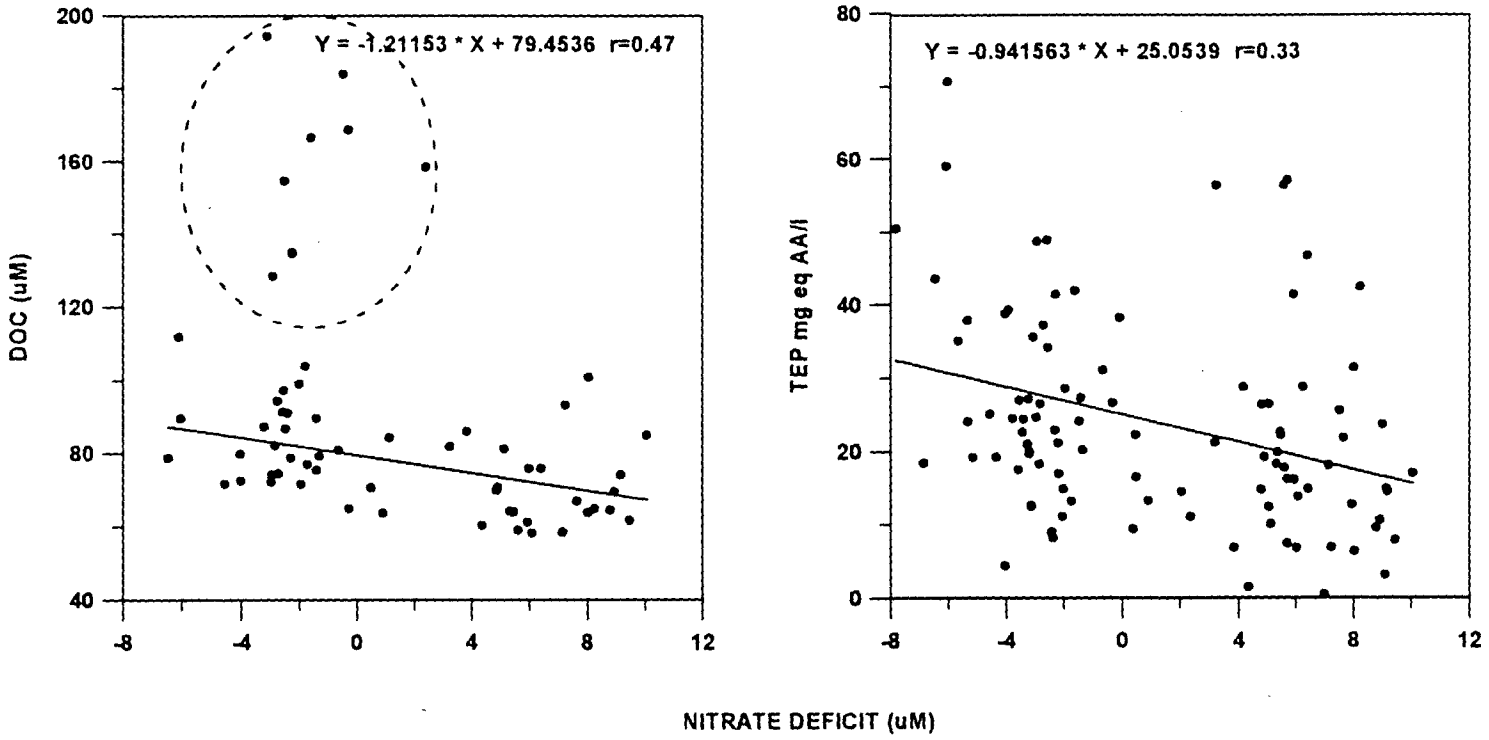

Fig. 5.7. Relations of nitrate deficit with DOC and TEP (mg equivalents of AA l^{-1}) in the Arabian Sea. Points within the dashed circle were not taken into account in regression.

demands in subsurface layers of the Arabian Sea. For instance, using a density difference between particle and water of 10-6 g cm^{-3}, particle area of $25x10^{-6}$ cm^2, viscosity of sea water, corresponding to subthermocline depth with 10° C and 35 psu, of $1.3866x10^{-2}$ $cm^{-2}s^{-1}$ and acceleration due to gravity of 981 cm s^{-2} the estimated stokes settling velocity of transparent particle is calculated to be 3.395 $gm^{-2}d^{-1}$. Therefore assuming 10% of TEP would be constituted by organic carbon, the sinking carbon flux in form of TEP could be 340 $mgCm^{-2}d^{-1}$. Hence, TEP carbon appears to sustain significant bacterial production/respiration in intermediate layers of the Arabian Sea.

Positive relationships appear to exist between bacterial carbon and concentrations of TEP and DOC (Fig. 5.8), even though the scatter appears to be large for the former. This indicates that the bacterial metabolism is fuelled by the availability of labile fractions of organic carbon in the Arabian Sea. Overall primary production exhibited poor correlations with DOC and TEP (Fig. 5.9) indicating that these organic forms in surface layers do not depend on productivity alone but on regeneration also, i.e. net metabolic activities. The particulate and dissolved organic components are assimilated by water column bacteria, which in turn are important for sustaining moderate to higher numbers of microzooplankton (10-85 l^{-1}) in waters immediately below thermocline (200-400 m) in the Arabian Sea. Comparison between the concentrations of DOC and bacterial abundance suggests that the DOC in deep layers is somewhat

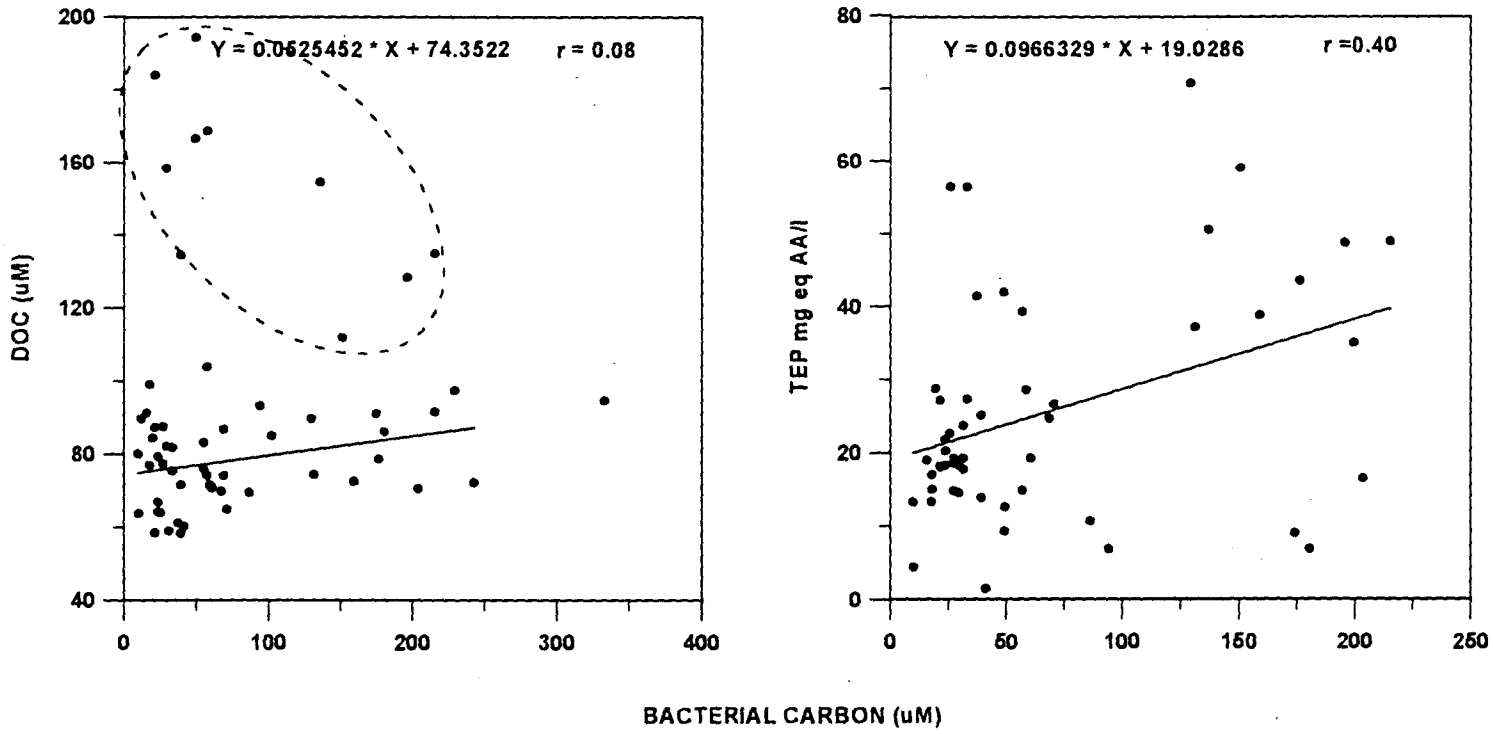

Fig. 5.8. Relations of Bacterial carbon with DOC and TEP (mg equivalents of AA l^{-1}) in the Arabian Sea. Points in dashed circle were not taken into account in regression.

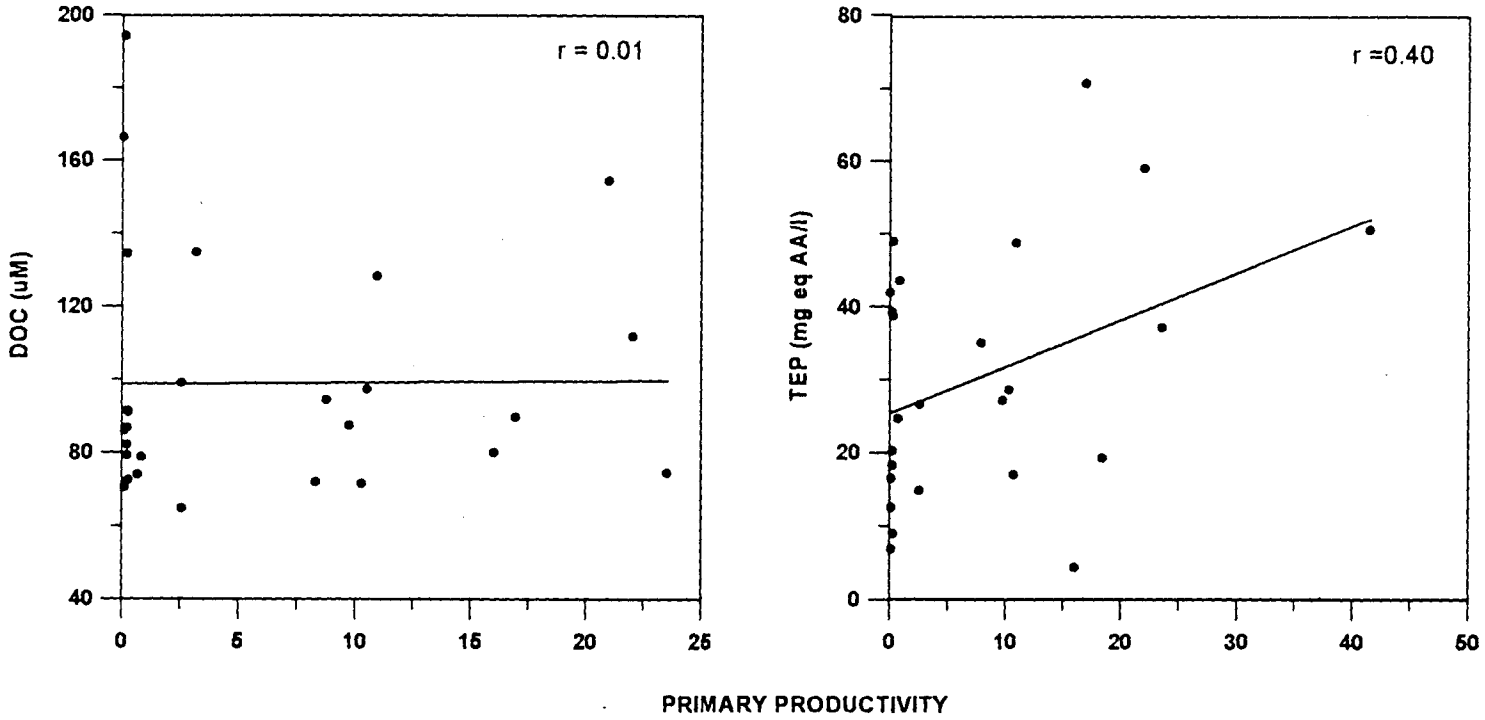

Fig. 5.9. Relations of Primary productivity (mgC $m^{-2}d^{-1}$) with DOC and TEP (mg equivalents of AA l^{-1}) in the Arabian Sea.

recalcitrant and, unlike TEP, is not easily consumable to bacteria. It is estimated, by assuming 20-33% efficiencies in bacterial growth rates, their carbon demand could be in the range of 0.04 to 3.6 - 0.06 to 5.0 $\mu gC\ l^{-1}\ h^{-1}$ in surface waters (Dr. Ramaiah, personal communication).

Negative relationships in Fig. 5.10 suggest that DOC and TEP undergo oxidation to CO_2. The TCO_2 values increase by 20-160 µM in northern Arabian Sea than in the southern Arabian Sea with a decrease in DOC concentration from 20 µM to 60 µM. The net increase in TCO_2 in the oxygen minimum zone cannot be accounted for by DOC/TEP oxidation alone. Hence, it is probable that dissolution of biogenic carbonate minerals which are relatively more abundant in northern Arabian Sea also partially contributes to elevated TCO_2 values in the north.

The percentage of TEP harbouring mineral (terrestrial or marine solid) particles were more (75 to 86) in the Bay of Bengal than in the Arabian Sea (33 to 46). This trend is in concurrence with the total number of TEP counted microscopically (Table 5.1). Low numbers of TEP with mineral particles in the Arabian Sea could have been due to lower inputs primarily of terrigenous particles by rivers and atmosphere. Flux of terrigenous materials (Subramanian, 1993) into the Bay of Bengal is quite substantial in which rivers from the Indian sub-continent alone pour in $\sim 1387 \times 10^6$ tons y^{-1} while the

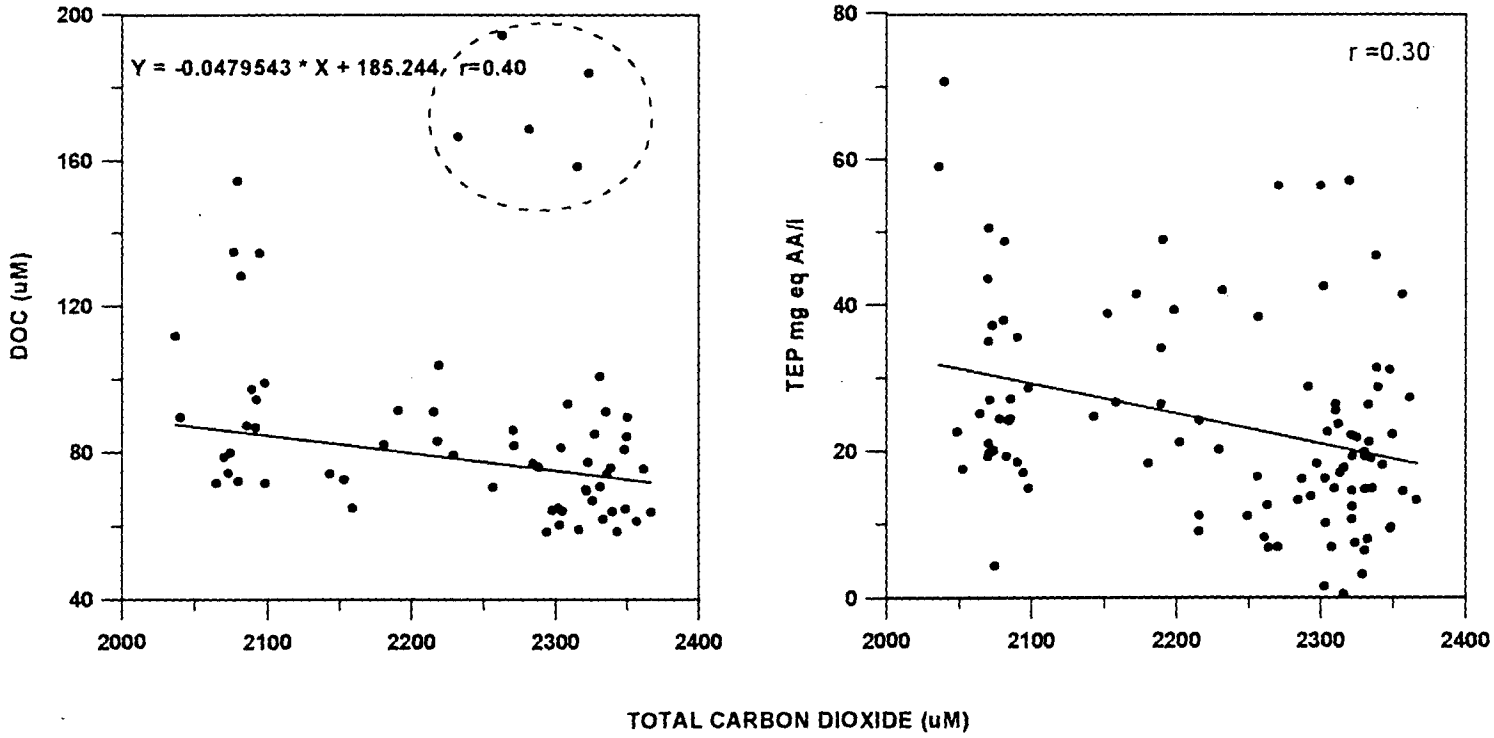

Fig. 5.10. Relations of TCO2 with DOC and TEP (mg equivalents of AA l^{-1}) in the Arabian Sea. Points in dashed circle were not taken into account in regression.

Arabian Sea receives only $195x10^6$ tons y^{-1}. Consequently, TEP can be more efficiently scavenged by mineral particles undergoing sedimentation from the surface layers in the Bay of Bengal (Fig. 5.1). This explains the higher sinking fluxes of organic carbon (2.04-3.59 and 1.53-1.80 gC m^{-2} y^{-1}, respectively) in the Bay of Bengal (Ittekkot *et al.*, 1991) than in the Arabian Sea (Nair *et al.*, 1989) and provides direct evidence to the mineral ballast hypothesis (Ittekkot *et al.*, 1992), that links the mechanism of long-term storage of atmospheric carbon dioxide in the ocean to the organic-mineral interactions in water column.

Important conclusions from Chapter 5 are:

1. **DOC levels are highly variable in location and depth**
2. **DOC is consumed in denitrification in the northern Arabian Sea**
3. **Negative relation was found between DOC and TEP**
4. **Bacteria appears to utilize TEP in denitrification**
5. **Bacterial carbon was linearly related to DOC and TEP**
6. **TEP-Mineral ballast hypothesis seems to work in the Bay of Bengal**

Chapter 6

AIR-SEA FLUXES OF CARBON DIOXIDE

The oceans are expected to absorb a significant proportion of anthropogenically emanated CO_2. The Indian Ocean has been shown to be a net sink of atmospheric carbon dioxide through a one-dimensional model (Louanchi *et al.*, 1996). Results from the North Indian Ocean indicated that the Arabian Sea is a source (Kumar *et al.*, 1992; George *et al.*, 1994; Sarma *et al.*, 1996) while the Bay of Bengal could be a seasonal sink (Kumar *et al.*, 1996). However, variability in CO_2 air-sea fluxes and processes controlling the distribution of surface pCO_2 in space and time is poorly known.

This chapter focuses on variations in surface pCO_2; effects of physical, biological and microbial processes on its distribution, also through a one-dimentional model; and diurnal, seasonal and inter-annual variability in air-sea fluxes of CO_2 in the Arabian Sea; and comparison of these pCO_2 fluxes to those from the Bay of Bengal and Andaman Sea.

6.1. Variability in surface pCO_2 in the Arabian Sea

The study area is a dynamic region with winter convection occurring in north during NE monsoon (Banse, 1984; Madhupratap *et al.*, 1996) and upwelling in SW monsoon (Shetye *et al.*, 1990; Muraleedharan and Prasanna Kumar, 1996), and highly stratified water column during inter-monsoon (Prasanna Kumar and Prasad, 1996). Due to these physical processes mixed layer is

deeper in winter and very thin during inter-monsoon. Such processes may have significant control on the distribution of surface pCO_2 along with biological ones. In this section we discuss the variability in surface pCO_2 and affect of physical and biological processes on its variations.

6.1.1. SW monsoon

The concentrations of dissolved substances in surface layers of the oceans are largely controlled by circulation which also determines the extent of primary production. The pCO_2 distribution in surface layers of the Arabian Sea along 64° E (Fig. 6.1) suggests super-saturation in the Arabian Sea surface waters, with respect to that in the atmosphere, in all seasons with values around 420 μatm. At 200m, however, lowest values occurred in 1995 SW-monsoon and inter-monsoon and the highest in winter and 1996 SW monsoon seasons. Primary productivity in the Arabian Sea is known to be the highest during SW-monsoon that led to localised low pCO_2 levels in surface layers, around 16° N in 1995, which is not the case in SW-monsoon 1996 (Fig. 6.1). Oxygen and nitrate have been found to be relatively higher in this region during 1995 SW-monsoon (nitrate ~4 μM; Figs. 3.2 and 3.3) whereas nitrate was around 1 μM during the same season in 1996. Near-surface pCO_2 differed by ~50 μatm between south and north with comparatively higher values around 16-20° N, except at 13 ° N in 1996 (Fig. 6.2). During 1996 SW monsoon, surface pCO_2

Fig. 6.1: Distribution of partial pressure of carbon dioxide (uatm) in the central Arabian Sea

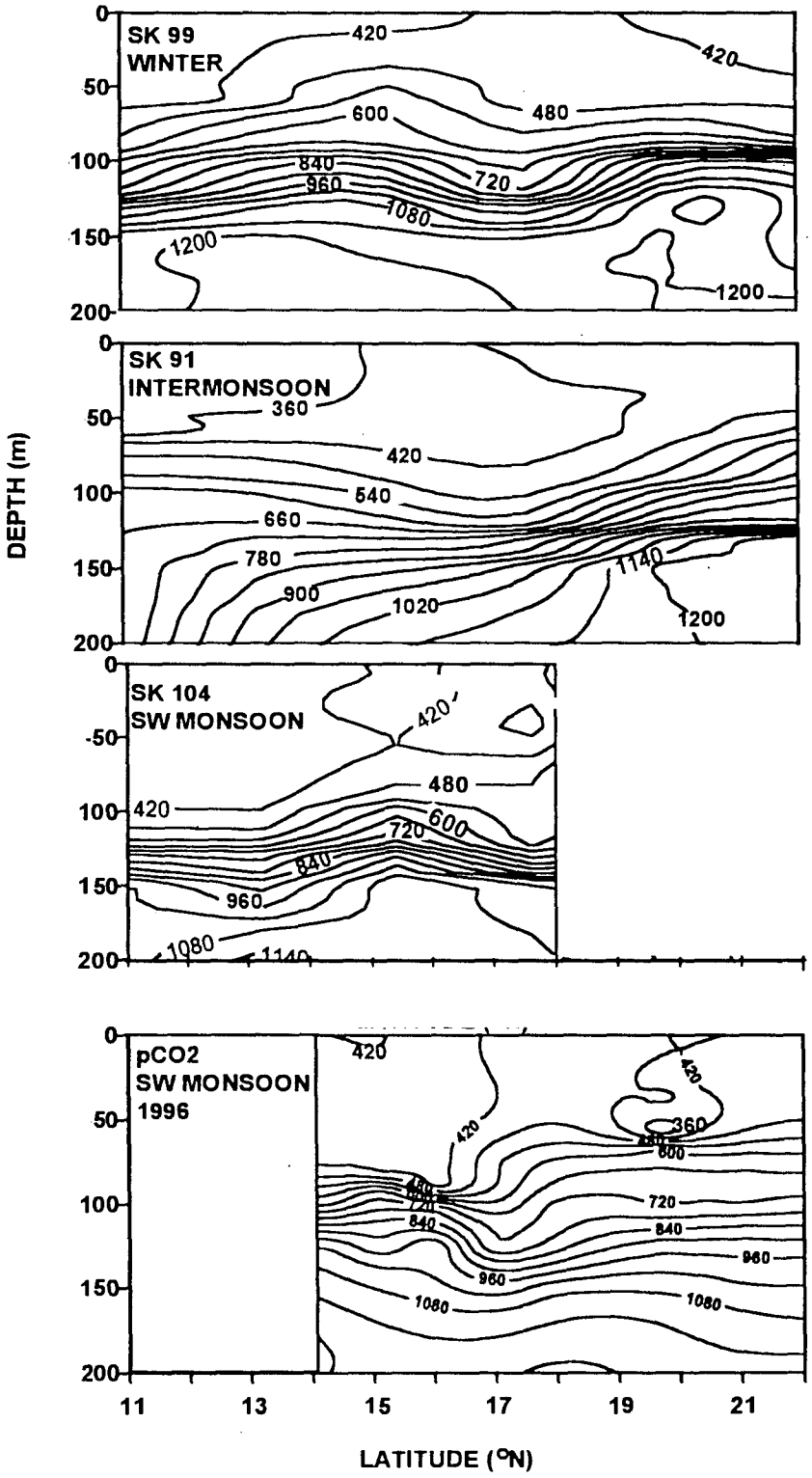

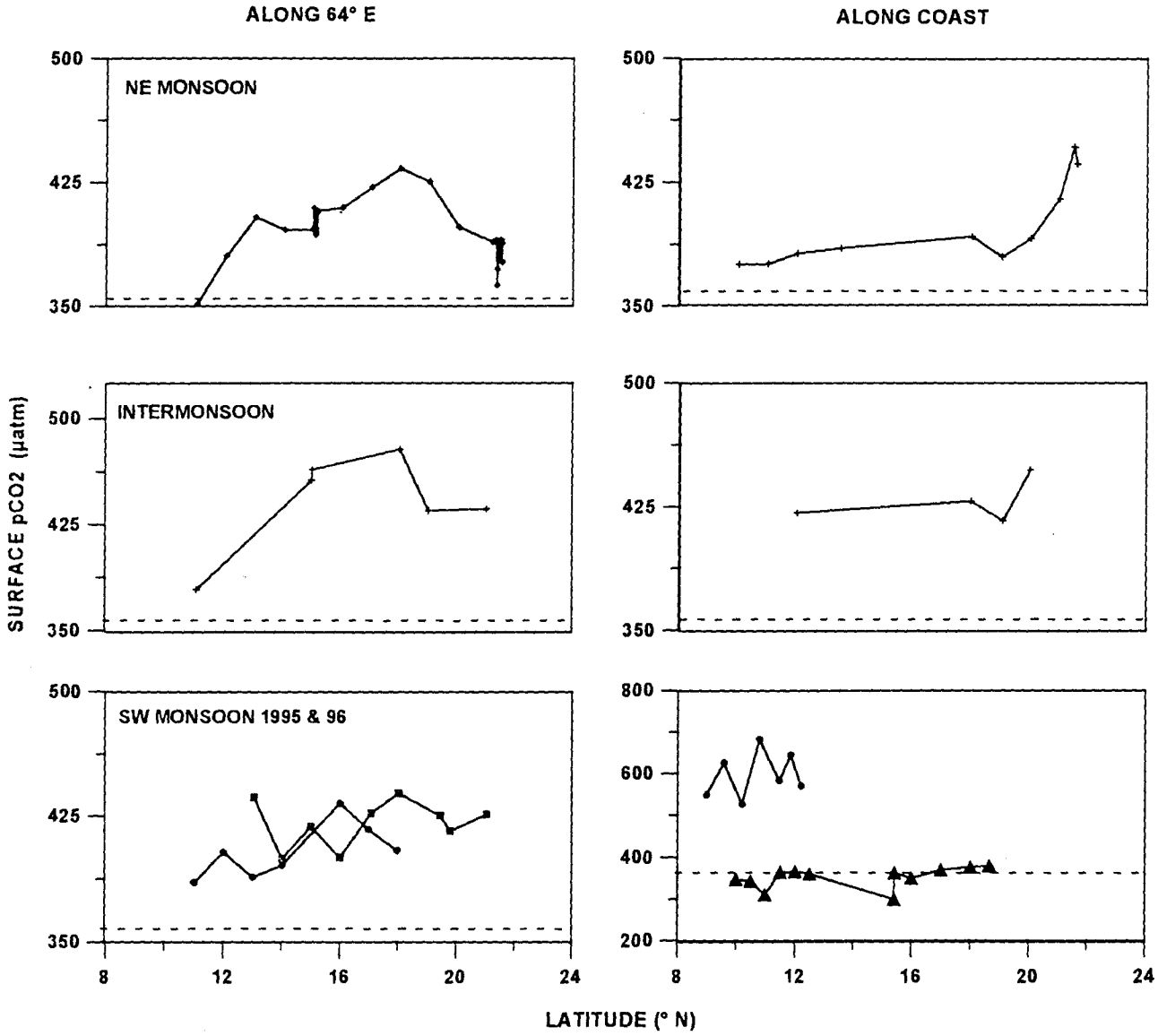

Fig. 6.2. Meridional variability in near surface pCO_2 in the Arabian Sea. Dashed lines indicates atmospheric pCO_2 value of 356 uatm.

data were collected using an underway continuous pCO_2 system. Figure 6.3 shows the underway-surface pCO_2 distribution along 64° E. There is an increasing trend towards north with values ranging from 320 to ~385 µatm. High pCO_2 levels (385 µatm) at 17-19°N could be the effect of Findlater jet. The underway data are comparatively lower than the values computed from TCO_2 and pH_T. This discrepancy might have arisen because of two different methods used. Phytoplankton blooms were noticed during 1996 and hence the elevated pCO_2 levels might have been due to rapid regeneration of organic material in upper layers itself, in addition to that laterally advected (Waniek, *et al.*, 1996). The Findlater Jet is expected to drive upwelling to the north of its axis in the Arabian Sea (Muraleedharan and Prasanna Kumar, 1996) that led to the observed patterns in nitrate (Fig. 3.3) and pCO_2 in 1995 (Figs. 6.1 and 6.2).

Figure 6.4 depicts longitudinal variations in near-surface pCO_2 along 11° N, which varied from 340 to 400 µatm where lower values came from the coastal regions, influenced by fresh water input by rivers. The surface salinity varied from 33.300 to 36.300 from the coast to open sea. In agreement with such a decrease in pCO_2 in runoff afftected coastal waters Fig. 6.5 also shows lowest values obtained using the underway measurement system along the west coast of India. Very low pCO_2 at the surface (200 µatm) was observed along the coast off Bombay due to monsoonal discharge from Narmada river that is carried by the southerly currents. The observed low pCO_2 values could also

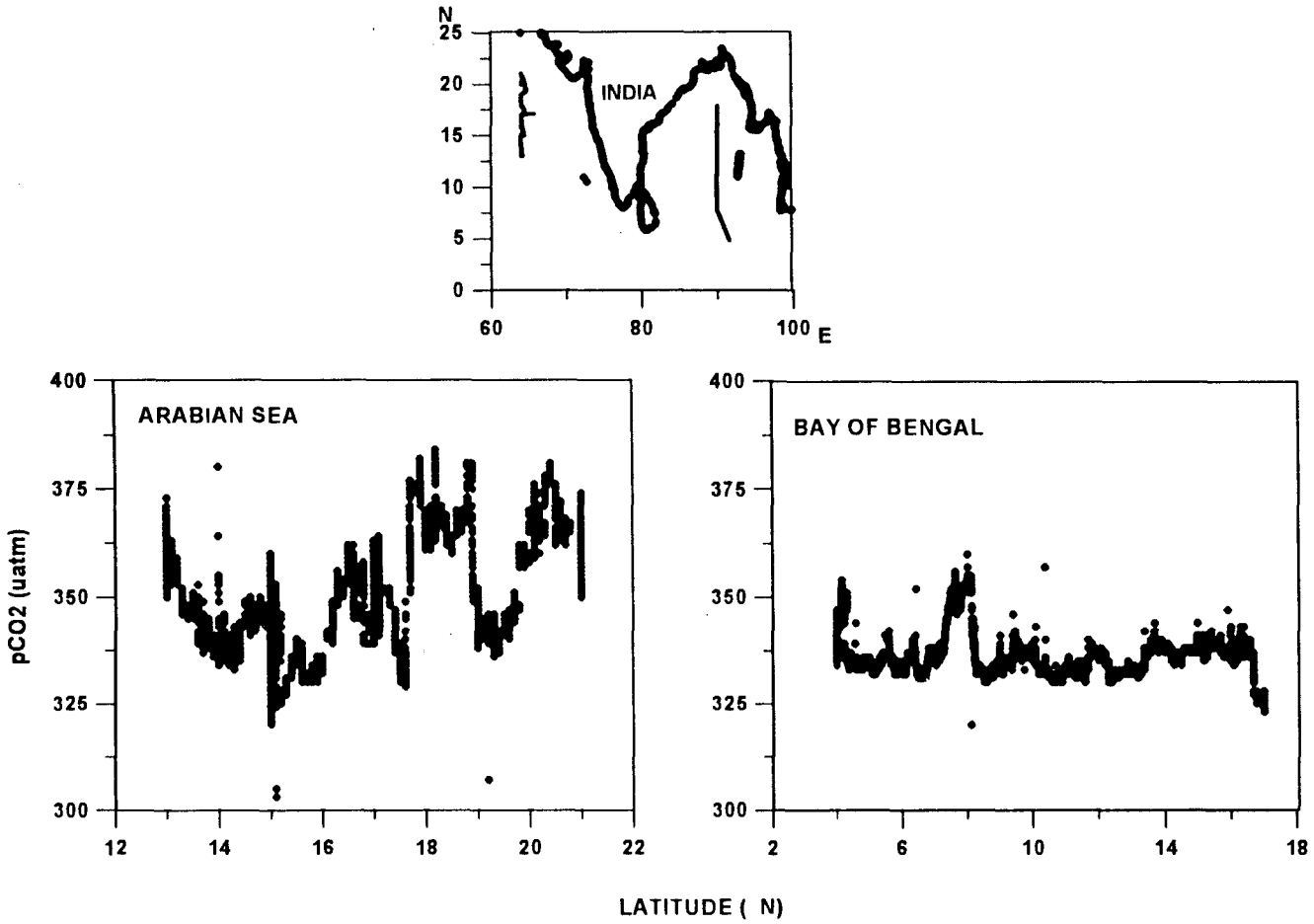

Fig. 6.3. Surface pCO2 distribution in the north Indian Ocean measured by continous underway measurement system.

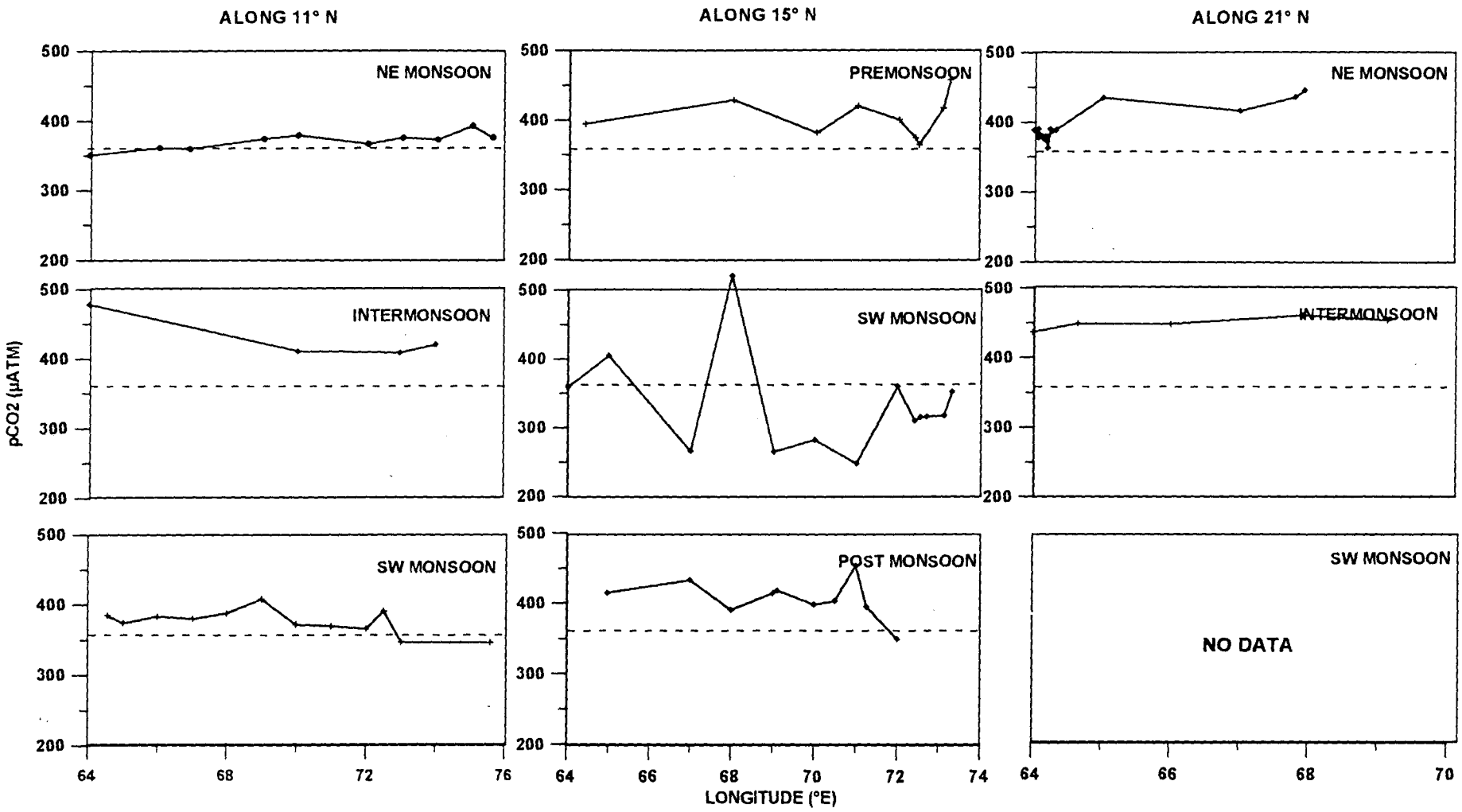

Fig. 6.4. Zonal variability (along 11° N, 15° N and 21° N) of surface pCO2 (µatm) in the Arabian Sea. Dashed line indicates atmospheric pCO2 value of 356 uatm.

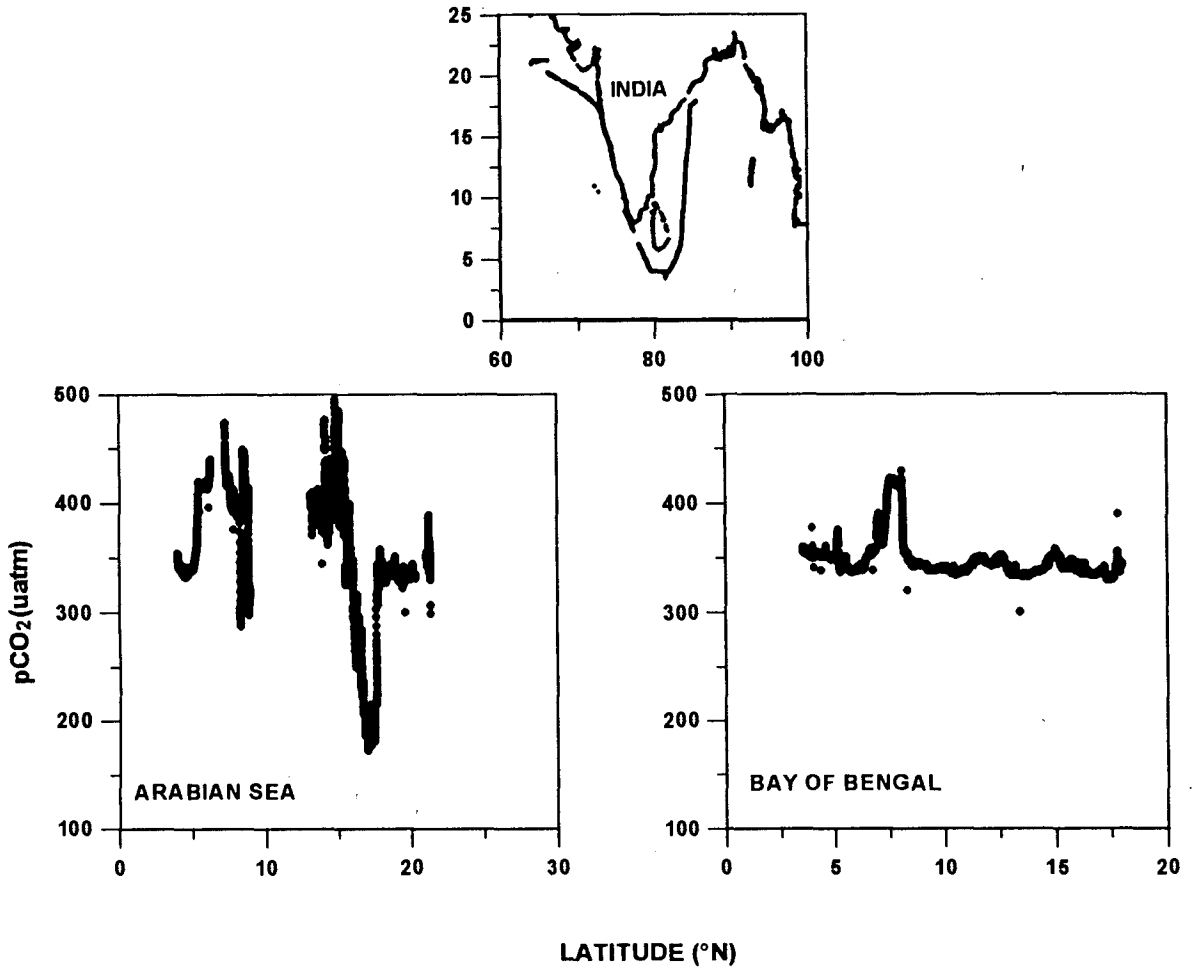

Fig.6.5. Near coastal surface pCO2 distribution in the North Indian Ocean measured by continous underway measurement system.

arise from biological fixation triggered by terrigenous nutrient inputs, as has been found in the Bay of Bengal (Kumar *et al.*, 1996). This is in addition to the fact that river waters contain ≤700 μM of TCO_2 and therefore has relatively low pCO_2 (Kumar *et al.*, 1996). Despite the occurrence of higher pCO_2 below the mixed layer the same can not be pumped up because of the prevailing lens of low salinity surface water which prevents vertical mixing. This leads to the drawing of atmospheric CO_2 through biological production.

The pCO_2 increase (to 500 μatm) around 15° N in Fig. 6.4 is due to wind induced upwelling. The sea surface temperatures were in the range 25-27° C at this location confirming the occurrence of upwelling. Data to the north of 10° N in Fig. 6.5 were collected during SK 115 cruise while those to the south of this latitude were taken during SK 116 cruise. Low values were found just south of 10° N because of the run-off influence from River Kali. Figure 6.4 shows surface pCO_2 distribution along 15° N where again coastal regions were occupied by low salinity waters (~35.200 psu). pCO_2 mostly ranged between 250 and 350 μatm in coastal waters whereas it was above 400 μatm in the open sea. The high pCO_2 of 500 μatm seen in Fig. 6.5 (SK 115) is absent in Fig. 6.3 (SK 104) because of the different periods of sampling. During July-August 1995, low values (~266 μatm) also occurred along Goa-Mangalore coast due to fresh water influence, as indicated by a salinity of 31.500 psu. Although, the coastal regions receiving freshwater inputs appear to act as a

sink of atmospheric carbon dioxide some of these regions act as sources since intense upwelling occurs. In June-July 1995, the pCO_2 value along the Southwest Indian coast was between 520 and 685 µatm as a result of intense upwelling. This is the first ever high concentration known so far from any oceanic region. Simultaneously, Kortzinger *et al.* (1997) recorded high pCO_2 of ~700 µatm in the Omani upwelling region during the same period.

During the late-SW monsoon surface pCO_2 levels were higher than those in the atmosphere with a range between 360 and 460 µatm along 15° N (Fig. 6.3). This could be again due to increasing surface temperatures and regeneration of organic debris months, since there could be time lag for bacteria to respond to increased productivity. After the surface nutrients are depleted chlorophyll *a* may drop rapidly but pCO_2 would be released more slowly through decomposition of organic matter (Peng *et al.*, 1987). Closer to the coast, however, the values dropped (Fig. 6.3) because of freshwater influence.

6.1.2. NE monsoon

The highest surface pCO_2 in winter, particularly in the north, is attributed to winter convection. This convection also resulted in relatively high nitrate (~2 µM) and oxygen ranged between 190 and 270 µM along 64° E (Figs. 3.2 and 3.3). These concentrations were increased from south to 16° N then decreased

around 17° N followed by an increase further north. Low oxygen concentrations at 17° N could be attributed due to intense winter mixing where the deepest mixed layer of 120 m was observed (Fig. 3.1). pCO_2 increased from 351 µatm in the south (11° N) to 433 µatm at 18°N but decreased to 375 µatm further north (Figs. 6.1 and 6.2). Madhupratap *et al.* (1996) observed that intense winter mixing around 17° N leads to a relatively high productivity north of 15° N (447 to 643 mgC m^{-2} d^{-1}). Reduced convection to the north of 18° N resulted in low surface pCO_2. pCO_2 marginally increased towards the coast (Fig. 6. 4), although, salinities decreased but not as much as they did during the SW monsoon. High pCO_2 levels in which compared to the SW monsoon are probably due to the absence of river run-off. Along 21° N, surface pCO_2 levels ranged between 370 to 445 µatm with an increase towards the coast (Fig. 6.4). High values towards the coast are because of vigorous winter mixing which is much stronger in the north (Fig. 3.6). Shetye *et al.* (1992) observed intense winter cooling close to the Saurashtra coast.

During the NE monsoon of 1997, time series observations were made for 14 days at 21° N and 64° E. Surface pCO_2 varied from 368 to 494 µatm and the oscillations of high and low coincided with surface temperature and chlorophyll suggesting a close coupling (Fig. 6.6).

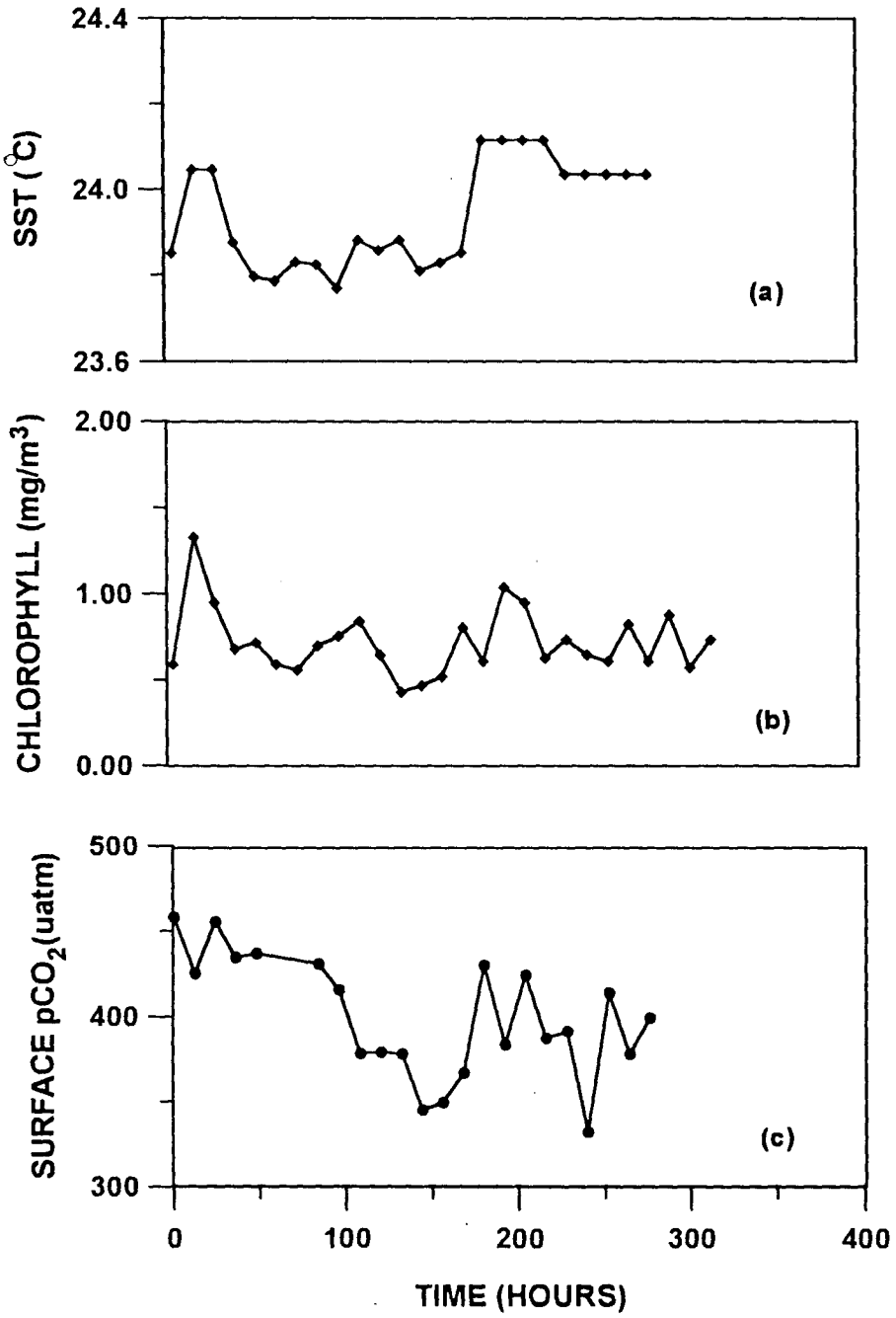

Fig. 6. Diurnal variations of (a) surface pCO2, (b) Chlorophyll and (c) SST during NE monsoon 1996 at 21 N, 64E in the Arabian Sea

6.1.3. Inter-monsoon (Pre SW-monsoon)

Although, the upwelling or convection do not occur during the inter-monsoon, pCO_2 levels remained higher than the atmospheric value along 64° E ranging between 379 and 478 µatm with the highest value occurring in the northern Arabian Sea at ~18° N (Figs. 6.1 and 6.2). Its range was 350-450 µatm along 15° N while it was well above the atmospheric concentration at 11 and 21° N (Fig. 6.3). Increased solar radiation (Prasanna Kumar and Prasad, 1996) and higher bacterial activity might have led to higher surface pCO_2 during this season. Bacteria are found to be more abundant during inter-monsoon which can not be supported by primary production (Ramaiah *et al.*, 1996), and hence such higher bacterial respiration might have resulted in higher pCO_2. For instance, the bacterial abundance have been reported to be 0.24-0.9 x 10^9 l^{-1} in inter-monsoon, 0.13-0.64 x 10^9 l^{-1} in SW monsoon and 0.05-0.09 x 10^9 l^{-1} in winter monsoon (Ramaiah *et al.*, 1996). Importantly, the bacterial carbon far exceeded the phytoplankton carbon during this season. Unlike, the SW monsoon season, the fresh water influence was absent in the coastal regions where pCO_2 remained in the high range of 416-428 µatm.

Interestingly, surface pCO_2 values were higher between 16 and 20° N in the central Arabian Sea in all seasons (Fig. 6.1 and 6.2). This region houses the most intensely denitrifying waters at intermediate depths (Naqvi, 1991). Hence,

higher pCO_2 between these latitudes could have arisen from the relative increase in upward pumping from subsurface layers as suggested by Kumar *et al.* (1992).

Highlights of surface pCO_2 distribution are:

- **Seasonally and spatially variable pCO_2 abundance was observed**
- **Highest pCO_2 values were associated with coastal upwelling**
- **pCO_2 Levels were supressed by river discharge in near-shore surface waters**
- **Consistently higher values were found at 16-20° N in the central Arabian Sea driven by upward pumping**

6.2. Control of surface pCO_2 in the Arabian Sea

6.2.1. Controlling factors from relations

Different processes - physical, chemical and biological - determine the levels of surface pCO_2. Contribution from each of these may change with season. The pCO_2 in euphotic zone (0-80 m) and the surface mixed layer (depth varies seasonally and regionally, from 10m to 30-120 m) can be influenced by biological production/regeneration, and physical processes such as run-off,

upwelling and winter convection. The variable depth ranges necessitate the consideration of a definite depth interval so as to understand the dominance of physical or biological processes in regulating the pCO_2 distribution in surface waters. Therefore, data obtained from the upper 60 m of the water column were utilised.

Figure 6.7 depicts the seasonal near surface dissolved oxygen. Along 64° E oxygen ranged between 190 and 270 µM in all seasons whereas in coastal waters it varied from 90 to 245 µM. Despite the conspicuous seasonal variability in the levels of oxygen the gradients were not significant between the south and the north. While the SW monsoonal upwelling signature of low oxygen was obvious along the Southwest Indian coast its concentration was the highest in winter in coastal as well as in the central Arabian Sea. Inter-monsoon and SW monsoon levels along 64° E were nearly the same. Higher values in winter could have been due to convection driven higher biological production. Less turbulence at the interface, due to low wind speeds in this season (Sarma *et al.*, 1998) might have restricted the oxygen ejection to atmosphere. Clustered points at 15° and 21° N along 64° E in winter indicate the results of two time series experiments (Fig. 6.7).

While oxygen varied between 195 to 260 µM in all seasons it exhibited the highest values in winter at 21° N, 64° E (Fig. 6.7). A decrease towards the

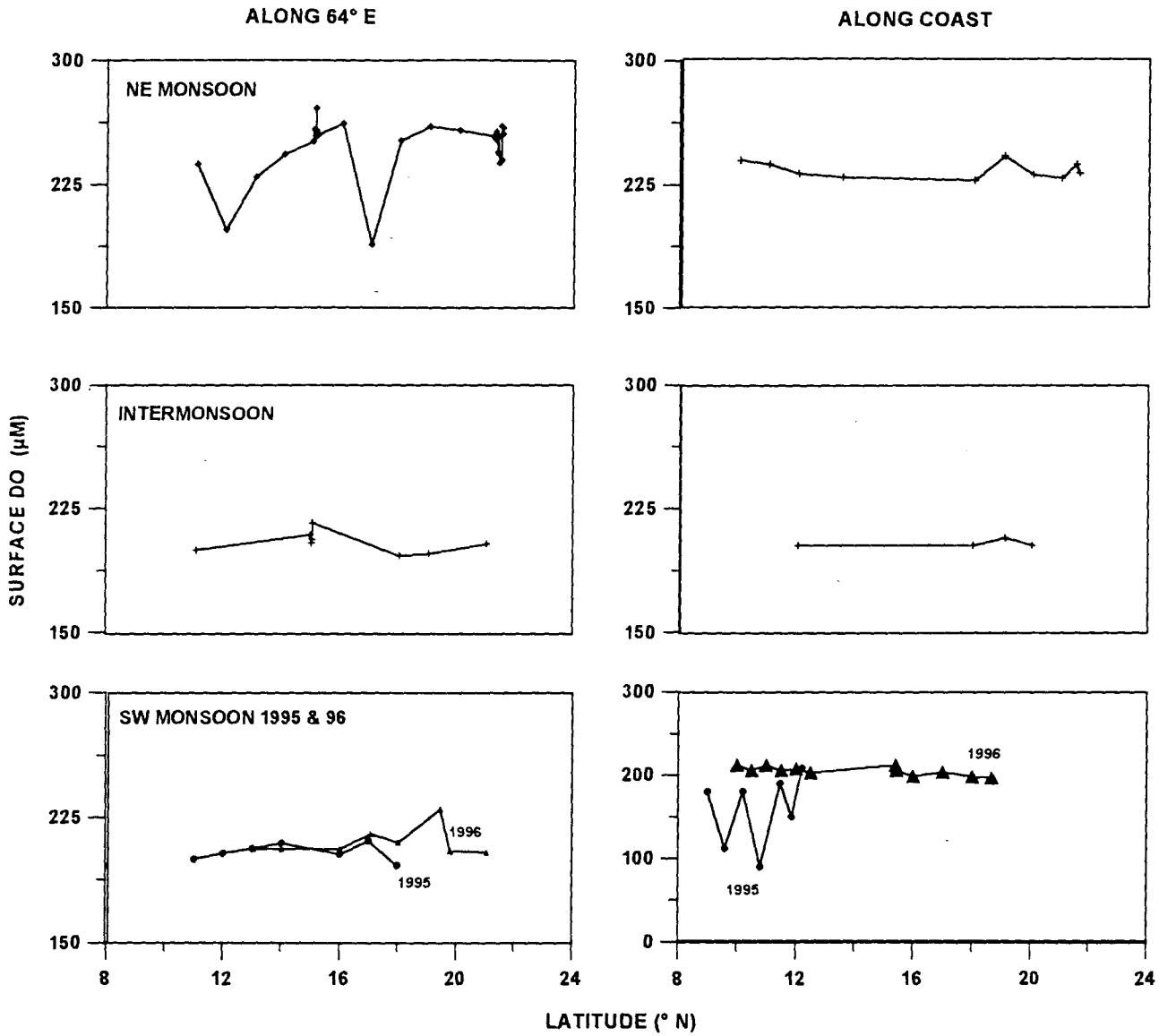

Fig. 6.7. Meridional variability in near surface dissolved oxygen in the Arabian Sea.

coast along this latitude is obvious since the convective mixing was more vigorous here (Fig. 3.6) than in the open sea (Fig. 3.2). Higher values were observed near the coast during winter and SW monsoon due to winter cooling and coastal upwelling. Chlorophyll data at 21° N and 64° N showed higher values in SW (29 mgC m^{-3}) and NE (19 mgC m^{-3}) monsoons than in inter-monsoon (7.6 mg m^{-3}).

Chlorophyll *a*, in the upper 60 m, varied in ranges of 0.014-0.433, 0.027-0.458 and 0.045-1.343 mgC m^{-3} during inter-, winter and SW- monsoon seasons, respectively. The corresponding surface primary production ranges were 0.37-20.89, 0.6-43.8 and 0.3-98.3 mgC m^{-3} d^{-1} (Dr. M. Madhupratap, personal communication 1996). High chlorophyll *a* values in SW monsoon were in response to upwelling whereas those in winter were due to convective mixing.

The near surface pCO_2 levels in the study area were almost always higher than in the atmosphere throughout the year (Fig. 6.2 and 6.4). Except in inter-monsoon, pCO_2 (Fig. 6.8) and oxygen (Fig. 6.9) exhibited specific relations with temperature due to winter cooling and SW monsoonal upwelling, that bring cold and carbon dioxide rich sub-surface waters to the surface. Such processes do not occur during inter-monsoon. While pCO_2 showed negative relations in all seasons, it was so with oxygen only in winter (Table 6.1). The biological properties, however, did not show any specific trends in relation to

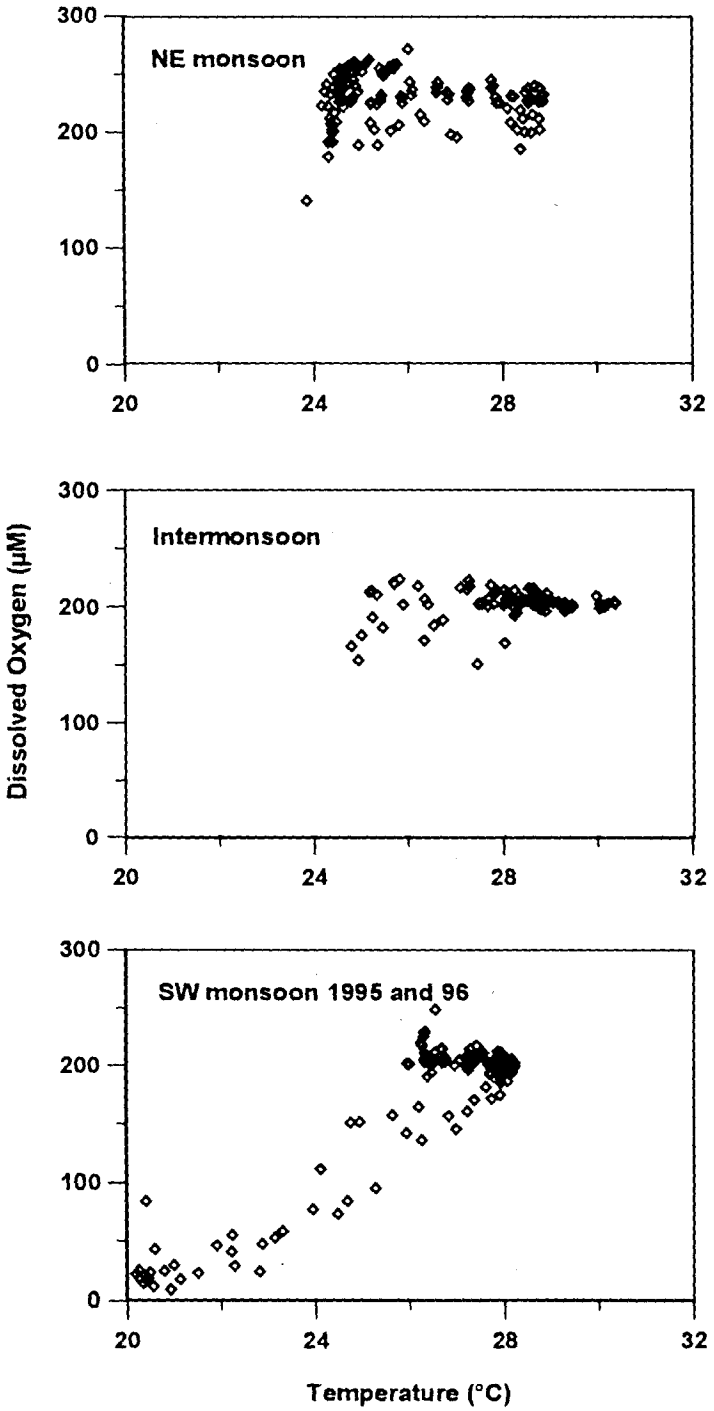

Fig. 6.8. Relations between temperature and dissolved oxygen in the Arabian Sea during different seasons.

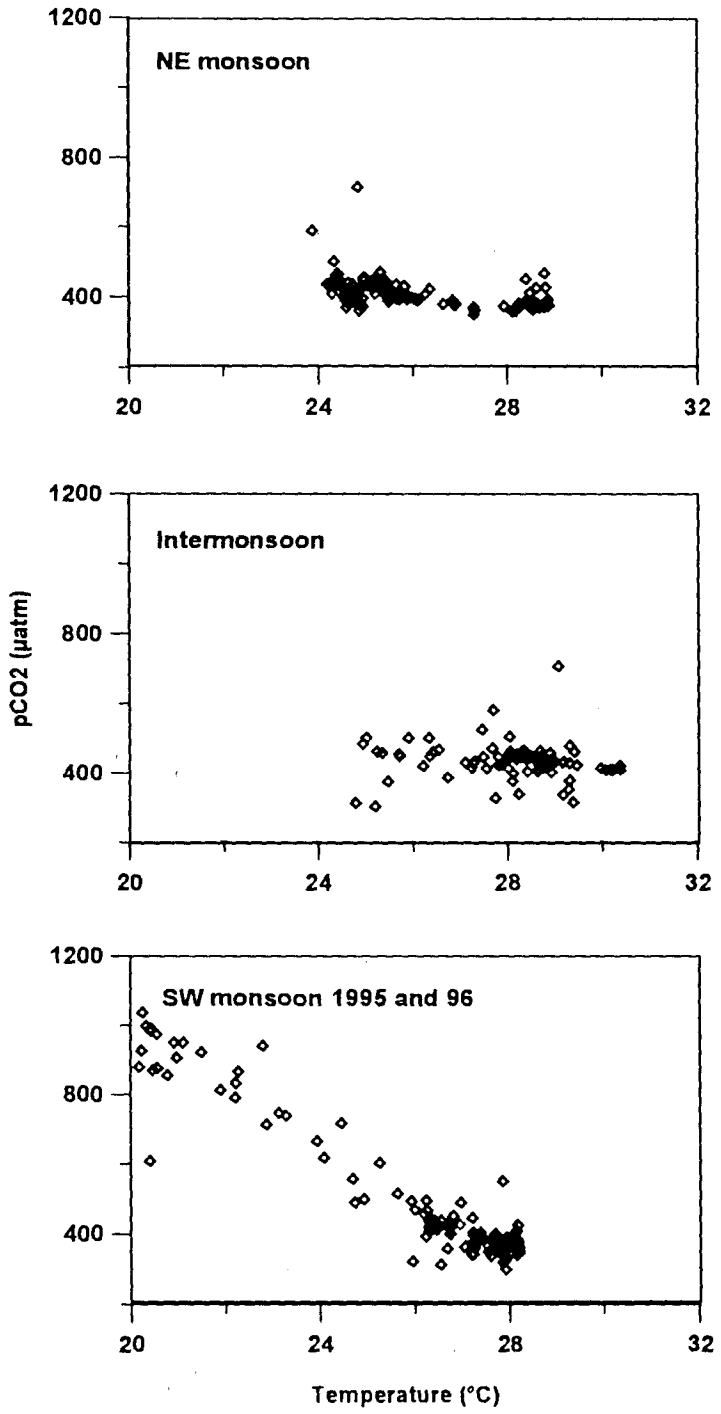

Fig. 6.9. Relation between surface temperature (°C) and surface pCO2 (µatm) in the Arabian Sea during diffferent seasons.

changes in pCO_2 (Fig 6.10 and 6.11). Inter-monsoon characterized by the most oligotrophic conditions that resulted in low chlorophyll *a* and primary productivity. Surface layer was relatively well stratified from north to south in inter-monsoon compared to that in other seasons (Prasanna Kumar and Prasad, 1996; Madhupratap *et al.*, 1996). When the CO_2 at surface is fixed by photosynthesis and is not rapidly replenished by upward pumping due to stratification, the continued release of CO_2 through decomposition of organic matter by the bacteria becomes dominant which would have led to the poor correlation (Table 6.1) in inter-monsoon. Increase in bacterial abundance in inter-monsoon has been related to the decay of organic matter produced during winter (Ramaiah *et al.*, 1996) by phytoplankton blooms (Ducklow, 1993).

Table 6.1. Relationships for temperature (°C) with oxygen (μM) and pCO_2 (μatm) in different seasons in the Arabian Sea.

Season	Slope	r^2
(a) temperature *vs* oxygen		
Intermonsoon	1.9	0.04
NE monsoon	-2.8	0.05
SW monsoon	25	0.84
(b) temperature *vs* pCO_2		
Intermonsoon	-2.8	0.01
NE monsoon	-9.0	0.22
SW monsoon	-75	0.90

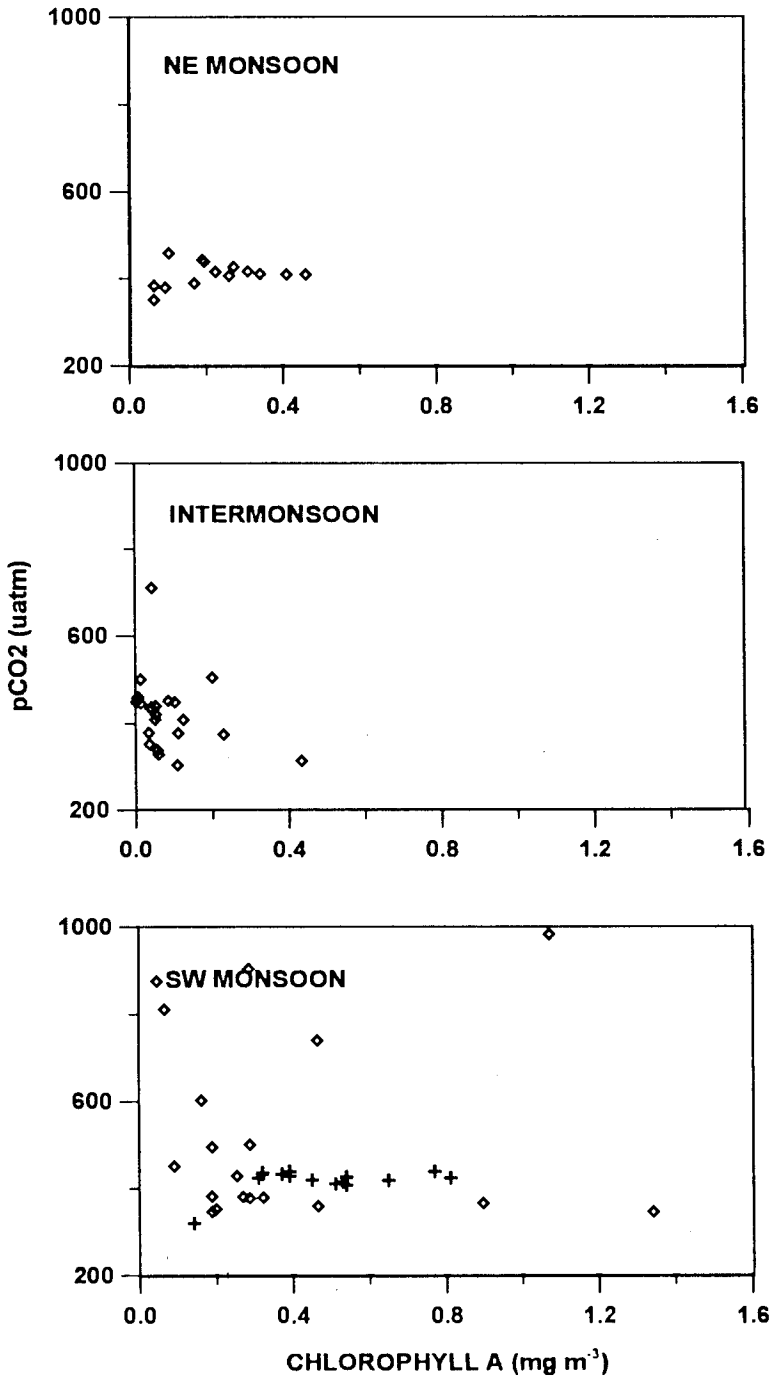

Fig. 6.10. Relation between chlorophyll a and pCO_2 in the Arabian Sea during diffferent seasons.

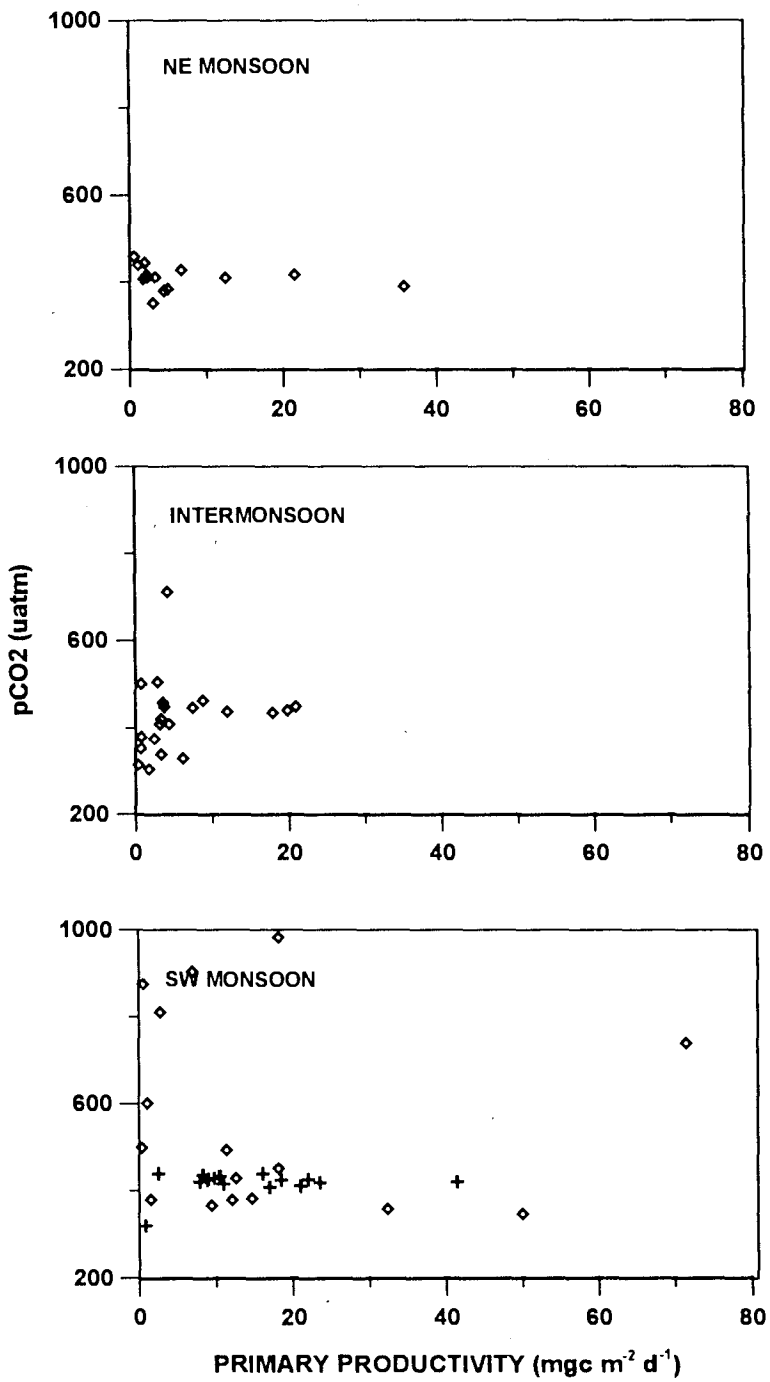

Fig. 6.11. Relations between primary productivity and pCO2 in the Arabian Sea during diffferent seasons.

The data from the North Atlantic between 47° N and 60° N showed large spatial variations with strong to weak negative correlations between chlorophyll *a* and surface pCO_2 during the spring (Watson *et al.*, 1991) suggesting a possible biological control. The present results, however, indicate weak relations for pCO_2 with biological parameters (Fig. 6.10 and 6.11) than with temperature (Fig. 6.9; Table 6.1). This strongly suggests that pCO_2 in the Arabian Sea is largely controlled by physical rather than biological processes. Besides, a slope of -75 and correlation of r^2=0.9 (Table 6.1) reveals that the physical processes during the SW-monsoon led to a large change in pCO_2 (Fig. 6.9) than in any other season. The lesser slope with large scatter (r^2=0.2) in winter suggests a more important role of biological processes in regulating surface pCO_2, than in SW monsoon. For instance, the minimal pCO_2 values at temperatures <25°C might have resulted from higher biological fixation. This enhanced biological control of pCO_2 is augmented by the negative relation between temperature and oxygen caused by the linkage: winter overturning-nutrient pumping- photosynthetically produced oxygen. Poor correlations for oxygen and pCO_2 with temperature (Table.6.1), together with the higher surface abundance of pCO_2, than in winter (Fig. 6.1) and its unclear relations with Chlorophyll *a* and primary production, strongly suggest the biological (microbial) dominance over the physical processes in controlling the pCO_2 distribution during inter-monsoon.

6.2.2. A one-dimensional model

6.2.2.1. *The model*

Recently, Louanchi *et al.* (1996) have developed a model to quantify the influence of different processes on surface pCO_2. Although, this model may have limitations in identifying the role of biological pump in the Arabian Sea especially during inter-monsoon season when the euphotic zone is deeper than mixed layer depth, it is expected to identify major processes responsible in controlling the surface pCO_2.

This model consists of two boxes, a surface mixed layer box in which the physical and biogeochemical processes control the pCO_2 variations and a subsurface box in which dissolved inorganic carbon system is considered invariant with definite boundary conditions. Four processes are defined to control pCO_2 distribution; air-sea exchange, biological pump, exchange between two boxes and thermodynamic effects on the CO_2 system in the surface box. The variations in pCO_2 are expressed by:

$$\partial fl/\partial t = (\partial fl/\partial t)_B + (\partial fl/\partial t)_M + (\partial fl/\partial t)_F + (\partial fl/\partial t)_{T,S} \qquad (6.1)$$

where $\delta f/\delta t$ is the total pCO_2 variation within a time period of ∂t; $(\partial f/\partial t)_B$ is the biological contribution to pCO_2 change; $(\partial f/\partial t)_M$ is the contribution from mixing processes; $(\partial f/\partial t)_F$ is the air-sea exchange contribution; and $(\partial f/\partial t)_{T,S}$ is the thermodynamical contribution.

First three terms in eq. 6.1 are estimated from total dissolved inorganic carbon (TC) and total alkalinity (TA) variations:

$$\partial TC/\partial t = (\partial TC/\partial t)_B + (\partial TC/\partial t)_M + (\partial TC/\partial t)_F \quad (6.2)$$

$$\partial TA/\partial t = (\partial TA/\partial t)_B + (\partial TA/\partial t)_M \quad (6.3)$$

fugacity of carbon dioxide (fCO_2) is computed at each step as a function of TC and TA according to Peng *et al.* (1987) and using dissociation constants K_1 and K_2 of Goyet and Poisson (1989).

6.2.2.2. *Biological effect on fCO_2 variations*

Variations in TC and TA are linked to biomass production/decomposition and calcite formation in the euphotic zone. These variations are considered in biological effects on fCO_2 changes

$$(\partial TC/\partial t)_B = (\partial IN/\partial t)_B * RCN - S_b \quad (6.4)$$

$$(\partial TA/\partial t)_B = -2 * S_b \qquad (6.5)$$

Whereas $(\partial IN/\partial t)_B$ represents the inorganic nitrogen (IN) variation with time, resulting from photosynthesis, respiration and mortality, which is expressed in terms of carbon units. This variation is calculated using the following equation

$$(\partial IN/\partial t)_B = - (u - r * q) * Chl * RN \qquad (6.6)$$

where u is the growth rate which depends on the maximal growth rate u_m and on the single nutrient (inorganic nitrogen, IN) following a Michaelis-Menten formulation [$u=u_m*IN/(IN+K_m)$] where K_m is the half-saturation constant. u is computed at each time step, r is the removal factor and q, which represents the respiration, mortality and grazing rate, is calculated at each time-step using the following equation

$$\partial Chl/\partial t = (u-q) * Chl \qquad (6.7)$$

Where $\partial Chl/\partial t$, the temporal variation in chlorophyll, is known and used as constraint in the model. RN is the N:Chl Redfield ratio (Table. 6.2).

The second term in the equation 6.4, S_b represents the temporal variation of calcite concentration which is expressed as 20% of the total export production according to Broecker and Peng (1982)

$$S_b = 0.2 * (\partial P_{exp} / \partial t) \quad (6.8)$$

The export production, P_{exp}, consists of two parts (inorganic and organic carbon) and is computed in terms of carbon at each time step by

$$(\partial P_{exp}/\partial t) = (1 - r) * q * Chl * RCC \quad (6.9)$$

where RCC is the C:Chl Redfield ratio

The quantity, TA, is assumed to be unchanged during the production of organic carbon.

These formulations imply that the chlorophyll and inorganic nitrogen changes adequately represent biological pump. The former one is a constraint of the model and the latter one a computed variable. The biological coefficients used in the model are given in Table 6.2.

Table:6.2 Biological coefficients which are used in this model

Parameter	Symbol	Value	Units
Removing factor	r	0.5	
Maximal growth rate	U_m	2.0	day^{-1}
Michaelis-menten half-saturation constant	K_m	0.11	$\mu mol\ kg^{-1}$
C:N	ECN	6.0	
C:Chl	RCC	40.0	

K_m, RCN and RCC taken from Tayler et al., 1991 and U_m is taken from Louanchi et al., 1995.

6.2.2.3. *Mixing effect on fCO_2 variations*

Entrainment-detrainment model of Peng *et al.* (1987) was used to estimate $(\partial TC/\partial t)_M$, $(\partial TA/\partial t)_M$ and $(\partial IN/\partial t)_M$ terms in the surface layers.

For $Z \geq 0$ concentration variations after entrainment are:

$$\partial Y_s = (Y_b - Y_s) * \partial Z/Z_m \qquad (6.10)$$

where Y is the dissolved substance (TC, TA and IN) in the surface layer (Y_s) and the subsurface layer (Y_b). The surface properties do not change when Z_m decreases (Y_s=0) (Louanchi *et al.*, 1996). Therefore, the terms $(\partial TC/\partial t)_M$, $(\partial TA/\partial t)_M$ and $(\partial IN/\partial t)_M$ are affected by the sub-surface conditions of TC, TA and IN, respectively.

6.2.2.4. *Effect of air-sea exchange*

The quantity of CO_2 lost or gained by the mixed layer because of the air-sea exchange is given by:

$$(\partial TC/\partial t)_F = F/Z_m \qquad (6.11)$$

where ∂TC is the variation due to the accumulation or out-gassing of CO_2 over time interval δt. F is the air-sea CO_2 flux and Z_m is the mixed layer depth at the end of the time step.

6.2.2.5. *Thermodynamic effect on fCO_2 variations*

The effect of SST and salinity variations on fCO_2 is estimated using the relation proposed by Goyet *et al.* (1993).

This model was used for 3 stations in the central Arabian Sea at 21° N, 15° N and 11° N along 64° E. Results of this model are given in Table 6.3.

Table: 6.3: The result of model on effect of different processes on surface pCO_2

21° N, 64° E	**Biology**	**Mixing**	**Flux**	**Thermo-dynamics**	**pCO_2 (model)**	**pCO_2 (observed)**
Intermonsoon	-0.010	0.00	118.8	-32.1	441.7	437.4
SW monsoon	-14.78	70.33	21.45	7.03	439.0	432.5
NE monsoon	-12.46	53.5	0.82	29.25	426.1	442.0
15° N, 64° E						
Intermonsoon	-0.024	0.00	8.10	-20.77	343.2	450.2
SW monsoon	0.062	45.5	2.14	10.84	413.5	417.1
NE monsoon	-25.18	6.16	14.72	14.06	364.7	426.5
11° N, 64° E						
Intermonsoon	-0.005	0.00	12.6	-64.63	303.0	365.3
SW monsoon	-10.15	36.37	1.13	5.38	387.7	381.0
NE monsoon	-6.82	-21.70	2.04	6.28	334.8	377.1

These results reveal that mixing processes dominated during the SW monsoon at all the three stations and is the major contributor in maintaining the high surface pCO_2 levels followed by flux effects at 21° N and thermodynamic effects in south.

During inter-monsoon, fluxes contribution is more significant probably due to higher surface temperatures in response to increased solar radiation. Here regenerated fraction is probably underestimated because the model assumes that 50% organic matter is regenerated in the mixed layer and taken as a constant in all seasons. In fact, during this season the carbon regenerated was actually produced in the previous season (NE monsoon). Biological uptake was also underestimated since the light penetrates beyond the mixed layer depth.

The major effects during winter season are thermodynamics and mixing. Due to surface cooling by 4-5°C compared to that in inter-monsoon, inorganic carbon system shifts towards the formation of carbonate ions leading to the absorption of atmospheric carbon dioxide. As a result of convective mixing carbon dioxide will be pumped up. Effect of winter convection was seen north of 17° N (Fig. 6.1). As a result, mixing effect is high at 21° N. Fluxes effect is small except at 15° N where it is the determining factor.

Highlights on pCO_2 controlling factors are:

- **Better pCO_2 correlaions were observed with physical than biological parameters**
- **Physical processes largely controlled surface pCO_2 distribution**
- **Physical to biological dominance appeared in the sequence from SW, NE and inter-monsoons**
- **Inter-relations and model results concur on the dominance of mixing processes in regulating pCO_2 in SW and NE monsoons**
- **Relations suggest biological processes while the model projects thermodynamics to control pCO_2 in surface layers in inter-monsoon**

6.3. Variability in air-sea fluxes

The quantum of flux depends on transfer velocity of carbon dioxide which is largely determined by wind speeds while direction of flux is determined by the gradient across the air-sea interface. Intensity of wind varies with season leading to changes in the magnitudes of fluxes. Hence, the spatial, seasonal and inter-annual variability in fluxes were studied by dividing the Arabian Sea into 8 areas (see Fig. 6.12). The data were pooled and average flux values evaluated are given in Table 6.4. The numbers in the parentheses show

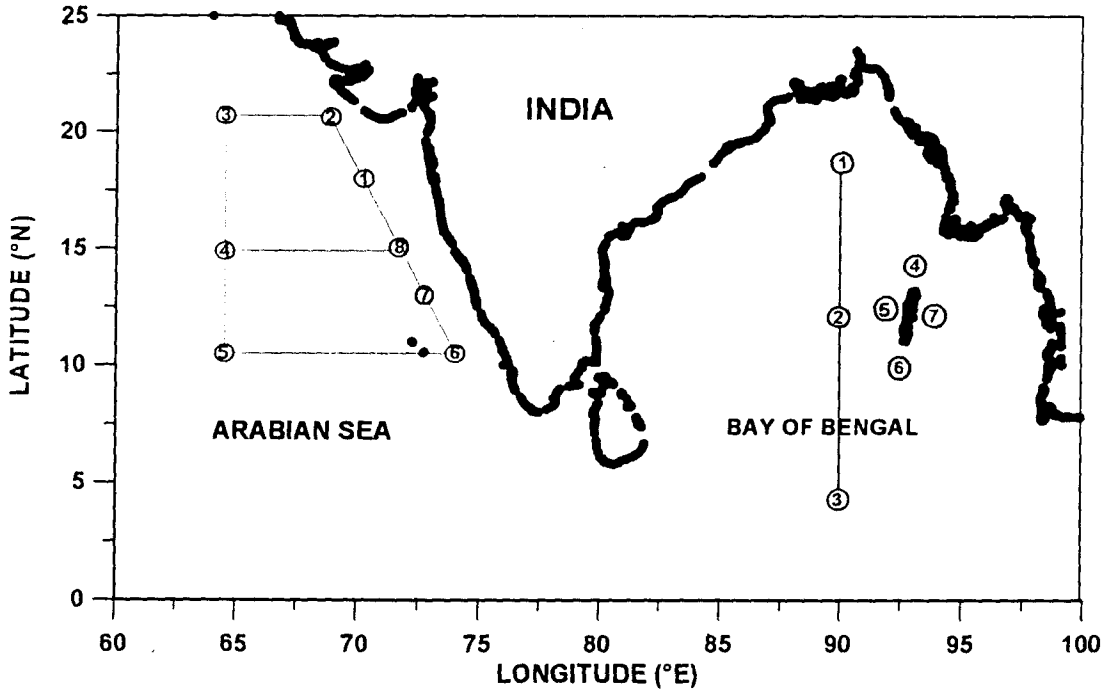

Fig. 6.12. Locations of averaged air-sea fluxes of carbon dioxide was given in table 6.4.

number of data points used for averaging.

6.3.1. SW monsoon

Strong upwelling manifested by high nutrient levels (nitrate up to 16 μM) and extremely high pCO_2 concentration (682 μatm) at surface were found off Kerala coast (Fig. 4.33). This is the highest values recorded so far in the eastern Arabian Sea. Therefore, this region may act as a large source of carbon dioxide to the atmosphere in this season. During this season, the winds have strong cross-shore component with positive trends from south to north and relatively weak long-shore component with a similar trend, except at 15° N where a steep rise in wind speed is noticed (Muraleedharan and Prasanna Kumar, 1996). The winds along the Southwest coast of India ranged between 4 and 9 m s^{-1}. This led to a very high flux along the Southwest coast of India (58 $mmol.m^{-2}$ d^{-1}) where strong upwelling occurred. In the central Arabian Sea, wind speeds were 5 m s^{-1} in the south increasing to 10 m s^{-1} at 17° N at axis of the Findlater Jet. A patch of high surface pCO_2 was observed at ~16° N (Fig. 4.39). The flux was about 45 $mmol.m^{-2}$ d^{-1} around 16° N in the Arabian Sea, where a gyral upwelling or lateral advection occurred, while it was ~8 mmol m^{-2} d^{-1} in the south. Gas fluxes at the air-water interface, however, depend not only on the concentration gradient between the two phases (air and water) but

Table 6.4. Seasonal and temporal variability in sea-to-air fluxes (mmol m^{-2} d^{-1}) of carbon dioxide in the northern Indian Ocean. Areas are shown in Fig. 6.12. Numbers in square brackets denotes number of measurements made in the respective area and wherein parenthesis wind speeds (m s^{-1}).

AREA / SEASON	1	2	3	4	5	6	7	8
			ARABIAN SEA					
NORTHEAST MONSOON 1995	7.20 [2] (7)	3.62 [5] (6)	0.98 [12] (3.3)	1.94 [12] (3.6)	0.28 [5] (5.2)	1.67 [3] (4.2)	1.39 [2] (4.4)	—
NE MONSOON 1997	—	—	5.35 [23] (3.6)	—	—	—	—	—
INTER MONSOON 1994	4.10 [2] (5)	18.5 [3] (8.8)	13.2 [4] (5.6)	0.85 [3] (2)	0.08 [3] (2)	3.52 [2] (5)	1.10 [1] (2.6)	—
INTERMONSOON 1996	—	—	—	1.36 [2] (5)	—	—	—	1.42 [6] (5)
SOUTHWEST MONSOON 1995	—	—	41.5 [1] (16)	24.4 [2] (12)	6.94 [3] (9.6)	1.02 [5] (6.6)	-10.2 [2] (5.4)	-0.80 [6] (9)
SOUTHWEST MONSOON 1996	—	—	14.3 [4] (6.5)	13.9 [4] (6)	6.15 [1] (3)	—	—	—
LATE SW MONSOON 1995	—	—	—	3.07 [1] (3)	—	—	—	3.77 [4] (3)
			BAY OF BENGAL					
SW MONSOON 1996	2.41 [3] (6.2)	2.82 [3] (5.7)	4.26 [3] (6)	—	—	—	—	—
POST MONSOON 1996	—	—	—	2.00 [8] (6.2)	-0.60 [4] (5)	1.49 [8] (2.6)	3.17 [4] (6.3)	—

winds, in fact, plays a major role in driving these fluxes. Usually higher fluxes were found from areas 3 and 4 in Table 6.4, particularly during this season.

During the SW monsoon coastal regions receive enormous amounts of fresh water from the continents which substantially brings down the surface pCO_2. For instance, very low pCO_2 (200 μatm) was recorded off Bombay where freshwater influence was evident. Low salinity water was also found at 15° N due to fresh water discharge by Mandovi and Zuari rivers. CO_2 flux of -16 $mmol.m^{-2}\ d^{-1}$ (air to sea) was recorded in these regions with an average of –10.2 $mmol.m^{-2}\ d^{-1}$ (Table 6.4). An extrapolation of the average flux in this season to the study area of $1.6x10^{12}\ m^2$ (assuming ¼ of the total Arabian Sea area) yielded 22 and 20 $Tg.season^{-1}$, respectively, for SW monsoons of 1995 and 1996.

6.3.2. NE monsoon

Convective mixing largely controlled the pCO_2 gradient at the air-sea interface. The winds were typically north/northeasterlies (average winds of 4 $m\ s^{-1}$) along 64° E. During this season, CO_2 flux amounted to 0.28-7.20 $mmol\ m^{-2}d^{-1}$. Low fluxes during this season were due to relatively weak winds. As shown in Table. 6.4, fluxes were higher in the northern Arabian Sea than in the south. Fluxes in coastal regions were several folds higher than in offshore regions in

the northern Arabian Sea. This is due to the high wind speed (5-10 m s^{-1}) in the coastal region where overturning also appeared to be high (Fig. 3.6). The CO_2 flux ranged between 0.16 and 5.70 mmol m^{-2} d^{-1} near the Southwest coast whereas in the southern Arabian Sea it varied from -0.15 to 1.54 mmol m^{-2} d^{-1}. Average flux to atmosphere from the study region was calculated to be 4 Tg. $season^{-1}$.

During NE monsoon 1997, time series observations were made for 14 days at 21° N, 64° E. Surface pCO_2 varied from 368 to 494 µatm during the study period. The wind speeds were between 1 and 6.5 m s^{-1} and as a result CO_2 fluxes varied widely from 0.18 to 13.2 mmol m^{-2} d^{-1}. There is not much difference in fluxes observed between NE monsoon seasons of 1995 and 1997. when time series observations were performed. During 1995 NE monsoon, fluxes varied from 0.35 to 8 mmol m^{-2} d^{-1} over a period of 5 days at the same location.

6.3.3. Inter-monsoon

Fig. 6.13 compares the solubility of carbon dioxide during different seasons revealing low solubility for carbon dioxide in inter monsoon than in SW monsoon due to higher temperatures during the former season. Consequently, higher fluxes were found in the central northern Arabian Sea (13-18 mmol m^{-2} d^{-}

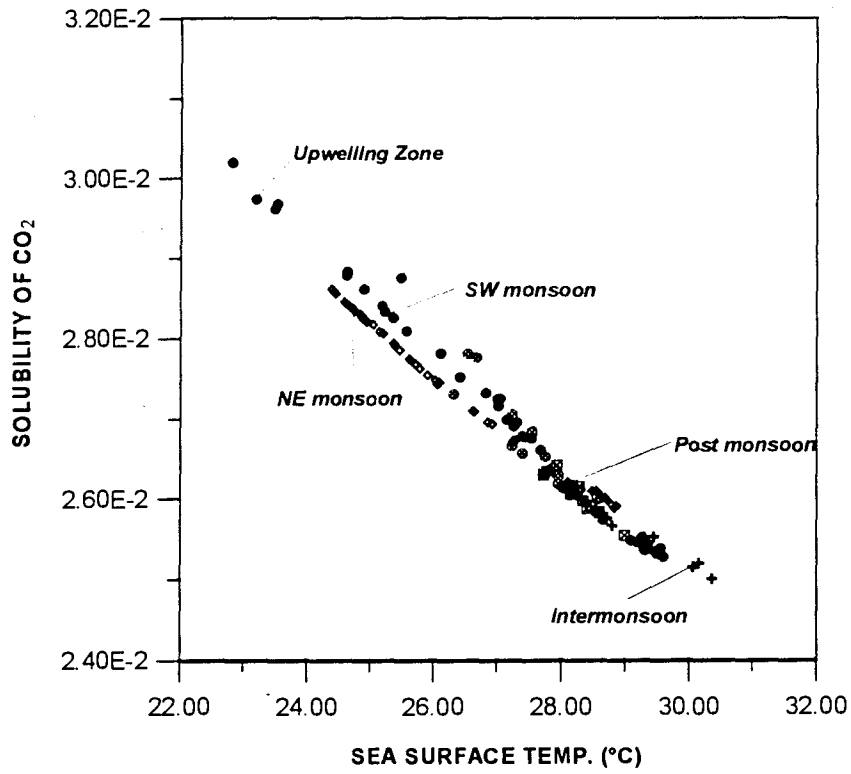

Fig. 6.13. Solubility of carbon dioxide with sea surface temperature during different seasons in the Arabian Sea.

^{1}) whereas these were lower in the south (0.08 mmol m^{-2} d^{-1}) due to changes in wind speeds. Coastal regions of the northern Arabian Sea seem to emit relatively higher fluxes of 4.1 mmol m^{-2} d^{-1} than in the southern Arabian Sea (1-3.5 mmol m^{-2} d^{-1}) due to higher wind speeds in north (3.7 to 6.3 m s^{-1}). It is estimated that the study region emanates ~10 Tg.season^{-1} of carbon dioxide to the atmosphere.

6.3.4. Late SW-monsoon

Although winds are weak, the CO_2 fluxes ranged between 1-8 mmol m^{-2} d^{-1} due to higher pCO_2 concentrations resulting from intense bacterial decomposition of organic matter and high sea surface temperatures. High fluxes were observed in the coastal waters (5-8 mmol m^{-2} d^{-1}) than in open sea regions (3-5 mmol m^{-2} d^{-1}). This might be due to higher pCO_2 resulting from the decomposition of organic matter produced in coastal regions driven by SW monsoonal upwelling. No difference was found between the fluxes from coastal and off-shore regions along 15° N. The study region acts as a source of atmospheric carbon dioxide to an extent of 9 Tg.season^{-1} during this period.

6.3.5. Inter-annual variations (SW monsoon of 1995 & 1996; NE monsoon of 1995 & 1997; Inter-monsoon of 1994 & 1996)

The present results show significant inter-annual pCO_2 variations during SW

monsoon and winter seasons due to changes in physical and biological processes. These variations were not only significant in the surface layers but also extended below the thermocline (Fig. 4.39 and 6.1). From the wind speeds and chemical data, it can be deduced that the influence of Findlater jet was more intense during the SW monsoon of 1995 than in 1996. The surface pCO_2 at the axis of the Findlater jet did not show much variation (432 and 426 µatm) but the mixed layer nitrate varied from 4 to 1 µM, respectively. Air-sea flux of carbon dioxide at the Findlater jet was several folds higher during the 1995 SW monsoon (45 mmol m^{-2} d^{-1}) than that in 1996 monsoon (13 mmol m^{-2} d^{-1}) which is due to high wind speeds during the former year. Inter-annual variations during NE monsoon were studied at 21° N, 64° E. Low SST and higher salinities were observed during 1997 than in 1995. No significant variations were observed in wind speeds (range 2-6 m s^{-1}). pCO_2 concentrations were higher during 1997 compared to those in 1995 by at least 50 µatm which was due to more intense convective mixing during 1997 than in 1995. In 1997 nitrate concentration of ~ 4 µM occurred whereas it was ~ 2 µM in 1995 at the air-sea interface, indicating the higher intensity of convective mixing in the former year. Air-sea fluxes of carbon dioxide were higher during 1997 with a range between 0.18 and 13.2 mmol. m^{-2} d^{-1} whereas it varied from 0.35 to 8 mmol. m^{-2} d^{-1} during 1995 at 21° N.

Pre-SW monsoon variations at 15° N, 64° E were not very significant with respect to pCO_2 distribution but in case of air-sea fluxes due to variations in wind speeds. pCO_2 varied from 456 to 464 µatm during inter-monsoon of 1994 whereas it was 415 µatm in 1996 (SS141). Air-Sea fluxes of CO_2 amounted to 1.54-1.81 mmol.m^{-2}.d^{-1} and 1.69 mmol.m^{-2}.d^{-1} during inter-monsoon seasons of 1994 and 95, respectively.

Air-sea fluxes of carbon dioxide, in general, showed significant seasonal and spatial variability. Average fluxes of carbon dioxide from different regions are listed in Table 6.4. These ranged between 0.08 and 18.5 mmol m^{-2} d^{-1} in inter-monsoon but varied from 0.28 to 7.2 and –10.2 to 41.5 mmol m^{-2} d^{-1}, respectively, during NE- and SW monsoon 1995. High spatial variability during this season was caused by river runoff in the coastal zone as well as upwelling. As upwelling brings subsurface waters to the surface it leads to higher fluxes whereas fresh water acts as a sink for atmospheric carbon dioxide. Interannual variations seem to be significant in SW monsoon. Higher fluxes were observed in 1995 (-17.8 to 53.8 mmol m^{-2} d^{-1}) than in 1996 (0.1 to 25 mmol m^{-2} d^{-1}). Inter-NE monsoonal variations at 15° N, 64° E seem to be only marginal between 1995 and 1997 as they varied from 0.1 to 13.5 mmol m^{-2} d^{-1} in 1995 but from 0.1 to 8 mmol.m^{-2} d^{-1} during 1997. Inter-premonsoonal variability was also observed at 15° N, 64° E during 1994 and 1995 where fluxes varied from 1.54 to 1.81 and ~1.69 mmol m^{-2} d^{-1}, respectively. These data results that Arabian

Sea exhibits high spatial and seasonal variability in CO_2 fluxes which are especially high during the SW monsoon.

Highlights of CO_2 fluxes from the Arabian Sea are:

- **Fluxes were highly variable being functions of wind speeds and pCO_2 gradients**
- **Most of the SW monsoonal efflux seemed to occur in the central Arabian Sea**
- **Sea-to-air fluxes from coastal regions in SW monsoon were reduced because of low salinity surface lens resulting from river discharge**
- **Fluxes in winter and inter-monsoon were more in north than in south**
- **Significant inter-seasonal and inter-annual variability was found**

6.4. Fluxes from the Northern Indian Ocean

Kumar *et al.* (1996) highlighted the influence of freshwater on pCO_2 distribution in the Bay of Bengal where freshwater discharge from rivers of the Indian sub-continent exerts a dominant control over TCO_2 and pCO_2 distributions in surface waters. Low pCO_2 levels occur within the low-salinity zones. Therefore, a large area in the north-western bay acts as a sink of atmospheric CO_2. Only a part of the observed pCO_2 variation can be accounted for by the effect of

salinity. The rest could be due to biological production supported by external nutrient inputs in conjunction with strong thermohaline stratification which seems to be more important in lowering surface water pCO_2 by >100 µatm relative to that in atmosphere.

Here, a comparison is made to understand the variability in CO_2 fluxes in the central parts of the Arabian Sea and the Bay of Bengal during SW monsoon. The data were collected during SW monsoon along 90° E in the Bay of Bengal and along 64° E in the Arabian Sea in 1996. As the coulometer developed technical problems the pCO_2 data in the Bay of Bengal were calculated from TA and pH_T. During this season, the surface pCO_2 levels were higher than the atmospheric values with variation between 400 and 440, and 360 and 411 µatm. respectively, in the Arabian Sea and Bay of Bengal. Wind was stronger in the Arabian Sea (to a maximum of 12 m s^{-1}) than in the Bay of Bengal (3.6 m s^{-1}). This together with higher pCO_2 (than in atmosphere) resulted in CO_2 evasion from the Arabian Sea as well as from the Bay of Bengal during this season. The fluxes varied from 2 to 22 mmol.m^{-2}.d^{-1} in the Arabian Sea and from 0.6 to 3.5 mmol.m^{-2}.d^{-1} in the Bay of Bengal (Table. 6.4). These values indicate that the Arabian Sea a much stronger source of atmospheric carbon dioxide, in concurrence with earlier observations (Kumar *et al.*, 1992; George *et al.*, 1994) in Southwest monsoon as well (Sarma *et al.*, 1998). On the other hand, unlike the northwestern Bay of Bengal, the central Bay also acts a mild

source during this period. No significant north-south gradients occur in fluxes in the central Arabian Sea except for the higher values at 18 and 19° N due to divergence. However, there is a general gradual northward decrease in the sea-to-air fluxes in the Bay of Bengal. Thus, CO_2 air-sea fluxes during SW monsoon seem to be much higher than those in other seasons both from the Arabian Sea and the Bay of Bengal. It is estimated that a flux of (2 mmol.m^{-2} d^{-1}; area 4.087 x 10^6 km^2) 8.4 Tg y^{-1} is pumped out to the atmosphere from the Bay of Bengal. George *et al* (1994) reported that the Bay of Bengal is emits about 6 Tg y^{-1} of carbon into the atmosphere. Our estimate of the Bay of Bengal may be an overestimation as low salinity coastal regions act as a sink for atmospheric carbon dioxide.

The data from the Andaman Sea (Fig. 6.11) were collected during post monsoon season. pCO_2 varied from 354 to 394 µatm in the study region except for one value (479 µatm) at 11.5° N, 93.5° E where low salinity (31.95) and warm (>32.1) waters, compared to rest of the Andaman Sea were encountered. Although the winds varied from 1 to 10 m s^{-1}, the air-sea fluxes of carbon dioxide were low and ranged between -0.11 and 7.75 mmol m^{-2} d^{-1}. On an average the flux was around 0.2 mmol m^{-2} d^{-1}. This suggests that the Andaman Sea also acts as a mild source (0.7 Tg y^{-1}) of atmospheric carbon dioxide in this season.

Arabian Sea seems to act as a source of atmospheric carbon dioxide except in the coastal areas during SW monsoon season. The average flux amounts to 6.4 mmol $m^{-2}d^{-1}$ which is equivalent to ~45 Tg y^{-1}. These fluxes far exceed the earlier estimates: 60 Tg.y^{-1} for the North Indian Ocean (Takahashi, 1989) 74, 79 and 8.4 Tg y^{-1} for the entire Arabian Sea (Somasundar *et al.*, 1990; George *et al.*, 1994; Goyet *et al.*, 1998, respectively). Goyet *et al.* (1998) used an interpolation of surface temperatures for pCO_2 evaluations, without taking into accound biological effects, and hence their fluxes could have been an under-estimate. Kortzinger *et al.*, (1997) reported that Arabian Sea in general, and the areas of upwelling in particular, represent a significant source of atmospheric CO_2 with flux densities varying from 2 mmol m^{-2} d^{-1} in the open ocean to 119 mmol m^{-2} d^{-1} in the coastal upwelling zones. Present fluxes also seem to be higher since Fig.8 of Louanchi *et al.* (1996) indicates an average flux of 10 Tg $month^{-1}$ (~120 Tg y^{-1}) for the region between 10° S and 20° N in the Indian Ocean. Hence, the Arabian Sea is a significant and perennial source of atmospheric CO_2 except in coastal pockets influenced by run-off. It should, however, be noted that the present data sets do not cover the most intense Somali and Omani upwelling regions in the Arabian Sea from where even higher fluxes are expected. Biological $CaCO_3$ precipitation releases CO_2 to water (Anderson and Dyrssen, 1994) that could further enhance the above estimated fluxes specifically in the western regions.

Highlights of CO_2 fluxes in the North Indian Ocan are:

- **Central Bay of Bengal and Andaman Seas act as mild sources of atmospheric CO_2 in SW Monsoon**
- **Arabian Sea is a perennial source of atmospheric carbon dioxide**

Chapter 7

CARBON BUDGETS

In order to understand the biogeochemical cycling of an element it is essential to quantify its fluxes among various major reservoirs (physical, biological and geological) as well as between compartments (dissolved and particulate) in each reservoir. The situation in the Indian Ocean is complicated by the presence of marginal water bodies that continuously exchange water and solutes with the Arabian Sea. Inputs of waters from the Gulf of Oman and the Gulf of Aden into the northwestern Indian Ocean and from the southern Indian Ocean could significantly influence the carbon budgets of this region (Somasundar *et al.*, 1990). Bethoux (1988) observed a temporary subsurface outflow and surface inflow in the Red Sea during SW monsoon. Attempts have been made by Somasundar *et al.* (1990) and Kumar *et al.* (1995) to quantify carbon budgets of the Arabian Sea. Somasundar *et al.* (1990) have found the carbon in the Arabian Sea to be negatively balanced by ~84 MtC y^{-1} and proposed that this deficit could be balanced by input through northward flowing Antarctic Bottom Water. In the earlier budget evaluations the surface layer has been assumed to be in equilibrium, as it has been in continuous exchange, with the atmospheric carbon dioxide (see Somasundar *et al.*, 1998). Further, detailed exchanges of water laterally and vertically, and influence of such exchanges on carbon turnover have not been addressed. Thus, in the present model we considered carbon exchanges laterally with watermasses as well as vertically across 100m boundary layer and across air-sea interface.

7.1 Computations

Earlier studies have been based on limited data sets and with several approximations assumed. Therefore, an attempt has been made here to evaluate carbon fluxes in the surface 100m of our study region (Fig. 7.1) with detailed data sets obtained in the present cruises (Table 2.1) and from Modular Ocean Models (MOM). The eastern boundary of the box was the section along the Indian coast (Fig. 7.1) while 21° N has been chosen to be the northern boundary. Sections along 64° E and 11° N act as western and southern boundaries, respectively. The model inputs are physical, biological and geological parameters. Physical inputs include velocities of water across the boundaries of the box laterally and vertically. The horizontal and vertical velocities were obtained from the runs of MOM model (courtesy Dr. P. S. Swathi, C-MMACS, Bangalore). Horizontal and vertical fluxes of water in to/out of the box were computed at one degree interval. Figures.7.2 and 7.3 show water and carbon transports in to and out of the surface box, seasonally and annually. Carbon fluxes are products of net water transport and total dissolved carbon concentration, of the source, along the section in question.

7.2 Water and carbon Fluxes

Along 21° N, 9.6×10^{12} m^3 of water goes out of the surface box which carries 0.26×10^3 Tg of carbon during NE monsoon whereas 7 and 19×10^{12} m^3 of

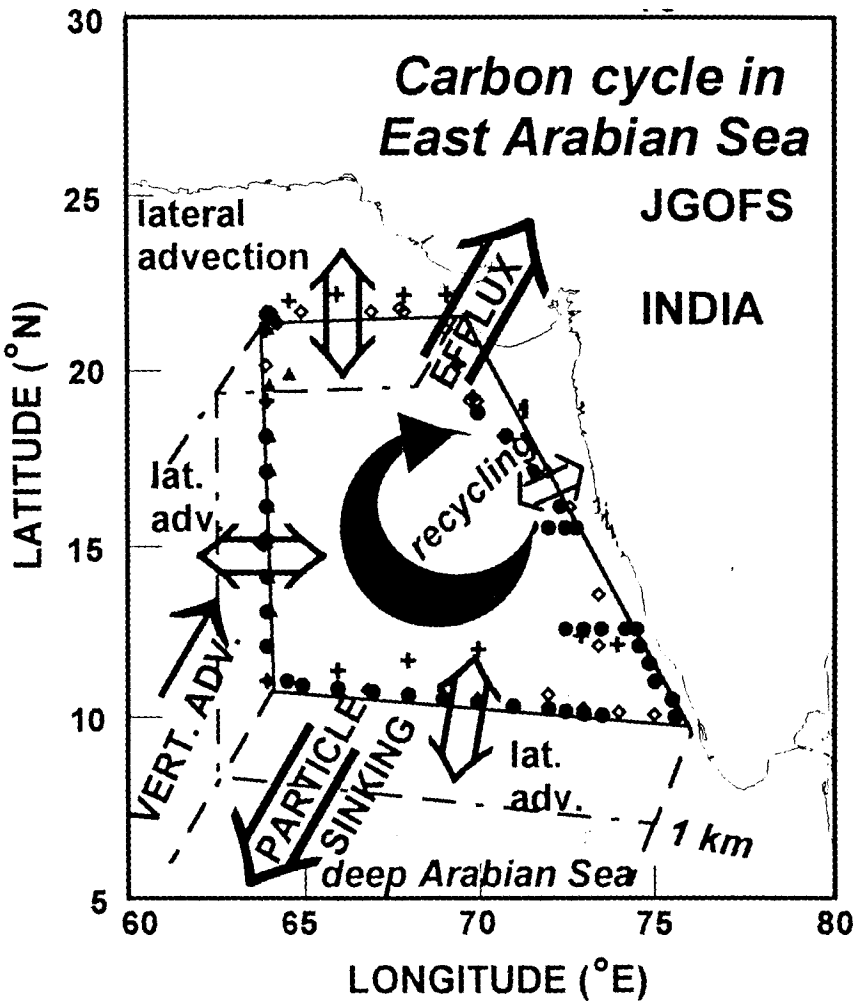

Fig. 7.1. Physical and biogeochemical model considered for the study area in the Arabian Sea. Recycling in the surface layer means primary production and remineralization of the produced carbon.

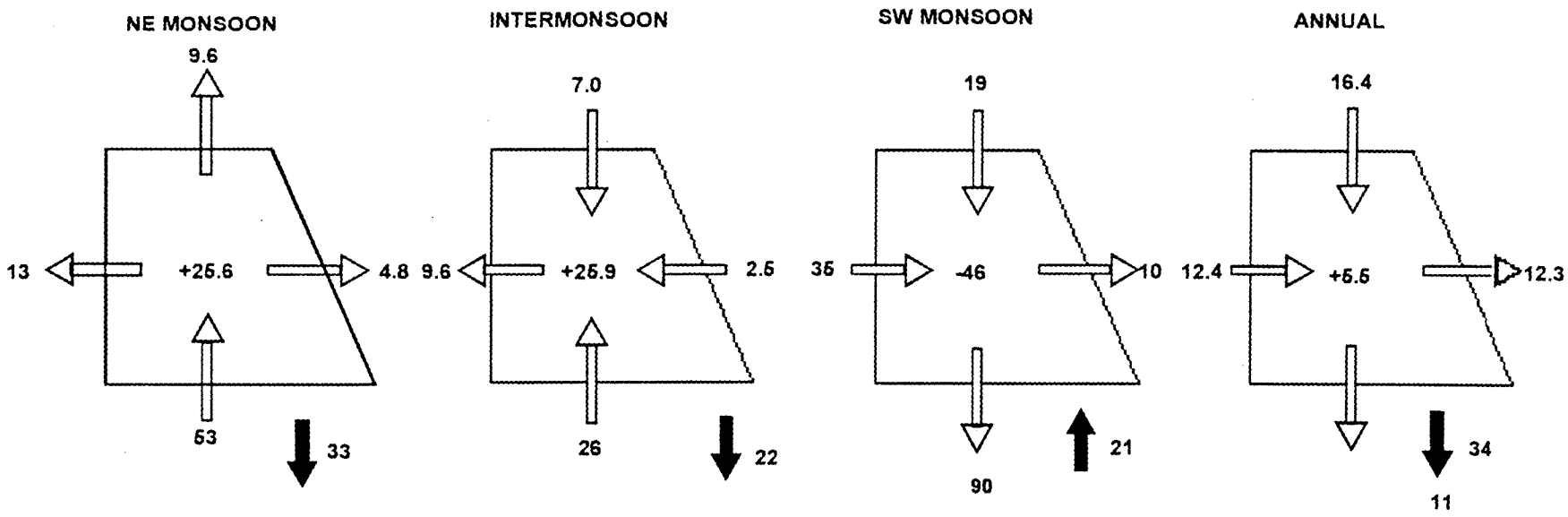

Fig. 7.2. Volume transports in the mixed layer of the study region (x $10^{12}m^3$)

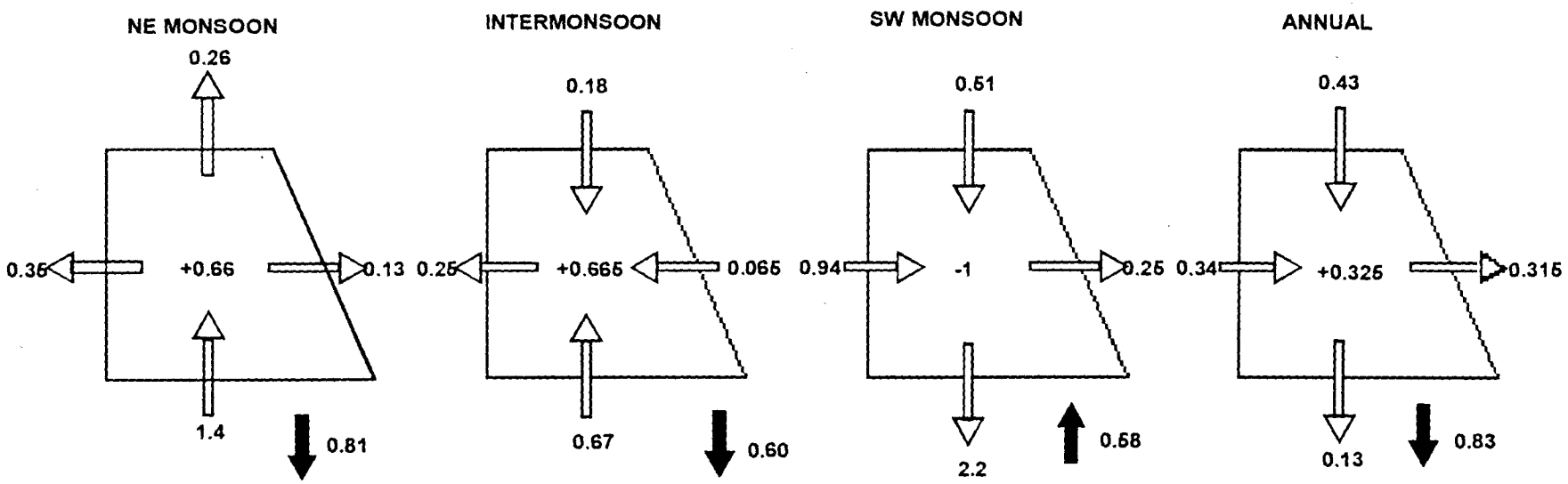

Fig. 7.3. Carbon transports in the mixed layer of the study region (x 10^3 Tg)

water enter during inter- and SW monsoon seasons, respectively, thus bringing 0.18 and 0.51 x 10^3 TgC in to the box. Therefore, the annual input of carbon into the surface box across 21° N amounted to 0.43 x 10^3 TgC. About 13 and 9.6 x 10^{12} m^3 of water seem to be transported westward, respectively, across 64° E boundary of the box during NE- and inter-monsoon seasons but 35 x 10^{12} m^3 water enters the box during SW monsoon. These amount to carbon transports of 0.35, 0.25 and 0.94 x 10^3 TgC in the three seasons, with an annual flux of 0.34 x 10^3 TgC in to the box. The resultant net transport of carbon out of the box amounts to 0.31 x 10^3 TgC y^{-1} through the eastern boundary, across which water transport was towards the coast in NE- (4.8 x 10^{12} m^3) and SW- (10 x 10^{12} m^3) monsoons but in to the box in inter- (2.5 x 10^{12} m^3) monsoon (Fig. 7. 2). Along the southern boundary (11° N) the transport is poleward during NE- (53 x 10^{12} m^3) and inter-monsoon (26 x 10^{12} m^3) seasons whereas it is equatorward in SW monsoon with a voluminous transport of 90 x 10^{12} m^3. These amounted to 1.4, 0.67 and 2.2 x 10^3 TgC fluxes in respective seasons with a net annual outflux of 0.13 x 10^3 TgC. These results indicate that the surface box is positively balanced during NE monsoon (0.92 x 10^3 TgC) and inter-monsoon (0.305 x 10^3 TgC) but is negative in SW monsoon (1.0 x 10^3 TgC). The annual carbon budget in the surface box is +1.96 x 10^3 TgC with flows of west to east and north to south.

The vertical fluxes of water (Fig. 7.2) indicate downwelling from surface layer in NE- (33 x 10^{12} m^3) and inter- (22 x 10^{12} m^3) monsoon seasons while it upwelled in SW monsoon (21 x 10^{12} m^3). These water flows lead to a sinking carbon of 0.81 x 10^3 TgC and 0.6 x 10^3 TgC and to an upwelled carbon of 0.58 x 10^3 TgC. Therefore, the net dissolved sinking carbon flux is 0.83x 10^3 TgC (Fig. 7.3).

7. 4 Cycling of carbon

Although considerable geographical variation in column productivity within the Arabian Sea is observed, an average value of 700 mgC m^{-2} d^{-1} was used here. The actual values varied from 281 to 1760 mgC m^{-2} d^{-1} in coastal regions and 193 to 1097 mgC m^{-2} d^{-1} in open sea regions (Bhattathiri *et al.*, 1996). On an average, 0.41 x 10^3 TgC y^{-1} is fixed annually through primary productivity in the study region (Fig. 7.4).

Most of the organic material thus derived from the first trophic level may be remineralized through various metabolic activities in the surface mixed layer and the remaining portion escapes the euphotic zone. The sediment trap and and Th-scavenging studies during the JGOFS cruises yielded a sinking flux (Fig. 7.4) of 0.11 x 10^3 TgC y^{-1} (Dr. V. Ramaswamy, personal communication, 1998). This reveals that nearly three-fourths of the photosynthetically fixed carbon gets remineralised in the surface layer itself.

Fig. 7.4. Carbon budget for the surface mixed layer for the study region (Tg y^{-1})

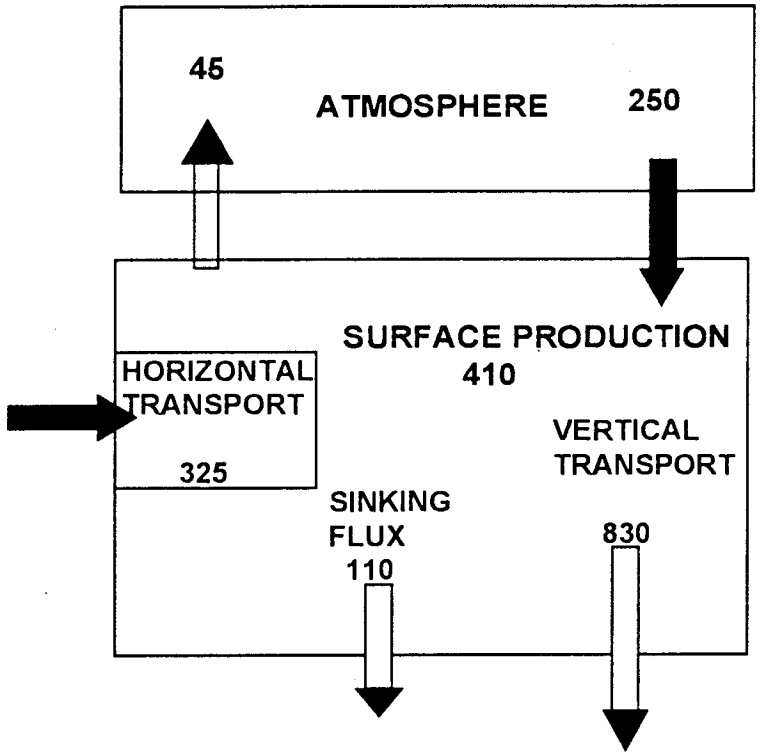

The laterally transported (325 TgC y^{-1}) and photosyrithetically fixed (410 TgC y^{-1}) carbon appeared to be the sources to that in surface layer box. The sum of these, however, is less than the total outflux of 985 TgC y^{-1} (=830+110+45) x 10^3 TgC y^{-1}) by 250 TgC y^{-1}. The only other carbon source to this surface layer box can be atmospheric carbon dioxide. Therefore, the present study reveals that although the study area perennially emits carbon dioxide to atmosphere (45 TgC y^{-1}) this region absorbs nearly 5 times of the emitted. Ironically, the surface layer of the study region is almost always supersaturated, sustained by very high pCO_2 gradient between surface and intermediate layers, with respect to atmospheric carbon dioxide. Hence, it is difficult to specify the actual mechanism of absorption which, nevertheless, is presumably driven by a combination of intense physical, chemical and biological forcings. The carbon proportion of biologically fixed to emitted (410/45 = 9.1) in the study area is out of prortion compared to that of global values (45,000/90,000 = 0.5). This could be due to the rapidity of processes occurring in the Arabian Sea with respect to productivity and circulation patterns, atypical of those in the rest of the world oceans. The sinking of carbon from surface layers seem to be logical since evaporation at the surface results in the formation of high density Arabian Sea High salinity Water. Moreover, biological processes catalyse the absorption of atmospheric carbon dioxide although not directly, unlike those of physical processes.

Highlights

- **Nearly three-fourths of the photosynthetically produced carbon remineralizes in the surface layer itself**
- **Despite the perennial emission, carbon budget, in toto, suggests the surface Arabian Sea to be a net sink**

Chapter 8

BEHAVIOUR OF CARBON DIOXIDE COMPONENTS IN ESTUARIES

Estuaries are the zones where river water mixes with sea water under the continuous influence of physical processes. The intensity of mixing depends on tidal, wind forces and of run-off. The estuaries represent very complex and important systems through which the continental materials are transported to oceans. The materials present in both dissolved and suspended forms, originate from weathering and biological activities on land. It has been estimated that nearly 25 $x10^3$ Tg y^{-1} of material is put into the sea of which ~85% passes through the estuarine environment (Garrels and Mackenzie, 1971). The mixing of fresh and saline water in the estuaries controls the distribution and speciation of chemical substances.

Biogeochemical processes occurring in estuaries may modify the concentrations of river or sea water borne substances. Such modification in a property is generally assessed through the comparison of the said property against a conservative property, chlorinity or salinity (Liss, 1976). If the observed concentrations of a property fall nearly on the theoretical dilution line, that joins the property levels in freshwater and sea water end-members, then the respective property is said to be behaving conservatively. On the other hand, when the property distribution deviates from the theoretical dilution line, either positively or negatively, its behaviour is termed as non-conservative. Positive deviation in a property could arise from regeneration, desorption/dissolution and inputs from sediments whereas negative deviation

can occur through biological removal, adsorption and precipitation process occurring within the estuarine zone.

The TCO_2 in average global river water is ~720 μM whereas in sea water it is ≥1800 μM. However, the behaviour of TCO_2 in estuaries is not much known. It is important to understand the dynamics of TCO_2 in this zone since these are highly productive regions where the organic carbon regeneration is quite significant. These biological processes may not only alter the TCO_2 but can also bring out changes in pH of these waters. Although the pH of sea water varies over a narrow range 7.8 - 8.3, the pH of river waters varies widely as it is governed by the nature of rocks in the catchment area. If the terrain rocks are acidic, the pH will be in the acidic range. If so, this will result in an increase in pCO_2 in water. Discharge of industrial and aquaculture effluents can also alter the carbonate equilibria based on the nature of the effluents. Changes in pH in sea water are largely because of changes in CO_2 system which is not the case for estuaries. This is because of the fact that pH of waters in proximity to land can be altered by other means such as pollution or a natural addition of substances other than carbon. Thus, the changes in dissolved pCO_2 will lead to change in its gradient between air and water that determines the direction as well as the magnitude of the flux.

8.1. Behaviour of pH in the Mandovi-Zuari estuarine complex

The behaviour of pH during estuarine mixing has not been given its due

importance and hence remains largely unknown. This is particularly required because of the relatively high productivity in estuaries that can alter pH and thus acid-base reactions. For instance, intense regeneration of organic matter may lower the pH substantially that would result in the build-up of pCO_2 in water. The pH may also be altered by the river transported suspended material or the resuspended bottom sediments. Since, this estuarine system is used by barges for the export of iron and manganese ores a change in pH, if any, is expected due to rock-water interaction which might alter the chemical equilibria.

8.1.1. Field measurements on behaviour of pH

The pH of river water did not change much during the study period. It remained in acidic range (~6.8). Sea water pH was relatively less compared to that of normal surface sea water of 8.1±0.2. The pH values seemed to somewhat follow the curve expected from the linear mixing between river and sea water in the Mandovi-Zuari estuarine system. (Fig. 8.1). This suggests that the pH largely behaves conservatively in the study area. The low salinity (1.300 psu) water in the Mandovi - Zuari Estuarine system has an average pH of 6.80 while the sea water with a salinity of 34.4 psu has a pH of 7.85. Significant deviation was observed around a salinity of 10-15 psu where several observed pH values were substantially higher than expected from the regular trend. Waters

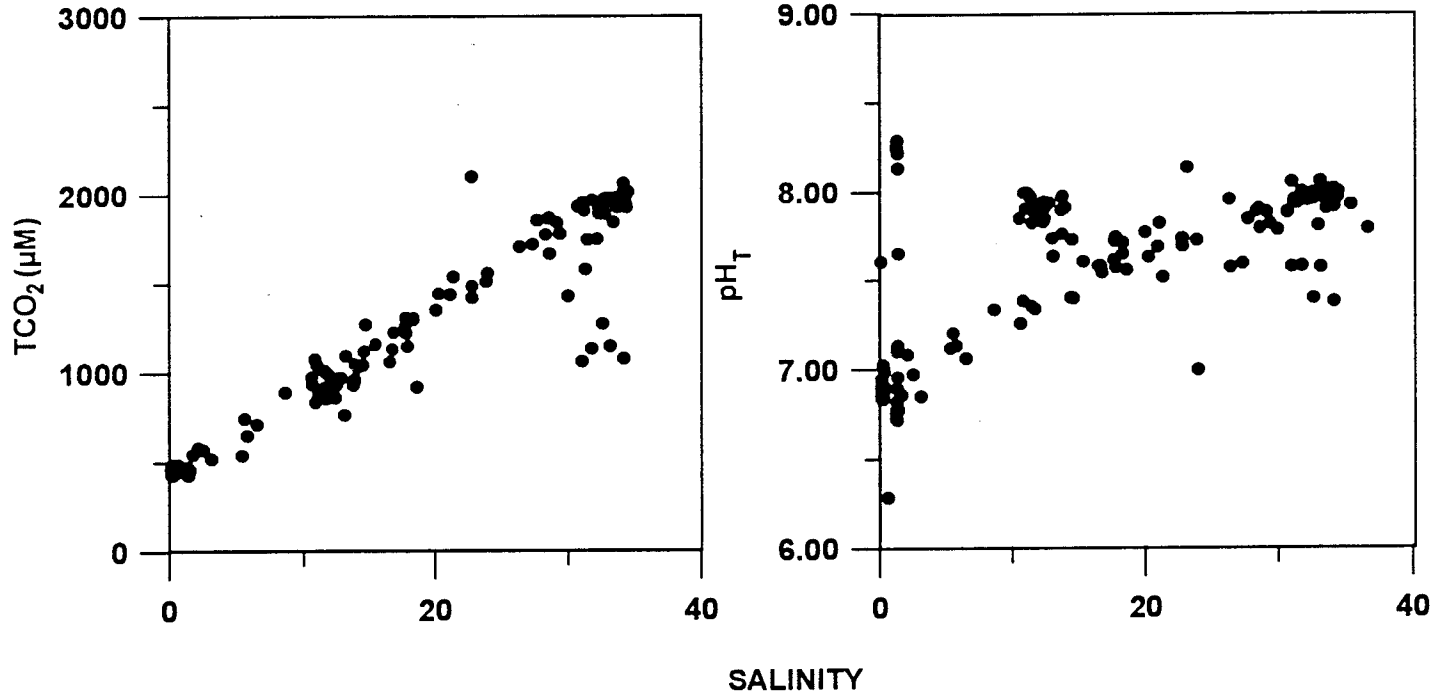

Fig. 8.1. Variations in TCO_2 (µM) and pH_T with salinity in the Mandovi-Zuari estuarine system.

of these high pH values were found to have higher salinities (~12 psu), compared to the neighbouring water salinities of ~5 psu, due to discharge from salt pans. Wide variations in pH observed at any salinity is due to CO_2 exchange with the atmosphere, productivity/regeneration processes in water column/sediments and/or mineral-water proton exchange equilibria. The increase in CO_2 absorption from atmosphere lowers the pH of a solution while its ejection raises it. In biochemical reactions, the synthesis of a particulate organic molecule consumes protons whereas regeneration releases them (Anderson and Dyrssen, 1994). Low salinity waters dominate the present estuarine system during SW monsoon when low pH were observed. Occurrence of these low pH values is of vital importance for the CO_2 system since this would enhance the partial pressure of CO_2 in water. This will enable the escape of larger quantities of this greenhouse gas to the atmosphere from this region.

8.1.2. Laboratory experiments

Due to comparatively higher pH values observed between salinities of 10-15 psu (Fig. 8.1), mixing experiments were conducted in the laboratory to ascertain whether or not the pH behaves conservatively, and if not, what are the controlling processes. These mixing experiments were conducted with and without minerals (iron and manganese) ore/sand soils.

8.1.2.1. *Behaviour of pH during mixing of river and* sea waters

The end-members of sea water and river water were mixed in varying proportions, to obtain a full range of salinities, under nitrogen atmosphere and the positive pressure maintained by over head nitrogen prevented CO_2 exchange. For this purpose we obtained water from the upper reaches of the Mandovi river was used. Three rounds of such experiments were conducted during the study period. The pH exhibited a non-conservative behaviour with a rapid rise from ~6.6 in river water to ~7.9 at 15 psu (Fig. 8.2). Thereafter a slight drop in pH was noticed up to about 35 psu. The rise in pH at lower salinities could be attributed to the complexation of proton by anions, such as sulphate and carbonates, which are abundant in sea water as compared in river water (Turner *et al.*, 1981). In view of the higher abundance of H^+ at salinities <20 this ion would also compete with Ca^{+2} and Mg^{+2} for complexation with anions. The minor drop in pH at >20 psu could have been due to a release of a few H^+ ions because of the heavy competition from highly abundant alkaline earth ions at higher salinities. Burton (1976) attributed pH changes during mixing between sea and brackish waters to variations in anionic composition. Equilibrium model calculations of Turner *et al.* (1981) indicate that free anions are much higher in sea water than in freshwater of pH 6. Hence, the observed and seemingly near conservative pH behaviour in the Mandovi-Zuari estuarine system in Fig. 8.1 is caused by a process other than simple

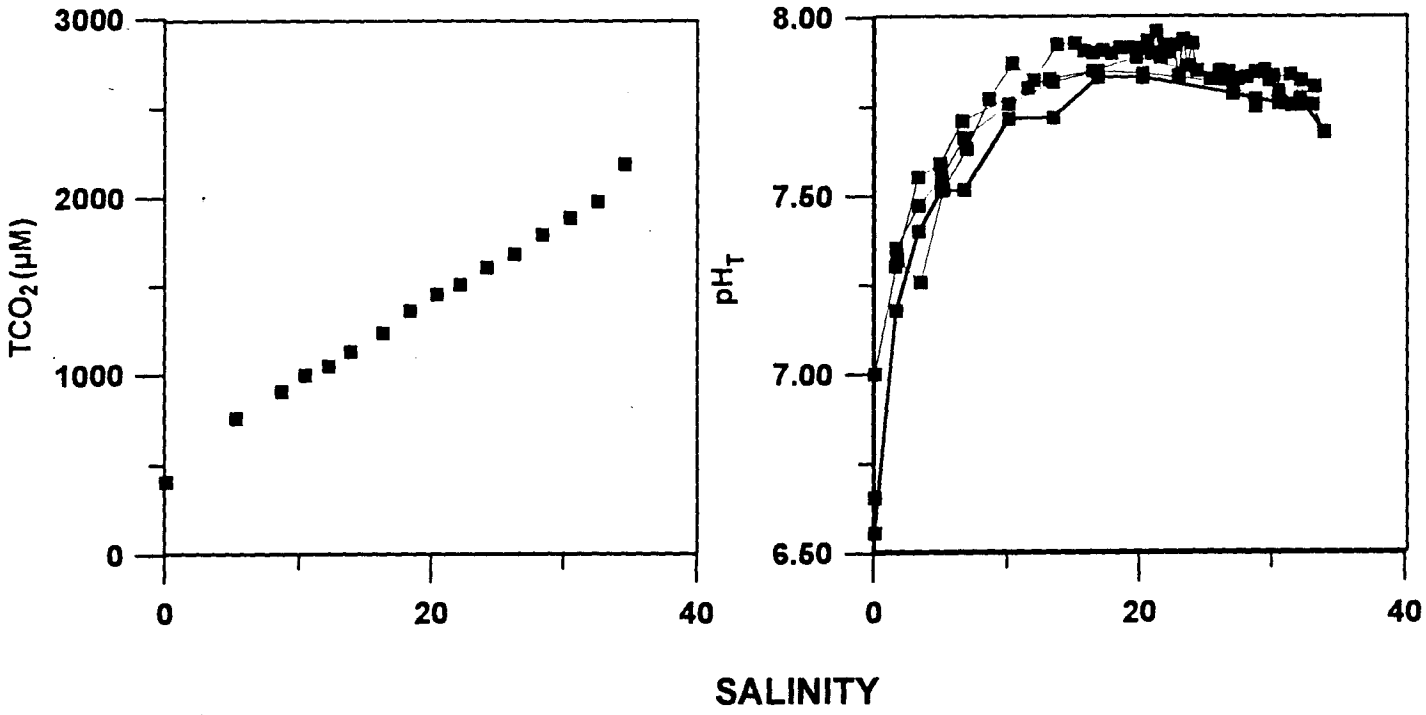

Fig. 8.2. Variations of TCO_2 (µM) and pH_T with salinity (psu) during laboratory mixing experiment.

mixing of end members. On the other hand, the dissolved organic material from rivers could also contribute to low pH in fresh waters. This organic material is likely to flocculate during the early estuarine mixing (Aston, 1978). Hence, the non-linear behaviour of pH in our mixing experiments could have been a result of complexation of rivers borne H^+ by free anions present in sea water and to some extent to the flocculation of dissolved organic materials.

Comparision of our field and mixing experiments reveal a clear incompatibility in the pH behaviour. The pH values from field measurements were lower than those obtained from simple mixing experiment. For instance, the difference was about 0.4 pH units around 15 psu. This is a significant decrease which can not result from the dominance of regeneration over production. Since, these are shallow rivers, an alternative mechanism to account for the lowered pH is the role of resuspended particulate matter. The estuarine sediments are rich in organic carbon that is conducive for microbial reactions in the presence of oxygen or any other oxidant. Thus the decomposition of organic matter releases proton to pore waters. The continuous tidal mixing leads to the resuspension of bottom sediments where the pore fluids are released to overlying waters. Thus a reduction in pH occurred in estuarine waters of Mandovi-Zuari estuarine complex compared to that expected from mixing. On the other hand, whether or not interaction of estuarine water with the drained soils from catchment areas or spilled ores from barges would lower the pH of

water is unknown. Therefore, further experiments were conducted in the laboratory using these mineral substances.

8.1.2.2. *Influence of soils*

These experiments were performed in almost the same way as in simple mixing experiments but with ore or soil materials in required quantities. The behaviour of pH noted in Fig. 8.2 was totally different from the results of experiments using ore and soils (Fig. 8.3). A pH decrease compared to those expected from the simple mixing experiments was found. However, the decrease was more significant with the soil than with ore materials. For instance, the initial experiments conducted with 1 g of soil resulted in pH values much lower than ~6.5. Hence, in the actual experiments we used only 0.25 g (Fig. 8.4). Even with the smaller quantities of soils (0.25 g) the pH decrease was more significant compared to that obtained using 1 g of ore materials (Fig.8.3). Hence, the pH in the Mandovi-Zuari estuarine system seems to be largely maintained by solid-solution interactions, with the soils in particular. These rivers and the estuarine system are shallow and therefore there is a continuous resuspension of solid materials. In fact, large amounts of soil from the catchment areas are transported through these estuaries following heavy rains (~300 cm y^{-1} on an average) during the Southwest monsoon; when the coastal waters are quite turbid and brownish in color.

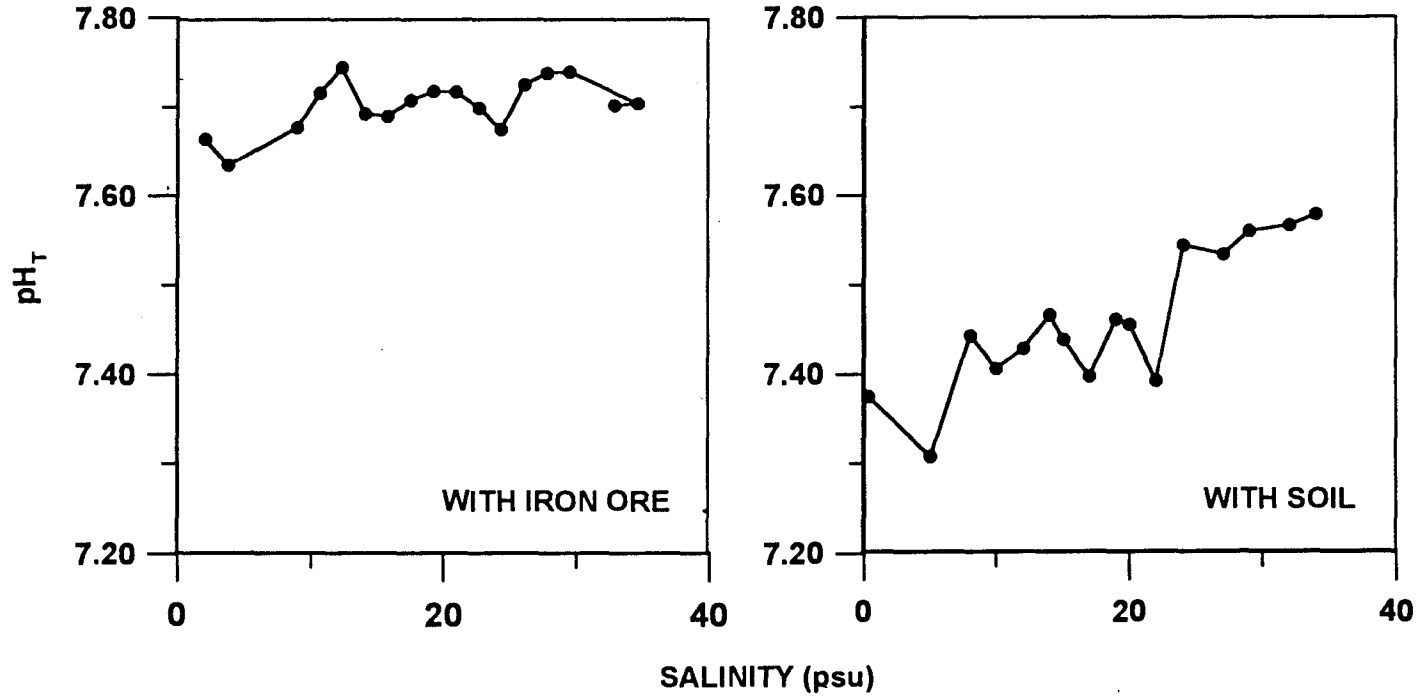

Fig. 8.3. Variations in pH with salinity during the interaction of water with 1 gm of iron ore and 0.25 gm of soil.

8.1.3. Effect of interaction with soil on pH in estuarine waters

Figure 8.4 shows a composite diagram on the behaviours of pH found in Figs. 8.1-3. These data clearly underscore the fact that the lowering of pH in the estuarine waters of Goa is mainly because of the interactions with the soils. This decrease in pH could have been a result of proton release and also leaching of organic matter from the soils. This could more likely be the humic material which is copiously present in the soils. Interestingly, at extremely low salinities in the mixing experiments with soil/ore resulted in a slight increase in pH was observed, possibly, because of the consumption of proton in river water by the humic material on the particulates. However, at higher salinities the protons complexed with humic materials in soils may be released due to heavy competition from Ca^{+2} and Mg^{+2} in sea water, thus resulting in lowest pH values. Simultaneously, dissolved organic materials may also be leached from soils. Hence we estimated these, in terms of dissolved organic carbon (DOC), using high temperature catalytic (platinum) oxidation method (see 2.2.6.).

8.1.4. Effect of Dissolved Organic Carbon leaching from soils

Fig. 8.5 depicts the behaviour of DOC in mixing experiments using 0.25 g of soil. DOC increased with increasing salinity from 0 to 20 psu with no significant variation at higher salinities. The increase at these salinities is apparently due

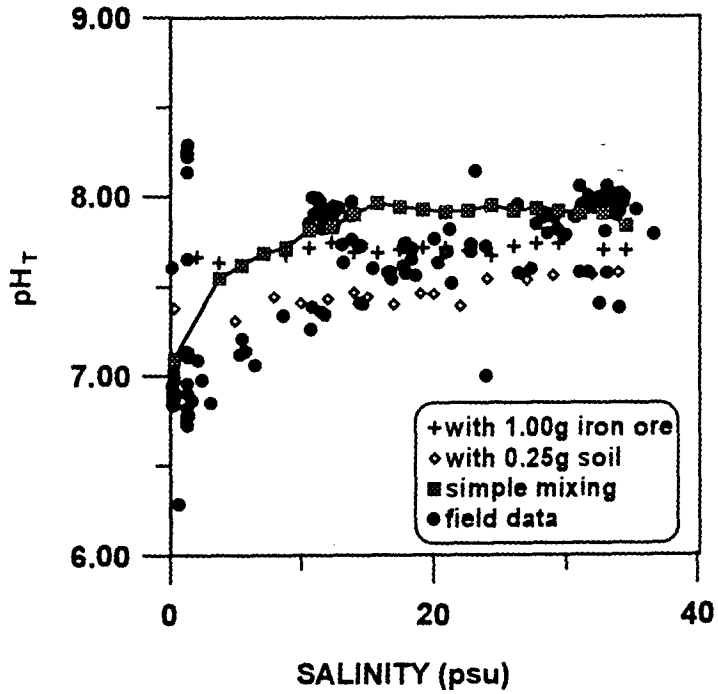

Fig. 8.4. Composite diagram of Figs. 8.1 to 8.3.

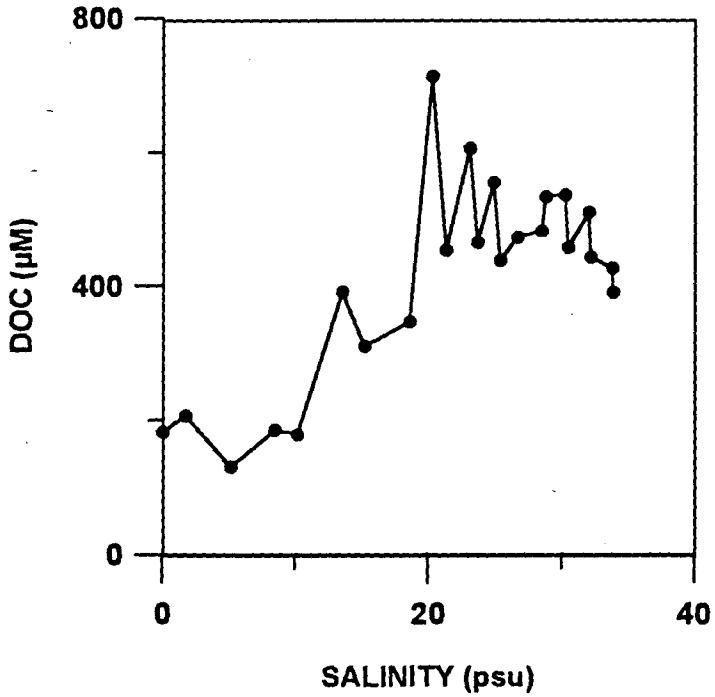

Fig. 8.5. Leaching of DOC from 1 g of soil at various salinities

to leaching of humic acids from the soil. The measured DOC would in fact also represent some fraction of colloidal form since the samples after the mixing experiments were not filtered before the analysis (Fig. 8.5). However, this fraction could be of minor importance as the sample, after the experiments, was found to be clear. Insignificant variations at salinities <10 might be due to a possible balance between leaching and coagulation processes. Aggregation of DOM is important at lower salinities (Sholkovictz, 1976). Humic acid acts as a chelating ligand because of phenolic and carboxylic groups (Reuter and Perdue, 1977; Perdue, 1978). The metal-humic acid association constants have been found to correlate reasonably well with the corresponding hydroxide and carbonate stability constants (Turner *et al* 1981). Humic acid complexation is therefore most significant for cations which are bound to carbonate and hydroxides. It has been observed that copper (II), manganese(II), cobolt(II), nickel (II), zinc (II), cadmium (II), mercury (II) and lead (II) are significantly complexed by the humic acid in sea water at pH 8.2 (Turner *et al* 1981). In fresh waters low amounts of organic ligand is bound by the major cations where trace metal complexation is also weaker (Mantoura *et al* 1978). Ong and Bisque (1968) examined the coagulation by metal ions of an alkali-soluble fraction of peat. Trivalent cations were shown to be more effective than divalent cations in coagulating humic matter and divalent ions more effective than univalent. Fig. 8.5 essentially confirms the fact that the catchment soils contain significant qualities of organic matter that is leachable during estuarine mixing.

This increased leaching at higher salinities could be aided through complexation and dissolution of organic acids in soils by cations in sea waters. These reactions release protons to water which result in pH decrease (Fig. 8.4) in Mandovi-Zuari estuarine system than expected from simple mixing of end members.

Highlights of pH behaviour are:

- **Behaviour of pH in the estuarine waters appeared to be conservative**
- **Simple laboratory mixing studies revealed its non-conservative behaviour**
- **Expected non-conservative behaviour was modified by soil-water interactions**
- **Leaching of soil organics contribute to decreased pH during soil-water interaction**

8.2. Behaviour of TCO_2

The TCO_2 in river water is lower (720 μM, Meybeck, 1982) than that in surface sea water (1800-2100 μM). Whether the TCO_2 behaves conservatively during the estuarine mixing or not is not known. In the Mandovi-Zuari estuarine system the TCO_2 of the low salinity end-member (0.079 psu) was 438 μM whereas the

highest TCO_2 obtained in sea water of 34.59 psu was 2103 μM. The TCO_2 content of river waters is much less than that of global average (720 μM, Meybeck, 1982). The behaviour of TCO_2 in the Mandovi-Zuari estuarine complex indicates that total carbon dioxide behaved conservatively during the study period, i.e., the TCO_2 in sea water has been largely diluted by the TCO_2 in river to yield the linear relationship in Fig. 8.1. The reasons for a few low TCO_2 values at salinities >30 psu are not known at present. The carbon dioxide in surface waters could also be effected by biological and air-sea exchange processes (Baes, 1982). The deviation of a few data points in Fig. 8.1 could have been due to biological and exchange processes but this does not greatly influence the apparent conservative behaviour of TCO_2 in Mandovi-Zuari estuarine complex. The effect of mixing between river and sea water on TCO_2 distribution was studied in laboratory experiments. The results were shown in Fig. 8.2 that confirm the conservative behaviour of TCO_2. This figure includes the results of mixing experiments conducted in 3 batches.

Highlights of TCO_2 behaviour are:

- **Lower TCO_2 values were found Mandovi-Zuari river waters than in average global river water**
- **Behaved conservatively in field and laboratory experiments**

8.3. Variations in pCO_2

The bicarbonate-carbonate equilibrium governs the pH in aqueous solutions. Biological processes largely modify this equilibrium. For instance, removal of carbonate for the formation of skeletal material leads to bicarbonates conversion to carbonates resulting in a build up of CO_2 (eq. 4.8). However, pCO_2 variations in Mandovi-Zuari estuarine complex is of particular interest since pH is substantially lower than expected from simple mixing. The pCO_2 in the study region showed large variability at the freshwater end (Fig. 8.6). At lower salinity ranges pCO_2 varied from ~60 to 140 µatm without any definite trend. At salinities >10 psu pCO_2 varied between 300 and ~1000 µatm. Interestingly, pCO_2 levels were found to be higher at the fresh water end and decreased towards the sea water end. This trend coincides with the large difference found in pH values between the observed distribution in estuarine waters and in mixing experiments. The field pCO_2 data have been compared with laboratory experimental data (based on pH variation in Fig. 8.2) in Fig. 8.7. These were high about 750 µatm at lower salinity and decreased to 380 µatm with a further increase to 750 µatm. Thus the lowered pH values in estuarine waters, due to soil-water interaction, leads to enhanced pCO_2 levels in the Mandovi-Zuari estuarine system.

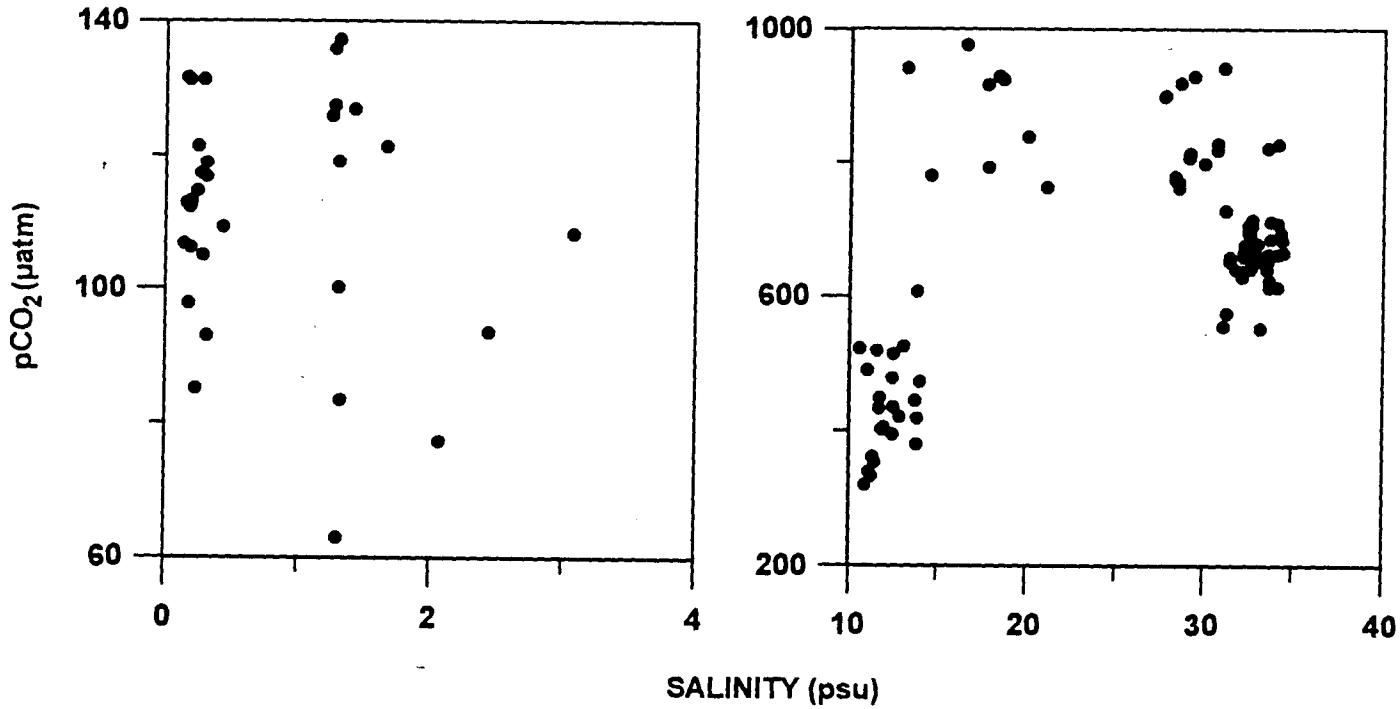

Fig. 8.6. Variations in pCO_2 (µatm) with salinity in Mandovi and Zuari estuarine complex.

Highlights of pCO_2 behaviour are:

- **Large variability was found in pCO_2 abundance at lower salinities**
- **Soil-water interaction enhances pCO_2 levels compared to those from simple mixing**

8.4. Air-Sea fluxes in estuaries

The carbon dioxide in natural waters is in continuous exchange with that in atmosphere. The difference in CO_2 between the atmosphere and water determines the direction of the flux at the interface but winds play a more important role in determining the magnitude of the flux. It is obvious that the low salinity waters shall absorb atmospheric carbon dioxide while those of intermediate and higher salinities emit the CO_2. Figure 8.7 compares air-sea fluxes computed based on experimental data without soil interactions and that of field measurements. It shows that CO_2 fluxes evaluated from experimental pH (Fig. 8.2) varied from 2-~40 mM m^{-2} d^{-1} and mainly centred at 15 mM m^{-2} d^{-1}. While field data show flux variation from -24 to ~150 mM m^{-2} d^{-1}. Based on these results it is suggested that the lowered pH values, because of soil-water interaction, result in higher pCO_2 levels than expected by simple mixing and hence make the Mandovi-Zuari estuarine system a disproportionately large source of atmospheric carbon dioxide. For instance, even with the strongest

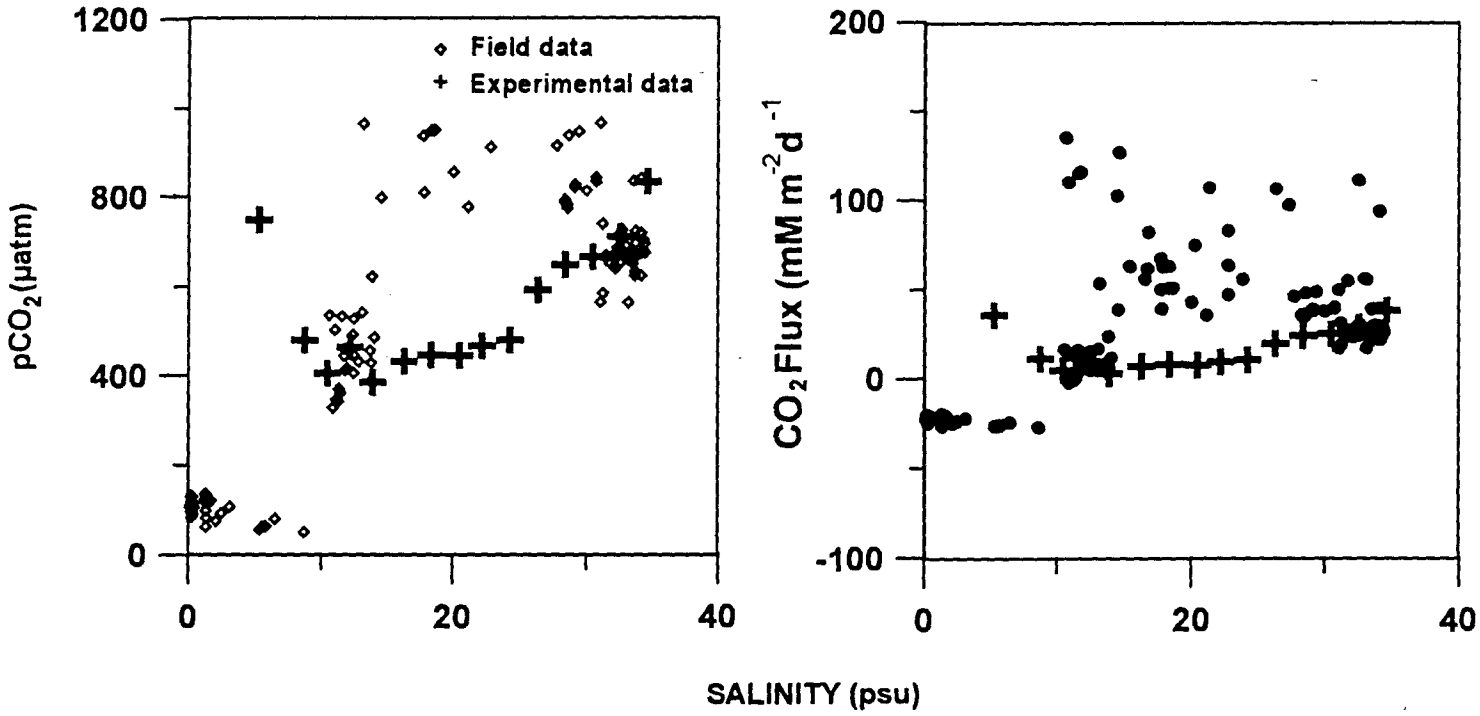

Fig. 8.7. Variations in pCO_2 and air-sea fluxes of carbon dioxide with salinity based on field and laboratory experimental data.

divergence in 1995 occurred at ~17° N the sea-to-air flux was only ~41.5 mM m^{-2} d^{-1} while the fluxes in Fig. 8.7 reached 100 mM m^{-2} d^{-1} at moderate salinities.

Hence although river influenced coastal waters found to be sinks for atmospheric carbon, those waters where soil-water interaction is intense may emit carbon dioxide depending on the nature of interaction, such as that occuring in Mandovi-Zuari estuarine system.

Highlights of CO_2 fluxes are:

- **Fluxes varied very widely**
- **Soil-water interactions lead to disproportionately large fluxes from estuaries**

Chapter 9

SUMMARY AND CONCLUSIONS

The Arabian Sea is one of the most productive regions of the world oceans where the biological fixation of carbon is largely driven by monsoonal forcings. Though many studies have been carried out on the distribution of dissolved inorganic carbon (DIC) and dissolved organic carbon (DOC) in other oceans, the dynamics of these constituents in the Arabian Sea are nearly unexplored. In view of this, the present work has been undertaken to study spatial and seasonal variability in inorganic carbon components and their fluxes at the air-water interface, and to understand their physical and biological controls. This work has been carried out as a part of the Joint Global Ocean Flux Study, a national programme of International Geosphere-Biosphere Programme, supported by the Development of Ocean Development, Government of India, New Delhi.

Ten cruises were undertaken in the Arabian Sea and Bay of Bengal. Besides hydrographic parameters and nutrients, inorganic extensive data on carbon components such as pH, total alkalinity (TA) and total carbon dioxide (TCO_2), were collected. From these data, partial pressure of carbon dioxide (pCO_2), and carbonate ion (CO_3^{2-}) were computed. Simultaneously collected physical and biological and microbiological data were utilised to understand the carbon cycling. Study has been carried out using the latest methodologies to obtain high precision data of international standards. This study covers estuarine, coastal and open sea regions of the Arabian Sea wherein the latter two areas

were studied for seasonal and spatial variations. The salient findings of this study in summary are described below:

The wind direction and speeds exhibited highly seasonal and spatial variations. They are mostly northerlies and weak in NE-; westerlies in north and northerlies in south with moderate speeds in inter-monsoon; and predominantly westerlies and strong in SW monsoons. The surface mixed layer was controlled by different physical processes in various seasons, i.e., convection in NE-, stratification in inter-monsoon and upwelling/divergence in SW monsoon. The surface mixed layer depth showed large seasonal variability. It was deep in north (120 m at 17° N) but shallow in south (~60 m) in NE-; shallow without north-south variation in inter-monsoon; and deep in south but shallow in SW-monsoon in the north. The north-south variations in mixed layer depth in winter and summer monsoons were due to convection and divergence, respectively.

The intensity of the coastal upwelling seems to have been reduced by monsoonal river discharges. Low saline waters at the surface prevent the upwelled waters to reach the surface. Highly variable productivity patterns, driven by injection of nutrient rich waters into the surface by convection and upwelling processes, were observed. The observed seasonally invarient north-south gradients in oxygen and nitrate in intermediate layers were a result of

high surface production and ageing of subsurface waters in the northern Arabian Sea. As a result, perennial denitrification was observed with the reducing conditions intensifying northward.

TA, TCO_2 and pCO_2 showed very high spatial and temporal variability driven by physical and associated biological processes. No seasonal or spatial variations in pH_T were observed since physical and biological processes contribute to different magnitudes and with opposite effects. Organic matter decomposition leads to lower pH_T, TA and carbonate ions in suboxic waters, but to high pCO_2 levels in the northern intermediate layers in all seasons, reaching to a maximum of ~1200 µatm. Physical processes largely controlled surface TA variability and mainly upwelling A complimentary behaviour between TCO_2 and nitrate in all seasons were observed. Significant north-south gradients in TA in suboxic waters were due to a large flux of protons released by intense organic matter decomposition in the north. Significant gradients in TCO_2 and TA between Arabian Sea and Bay of Bengal were due to different surface hydrographical regimes where the influence of river discharge reduced their abundance in the bay.

High pCO_2 values were associated both with nitrate enriched (upwelled) surface water and nitrate depleted (OMZ) waters in subsurface layers. Upwelling brings very high pCO_2 levels to surface thus facilitating the pumping

of carbon into the atmosphere, which, however, depends on the intensity of wind speeds. Inter element-relations and a one-dimensional model results reveal that physical processes largely control surface pCO_2 distribution. The shift in control factors from physical to biological ones occurred in the order SW-, NE- and inter-monsoon. Highly variable CO_2 fluxes, being functions of wind speeds and levels of surface pCO_2, were found to be large in SW monsoon because of divergence in the central Arabian Sea (~17° N) and waters of southwest coast of India. Sea-to-air fluxes from these coastal upwelled waters were not large as expected as these were reduced because of the prevalence of low salinity water lense. Significant inter-annual variability in fluxes were observed. These results reveal the Arabian Sea to be a perennial source to atmospheric CO_2 whereas Bay of Bengal and Andaman Sea are mild sources to atmosphere.

DOC concentrations were highly variable in agreement with the patchiness in the productivity pattern. North-south gradients in subsurface DOC indicate that it fuels denitrification in north leading to subsurface minima. DOC exhibited linear relations with AOU, nitrate deficit, TEP and bacterial carbon and thus suggesting its pivotal role in the biogeochemical cycling of carbon in this region. TEP were minimal in the oxygen minimum zone indicating their consumption by bacteria during denitrification. Bacterial carbon was linearly related to DOC and TEP suggesting a close coupling among these

reservoirs. A general negative relation between DOC and TEP indicates possible interconversions between them. Low TEP concentrations and their association with mineral particles in the Bay of Bengal supports mineral-ballast theory that explains faster scavanging of organic particles from the water column. Estimation of regenerated carbon using elemental ratios (Redfield ratios), and circulation changes (Kroopnick's formulations) differed significantly due to seasonal changes in stoichiometry in case of the former and due to incompatibility of the generalised world ocean formulations to those occurring in the Arabian Sea, in case the latter.

Physical and biogeochemical carbon box-model for the study region revealed that nearly three-fourths of the photosynthetically produced carbon remineralises in the surface layer itself. But despite the perennial emission, carbon budget, in toto, suggests the surface Arabian Sea to be a net sink of atmospheric CO_2, that is to be ascertained in future studies.

Soil-water interactions modified the expected pH behaviour in the estuarine waters of Goa, west coast of India. Leaching of organics from soil appears to contribute to a pH decrease. Nevertheless, TCO_2 behaved conservatively both in field and laboratory experiments. Our studies reveal that soil-water interactions significantly influence pCO_2 levels in the estuarine system of Goa and thus leading to higher fluxes, than expected from simple mixing between

river and sea waters. As a result disproportionately large CO_2 fluxes from water-to-air occurred in these estuaries. This study therefore suggests that the role of estuarine /coastal waters to act as sink or source of atmospheric CO_2 shall depend with the nature of catchment soil and soil-water interactions.

From the results obtained in this detailed study and the salient features identified the recommendations for the future work are:

Understanding the carbon dioxide dynamics in surface layers of the ocean is very important. Its cycling within the surface layer and its exchanges with atmosphere and subsurface layers is still to be understood satisfactorily. Further, an integrated, systematic and detailed measurements on all carbon components with concomitant physical and biological parameters are essential to quantify carbon exchanges. Use of stable isotopes of carbon will be of extreme importance in measuring the extents of atmospheric carbon absorption by Arabian Sea surface waters. This study suggested the Arabian Sea to be a net sink of atmospheric carbon dioxide, if found true, this region will be the most significant among the world oceans to absorb anthropogenic carbon dioxide.

It is also important to monitor the surface pCO_2 concentrations using the continuous monitoring sensors on moored buoys that are being placed at

several places in the oceans as a part of the Global Ocean Observing System (GOOS), World Climate research Programme (WCRP) etc. Such automatic and continuous recording of data particularly in the North Indian Ocean would enable understand the variability of this region with respect to sink/source of atmospheric CO_2.

Intense measurements on CO_2 components in estuarine and coastal waters of India are required as the North Indian Ocean, Bay of Bengal in particular, receives enormous amounts of run-off and suspended loads. The nature of soil-water interactions might differ from region to region based on the characteristics of drainage basin and soil of the terrain. Therefore, it is important to understand these interactions through *in situ* and *in vitro* studies in Indian rivers, estuaries and coastal waters around India..

Very little is known on the carbon dynamics in the Bay of Bengal, a region of intense land-ocean-atmosphere interactions. Low salinity regions in the open bay act as sinks of atmospheric carbon. The mineral particles, land derived or of marine origin, enhance the rate of organic carbon deposition in the bay. However, the detailed linkages and actual mechanisms of carbon turnover is still to be known. Hence, the Bay of Bengal should be aimed for extensive measurements of carbon components in the near future.

REFERENCES

References

Alldredge, A.L., Passow, U and Logan, B.E. 1993. The abundance and significance of a class of large, transparent organic particles in the ocean. Deep-Sea Res., 40, 1131-1140.

Alldredge, A.L.1998. The carbon, nitrogen and mass content of marine snow as a function of aggregate size. Deep-Sea Res., 45, 529-541.

Anderson, L. and Dyrssen, D. 1994. Alkalinity and total carbonate in the Arabian Sea. Carbonate depletion in the Red Sea and Persian Gulf. Mar. Chem., 47, 195-202.

Anderson, L.A. and Sariemento, J.L. 1994. Redfield ratios of remineralization determined by nutrient data analysis. Global Biogeochem. Cycles, 8, 65-80.

Antoine, D., Andre, J-M. and Morel, A. 1996. Oceanic primary production 2. Estimation at global scale from satellite (coastal zone color scanner) chlorophyll. Global Biogeochem. cycles, 10, 57-69.

Aston, S.R.1978. Estuarine Chemistry, In: Chemical Oceanography, Edited by J.P. Riley and R. Chester, 2nd edition, 7, Academic Press, London, 361-446.

Azam, F., Steward, G.F;, Smith, D.C., and Ducklow, H.W. 1994. Significance of bacteria in carbon fluxes in the Arabian Sea. Proc. Indian Acad. Sci., (Earth Planet. Sci.), 103, 341-351.

Babenerd, K and Krey, J. 1974. Indian Ocean: Collected data on primary production, phytoplankton pigments, and some related factors. Institut für Meereskunde an der Universität Kiel, Germany, 521 pp.

Baeber, R., Marra, J, K., Bidigare, R., Halpern, D., Codispoti, L. and Smith, S. 1998. Deep-Sea Res., (submitted)

Baes, C.F., Jr. 1982. Role of the oceans in the carbon cycle. Conf. on climate and energy, carbon dioxide, Erice (Italy), 16 July 1982.

Banse, K. 1968. Hydrography of the Arabian Sea Shelf of India and Pakistan and effects on demersal fishes. Deep-Sea Res., 15, 45-79.

Banse, K. 1984. Overview of the hydrography and associated biological phenomena in the Arabian Sea, off Pakistan. In: Marine Geology and Oceanography of Arabian Sea and Coastal Waters, edited by B.U.Haq and J.D. Milliman, Van Nostrand Reinhold Co., NY, 271-303.

Banse, K. 1994. On the coupling of hydrography, phytoplankton, zooplankton, and settling organic particles offshore in the Arabian Sea. Indian Acad. Sci., (Earth Planet. Sci.,), 103, 125-161.

Bauer, S., Hitchcock, G.L., and Olson, D.B. 1991. Influence of monsoonally-forced Ekman dynamics upon the surface layer depth and plankton biomass distribution in the Arabian Sea. Deep-Sea Res., 38, 531-553.

Baumgartner, A and Reichel, E. 1975. The World Water Balance: Annual Global Continental and Maritime Precipitation, Evaporation and Runoff, 31 charts, Elsevier Sciences, New York, 179 pp.

Benson, B.B. and Krause, D. Jr. 1984. The concentration and isotopic fractionation of oxygen dissolved in fresh water and seawater in equilibrium with the atmosphere. Limnol.Oceanogr. 29, 620-632.

Bethoux, J.P. 1988. Red Sea geochemical budgets and exchanges with the Indian Ocean. Mar. Chem., 24, 83-92.

Bhattathiri, P.M.A., Pant, A., Sawant, S., Gauns, M., Matondkar, S.G.P. and Mohanraju, R. 1996. Phytoplankton production and chlorophyll distribution in the eastern and central Arabian Sea in 1994-1995. 1996. Curr. Sci., 71, 857-862.

Bhosle, N.B., and Wagh, A.B., 1989. Particulate carbohydrates in the Arabian Sea. Oceanol. Acta, 12, 57-63.

Breland II, J.A. and Byrne, R.H. 1993. Spectrophotometric procedures for determination of seawater alkalinity using bromocresol green. Deep-Sea Res., 40, 629-641.

Brewer, P.G. and Dyrssen, D. 1985. Chemical Oceanography of the Persian Gulf, Essays on oceanography: A Tribute to John Swallow, edited by J. Crease, W.S, Goulet and P.M. Saunders, 14, 41-55.

Brock, J.C, C.R. McClain, M.E. Luther and W.W. Hay. 1991. The phytoplankton bloom in the northwestern Arabian Sea during the southwest monsoon of 1979. J. Geophys. Res., 96, 20,613-20,622.

Broecker, W.S. 1974a. Chemical Oceanography, Harcourt Brace Jovanovich, New York , 79pp

Broecker, W.S. 1974b. 'NO', a conservative water mass tracer. Earth Planet. Sci. Lett., 23, 100-107.

Broecker, W.S., and Peng, T.H. 1992. Interhemispheric transport of carbon dioxide by ocean circulation, Nature, 356, 587-589, 1992.

Broecker, W.S., and Peng, T.H., 1982. Tracers in the Sea. Edited by LDGO, University of Columbia, Palisades, NY.

Broecker, W.S., Takahashi, T., 1978. The relationship between lysocline depth and insitu., carbonate ion concentration, Deep-Sea Res., 25, 65-95.

Broecker, W.S., Takahashi, T., Simpson, H.J. and Peng, T.H. 1979. Fate of Fossil Fuel Carbon Dioxide and the Global Carbon Budget, Science, 206, 4417, 409-418.

Bryden, H.L. 1973. New polynomials for thermal expansion, adiabatic temperature gradient and potential temperature of sea water. Deep-Sea Res., 25, 315-322.

Burton, J.D. 1976. Basic properties and processes in estuarine chemistry. In: Estuarine Chemistry, Edited by J.D. Burton and P.S. Liss, Acadamic Press, London and New
York, 1-36 pp.

Byrne, R.H. and Breland, J.A., 1989. High precision multiwavelength pH determination in seawater using Cresol Red. Deep-Sea Res., 36, 803-810.

Calvert, S.E., T.F. Pedersen, P.D. Naidu and U. von Stackelberg. 1995. On the organic carbon maximum on the continental slope of the eastern Arabian Sea, J. Mar. Res., 53, 269-296.

Carpenter, J.H. 1965. The Chesapeake Bay Institute technique for the winkler dissolved oxygen method. Limnol. Oceanogr., 10, 141-143.

Cho, B.C. and Azam, F. 1988. Major role of bacteria in biogeochemical fluxes in the ocean's interior. Nature, 332, 441-443.

Clayton, T. and Bryne, R.H. 1993. Calibration of m-cresol purple on the total hydrogen ion concentration scale and its application to carbon dioxide system characteristics in sea water. Deep-Sea Res., 40, 2115-2129.

Codispoti, L.A., Friederich, G.E., Sakamoto, C.M., Elkins, J., Packard, T.T., and Yoshinari, T. 1992. Nitrous oxide cycling in upwelling regions underlain by low oxygen waters, in Oceanography of the Indian Ocean, edited by B.N. Desai, Oxford & IBH, New Delhi, 271-284.

Craig, H. 1971. Deep metabolism: oxygen consumption in abyssal ocean water. J. Geophys. Res., 76, 5078-5086.

Culberson, C. and Pytkowitcz, R.M. 1968. Effect of pressure on carbonic acid, boric acid and the pH in sea water. Limnol. Oceanogr., 13, 403-417.

Cutler, A.N., and Swallow, J.C. 1984. Surface currents of the Indian Ocean (To 25°S, 100°E): compiled from historical data archived by the Meteorological office, (Bracknell, UK, : Institute of Oceanographic Sciences, Wormley, Report No. 187, 36 Charts), 8pp.

de Sousa, S.N., Kumar, M.D., Sardessai, S, Sarma, V.V.S.S., and Shirodkar, P.V., 1996. Seasonal variability in oxygen and nutrients in the central and eastern Arabian Sea. Curr. Sci., 71, 847-851.

Dickson, A.G., 1993. The measurement of seawater pH. Mar. Chem., 44, 131-142.

Dietrich, G. 1973. The unique situation in the environment of the Indian Ocean. In: The Biology of the Indian Ocean, edited by B. Zeitzschel, Springer Verlagm 1-6 pp.

Druffel, E.R.M., Williams, P.M., and Suzuki, Y., 1989. Concentrations and radio carbon signatures of Dissolved Organic Matter in the Pacific Ocean, Geophy. Res. Lettrs., 16, 991-994.

Ducklow, H.W., 1993. Bacterioplankton distributions and production in the northwestern Indian Ocean and Gulf of Oman, September 1986. Deep-Sea Res., II, 40, 753-771.

Dugdale, R.C. and Goering, J.J. 1967. Limnol. Oceanogr. 12, 196.

Duing, W., 1970. The monsoon regime of the currents in the Indian Ocean, (Honolulu: East-West center Press) contribution No. 330 from the Hawaii Institute of Geophysics, University of Hawaii, 68 pp.

Dyrssen, D., 1992. Processes determining the pH of seawater, Vatten, 48, 246-250.

Emery, K.O., and D.G. Aubrey. 1989. Tide gauges of India. J. Coastal Res., 5, 489-501.

Findlater, J. 1969. A major low-level air current near the Indian Ocean during the northern summer. Quarterly Journal of the Royal Meterological Society, 95, 362-380.

Findlater, J. 1974. The low-level cross-equatorial barrier between the Indian and Pacific Oceans and a likely cause for Wallace's line. Unesco Technical Papers in Marine Science, 49, 84-97.

Fofonoff, N.P., Millard, R.C., Jr. 1983. Algorithms for computation of fundamental properties of seawater, UNESCO-Tech.-pap. Mar. Sci., Paris, France, Unesco, 44, 53pp.

Garrels, R.M. and F.T. Mackenzie, 1971. Evolution of sedimentary rocks. W.W. Norton & Co., New York, 397.

George, M.D., Kumar, M.D., Naqvi, S.W.A., Banerjee, S., Narvekar, P.V., de Sousa, S.N. and Jayakumar, D.A. 1994. A study of the carbon dioxide system in the northern Indian Ocean during premonsoon. Mar.Chem., 47, 243-254.

Goyet, C., and Poisson, A. 1989. New determination of carbonic acid dissociation constants in seawater as a function of temperature and salinity. Deep-Sea Res., 36, 1635-1654.

Goyet, C., Millero, F.J., O'sullivan, D.W., Eischeid, G., McCue, S.J., and Bellerby, R.G.J. 1998. Temporal variations of pCO_2 in surface seawater of the Arabian Sea in 1995. Deep-Sea Res., 45, 609-624.

Goyet, C., Millero, F.J., Poisson, A. and Shafer, D.K. 1993. Temperature dependence of CO_2 fugacity in seawater. Mar. Chem., 44, 205-219.

Goyet, C. and Snover, A.K. 1993. High-accuracy measurements of total dissolved inorganic carbon in the ocean: comparison of alternate detection methods. Mar. Chem. 44, 235-242.

Grasshoff, K. 1975. The hydrochemistry of landlocked basins and fjords. In: Chemical Oceanography, Vol. 2, edited by J.P. Riley and G. Skirrow, Academic Press, New York, pp. 455-597.

Grasshoff, K., Ehrhardt, M. and Kremling, K. (Eds) 1983. Methods of Seawater analysis, 2nd edition, VCH publishers, Wainheins, Germany.

Grasshoff, K. 1969. Zur chemie des Roten Meeres und des inneren Golfs von Aden nach Beobachtungen von F.S. 'Meteor' wahrend der Indischen Ozean Expedition 1964/65. Meteor Forschungsergeb., Reihe A, No. 6, 76 pp.

Hama, T., and Handa, N. 1983. The seasonal variation of organic constituents in a eutrophic lake, Lake Suwa, Japan, Part 2. Dissolved Organic Matter, Arch. Hydrobiol., 98, 443-462.

Hama, T., and Handa, N. 1987. Pattern of organic matter production by natural phytoplankton population in a eutrophic lake. 2. Extracellular products, Arch. Hydrobiol., 109, 227-243.

Hansson, I. 1973. A new set of pH scales and standard buffers for sea water. Deep-Sea Res., 20, 479-491.

Hartman, M., Mange, H., Scibold, E., and Walgner, E., 1971. Oberflachensedimente im Persichen Golf und Folf von Oman, J. Geologisch-hydrologischer Rahmen und erste Sedimentologisch Ergebnisse, "Meteor" Forschungsergebn., Berlin, 1-76.

Hastenrath, S., and Lamb, P.J. 1979. Climate Atlas of the Indian Ocean, Part 1 (Madison: University of Wisconsin Press) 97 charts.

Howell, E.A., Doney, S.C., Fine, R.A. and Olson, D.B. 1997. Geochemical estimates of denitrification in the Arabian Sea and the Bay of Bengal during WOCE. Geophys. Res. Lett., 24, 2549-2552.

Ittekkot, V., Haake, B., Bartsch, M., Nair, R.R., and Ramaswamy, V. 1992. Organic carbon removal in the sea: The continental connection in upwelling systems: Evolution since the Miocene, edited by C.P. Summerhayes et al., Geol. Soc. Spec. Publ., 64, 167-176.

Ittekkot, V., Nair, R.R., Honjo, S., Ramaswamy, V., Bartsch, M., Manginini, S. and Desai, B.N. 1991. Enhanced particle fluxes in Bay of Bengal induced by injection of fresh water. Nature, 351: 385-387.

Jackson, G.A, 1990. A model of the formation of marine algal flocs by physical coagulation processes. Deep-Sea Res., 37, 1197-1211.

Jackson, G.A., and Williams, P.M. 1988. Measures of net oxidant concentration in seawater, Deep-Sea Res., 35, 209-225.

Johnson, K.M., Wills, K.D., Butler, D.B., Johnson, W.K. and Wong, C.S. 1993.. Coulometric TCO_2 analyses for marine studies: maximizing the performance of an automated gas extraction system and coulometric detector. Mar. Chem. 44, 167-187.

Kabanova, Y.G. 1968. Primary production of the northern part of the Indian Ocean.. Oceanol., 8, 214-225.

Kauppi, P.E., Mielikainen, K, and Kuusela, K.1992. Biomass and carbon budget of European forests, Science, 256, 70-74.

Keeling, C.D. 1968. Carbon dioxide in surface ocean waters. 4. Global distribtuion. J. Geophys. Res., 73, 4543-4553.

Keeling, C.D., and Heimann, M. 1986. Meridional eddy diffusion model of the transport of atmospheric carbon dioxide, 2, Mean annual carbon cycle, J. Geophys. Res., 91, 7782-7796.

Keeling, C.D., Piper, S.C. and Heimann, M. 1989. A three-dimensional model of atmospheric carbon dioxide transport based on observed winds, 4, Mean annual gradients and interannual variations. In Aspects of Climate Variability in the Pacific and the Western Americas, Geophys. Monogr. Ser., vol. 55, edited by D.H. Peterson, AGU, Washington, D.C., 305-363 pp.

Keil, R.G. and Kirchman, D.L. 1993. Dissolved combined aminoacids: chemical form and utilization by marine bacteria. Limnol. and Oceanogr. 38, 1256-1270.

Kepkay, P.E.1994. Particle aggregation and the biological reactivity of colloids. Mar. Ecol. Prog. Ser., 109, 293-304.

Koczy, F.F. 1956. The specific alkalinity. Deep-Sea Res., 3, 279-288.

Kolla, V.L., Sullivan, S., Strecter, S. and Langseth, M.G. 1976. Spreading of the Antarctic Bottom water and its effects on the Indian Ocean inferred from bottom water potential temperature, Turbidity and seafloor photography, Mar. Geol., 21, 171-189.

Koroleff, F. 1983. Determination of phosphorous, In: Methods of seawater analysis. Edited by K. Grasshoffm M. Ehrhardt and K.Kremling, Verlag chemie, pp. 126.

Kortzinger, A., Duinker, J.C. and Mintrop, L. 1997. Strong CO_2 emissions from the Arabian Sea during South-West Monsoon. Geophys. Res. Lettrs., 24, 1763-1766.

Kroopnick, P. M. 1985. The distribution of ^{13}C of ΣCO_2 in the world oceans. Deep-Sea Res I., 32, 57-84.

Ku, T.L., and S.Luo. 1994. New appraisal of Radium 226 as a large scale oceanic mixing tracer. J. Geophys. Res., 99, 10,255-10,273,

Kumar, M.D. and Li, Y.H. 1996. Spreading of water masses and regeneration of silica and ^{226} Ra in the Indian Ocean. Deep-Sea Res. II, 43, 83-110.

Kumar, M.D., Rajendran, A., Somasundar, K., Haake, B., Jenisch, A., Shuo, Z., Ittekkot, V., and Desai, B.N. 1990. Dynamics of dissolved organic carbon in the northwestern Indian Ocean, Mar. Chem., 31, 299-316.

Kumar, M.D., Rajendran, A.,Somasundar, K.,Ittekkot, V. and Desai, B.N., 1992. Processes controlling carbon components in the Arabian Sea. In: Oceanography of the Indian Ocean, edited by B.N. Desai, Oxford & IBH, New Delhi, pp. 313-325.

Kumar, M.D., Sarma, V.V.S.S., Ramaiah, N. and Gauns. 1998. Biogeochemical significance of transparent exopolymer particles in the Indian Ocean. Geophys. Res. Lett., 25, 81-84.

Kumar, MD., Naqvi, S.W.A., George, M.D., and Jayakumar, D.A. 1996. A sink for atmospheric carbon dioxide in the northeast Indian Ocean, J. Geophys. Res., 101, 18,121-18,125.

Lancelot, C. and Methot, S. 1985. Biochemical fractionation of primary production by phytoplankton in Belgian coastal waters during short and longterm incubations with ^{14}C-bicarbonate. II. *Phaeocystis pouchetti* colonial population. Mar. Biol., 86, 227-232.

Lancelot, C., 1984. Metabolic changes in *Phaeocystic pouchetti* (Hariot) Lagerheim during the spring bloom in Belgian coastal waters. Estuar. Coastal Shelf. Sci., 18, 593-600.

Law, C.S. and Owens, N.J.P. 1990. Significant flux of atmospheric nitrous oxide from the northwestern Indian Ocean. Nature 346, 826-828.

Liss, P. and Merlivat, L. 1986. Air-sea gas exchange rates: Introduction and synthesis. In: The role of air-sea exchange in geochemical cycling, Edited by P. Buat-Menart, N.A.T.O.A.S.I. Series, vol. 185, pp. 113-128.

Liss, P.S., 1976. Conservative and non-conservative behaviour of dissolved constituents during estuarine mixing. In "Estuarine Chemistry", Edited by J.D. Burton and P.S. Liss, Academic Press, London, 93-130.

Longhurst, A.R., and Wooster, W.S. 1995. Abundance of oil sardine (*Sardinella longiceps*) and upwelling on the southwest coast of India. Can. J. Fish. Aquat. Sci., 47, 2407-2419.

Louanchi, F., Metzl, N. and Poisson, A. 1996. A modelling the monthly sea surface fCO_2 fields in the Indian Ocean, Mar. Chem. 55, 265-280.

Luther, M.E., O'Brien, J.J., and Prell, W.L. 1990. Variability in upwelling fields in the northwestern Indian Ocean; part1: Model experiments over the past 18,000 years. Paleoceanography, 5, 433-445.

Madhupratap, M., Kumar, S.P., Bhattathiri, P.M.A., Kumar, M.D., Raghukumar, S., Nair, K.K.C., and Ramaiah, N. 1996. Mechanism of the biological response to winter cooling in the northeastern Arabian Sea. Nature, 384, 549-552.

Maillard, L.C. 1913. Formation des materies humiques par action des acides amines sur les sucres; C.R. Acad. Sci. Paris, 156, 1159.

Mantoura, R.F.C., Law, C.S., Owens, N.J.P., Burkill, P.H., Woodward, E.M.S., Howland, R.J.M. and Llewellyn, C.A. 1993. Nitrogen biogeochemical cycling in the NW Indian Ocean. Deep-Sea Res., II 40, 651-672.

Mantoura, R.F.C., Dickson, A., and Riley, J.P. 1978. The complexation of metals with humic materials in natural waters. Estuarine. Coastal Mar. Sci., 6, 387-408.

Martin, J.M., Burton, J.D. and Eigma, D. (Eds). 1981. River inputs to the ocean systems, United Nations press, Geneva, Switzerland, 384 pp. .

Mehrbach, C., Culberson, C.H., Hawley, J.E. and Pytkowicz, R.M. 1973. Measurement of the apparent dissociation constants of carbonic acid in seawater at atmospheric pressure. Limnol. Oceanogr., 18, 897-907.

Menzel, D.W., 1964. The distribution of Dissolved Organic Carbon in the western Indian Ocean, Deep-Sea Res., 11, 757-766.

Menzel, D.W., and Ryther, J., 1968. Organic carbon and the oxygen minimum in the South Atlantic Ocean, Deep-Sea Res., 15, 327-337.

Meybeck, M. 1982. Carbon, nitrogen and phosphorus transport by world rivers. Am. J. Sci., 282, 401-450.

Millero, F.J. 1979. The thermodynamics of the carbonate system in seawater, Geochim. Cosmochim. Acta, 43, 1651-1661.

Millero, F.J., Byrne, R.H., Wanninkhof, R., Feely, R., Clayton, T., Murphy, P. a,d Mamb, M.F. 1993. The internal consistency of carbon dioxide measurements in equatorial Pacific. 44, 269-280.

Millero, F.J., Chen, C.T., Bradsha, A.L., and Schleiche, K. 1980. A new high pressure equation of State for Sea water. Deep-Sea Res., 27, 255-264.

Millero, F.J., Zhang, J-Z., Lee, K. and Cambell, D.M. 1993. Titration alkalinity of sea water. Mar. Chem., 44, 153-165.

Milliman, J.D., and Meade, R.H. 1982. World-wide delivery of river sediment to the oceans, Tech. Rep. Woods Hole Oceanogr. Inst. MA-USA-WHOI, 23pp.

Mintrop, L. Körtzinger, A. and Duinker, C. 1998. The carbon dioxide system in the northwestern Indian Ocean during south-west monsoon. Mar. Chem (submitted).

Morcos, S.A. 1970. Physical and chemical oceanography of the Red Sea. Oceanogr. Mar. Biol. Ann. Rev., 8, 73-202.

Mucci, A. 1983. The solubility of calcite and aragonite in seawater at various salinities, temperature and atmospheric total pressure. Am. J. Sci., 283, 780-799.

Muralidheeran, P.M. and Prasanna Kumar, S., 1996. Arabian Sea upwelling - A comparison between coastal and open ocean regions. Curr. Sci., 71, 842-846.

Naidu, P.D. 1993. Distribution pattern of recent panktonic foraminefera in surface sediments of the western continental margin of India. Mar. Geol. 110, 403-418.

Nair, R.R. and Hashimi, N.H. 1980. Holocene climatic influences from the sediments of the western Indian continental shelf. Proceedings of the Indian Academy of Sciences (Earth and Planetary Sciences), 89, 299-315.

Nair, R.R. and Hashimi, N.H. 1981. Mineralogy of the carbonate sediments-western continental shelf of India. Mar. Geol., 41, 309-319.

Nair, R.R., Ittekkot, V., Managanin, S.J., Ramaswamy, V., Haake, B., Degens, E.T., Desai, B.N. and Honjo, S. 1989. Increased particle flux to the deep ocean related to monsoons. Nature, 338, 749-751.

Naqvi, S.W.A. and Naik, S., 1983. Calcium:chlorinity ratio and carbonate dissolution in the northwestern Indian Ocean, Deep Sea Res., 30, 381-392.

Naqvi, S.W.A. 1991. Geographical extent of denitrification in the Arabian Sea in relation to some physical processes. Oceanol. Acta., 14, 281-290.

Naqvi, S.W.A. 1994. Denitrification processes in the Arabian Sea. Proc. Indian Acad. Sci. 103, 279-300.

Naqvi, S.W.A. and Reddy, C.V.G. 1975. Vertical distribution of the degree of calcium carbonate saturation in the Indian Ocean. Indian. J Mar. Sci., 4, 213-215.

Naqvi, S.W.A. and Sen Gupta, R. 1985. 'NO' a useful tool for the estimation of nitrate deficits in the Arabian Sea. Deep-Sea Res., 35, 665-674.

Naqvi, S.W.A., and Shailaja, M.S. 1993. Activity of the respiratory electron transport system and respiration rates within the oxygen minimum layer of the Arabian Sea. Deep-Sea Res., II, 40, 687-695.

Naqvi, S.W.A., Jayakumar, D.A., Nair, M., Kumar, M.D., and George, M.D., 1994. Nitrous Oxide in the western Bay of Bengal, Mar. Chem., 47, 269-278.

Naqvi, S.W.A., Kumar, M.D., Narvekar, P.V., De Sousa, S.N., Geroge, M.D., D' Silva, C., 1993. An intermediate nepheloid layer associated with high microbial metabolic rates and denitrification in the northwestern Indian Ocean, J. Geophys. Res., 98, 16,469-16,479.

Naqvi, S.W.A., Noronha, R.J., Somasundar, K., Gupta, R., 1990. Seasonal changes in the denitrification regime of the Arabian Sea. Deep-Sea Res., 37, 593-611.

Naqvi, S.W.A., Shailaja, M.S., Kumar, M.D. and Gupta, R.S. 1996. Respiration rates in subsurface waters of the northern Indian Ocean: Evidence for low decomposition rates of organic matter within the water column in the Bay of Bengal. Deep-Sea Res., 43, 73-81.

Naqvi, S.W.A.1987. Some aspects of the oxygen deficient conditions and denitrification in the Arabian Sea. J. Mar. Res., 45, 1049-1072.

Ogura, N. 1970. The relation between Dissolved Organic Carbon and Apparent Oxygen Utilization in the western North Pacific. Deep-Sea Res., 17, 221-231.

Olson, D.B., Hitchcock, G.L., Fine, R., and Warren, B.A. 1993. Maintenance of the low-oxygen layer in the central Arabian Sea. Deep-Sea Res., II 40, 697-710.

Ong, H.L. and Bisque., R.E. 1968. Coagulation of humic colloids by metal ions. Soil Sci., 106, 220-224.

Owens, N.J.P., Burkill, P.H., Mantoura, R.F.C., Woodward, E.M.S., Bellan, I.A., Aiken, J., Howland, R.J.M., Llewellyn, C.A. 1993. Size fractionated primary production and nitrogen assimilation in the NW Indian Ocean. Deep-Sea Res., II, 40, 697-710.

Pai, S., Gong, G. and Liu, K. 1993. Determination of dissolved oxygen in seawater by direct spectrophotometry of total iodine. Mar. Chem. 41, 343-351.

Paropkari, A.L., Prakash Babu, C. and Mascarenhas, A. 1992. A critical evaluation of depositional parameters controlling the variability of organic carbon in Arabian Sea sediments. Mar. Geol. 107, 213-226.

Passow, U. and Alldredge, A. L. 1994. Distribution, size and bacterial conlonization of Transparent Exopolymer Particles (TEP) in the ocean, Mar.Ecol.Prog.Ser. 113, 185-198.

Passow, U. and Alldredge, A. L. 1995. A dye-binding assay for the spectrophotometric measurement of Transparent Exopolymer Particles (TEP). Limnol. Oceanogr., 40, 1326-1335.

Pearman, G.I., Hyson, P., Fraser, P.J. 1983. The global distribution of atmospheric carbon dioxide: 1. Aspects of observations and modelling. J. Geophys. Res., 88, 3581-3590.

Peng, T.H., Takahashi, T., Broecker, W.S. and Olafsson, Jr. 1987. Seasonal variability of carbon dioxide, nutrients and oxygen in the northern North Atlantic surface water: observations and a model. Tellus, 39B, 439-458.

Perdue, E.M. 1978. Solution thermochemistry of humic substances - I. Acid-base equilibria of humic acid. Geochim. Cosmochim. Acta, 42, 1351-1358.

Prasanna Kumar, S. and Prasad, T.G., 1996. Winter cooling in the northern Arabian Sea, Curr. Sci.,71, 834-841.

Prasanna Kumar, S. Madhupratap, M., Kumar, M.D., Muraleedharan, P.M. Sawant, S., Gauns, M., de Sousa, S.N. and Sarma, V.V.S.S. 1998. High biological productivity in the interior Arabian Sea during summer monsoon driven by Ekman pumping and lateral advection. J Geophys. Res. (Communicated).

Prell, W.L., Marvil, R.E., and Luther, M.E. 1990. Variability in upwelling fields in the northwestern Indian Ocean; Part 2: Data-Model comparison at 9,000 years B.P. Paleoceanogr., 5, 447-457.

Qasim, S.Z. 1982. Oceanography of the Northern Arabian Sea, Deep-Sea Res., 29, 1041-1068.

Qasim, S.Z.1977. Biological productivity of the Indian Ocean. Indian J. Mar. Sci., 6, 122-137.

Quay, P.D., Tilbrook, B. and Wong, C.S. 1992. Oceanic uptake of fossil fuel CO_2: Carbon-13 evidence, Science, 256, 74-79.

Ramaiah, N., Raghukumar, S., and Gauns, M. 1996. Bacterial abundance and production in the central and eastern Arabian Sea. Curr. Sci., 71, 878-882.

Ramanathan, K.R., and Pisharoty, P.R., 1972. Water balance - Indian Ocean, in World Water Balance, vol. I, pp.39-41, Int. Assoc. of Hydrolo. Sci., Gentbrugge, Belgium.

Ramesh Babu, V., Varkey, M.J., Kesava Das, V. and Gouveia, A.D. 1980. Water masses and general hydrography along the west coast of India during early March. Indian J. Mar. Sci., 9, 83-89.

Rao, C.K., Naqvi, S.W.A., Kumar, M.D., Varaprasad, S.D.J., Jayakumar, D.A., George, M.D. and Singbal, S.Y.S. 1994. Hydrochemistry of Bay of Bengal: possible reasons for a different water-column cycling of carbon and nitrogen from the Arabian Sea. Mar.Chem. 47, 279-290.

Redfield, A.C., Ketchum, B.H., and Richard, F.A., 1963. The influence of organisms on the composition of seawater, In: M.N. Hill (Editor), The Sea, 2, Wiley, New York, NY.

Reuter, J.H. and Perdue E.M. 1977. Importance of heavy-metal-organic matter interactions in natural waters. Geochim. Coschim. Acta, 41, 325-334.

Ryther, J.H. and Menzel, D.W. 1965. On the production, composition and distribution of organic matter in the western Arabian Sea. Deep-Sea Res., 12, 199-209.

Sabine, C.L., Mackenzie, F.T., Winn, C. and Karl, D.M. 1995. Geochemistry of carbon dioxide in seawater at the Hawaii Ocean Time series station, ALOHA. Global Biogeochem. Cycles, 9, 637-651.

Sarin, M.M., Rengarajan, R. and Ramaswamy, V. 1996. ^{234}Th scavenging and particle export fluxes from the upper 100 m of the Arabian Sea. Curr. Sci., 71, 888-893.

Sarma, V.V.S.S., Kumar, M.D., and George, M.D., 1998. The eastern and Central Arabian Sea as a pernial source for atmospheric carbon dioxide. Tellus,50B, 179-184.

Sarma, V.V.S.S., Kumar, M.D., George, M.D. and Rajendran, A. 1996. Seasonal variability in inorganic carbon components in the central and eastern Arabian Sea, Curr. Sci., 71, 852-856.

Sarmiento, J.L., Orr, J.C. and Siegenthaler, U. 1992. A perturbation simulation of CO_2 uptake in an ocean general circulation model, J. Geophys. Res., 97, 3621-3645.

Sathyendranath, S., Gouveia, A.D., Shetye S.R,, Ravindran P, and Platt T. 1991. Biological control of surface temperature in the Arabian Sea. Nature, 349, 54-56.

Sawant, S. and Madhupratap, M. 1996. Seasonality and composition of phytoplankton in the Arabian Sea. Curr. Sci., 71, 869-873.

Schott, F. 1983. Monsoon response of the Somali Current and associated upwelling. Prog. Oceanogr., 12, 357-381.

Schott, F., Swallow, J.C., and Fieux, M. 1990. The Somali Current at the equator: Annual cycle of currents and transports in the upper 1,000 m and connection to neighbouring latitudes. Deep-Sea Res., 37, 1825-1848.

Sen Gupta, R. and Pylee, A. 1968. Specific alkalinity in the northern Indian Ocean during the southwest monsoon. Bull. Natl. Inst. Sci. India, 38, 324-333.

Sen Gupta, R., Rajagopal, M.D. and Qasim, S.Z. 1976. Relationship between dissolved oxygen and nutrients in the northwestern Indian ocean. Indian J. Mar. Sci., 5, 201-211.

Shankar, D. and Shetye, S.R. 1997. On the dynamics of the Lakshadweep high and low in the southeastern Arabian Sea. J. Geophys. Res., 102, 12551-12562.

Sharma, G.S. 1968. Seasonal variation of some hydrographic properties of the shelf waters off the west coast of India. Bull. Natl. Inst. Sci. India, 38, 263-275.

Shetye, S.R., Gouveia, A.D., Shenoi, S.S.C., Sundar, D., Michael, G.S., Almeida, A.M., and Santanam, K. 1990. Hydrography and circulation off the west coast of India during the southwest Monsoon 1987. J. Mar. Res., 48, 359-378.

Shetye, S.R., 1993. The movement and implication of the Ganges-Brahmaputra runoff on entering the Bay of Bengal, Curr. Sci., 64, 32-38.

Shetye, S.R., and Shenoi, S.S.C. 1988. The seasonal cycle of surface circulation in the coastal north Indian Ocean, Proc. Indian Acad. Sci., (Earth Planet Sci.,) 97, 53-62.

Shetye, S.R., Shenoi, S.S.C., Antony, M.K., Krishna Kumar, V., 1984. Monthly mean wind stress distribution along the coast of the Northern Indian Ocean, Tech. Rep. Natl.Inst.Oceanogr., Donapaula, India, No. 1/84, 54pp.

Shetye, S.R., Gouveia, A.D., Shenoi, S.S.C. 1992. Does winter cooling lead to the subsurface salinity minimum off Saurashtra, India? In: Oceanography of the Indian Ocean, edited by B.N. Desai, oxford press, New Delhi, pp 617-626.

Sholkovitz, E.R. 1976. Flocculation of dissolved organic and inorganic matter during the mixing of river water and seawater. Geochimca et Cosmochimica Acta., 40, 831-845.

Siegenthaler, U and Sarmiento, J.L. 1993. Atmospheric carbon dioxide and the ocean. Nature, 365, 119-125.

Skirrow, G., 1975. The dissolved gases - Carbon dioxide. In: Chemical Oceanography, vol.2, 2nd edition (edited by. J.P. Riley and G. Skirrow), Academic Press, 1-181.

Slater, R.D. and Kroopnick, P. 1984. Controls of dissolved oxygen distribution and organic carbon deposition in the Arabian Sea. In: Marine geology and Oceanography of the Arabian Sea and coastal Pakistan. (edited by. J. Milliman), pp. 305-313.

Smith, D.C., Simon, M., Alldredge, A.L. and Azam, F. 1992. Intense hydrolytic enzyme activity on marine aggregates and implications for rapid particle dissolution. Nature, 359, 139-142.

Smith, R.L. and Bottero, J.S. 1977. On upwelling in the Arabian Sea. In: A Voyage of Discovery, edited by M. Angel, Pergamon Press, Oxford, pp. 291-304.

Smith, R.L. and Bottero, J.S. 1977. On upwelling in the Arabian Sea. In: A Voyage of Discovery, edited by M. Angel, Pergamon Press, 291-304.

Somasundar, K., Naqvi, S.W.A., 1988. On the renewal of the denitrifying layer in the Arabian Sea, Oceanol. Acta, 11, 167-172.

Somasundar, K., Rajendran, A., and Kumar, M.D. 1987. Property, Property relations: 22° and 9° discontinuities in the Arabian Sea, Oceanol. Acta., 10, 293-299.

Somasunder, K., Rajendran, A., Kumar, M.D. and Sen Gupta, R. 1990. Carbon and nitrogen budgets of the Arabian Sea. Mar. Chem., 30, 363-377.

Strickland, J.D.H., and Parsons, T.R., 1972. A practical Hand book of seawater Analysis, Bull. Fish. Res. Board. Can., 2nd Edn. No. 167, 311 pp.

Subramanian, V. 1993. Sediment load of Indian waters. Curr. Sci., 64, 928-930.

Suess, E. 1980. Particulate organic carbon flux in the oceans - surface productivity and oxygen utilization, Nature, 288, 260-263.

Sugimura, Y. and Suzuki, Y. 1988. A high temperature catalytic oxidation method for the determination of non-volatile dissolved organic carbon in sea water by direct injection of a liquid sample. Mar. Chem. 24, 105-131.

Sverdrup, H.U., Johnson, M.W. and Fleming, R.H. 1942. The Oceans: their physics, chemistry and general biology. Prentice Hall, New Jersey: 696 pp

Swallow, J.C. 1984. Some aspects of the physical oceanography of the Indian Ocean. Deep-Sea Res., 31, 639-650.

Szebellédy, L. and Somogyi, Z. 1038. Die coulometrische analyse als präzisims methode. Anal. Chem. 112, 313-323.

Takahashi , T., Broecker, W.S., and Langer, S. 1985. Redfield ratios based on chemical data from isopycnal surfaces. J. Geophys. Res., 90, 6907-6924.

Takahashi, T. 1961. Carbon dioxide in the atmosphere and in Atlantic Ocean water. J. Geophys. Sci., 66, 477-494.

Takahashi, T. 1975. Cushman Found, Foraminiferal Res. Spec. Publ. 11, 11 .

Takahashi, T. 1989. Only half as much CO_2 as expected from industrial emissions is accumulating in the atmosphere: could the oceans be the store house for the missing gas? Oceanus, 32, 22-29.

Takahashi, T. 1989. The carbon dioxide puzzle. Oceanus, 32, 22-29.

Takahashi, T., Broecker, W.S., Werner, S.R. and Bainbridge, A.E. 1982. Carbonate Chemistry of the surface wters of the world oceans. In:E.D. Goldberg, Y. Horibe and K. Saruhashi (Editors), Isotope Marine Chemistry. Uchida Rokakuho, Tokyo, pp. 291-326.

Tans, P.P. and White, J.W.C. 1998. The global carbon cycle: In balance, with a little key from the plants. Science, 281, 183-185.

Tans, P.P., Fung, I.Y. and Takahashi, T. 1990. Observational constraints on the global atmospheric CO_2 budget. Science, 247, 1431-1438.

Toggweiler, J.R. 1988. Deep sea carbon, a burning issue, Nature, 334, 465.

Turner, D.R., Whitfield, M. and Dickson, A.G. 1981. The equilibrium speciation of dissolved components in freshwater and seawater at 25°C and 1 atm pressure. Geochim. Cosmochim. Acta, 45, 855-881.

UNESCO, 1979. The carbon dioxide budget of the oceans. UNESCO Tech. Pap.Mar. Sci., 34, 51pp

UNESCO, 1987. Thermodynamics of the carbon dioxide system in seawater. Report by the carbon dioxide sub-panel of the joint panel on oceanographic tables and standards, UNESCO-Tech Pap. Mar. Sci. 60, 41 pp.

Varkey, M.J., Murty, V.S.N. and Suryanarayana, A. 1996. Physical oceanography of the Bay of Bengal and Andaman Sea. In: Oceanography and Marine Biology: An annual Review, editor A.D. Ansell, R.N. Gibson and M. Barnes, UCL Press, 34, pp 1-70.

Veldhuis, M.J.W., Kraay, G.W., Van-Bleijiswijk, J.D.L. and Baars, M.A. 1997. Seasonal and spatial variability in phytoplankton biomass productivity and growth in the northwestern Indian Ocean: The southwest and northeast monsoon, 1992-1993. Deep-Sea Res., 44, 425-449.

Venkateswaran, S.V. 1956. On evaporation from the Indian Ocean. Indian J. Meteorol. Geophy., 7, 265-284.

Von Stackelberg, U. 1972. Faziesverteilung in Sedilenten des indisch-pakistanischen Kontinentalrandes (Arabisches Meer). Meteor Forschungs-Ergebnisse, C9, 1-73.

Wangersky, P.J. 1978. Production of Dissolved Organic Matter. In: O. Kinne (Editor) Marine Ecology, 4, Wiley-Inter Science, Chichester, 115-220.

Waniek, J. and Zeitzschel, B. 1996. The cold water structure at 17° N, 65° E: Hydrography and nutrients. EOS 76, OS4 (OS11B-10).

Wanninkhof, R. and Thoning, K. 1993. Measurement of fugacity of CO2 in sea water using continuous and discrete sampling methods. Mar. Chem., 44, 189-204.

Wanninkhof. R. 1992. Relationship between wind speed and gas exchange over the ocean. J. Geophys. Res., 97, 7373-7382.

Warren, B.A. 1978. Bottom water transport through the southwest Indian Ridge, Deep-Sea Res., 25, 315-321.

Watson, A.J., Robinson, C., Robinson, J.E., Williams, P.J. le B. and Fasham, M.J.R. 1991. Spatial variability in the sink for atmospheric carbon dioxide in the North Atlantic. Nature, 350, 50-53.

Wattenberg, H. 1933. Kalzium Karbonat-und Kohlenäuregehalt des Meerwassers. Wiss. Ergebn. dt. atlant. Exped. 'Meteor', 8.

Weiss, R.F. 1970. The solubility of nitrogen, oxygen and argon in water and seawater. Deep-Sea Res., 17, 721-735.

Weiss, R.F. 1974. Carbon dioxide in water and seawater: The solubility of a non-ideal gas, Mar. Chem., 2, 203-215.

Weiss, R.F., Broecker, W.S., Craig, H. and Spencer, D. 1983. GEOSECS Indian Ocean Expedition, vol. 5, Hydrographic Data 1977-1978. U.S. Government Printing Office, Washington, D.C., 48 pp.

Williams, P.M.1990. Studies of the physical and chemical stability of natural sea surface films, Technical Report, Scripps Inst. of Oceanography, La Jolla, CA(USA), 3pp.

Wyrtki, K. 1971. Oceanographic Atlas of the International Indian Ocean Expedition. National science Foundation, Washington, 531pp

Wyrtki, K. 1973. Physical oceanography of the Indian Ocean. pp.18-36, In:B.Zeitzschel (Ed.), The Biology of the Indian Ocean, Springer-Verlag, New York.

Yentsch, C.S. and Phinney, D.A. 1992. The effect of wind direction and velocity on the distribution of phytoplankton chlorophyll in the western Arabian Sea. In: Oceanography of the Indian Ocean, edited by B.N. Desai, Oxford Press, New Delhi, pp 57-66.

Yoder, J.A., McClain, C.R., Feldman, G.C. and Esaias, W.E. 1992. Annual cycles of phytoplankton chlorophyll concentrations in the global ocean: a satellite view. Global Biogeochemical Cycles, 7, 181-193.

Yoshida, K. and Mao, H.L. 1957. A theory of upwelling of large horizontal extent. J. Mar. Res., 16, 40-57.